Version 2.0
January 2010

Cosmic Origins Spectrograph Instrument Handbook for Cycle 18

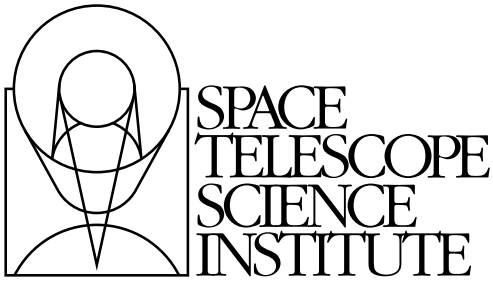

Space Telescope Science Institute
3700 San Martin Drive
Baltimore, Maryland 21218
help@stsci.edu

Operated by the Association of Universities for Research in Astronomy, Inc., for the National Aeronautics and Space Administration

User Support

For prompt answers to any question, please contact the STScI Help Desk.

- Send e-mail to: help@stsci.edu.
- Phone: 410-338-1082.
- Within the USA, you may call toll free: 1-800-544-8125.

World Wide Web

Information and other resources are available on the STScI COS World Wide Web site:

http://www.stsci.edu/instruments/cos

COS Handbook History

Version	Date	Editors
2.0	January 2010	Dixon, W. V., and Niemi, S.-M.
1.0	December 2007	Soderblom, D. R.

Additional Contributors

Please see the acknowledgments.

Citation

In publications, please refer to this document as
Dixon, W. V., et al. 2010, Cosmic Origins Spectrograph Instrument Handbook, Version 2.0 (Baltimore: STScI)

Send comments or corrections to:
Space Telescope Science Institute
3700 San Martin Drive
Baltimore, Maryland 21218
E-mail:help@stsci.edu

Table of Contents

Acknowledgments

The technical and operational information contained in this handbook is the summary of the experience gained by members of the STScI COS Team and by the COS IDT at the University of Colorado in Boulder.

Current and former members of the STScI COS Team include Alessandra Aloisi (lead), Tom Ake, Rossy Diaz, Van Dixon, Tom Donaldson, Linda Dressel, Scott Friedman, Parviz Ghavamian, Paul Goudfrooij, Phil Hodge, Mary Beth Kaiser, Tony Keyes, Claus Leitherer, Matt McMaster, Melissa McGrath, Derck Massa, Sami Niemi, Cristina Oliveira, Rachel Osten, Charles Proffitt, David Sahnow, Ken Sembach, Brittany Shaw, Ed Smith, David Soderblom, Katya Verner, Nolan Walborn, Alan Welty, and Brian York. All of these individuals contributed to this volume, as did Russ Makidon.

The COS IDT includes James Green (Principal Investigator), Cynthia Froning (Project Scientist), Steven Penton, Steven Osterman (Instrument Scientist), Stéphane Béland, Eric Burgh, and Kevin France, all of whom provided information and assistance. COS co-investigators are Dennis Ebbets (Ball Aerospace), Sara R. Heap (GSFC), Claus Leitherer (STScI), Jeffrey Linsky (University of Colorado), Blair D. Savage (University of Wisconsin-Madison), Ken Sembach (STScI), J. Michael Shull (University of Colorado), Oswald Siegmund (University of California, Berkeley), Theodore P. Snow (University of Colorado), John Spencer (Southwest Research Institute), and John T. Stocke (University of Colorado). K. Brownsberger, J. Morse, and E. Wilkinson have also been part of the COS IDT and have made significant contributions.

The prime contractor for COS is Ball Aerospace, Boulder, Colorado. The XDL detector was built at UC Berkeley by O. Siegmund, J. McPhate, J. Vallerga, and B. Welsh.

The Editor thanks Susan Rose (Technical Editor) for her contributions to the production of this handbook.

References and Additional Information

This document relies heavily on information provided by the COS team in Boulder. The primary documents used are

Morse, J. 2004, Cosmic Origins Spectrograph Science Operations Requirements Document (referred to as OP-01).

Wilkinson, E. 2002, COS Calibration Requirements and Procedures, rev. B. (referred to as AV-03).

Wilkinson, E. 2008, COS Prelaunch Calibration Data (referred to as AV-04).

We also used the *STIS Instrument Handbook* (Kim Ouijano et al. 2007, v8.0).

CHAPTER 1:

Introduction

In this chapter…

1.1 Purpose of This Handbook

This *COS Instrument Handbook* describes the design, performance, operation, and calibration of COS. It is meant to be the principal reference manual for users of the Cosmic Origins Spectrograph. This handbook is written and maintained at STScI. We have attempted to incorporate the best available information, but because COS was only recently installed on *HST*, tabulated parameters are likely to evolve as we learn more about its on-orbit performance.

There are three occasions upon which a reader would consult this handbook:

- when preparing a Phase I proposal to observe with *HST*;
- when writing a Phase II program once a proposal has been accepted; or
- when analyzing data from observations that have already been made.

This handbook is not meant to be the primary reference for COS data reduction or analysis; that information is provided in the *COS Data Handbook*. For quick reference, information on COS data products is provided in Chapter 13.

1.2 Document Conventions

This document follows the usual STScI conventions:

- Terms, words, or phrases which are to be entered by the user in a literal way in an HST proposal are shown in a typewriter or Courier font, such as "`COS/FUV`" or "`TIME-TAG`."
- Names of software packages or commands (such as **calcos**) are shown in boldface.
- Wavelengths in this handbook and in COS data products are always as measured in vacuum and are quoted in Ångstroms (Å).

CHAPTER 2:

Special Considerations for Cycle 18

In this chapter…

2.1 SM4 and the Installation of COS

COS was installed during Servicing Mission 4 (SM4) in May of 2009. This document presents the results of calibration and testing during the subsequent Servicing Mission Observatory Verification (SMOV). Instrument parameters and reference files will continue to be refined throughout Cycle 17.

2.2 Observing Considerations

2.2.1 The COS GTO Program

The COS Investigation Definition Team (IDT) was responsible for the development, management, and scientific oversight of COS prior to launch. As Guaranteed Time Observers (GTOs), the COS IDT has 555 orbits of guaranteed observing time, primarily during Cycle 17, but continuing into Cycles 18 and 19. The members of the COS IDT are listed in the "Acknowledgments" section.

As GTOs, the COS IDT has been granted exclusive access to the targets they will observe for the science they proposed. The COS GTO target list may be found at

`http://www.stsci.edu/hst/proposing/docs/COS-GTO`

GTO target protection policy is more fully explained in the *HST Call for Proposals*.

2.2.2 Survey and SNAP Programs with COS

The COS photon-counting detectors can be harmed by exposure to bright light. Because all COS observations must be checked at STScI by an Instrument Scientist to confirm that both the intended target and all nearby objects lie within safe-brightness limits, the total number of targets accepted from all Survey and SNAP programs for COS and STIS/MAMA will not exceed 300 per cycle. For more information on this and other policies pertaining to *HST* observing, please see the *Call for Proposals*.

2.3 Should I Use COS or STIS?

With the installation of COS and the repair of STIS, *HST* has two spectrographs with significant overlap in spectral range and resolving power. Each has unique capabilities, and the decision of which to use will be driven by the science goals of the program and the nature of the target to be observed.

The primary design goal of COS is to improve the sensitivity of *HST* to point sources in the far-UV (from about 1100 to 1800 Å). In this wavelength range, the throughput of the COS FUV channel exceeds that of the STIS FUV MAMA by factors of 10 to 30, and the combination of the spectroscopic resolving power (~ 20,000) and wavelength coverage (300 to 370 Å per setting) of the medium-resolution COS FUV modes results in a discovery space (throughput times wavelength coverage) for observations of faint FUV point sources that is at least 10 times greater for most targets than that of STIS modes with comparable resolution, and is as much as 70 times greater for faint, background-limited point sources.

In the near-UV (approximately 1700 - 3200 Å), COS and STIS have complementary capabilities. To accommodate the NUV detector format, the COS NUV spectrum is split into three non-contiguous stripes, each of which covers a relatively small range in wavelength. Obtaining a full NUV spectrum of an object requires several set-ups and exposures (6 or more for the medium-resolution gratings and 4 for G230L). When broad NUV wavelength coverage is needed, there will be circumstances in which obtaining a single STIS spectrum is more efficient than taking separate COS spectra. Because the background count rate for COS/NUV is substantially lower than for STIS, COS will often be superior for faint sources, even when more exposures are required to span the full wavelength coverage.

In particular, STIS has significantly higher dark current in the NUV, with initial post-repair values as much as 10 times higher than pre-failure dark-current measurements. This excess dark current is slowly decreasing, but even if by the beginning of Cycle 18 the STIS NUV MAMA dark current has decreased to pre-repair levels, which averaged about 1.2×10^{-3} counts pixel^{-1} s^{-1}, it will still be 17 times higher than the COS NUV dark current of about 7×10^{-5} counts pixel^{-1} s^{-1}. Thus, observers are advised to perform detailed calculations using both the COS and STIS ETCs and to consider carefully the relative instrument overheads to determine which combination of instruments and modes is best for their science.

For observations of extended sources, the spatial resolution offered by STIS must be weighed against the superior sensitivity of COS. One of the primary design goals of STIS was to provide spatially-resolved spectra in the UV, optical, and near-IR. The STIS long slits, when used with the first-order gratings, allow spatially-resolved observations that exploit the intrinsically high resolution of *HST* over the full width of the detectors (approximately 0.05 arcsec per 2-pixel spatial resolution element over a length of 25 arcsec with the NUV and FUV MAMAs, and ~ 0.1 arcsec per 2-pixel spatial resolution element over a length of 52 arcsec with the CCD).

COS was optimized for point-source observations, at the expense of extended sources. While COS has relatively large entrance apertures (2.5 arcsec diameter), flux from regions more than 0.5 arcsec from the aperture center is significantly vignetted. These large apertures also mean that objects extended in the dispersion direction will yield spectra with lower spectral resolution. In addition, the optical design of the FUV channel limits the achievable spatial resolution, making it impossible to separate multiple point sources in the aperture unless they are separated by about 1 arcsec in the cross-dispersion direction. The COS NUV channel uses a different optical design and has a spatial resolution comparable to that of the STIS first-order NUV modes (~ 0.05 arcsec), with somewhat better sampling; however, for sources extending more than 1 arcsec in the spatial direction, the various NUV spectral segments will begin to overlap.

The line-spread functions (LSFs) of both instruments exhibit non-Gaussian wings due to mid-frequency zonal (polishing) errors in the Optical Telescope Assembly (OTA). Using STIS, one can minimize their effects through the use of narrow apertures. On COS, narrow apertures are not available. The broad wings of the COS LSF, especially in the short wavelengths of FUV band, can affect the detectability of faint, narrow features and blend closely-spaced lines. Studies that require accurate knowledge of the line profile will require full consideration of the COS LSF. The non-Gaussian wings of the COS LSF should have only modest impact on science programs targeting broad lines and continuum sources.

Both COS detectors and the STIS MAMA detectors are prohibited from observing objects that exceed specific brightness levels (see Chapter 9 in this handbook and Sections 13.8 and 14.8 of the *STIS Instrument Handbook*). Some brightness limits have been established for the health and safety of the instrument, while others are practical limits that are set to ensure good data quality. Because STIS is less sensitive than COS, the brightness limits for STIS tend to be significantly less stringent. In the NUV range, the STIS G230LB and G230MB gratings can also be used with the STIS CCD, which has no bright-object limitations. STIS also has a number of small and neutral-density apertures that can be used with the MAMA detectors to attenuate the light of a too-bright object. COS has only a single neutral-density filter that attenuates by a factor of about 200 but also degrades the spectral resolution by a factor of 3 to 5. In most cases, some combination of STIS gratings and apertures will be a better choice for observing a UV-bright object than COS with its neutral-density aperture. Users are advised to compare results from the COS and STIS ETCs to decide on an appropriate strategy for their target.

The STIS high-dispersion echelle modes E140H and E230H have resolving powers of ~114,000 (or even R ~ 200,000 with the `0.1x0.03` aperture and specialized data reduction; see Section 12.6, "Improving the Sampling of the Line Spread Function," of the *STIS Instrument Handbook*), significantly higher than the best COS resolution. Also, STIS can obtain spectra in the optical and near-IR at wavelengths up to 10,200 Å, while the maximum wavelength observable by COS is about 3,200 Å.

Both STIS and COS can perform observations in `TIME-TAG` mode, whereby the time of each photon's arrival is recorded. STIS is capable of a much finer time resolution (125 microseconds vs. 32 milliseconds for COS), although few programs require such a high sampling rate. Due to its lower sensitivity, STIS may be able to observe a target in `TIME-TAG` mode that is too bright for `TIME-TAG` observations with COS. On the other hand, `TIME-TAG` data acquired with the COS FUV detector includes information on the pulse-height distribution, while `TIME-TAG` data acquired with the STIS and COS MAMA do not. Pulse-height information can be valuable in identifying and rejecting background counts in the spectra of faint sources.

CHAPTER 3:

An Introduction to COS

In this chapter…

3.1 The Location of COS in the HST Focal Plane

The location of the COS aperture in the *HST* focal plane is shown in Figure 3.1. Note the relative orientation of the *HST* V_2 and V_3 axes (the V_1 axis is along *HST*'s optical axis), as well as the relative locations and orientations of the other instruments. The COS aperture lies ~ 325 arcsec from the V_1 axis in the $+V_2$, $-V_3$ quadrant. Complete information on the locations of all *HST* instruments may be found at:

`http://www.stsci.edu/hst/observatory/apertures/siaf.html`

3.2 The COS User Coordinate System

Figure 3.2 presents a schematic layout of the COS focal plane. In this figure, the *X* and *Y* axes denote the COS user coordinate system. In this system, `X` lies along the wavelength (dispersion) axis and increases with increasing wavelength for both the FUV and NUV channels. For the NUV channel, *Y* increases with increasing wavelength in the cross-dispersion direction. All references to COS (including POS TARG specifications in APT, detector pixel coordinates, and science header keywords) employ this coordinate system.

Figure 3.1: A Schematic View of the HST Focal Plane.

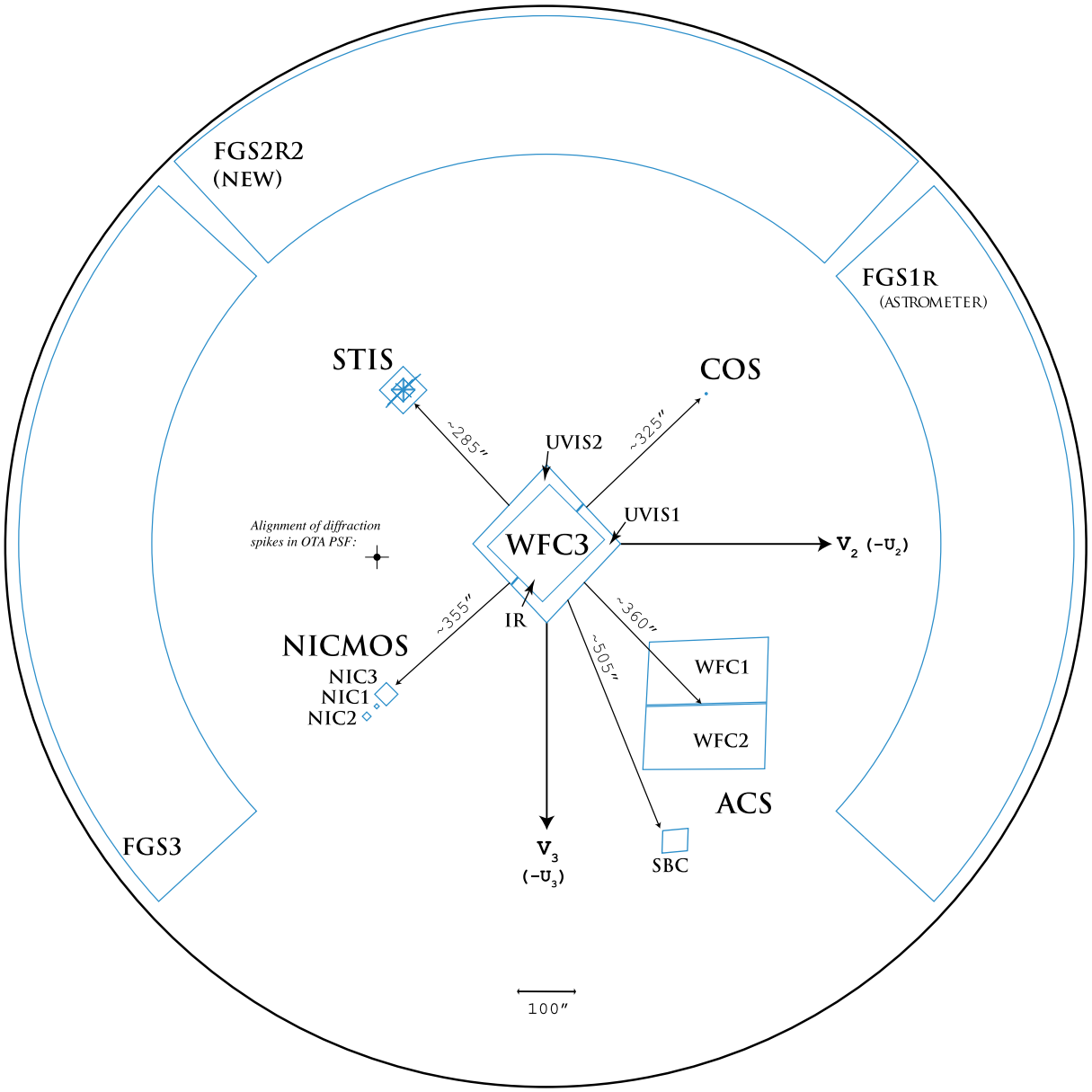

This drawing shows the entire *HST* focal plane and the apertures of the scientific instruments. The view is from the rear of the telescope looking forward toward the sky, the opposite of the sense of Figure 3.2.

Figure 3.2: Schematic Layout of the COS Detectors.

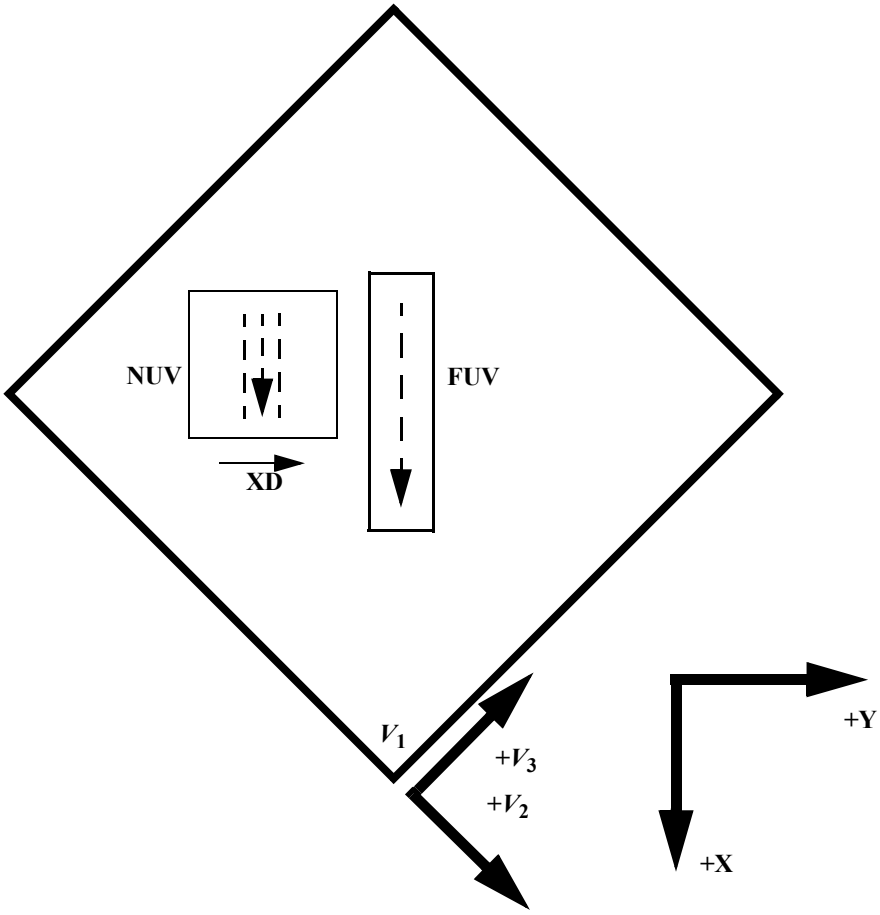

This view is from the front of the telescope looking aft. The dashed arrows show the direction of increasing wavelength for the two detectors, and "XD" indicates the direction of increasing wavelength for the NUV cross-dispersion direction. The X and Y axes denote the COS user coordinate system. For both the FUV and NUV channels, wavelength increases in the +X or ($+V_2$, $-V_3$) direction. Note that this diagram is purely schematic and it is intended to show only relative directions. This diagram does **not** show the locations of apertures. The bottom corner of this square (at V_1) corresponds to the center of the WF3 camera (see Figure 3.1).

3.3 The Optical Design of COS

In this section, the light from *HST* is followed as it progresses through COS to each optical element and mechanism. This path and its alternatives are shown schematically in Figure 3.3.

Figure 3.3: Schematic of the Light Flow Through COS.

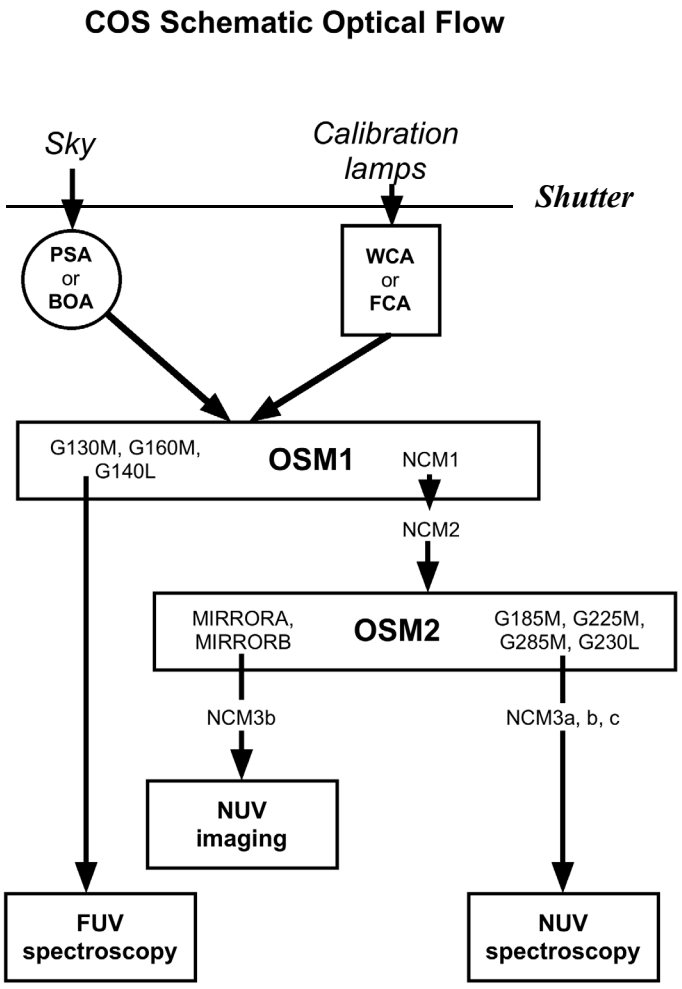

3.3.1 External Shutter

The external shutter is located at the front of the COS enclosure in the optical path before the aperture mechanism. When closed, the shutter blocks all external light from entering the COS instrument and prevents light from the COS internal lamps from exiting the instrument. The opening and closing of the external shutter does not define

the duration of an exposure, as the shutter may be opened before an exposure begins to allow for target acquisitions and bright-object checking. The external shutter will be closed autonomously by the COS flight software when an over-light condition is triggered by an external or internal source or when the *HST* take-data flag goes down, indicating loss of fine lock; see Section 9.5.

Table 3.1: COS Entrance Apertures.

Aperture	Full name	Purpose	Size (mm)
PSA	Primary Science Aperture	science aperture	0.700 circular
BOA	Bright Object Aperture	science aperture with ND2 filter	0.700 circular
WCA	Wavelength Calibration Aperture	wavecals with Pt-Ne lamp	0.020 × 0.100
FCA	Flat-Field Calibration Aperture	flat field with deuterium lamp	0.750 × 1.750

3.3.2 The Apertures and Aperture Mechanism

After passing through the external shutter, the light from *HST* first encounters one of the COS entrance apertures (Table 3.1), which are mounted on the Aperture Mechanism (ApM).

In most spectrographs, the light from the telescope is focused on a slit, and the instrument's optics then re-image the slit onto the detector. In such a design, the slit width and how the slit is illuminated determine the resolving power and line spread function (LSF). COS is different: it is essentially a slitless spectrograph with an extremely small field of view.

There are four apertures: two are used for science exposures and two for calibration. The two science apertures are the Primary Science Aperture (PSA) and the Bright Object Aperture (BOA). The two calibration apertures are the Wavelength Calibration Aperture (WCA) and the Flat-field Calibration Aperture (FCA). Selecting among these apertures can involve movement of the Aperture Mechanism.

Primary Science Aperture

The Primary Science Aperture (PSA) is a 2.5 arcsec (700 μm) diameter field stop located behind the *HST* focal surface near the point of the circle of least confusion. This aperture transmits ≥ 95% of the light from a well-centered, aberrated point-source image delivered by the *HST* optics. The PSA is expected to be used for observing in almost all instances. The PSA is in place, ready to use, at the start of a new visit. Note that, when the PSA is in place, the WCA (see below) is also in place and available for use.

Bright Object Aperture

The Bright Object Aperture (BOA) is also 2.5 arcsec (700 μm) in diameter, but has a neutral density (ND2) filter immediately behind it. The transmission of the BOA is

wavelength dependent, as shown in Figure 3.4. The BOA attenuates by about a factor of 200 at 2000 Å.

The BOA material has a slight wedge shape so that the front and back surfaces differ from one another by about 15 arcmin. This wedge is sufficient to degrade the spectroscopic resolution realized when the BOA is used. In fact, a secondary peak in the image is formed; see Section 8.4.2.

The BOA must be moved into place with the Aperture Mechanism to replace the PSA for science observations. Thus, science spectra obtained through either the PSA or BOA will use the same optical path and detector region (for a given channel), and so may employ the same flat-field calibrations. Moving the BOA into place for science use precludes simultaneous use of the WCA for a wavelength-calibration exposure, so an additional movement of the Aperture Mechanism is needed to obtain a wavecal when the BOA is used. For this reason, the BOA may not be used with TAGFLASH exposures (see Section 6.7).

The BOA is open to light from the sky when the PSA is used for science (and vice versa); bright-object screening for the field of view must therefore consider both apertures.

Figure 3.4: Measured Transmission of the COS BOA as a Function of Wavelength.

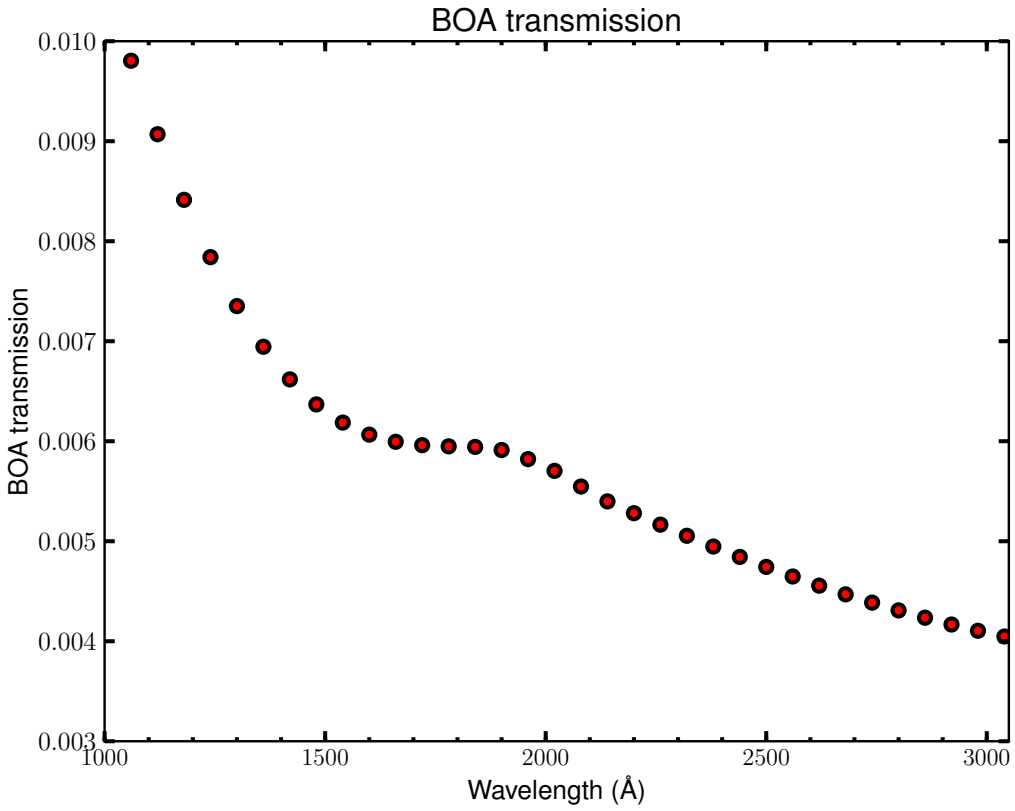

Wavelength Calibration Aperture

The Wavelength Calibration Aperture (WCA) is offset from the PSA by 2.5 mm (about 9 arcsec) in the cross-dispersion direction. Light from external sources cannot illuminate the detector through the WCA; instead the WCA is illuminated by one of two Pt-Ne wavelength calibration lamps. The wavelength calibration spectrum is used to assign wavelengths to the science spectra obtained through either the PSA or BOA. As noted above, both the PSA and WCA are available for use at the same time and no additional motion of the Aperture Mechanism is needed.

Flat-field Calibration Aperture

The Flat-field Calibration Aperture (FCA) is used only for calibration and is not available to observers. The FCA is used to obtain flat-field exposures using one of the two deuterium lamps.

Figure 3.5: The COS FUV Optical Path.

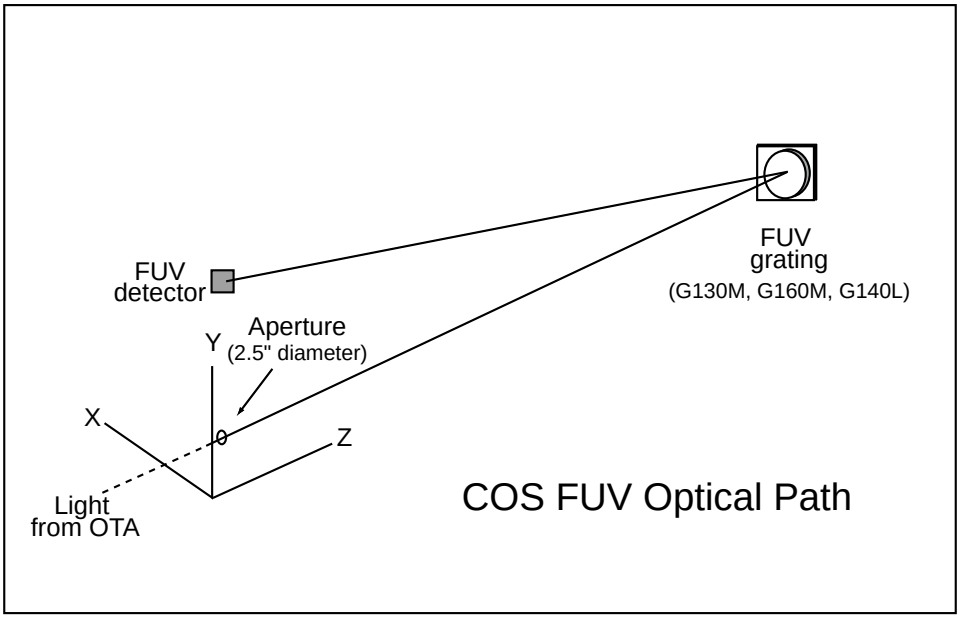

3.3.3 Gratings and Mirrors: The Optics Select Mechanisms

After passing through one of the COS apertures, light next encounters Optics Select Mechanism 1 (OSM1), a rotating mechanism that can bring one of four optical elements into the beam. These four optical elements are located at 90-degree intervals around OSM1. One of these, mirror NCM1, is a flat mirror that directs the beam to the NUV channel. The other three elements are gratings for the FUV channel.

FUV Channel Optical Design

The COS FUV optical path is illustrated schematically in Figure 3.5. The FUV channel of COS uses only a single optical element to image the sky onto the XDL detector (described in Chapter 4). Each of the three FUV gratings is holographically ruled to disperse the light and to focus it onto the detector. The gratings also have

optical surfaces configured to remove the spherical aberration produced by the HST primary mirror. Given the location of OSM1 in the *HST* optical path, it is possible for the FUV gratings to disperse, focus, and correct the beam optimally only for a point source that is centered in the aperture. Performance is degraded when the source is moved away from the aperture center; however, this degradation is low for displacements up to about 0.5 arcsec (see Section 8.3).

The COS FUV channel provides spectra from 900 to 2050 Å at low and moderate spectral resolution. (Its sensitivity at EUV wavelengths is under investigation.) The XDL detector is described fully in Chapter 4, but it is important to note that it consists of two independent segments with a small physical gap between them. The 14 to 18 Å of spectrum falling in the gap (with G130M or G160M grating) are not recorded. Though the gap prevents a single continuous spectrum from being obtained in one setting, the missing wavelengths can be recovered by shifting the grating, as described in Section 6.5. The gap can be made useful: in some configurations, the geocoronal Lyman-α line can be placed there, eliminating the local high count rates that this emission line can cause.

OSM2 and the NUV Channel

The COS NUV channel, illustrated schematically in Figure 3.6, provides coverage from about 1650 to 3200 Å at low and moderate spectral resolution. If the NUV channel is to be used, mirror NCM1 is placed into position on OSM1, directing the beam to mirror NCM2 -- which collimates the light -- and then to Optics Select Mechanism 2 (OSM2). OSM2 holds five optical elements: four plane diffraction gratings plus a mirror for target acquisitions or imaging. These five optical elements are located at 72-degree intervals around OSM2.

Dispersed light from the NUV gratings is imaged onto a MAMA detector by three parallel camera optics (NCM3a, b, c). For the medium-dispersion gratings, the spectra appear as three non-contiguous 35-40 Å stripes on the MAMA detector, allowing 105-120 Å wavelength coverage per exposure. The gratings can be shifted with slight rotations of OSM2 to cover the entire NUV wavelength band. The NCM3a,b,c mirrors are spaced such that several correctly-chosen exposures will produce a complete spectrum from the low end of the short-wavelength stripe to the high end of the long-wavelength stripe. The layout of the stripes is shown in Figure 4.4.

The low-dispersion grating, G230L, produces three stripes with ~ 400 Å coverage per stripe at a resolution of ~ 0.8 Å (R = 2100 to 3900). A first-order science spectrum from G230L over the full 1650-to-3200 Å region can be obtained in four separate exposures.

The plane mirror on OSM2 is designated as `MIRRORA` when used in direct specular reflection. `MIRRORB` refers to the arrangement in which OSM2 rotates the position of this mirror slightly so that the front surface of the order sorter filter on this mirror is used. This provides an attenuation factor of approximately 25 compared to `MIRRORA`. Because of the finite thickness of the order-sorting filter, `MIRRORB` produces an image with two peaks that may affect its use for imaging; see Section 8.4.2 for details. This doubled image is generally acceptable for acquisitions of bright targets.

Figure 3.6: The COS NUV Optical Path.

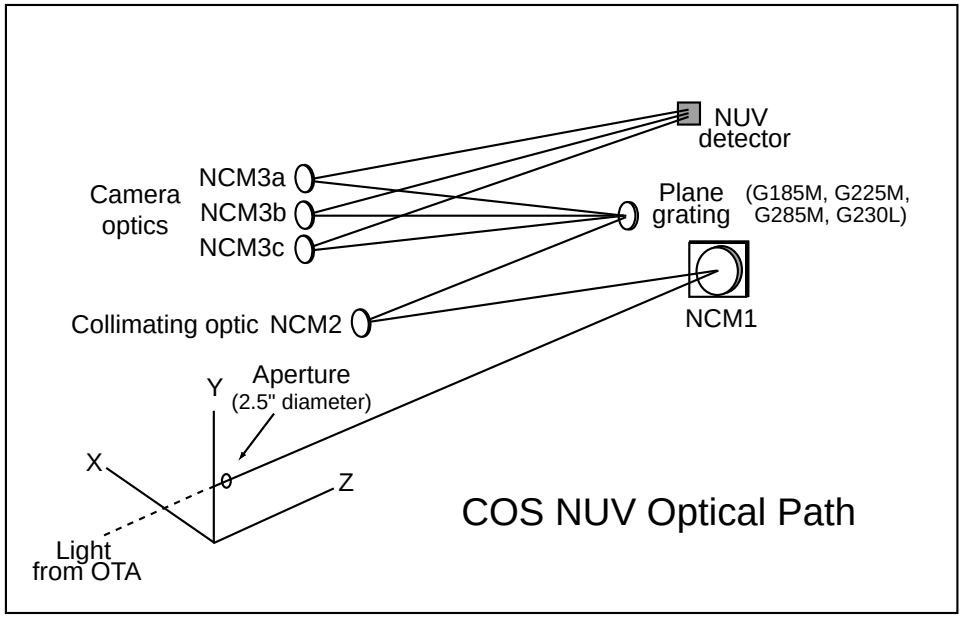

3.3.4 Detectors

The FUV and NUV channels employ separate detectors. The FUV detector is a photon-counting, cross delay line (XDL) device, similar to the *FUSE* detectors. Its two segments are separated by a small gap, as discussed above. The NUV detector is also a photon-counting device, a MAMA (multi-anode micro-channel array) similar to that used by STIS. The COS detectors are more fully described in Chapter 4.

3.3.5 On-board Calibration Lamps

Four calibration lamps are mounted on the calibration subsystem. Light is directed from the lamps to the aperture mechanism through a series of beam-splitters and fold mirrors.

Pt-Ne Wavelength Calibration Lamps

COS has two Pt-Ne hollow-cathode wavelength calibration lamps; their spectra are suitable for determining the wavelength scale of any spectroscopic mode. Either lamp may be used for wavelength-calibration exposures, but the choice is not user-selectable. We anticipate that one lamp will be used until it fails, when operations will be switched to the other.

The Pt-Ne lamps are used to obtain wavelength calibration ("wavecal") exposures. Light from the Pt-Ne lamp reaches the spectrograph through the WCA (wavelength calibration aperture). The WCA spectrum is displaced by ~ 2.5 mm from the target spectrum on the FUV detector. On the NUV detector, the corresponding WCA spectral stripe lies ~ 9.3 mm from the associated target stripe. For both FUV and NUV

channels, the COS optical design introduces a wavelength offset between the target and WCS spectra; this offset is compensated for during data reduction with **calcos**.

Note that the WCA and the PSA are available for use at the same time; this is what makes TAGFLASH mode possible. The Aperture Mechanism must be moved to bring the BOA into position, making it impossible to use TAGFLASH mode with the BOA; see Section 6.7.

The Pt-Ne lamps are also used during acquisitions to provide a reference point that will define the relationship between a known location at the aperture plane and the detector pixel coordinates in which the measurements are made.

Deuterium Flat-field Calibration Lamps

COS has two deuterium hollow-cathode flat-field calibration lamps. The deuterium lamps may also be used interchangeably. Use of these lamps for flat-field calibrations is restricted to observatory calibration programs. The light from these lamps enters the spectrograph through the FCA (flat-field calibration aperture).

3.4 Size of a Resolution Element

Throughout this document, we assume that a resolution element (resel) spans 6 × 10 pixels on the FUV detector and 3 × 3 pixels on the NUV detector (Table 3.2). These values were determined before launch; even then, it was known that the true size of a resel would vary with wavelength. Preliminary analysis of in-flight data suggest that the FUV resel is somewhat larger than previously assumed (see the discussion of the line-spread function in Chapter 5), while the NUV resel is smaller. We will continue to refine our analysis of the instrument parameters throughout Cycle 17. In the mean time, keep in mind that the COS Exposure Time Calculator uses the pre-flight resel sizes in all of its calculations. Users who adopt a larger or smaller resel should adjust the ETC results accordingly.

3.5 Basic Instrument Operations

3.5.1 Target Acquisitions

The COS entrance apertures are 2.5 arcsec in diameter. To ensure that the target is centered in the aperture, a target acquisition procedure must be performed at the beginning of each visit.

The COS flight software provides two methods for acquiring and centering a target in the aperture. The first method obtains a direct image of the aperture with the NUV channel and moves the telescope to the center of light. The second method centers the target using its dispersed spectrum and can be performed with either the NUV or FUV detector. For both methods, a target's center of light can be computed from a single exposure or from a series of exposures that map out a grid on the sky. Acquisitions are described in Chapter 8.

3.5.2 Observing Modes: TIME-TAG and ACCUM

COS provides two spectral observing modes, TIME-TAG and ACCUM. In TIME-TAG mode, the position, arrival time, and pulse height of each detected photon are recorded in the memory buffer. In ACCUM mode, only the location of arriving photons is recorded.

TIME-TAG mode is preferred, because it allows for more sophisticated data reduction. For example, an observer may compare data from the night and day sides of the orbit or compute the count rate of an object whose intensity varies on short time scales. TIME-TAG observations through the PSA allow the taking of occasional wavelength-calibration spectra during the course of a long exposure. These spectra are used by **calcos** to correct drifts in the spectrum due to small motions of the optics selection mechanism. ACCUM mode is designed for observations of targets too bright for TIME-TAG mode. Because the lower information content of ACCUM data reduces their utility for archival researchers, its use must be justified for each target.

Both TIME-TAG and ACCUM modes may be used with either the FUV or NUV channel. For more information comparing TIME-TAG and ACCUM, see Section 6.2.

3.5.3 Wavelength Calibration

COS is most efficiently used in TIME-TAG mode with FLASH=YES (the so-called "TAGFLASH" mode), in which science and wavelength-calibration spectra are obtained concurrently. Pt-Ne lamps provide the wavelength-calibration spectra, and the reduction to wavelength is performed automatically by **calcos**. ACCUM mode is required for brighter objects; in this mode, wavecals are also obtained automatically, but as separate images. It is possible to suppress the taking of wavelength-calibration spectra, but doing so significantly lessens the archival quality of COS data and must be justified on a case-by-case basis.

3.5.4 Typical Observing Sequences

In the majority of cases, the following sequence of events will produce high-quality data:

- Acquire the object using `ACQ/SEARCH`, followed by `ACQ/IMAGE`. This should take about ten minutes (see the examples in Chapter 10).
- Obtain spectra in `TIME-TAG` mode with `FLASH=YES` so the spectra can be corrected for any drifts. The COS Exposure Time Calculator (ETC) provides a means of calculating essential parameters such as `BUFFER-TIME`.
- Obtain more spectra during additional orbits to achieve the desired signal-to-noise.

3.6 COS Illustrated

Figure 3.7: The various subassemblies of COS and how they fit in its enclosure.

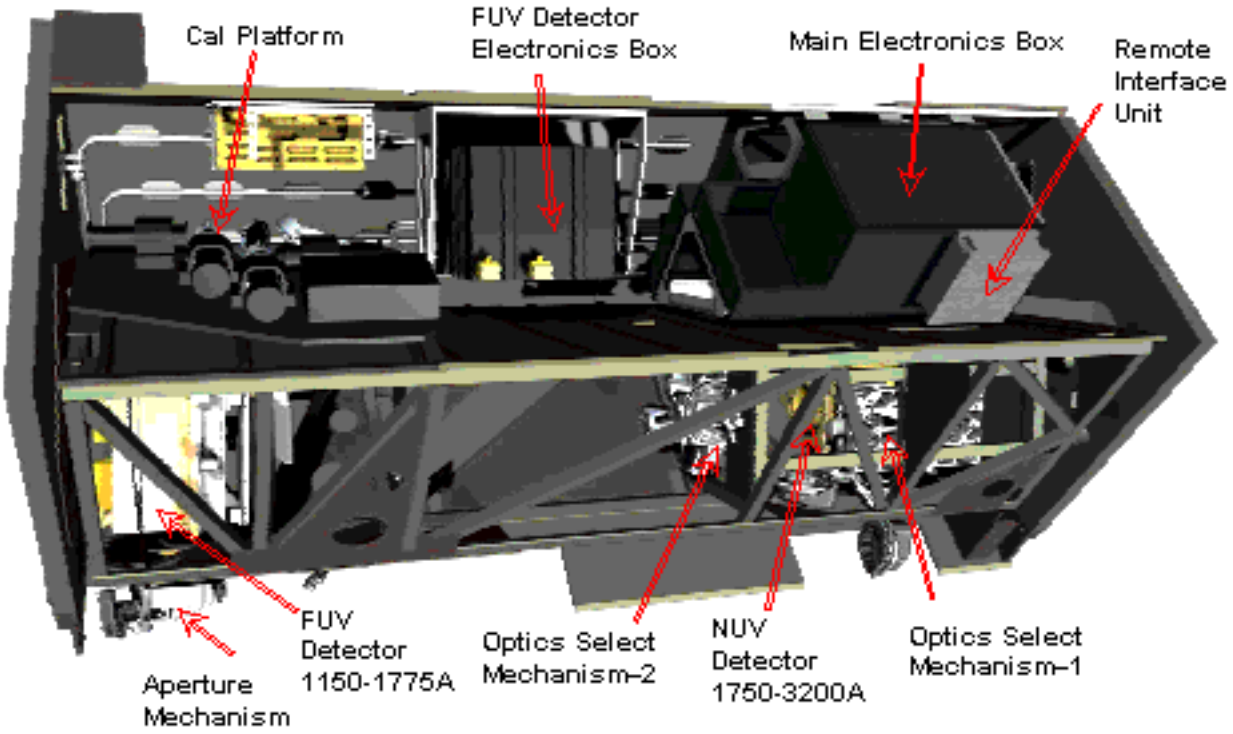

(CAD drawing courtesy of Ball Aerospace.)

Figure 3.8: The COS optical path and the locations of the mechanisms.

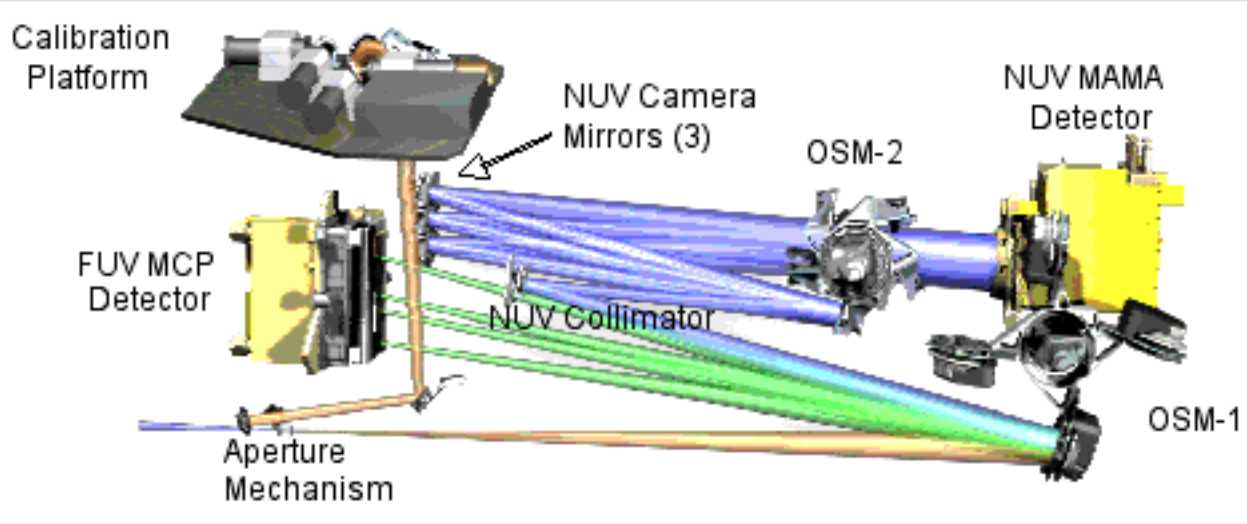

(CAD drawing courtesy of HSTP at GSFC.)

Figure 3.9: The COS flight instrument in its test stand at Ball Aerospace.

(Image courtesy of Ball Aerospace.)

3.7 COS Quick Reference Guide

Table 3.2: COS Instrument Characteristics

Property	FUV channel	NUV channel
Entrance aperture	2.5 arcsec round: clear (PSA) or attenuated (BOA)	
Detector plate scale (cross dispersion)	0.1 arcsec per pixel 1 arcsec per resel	24.3 mas per pixel 70.5 mas per resel

Table 3.3: COS Detector Characteristics

		FUV XDL	NUV MAMA
Photocathode		CsI (opaque)	Cs_2Te (semi-transparent)
Window		None	MgF_2 (re-entrant)
Wavelength range		< 900 – 2050 Å	1650 – 3200 Å
Active area		85 × 10 mm (two)	25.6 × 25.6 mm
Pixel format (full detector)		16384 × 1024 (two)	1024 × 1024
Image size recorded per spectrum		16384 × 128 (two, `ACCUM`) 16384 × 1024 (two, `TIME-TAG`)	1024 × 1024
Pixel size		6 × 24 μm	25 × 25 μm
Spectral resolution element size (= resel)		6 × 10 pix	3 × 3 pix
Quantum efficiency		~26% at 1335 Å ~12% at 1560 Å	~10% at 2200 Å ~8% at 2800 Å
Typical dark-count rate (away from SAA)		1.5 cnt s^{-1} cm^{-2} 2.2×10^{-6} cnt s^{-1} pix^{-1} 6.5×10^{-5} cnt s^{-1} $resel^{-1}$	11 cnt s^{-1} cm^{-2} 6.9×10^{-5} cnt s^{-1} pix^{-1} 6.2×10^{-4} cnt s^{-1} $resel^{-1}$
Detector global count rate limit	TIME-TAG mode	30,000 cnt s^{-1} (but counts lost at rates above ~21,000 cnt s^{-1})	
	ACCUM mode	~60,000 cnt s^{-1} per segment	~170,000 cnt s^{-1}
Local count rate limit		~100 cnt s^{-1} $resel^{-1}$ ~1.67 cnt s^{-1} pix^{-1}	~1800 cnt s^{-1} $resel^{-1}$ ~200 cnt s^{-1} pix^{-1}
Screening limits for bright objects		see Table 9.1	
Dead-time constant		7.4 μsec	280 nsec

Table 3.4: COS Calibration Accuracies

Property	FUV channel	NUV channel
Wavelength zero point: M gratings	15 km s^{-1}	15 km s^{-1}
Wavelength zero point: L gratings	150 km s^{-1}	175 km s^{-1}
Wavelength scale	15 km s^{-1}	15 km s^{-1}
Absolute photometry	5%	5%
Relative photometry (same object at a different time)	2%	2%
Flat field quality per resel, measured	30:1	100:1
Flat field quality per resel, goal	100:1	100:1

Table 3.5: Useful Figures and Tables

Topic	Source	Content
Usage planning	Table 6.1	COS grating parameters
	Table 6.4	FUV grating wavelength ranges
	Table 6.5	NUV grating wavelength ranges
	Table 9.1	COS count-rate screening limits
	Table 11.2	Earthshine and zodiacal light fluxes
	Table 11.3	Strengths of airglow lines
Aperture parameters and PSFs	Figure 3.1	*HST* focal plane and COS aperture
	Figure 3.4	BOA transmission
	Figure 5.1	Model LSFs for the COS FUV Channel
	Figure 5.2	Detector LSFs for the COS NUV Channel
	Figure 7.3	Two-dimensional COS imaging PSF
	Figure 7.4	Cross section of the COS imaging PSF
	Figure 8.1	Relative transmission of the COS PSA in the FUV
	Figure 8.2	Relative transmission of the COS PSA in the NUV
Effective Area	Figure 6.1	FUV spectroscopy
	Figure 6.2	NUV spectroscopy
	Figure 7.1	NUV imaging

Topic	Source	Content
Acquisitions	Figure 8.3	ACQ/IMAGE exposure times
	Figure 8.4	Cross section of image using MIRRORB
	Figure 8.5	NUV image of point source observed with BOA
	Figure 8.6	Point source observed with BOA and MIRRORB
	Figure 8.7	Example of 3 × 3 spiral search pattern
	Figure 8.8	Acquisition exposure times for FUV dispersed light
Detector characteristics	Figure 4.1	FUV XDL detector schematic layout
	Figure 4.4	NUV MAMA detector layout
	Table 11.1	Detector dark count rates
Overheads and observing parameters	Table 6.3	TAGFLASH exposure durations
	Table 10.1	Generic observatory overhead times
	Table 10.2	Overhead times for OSM1 movements
	Table 10.3	Overhead times for OSM2 movements
	Table 10.4	Science exposure overhead times
Celestial backgrounds	Figure 11.1	Sky background versus wavelength
	Figure 11.2	Moon and Earth background levels
	Figure 11.3	Galactic extinction model
Data quality	Figure 6.7	FUV flat-field example
	Figure 6.8	NUV flat-field example

CHAPTER 4:

Detector Description and Performance

In this chapter…

4.1 The FUV XDL Detector

4.1.1 XDL Properties

The COS FUV detector is a windowless cross delay line (XDL) device that is similar to the detectors used on the *Far Ultraviolet Spectroscopic Explorer (FUSE)*. The XDL is a photon-counting micro-channel plate (MCP) detector with two independently-operable segments. Each segment has an active area of 85 × 10 mm; they are placed end to end and separated by a 9-mm gap. When the locations of detected photons are digitized, they are placed into an array of 16384 × 1024 pixels, though the active area of the detector is considerably smaller. The long dimension of the array is in the direction of dispersion; increasing pixel number (the detector's *x* axis) corresponds to increasing wavelength. The XDL is shown schematically in Figure 4.1.

The FUV XDL is optimized for the 1150 to 1775 Å bandpass, with a cesium iodide photocathode on the front MCP. The front surface of the XDL is curved with a radius of 826 mm to match the curvature of the focal plane. When photons strike the photocathode, they produce photoelectrons that are amplified by a stack of micro-channel plates (MCPs). The charge cloud that comes out of the MCP stack, several millimeters in diameter, lands on the delay line anode. There is one anode for each detector segment, and each anode has separate traces for the dispersion (*x*) and cross-dispersion (*y*) axes. The location of an event in each axis is determined by measuring the relative arrival times of the collected charge pulse at each end of the

anode delay line for that axis. The results of this analog measurement are digitized to 14 bits in *x* and 10 bits in *y*. The total charge collected (the pulse height) is also saved (5 bits in TIME-TAG mode).

Figure 4.1: The FUV XDL Detector.

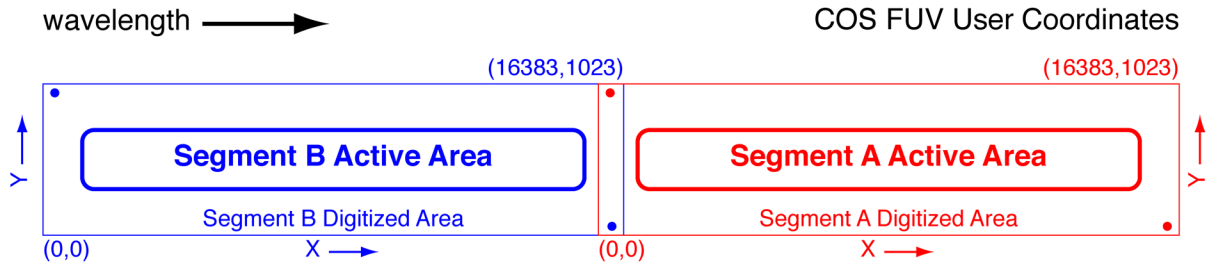

This diagram is drawn to scale, and the slight curvature at the corners is also present on the masks of the flight detectors. Wavelength increases in the direction of the increasing X coordinate. The red and blue dots show the approximate locations of the stim pulses. The numbers in parentheses show the pixel coordinates at the corner of the segment's digitized area; the two digitized areas overlap in the region of the inter-segment gap.

The detector electronics also generate pulses that emulate counts located near the edges of the anode, beyond the illuminated regions of the detector. These "stim pulses" (see Section 4.1.5) provide a means of tracking and correcting thermal distortions.

The XDL's quantum efficiency is improved by the presence of a series of wires, called the quantum-efficiency (DQE) grid, placed above the detector (i.e., in the light path). These wires create shadows in the spectrum that are removed during data reduction. The XDL also includes an ion-repeller grid that reduces the background rate by preventing low-energy thermal ions from entering the open-faced detector. They act as a 95% transmission neutral-density filter.

4.1.2 XDL Spectrum Response

COS is considerably more sensitive than STIS and earlier-generation *HST* instruments at comparable spectral resolutions in the far-UV. Effective area for the COS FUV gratings are shown in Figure 6.1.

4.1.3 XDL Background Rate

The XDL detectors have extremely low dark rates, below 10^{-6} per pixel per second; see Section 11.4.1.

Figure 4.2: Example of a COS FUV Spectrum.

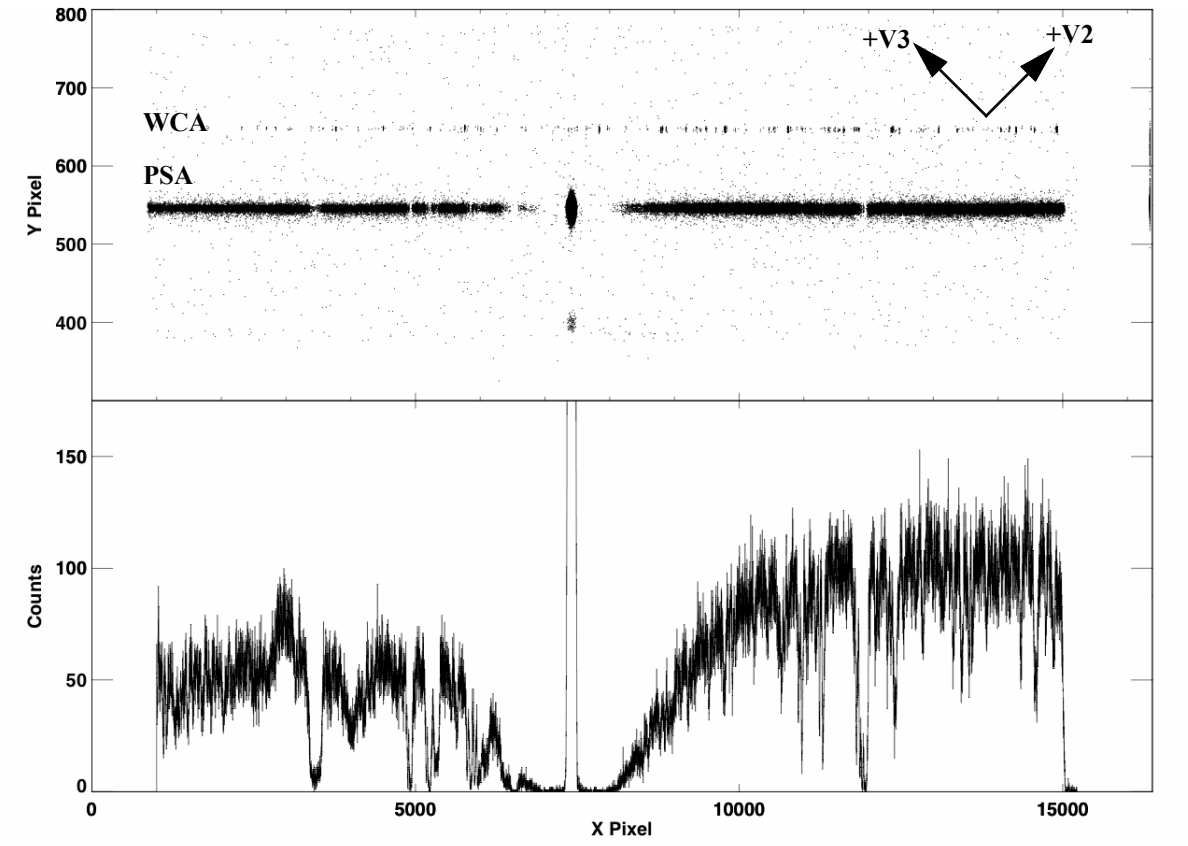

Upper panel: A stellar spectrum obtained with segment B of the COS FUV detector using the G130M grating at a central wavelength of 1309 Å. The wavelength calibration (WCA) spectrum is on top, and the stellar spectrum is below (PSA). The *HST* $+V_2$ and $+V_3$ axes are overplotted. Note the size of the active area compared to the overall digitized area (16384 ´ 1024). Lower panel: the extracted stellar spectrum. The bright emission feature is Lyman α; it is visible though both the PSA and the BOA (near y = 400).

4.1.4 XDL Read-out Format

The FUV channel creates two spectral stripes on each detector segment, one for the science spectrum and one for the wavelength-calibration spectrum. Figure 4.2 shows an example of an FUV spectrum obtained on orbit with segment B. The upper panel shows the two-dimensional image; the lower panel shows the extracted PSA spectrum. Note the difference in the *x* and *y* axis scales.

Although the gap between the two FUV detector segments prevents the recording of an uninterrupted spectrum, it also makes it possible to position spectra such that bright airglow features – Lyman α, in particular, when the G140L grating is used – fall in the gap. Such features could trigger excessive count rates in the detector. For suggestions on spanning the gap, see Section 6.5.

4.1.5 Stim Pulses

The signals from the XDL anodes are processed by Time-to-Digital converters (TDCs). Each TDC contains a circuit that produces two alternating, periodic, negative polarity pulses that are capacitively coupled to both ends of the delay line anode. These stim pulses emulate counts located near the edges of the anode, beyond the illuminated portions of the detector. Their nominal locations in (x, y) coordinates are (383, 33) and (15994, 984). Stim pulses are primarily used as a means to correct the temperature-dependent shift and stretch of the image during an exposure, and they provide a first-order check on the dead-time correction. They are recorded in both `TIME-TAG` and `ACCUM` modes. Both the detector electronics and the **calcos** pipeline treat the stim-pulse and photon events identically.

Four stim-pulse rates are available: 0 (i.e., off), 2, 30, and 2000 Hz per segment. These rates, which are only approximate, are **not** user selectable. Exposures longer than 100 sec will use the 2 Hz rate, those between 10 and 100 sec will use 30 Hz, and those shorter than 10 seconds will use 2000 Hz.

4.1.6 Pulse-height Distributions

The XDL detector generates pulse-heights along with the science data. The pulse-height distribution (PHD) is a histogram of the pulse heights for all events detected during an integration. The distribution of the pulse heights of photon events is peaked at the average gain of the MCPs with a width determined by MCP characteristics. Background events, both internal and cosmic-ray-induced, tend to have a falling exponential distribution in pulse height, with most events being at very low pulse heights. On-board charge threshold discriminators are used to filter out very large and small pulses to improve the signal-to-noise ratio. For the FUV XDL in `TIME-TAG` mode, the pulse height is recorded with each detected photon event and is used by **calcos** for data reduction. For the FUV XDL in `ACCUM` mode, only the integrated pulse-height distribution is recorded.

4.1.7 Non-linear Photon Counting Effects (Dead-time Correction)

The electronics that control the COS detectors have a finite response time t, called the dead time, which limits the rate at which photon events can be processed. If two photons arrive within time t, the second photon will not be processed. For the FUV channel, three factors limit the detected count rate. The first is the Fast Event Counter (FEC) for each segment, which has a dead time of 300 nsec. The FEC dead time matters only at count rates well above what is usable, introducing a 1% error at a count rate of 33,500 per segment per second.

The second factor is the time required to digitize a detected event. For a given true count rate C, the detected count rate D is:

$$D = \frac{C}{1 + C \cdot t}$$

where t is the dead-time constant. For the FUV XDL detector, t = 7.4 μsec, so the apparent count rate deviates from the true count rate by 1% when C = 1,350 counts sec^{-1} and by 10% when C = 15,000 counts sec^{-1}. Note that when the effect is near the 10% level, then the FUV detector is near its global count rate limit (see Table 9.1), so non-linear effects are effectively small.

Finally, the count streams for the two separate FUV segments must be combined in a single "round robin" Detector Interface Board (DIB) that takes signals from both the A and B segments and stores them in a single data buffer. The DIB interrogates the A and B segments alternately; because of this, a count rate that is high in one segment but not the other could cause a loss of data from both segments. The DIB is limited to processing about 250,000 events sec^{-1} in ACCUM mode and only 30,000 counts sec^{-1} in `TIME-TAG` mode (the highest rate allowed for `TIME-TAG` mode). Tests have shown that the DIB is lossless up to a combined rate for both segments of 20,000 sec^{-1}, and the loss is 100 sec^{-1} at a rate of 40,000 sec^{-1}. Thus this effect is less than 0.3% at the highest allowable rates. Furthermore, information in the engineering data characterizes this effect.

While dead-time corrections are automatically made in the **calcos** pipeline, they are not (at present) included in the ETC, which will over-predict count rates for bright targets.

4.1.8 Structures in the Dark Images

Deep FUV detector dark images show that the dark rate varies as a function of position on the detector and proximity to the South Atlantic Anomaly (SAA). Figure 4.3 shows the sum of a large number of dark exposures for both segments. While segment A appears relatively featureless, segment B exhibits several regions with higher count rates. In most cases, these features will have a negligible effect on the extracted spectra, since they are quite faint, only a few times the typical background rate of about 10^{-6} counts s^{-1} $pixel^{-1}$. In `TIME-TAG` mode, these features can be nearly eliminated by pulse-height filtering when the data are processed. They cannot be removed from `ACCUM` mode exposures, for which pulse-height information is not available. Since `ACCUM` mode is used only for bright targets, these features should constitute a negligible fraction of the total counts.

Figure 4.3: FUV Detector Dark Features.

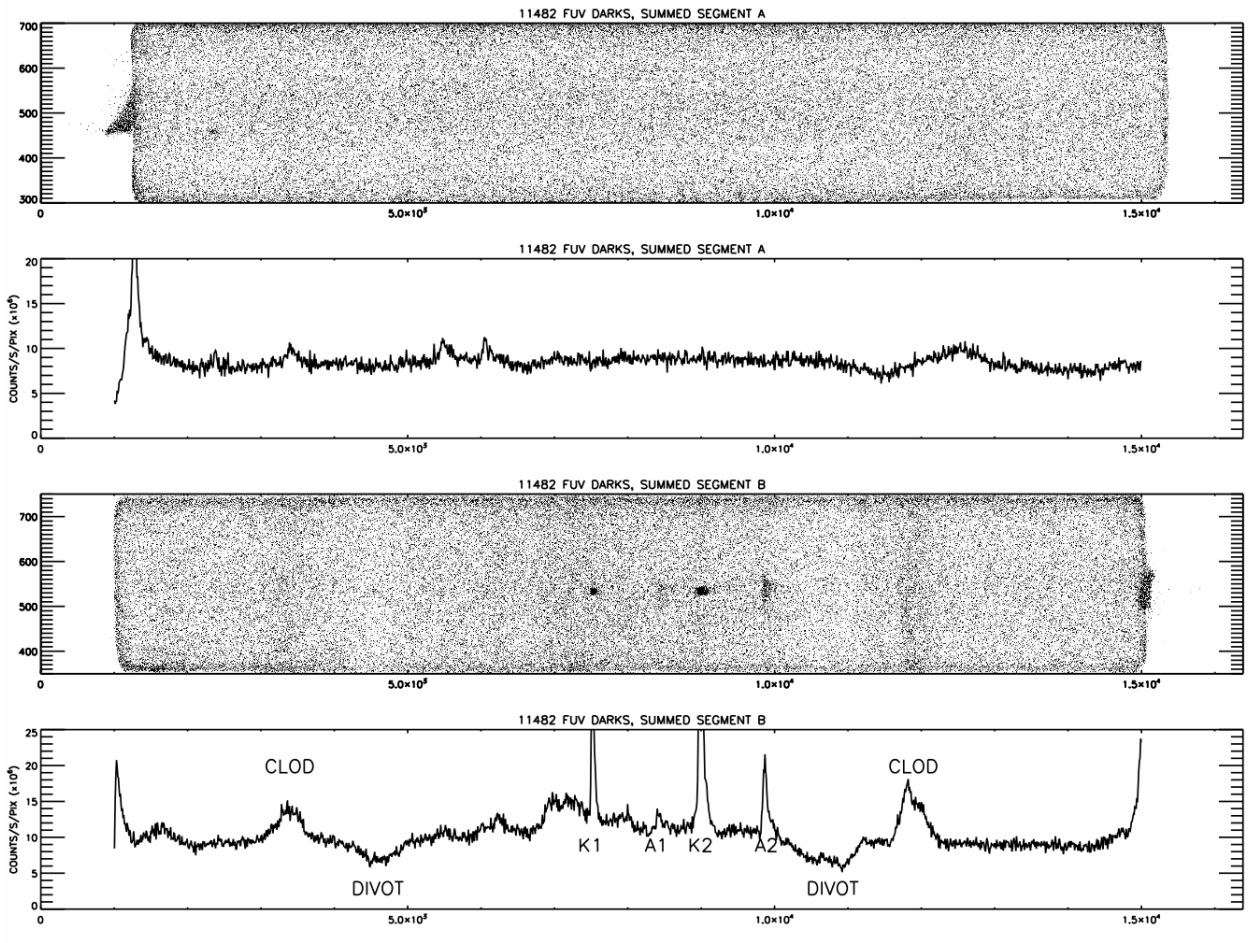

Summed raw dark frames from program 11482. Each segment is displayed as an image and as a projection onto the *x* axis (units are counts s^{-1} $pixel^{-1} \times 10^6$). No pulse-height screening is employed. While segment A appears relatively featureless, segment B shows four pseudo-emission lines, known as arcs and knots (and labeled A and K, respectively), as well as a pair of divot/clod features, which result when their large pulse heights cause photons to be mis-registered.

4.1.9 Detector Lifetime Sensitivity Adjustments

The FUV XDL MCPs are subject to gradual gain degradation, due to charge extraction over their lifetimes, that may reduce their effective sensitivity. The effect is small, but can be important in a localized region where the lifetime fluence is high, e.g., where a strong spectral feature such as geocoronal Lyman α falls on the detector.

The requirement for COS is to have no more than 1% loss in quantum efficiency after 10^9 events mm^{-2} have been collected. Estimates of planned COS usage show that the total number of events detected in the FUV channel over a seven-year mission would be a few times this value. The net effect is thus likely to be negligible, but nevertheless STScI will monitor any degradation of the XDL detector. There is a provision to move the spectrum in the cross-dispersion direction onto a previously-unused portion of the detector by offsetting the aperture mechanism. This can be done up to four times.

4.2 The NUV MAMA Detector

4.2.1 MAMA Properties

The COS NUV detector is a Multi-Anode Micro-channel Array (MAMA) that is essentially identical to that used for the NUV in STIS. (It is, in fact, the STIS NUV flight spare.) The COS MAMA has a semi-transparent cesium telluride photocathode on a magnesium fluoride window and is sensitive to photons with wavelengths from 1150 to 3200 Å.

The NUV optics focus light through the MgF_2 window onto the Cs_2Te photocathode. A photoelectron generated by the photocathode then falls onto a curved-channel micro-channel plate (MCP), which generates a cloud of electrons. The active area of the coded anode array is 25.6 mm square and is divided into 1024 × 1024 pixels on 25 μm centers. The window is stepped inwards, allowing the photocathode to protrude into the tube body to within 0.25 mm of the MCP. At this spacing and with a photocathode-to-MCP gap potential of 800 volts, the spatial resolution at 2500 Å is 35 μm FWHM.

4.2.2 MAMA Spectrum Response

The inherent spectral response of the COS NUV MAMA is essentially identical to that of the STIS NUV MAMA. However, the overall optical train of COS differs from STIS, so the COS throughputs are different (Figure 6.2).

4.2.3 MAMA Background Rate

COS NUV dark current is about 7×10^{-5} counts pixel^{-1} s^{-1}; see Section 11.4.1.

Figure 4.4: Example of a COS NUV Spectrum.

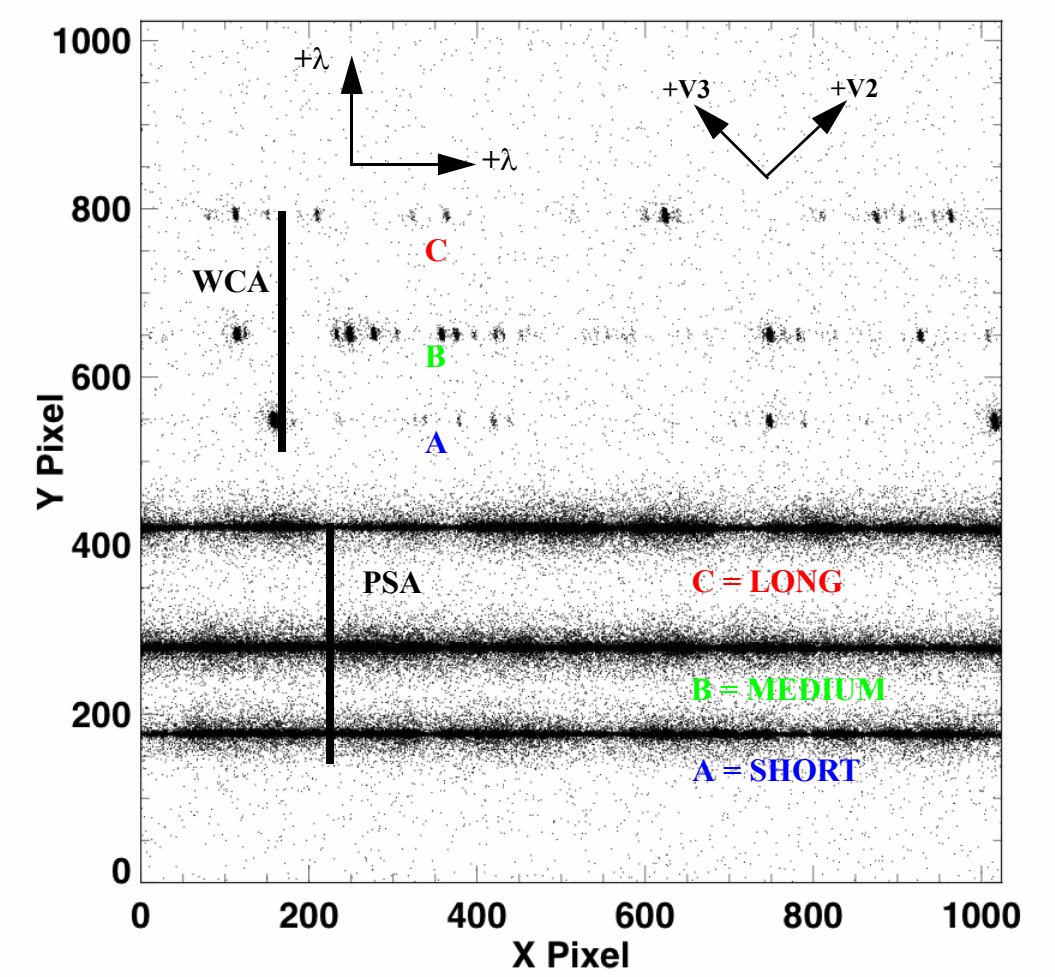

A COS NUV spectrum obtained in time-tag mode with `FLASH=YES`. The stellar spectrum is on the bottom and the wavelength calibration spectrum on the top; each has three stripes. From bottom to top, these stripes are designated A, B, and C as illustrated. Wavelength increases to the right and toward the top of the chip. The *HST* $+V_2$ and $+V_3$ axes are also shown. The SHORT, MEDIUM, and LONG designations are used in Phase II with the ACQ/PEAKXD command and the STRIPE Optional Parameter.

4.2.4 MAMA Read-out Format

The NUV channel creates six spectral stripes on the MAMA detector, three for the science data and three for the wavelength-calibration data. Stripes are separated by 2.80 mm (center-to-center) in the cross-dispersion direction, and there is a gap of 3.70 mm between the reddest science stripe and the bluest calibration stripe. The NUV detector is read out as a 1024 × 1024 array, but in all other respects the data are handled in the same way as for the FUV detector. As noted, no pulse-height information is provided for MAMA data. An NUV spectrum obtained in `TAGFLASH` mode is shown in Figure 4.4.

4.2.5 MAMA Dead-time Correction

The dead time for the COS NUV MAMA is 280 nsec, the same as for the STIS NUV MAMA. The 1% level of non-linearity is reached for $C = 36{,}000$ counts sec^{-1}.

CHAPTER 5:

The COS Line-Spread Function

In this chapter…

5.1 Mid-Frequency Wavefront Errors

Preliminary analysis of SMOV data suggests that the COS on-orbit spectroscopic line spread function (LSF) differs from that observed during pre-launch ground testing. While the COS optics successfully correct for the spherical aberration of the *HST* primary mirror, mid-frequency wavefront errors (WFEs) due to zonal (polishing) errors in the *HST* primary and secondary mirrors result in an LSF with extended wings and a core that is slightly broader and less deep than expected. These extended wings limit the detectability of faint, narrow spectral features. The effect is larger at shorter wavelengths, and it may have consequences for some COS FUV science. The most severely impacted programs are likely to be those that

- rely on models of the shapes of unresolved lines;
- search for very weak lines;
- need to measure line strengths in complex spectra with overlapping or nearly overlapping lines; or
- require precise estimates of residual intensity in very strong lines.

Figure 5.1: Model Line-Spread Functions for the COS FUV Channel

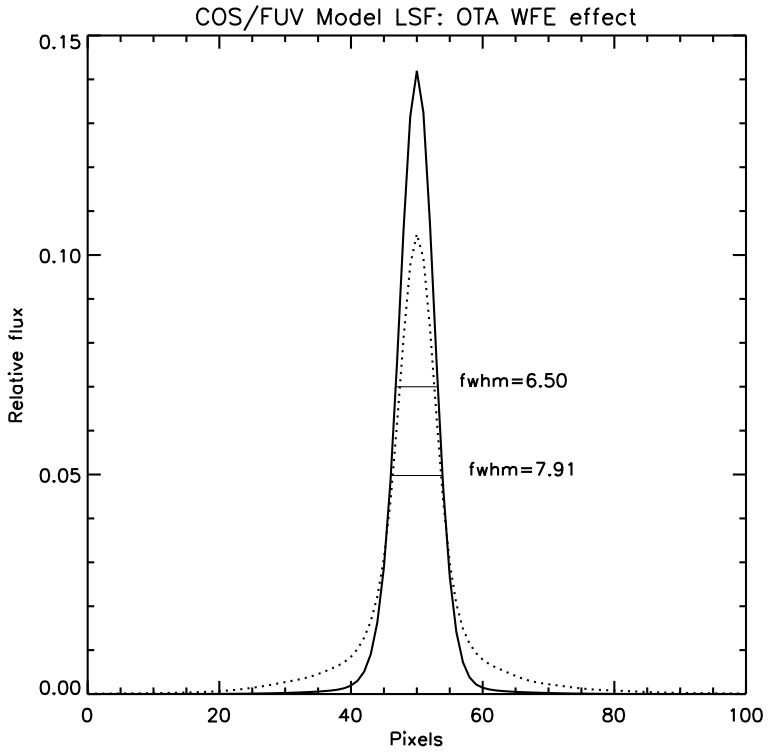

Model LSFs for G130M at 1309 Å, normalized to a sum of unity. The solid line represents a model LSF that incorporates the spherical aberration of the OTA; it is well-fit by a Gaussian with FWHM = 6.5 pixels. The dotted line represents a model that also includes the HST mid-frequency wave-front errors. It shows a larger FWHM and broad, non-Gaussian wings.

Figure 5.1 shows two model line-spread functions computed for grating G130M at 1309 Å. The solid line represents a model LSF incorporating the spherical aberration of the *HST* Optical Telescope Assembly (OTA); it is well-fit by a Gaussian with FWHM = 6.5 pixels. The dotted line represents a model that also includes the mid-frequency WFEs. Its FWHM is 7.9 pixels, slightly larger than that of the solid curve, and its broad wings could complicate the detection of nearby narrow features.

5.2 First Results

Initial results from an analysis of the on-orbit COS LSF are reported by Ghavamian et al. (2009) in COS Instrument Science Report 2009-01. They find that model LSFs incorporating *HST* mid-frequency WFEs are required to reproduce the absorption features observed in stellar spectra obtained with COS. Plots of these model LSFs are presented in Chapter 15, and tabular versions are available on the COS Web site. Additional information will be posted to the COS home page as it becomes available.

Figure 5.2: Detector LSFs for the NUV MAMA

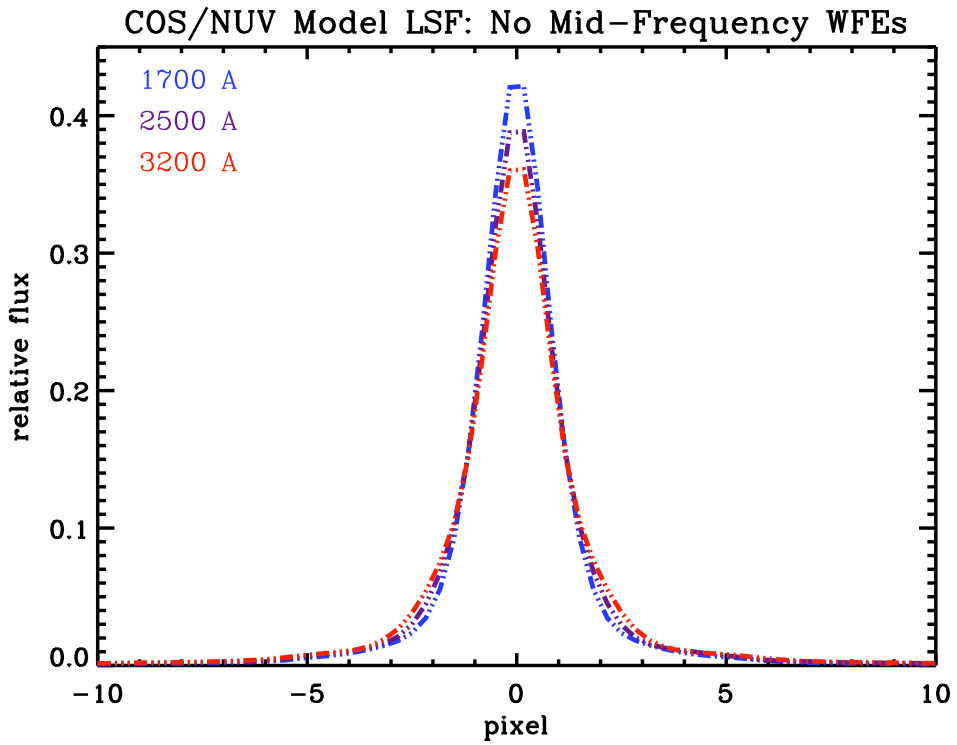

5.3 Non-Gaussian Wings in the MAMA PSF

While most NUV observations should be minimally affected by the mid-frequency WFEs, it is worth pointing out that the point-spread function of the COS MAMA detector exhibits faint, extended wings that are unrelated to the telescope optics. While the telescope-induced wings weaken as wavelength increases, the detector wings become stronger with increasing wavelength. Figure 5.2 shows model NUV detector LSFs at various wavelengths. Beyond 2500 Å, the detector wings dominate.

5.4 Quantifying the Resolution

When a substantial fraction of the power in an LSF is transferred to its extended wings, traditional measures of resolution, such as the FWHM of the line core, can be misleading. For example, an observer assuming that the resolution $R = 16{,}000$ quoted for the G130M grating represents the FWHM of a Gaussian may mistakenly conclude that COS can resolve two closely-spaced absorption features, when in fact it cannot. Nevertheless, the FWHM is a convenient tool, and we use it to describe the COS gratings in tables throughout this handbook. When using these tables, keep in mind that the quoted resolution R is the empirically-determined FWHM of the line core, and careful modeling may be needed to determine the feasibility of an observation or to analyze its result.

CHAPTER 6:

Spectroscopy with COS

In this chapter…

6.1 The Capabilities of COS

The two detectors and seven diffraction gratings (three for FUV, four for NUV) of COS enable high-sensitivity spectroscopy at low and moderate resolution across the FUV and NUV bands. The bandpass and resolution of each grating are presented in Table 6.1.

For each exposure, the observer selects a detector (FUV or NUV), a grating, a central wavelength and FP-POS setting for the grating, one of the two 2.5 arcsec apertures (PSA or BOA), and a data-taking mode (TIME-TAG or ACCUM). Chapter 15 provides detailed specifications for each grating and aperture. Note that the two channels cannot be used simultaneously, as the NUV channel is fed by a mirror on the FUV optics select mechanism.

Table 6.1: COS Grating Parameters

Grating	Useful Wavelength Range (Å)	Bandpass per Exposure (Å)	Inferred Resolving Power[1] $R = \lambda/\Delta\lambda$	Dispersion (mÅ pixel^{-1})
FUV Channel				
G130M	1150 –1450	292[2]	16,000 – 21,000	9.97
G160M	1405 – 1775	360[3]	16,000 – 21,000	12.23
G140L	< 900 – 2050	> 1150	1,500 – 4,000	80.3
NUV Channel				
G185M	1700 – 2100	3 × 35	22,000 – 28,000	37
G225M	2100 – 2500	3 × 35	28,000 – 38,000	33
G285M	2500 – 3200	3 × 41	30,000 – 41,000	40
G230L	1650 – 3200[4]	(1 or 2) × 398	2,100 – 3,900	390

1. Empirically-determined FWHM of the LSF through the PSA, which is not Gaussian, for observations through the PSA. The lesser value of *R* is realized for the low-wavelength end of the useful range, and *R* increases roughly linearly with wavelength.
2. The inter-segment gap spans 14.3 Å.
3. The inter-segment gap spans 18.1 Å.
4. Some shorter wavelengths are recorded in second-order light. They are listed in Table 6.5.

6.1.1 First-Order Sensitivity

COS is considerably more sensitive than STIS and earlier-generation *HST* instruments at comparable spectral resolutions, particularly in the far ultraviolet. Effective areas for targets observed through the PSA are shown in Figure 6.1 and Figure 6.2.

While the figures and tables in this handbook can be used to derive accurate estimates of count rates, exposure times, and the like, we recommend the use of the COS ETC in all cases, because it properly computes instrument throughput, accounts for detector and astronomical backgrounds, and checks for violations of local and global count-rate limits.

Figure 6.1: Effective Areas for the FUV Channel through the PSA.

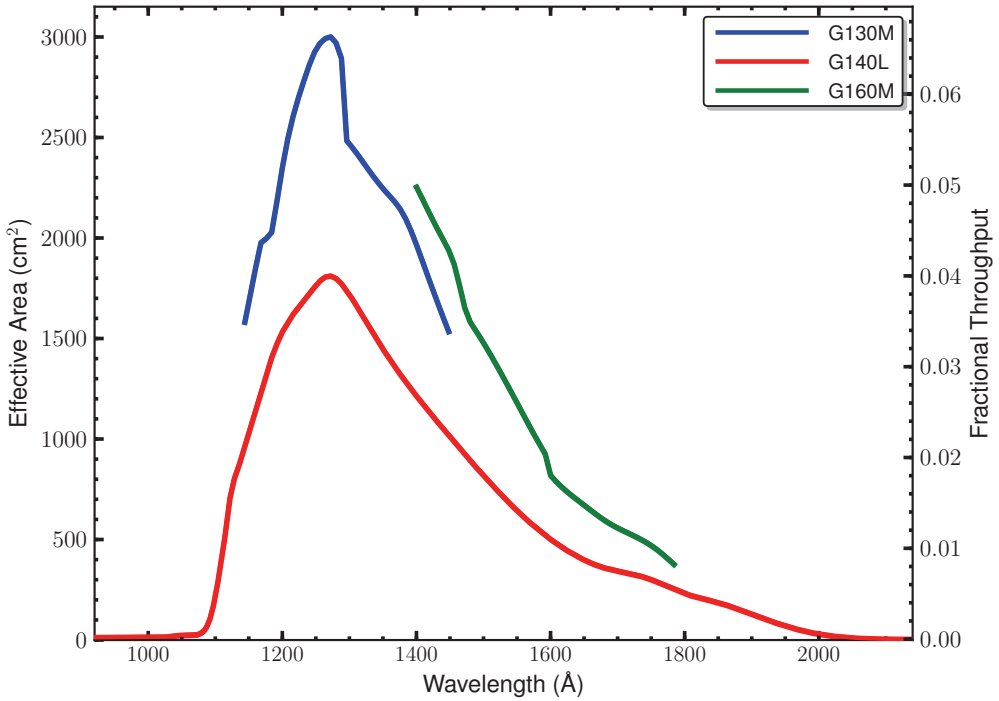

Figure 6.2: Effective Areas for the NUV Channel through the PSA.

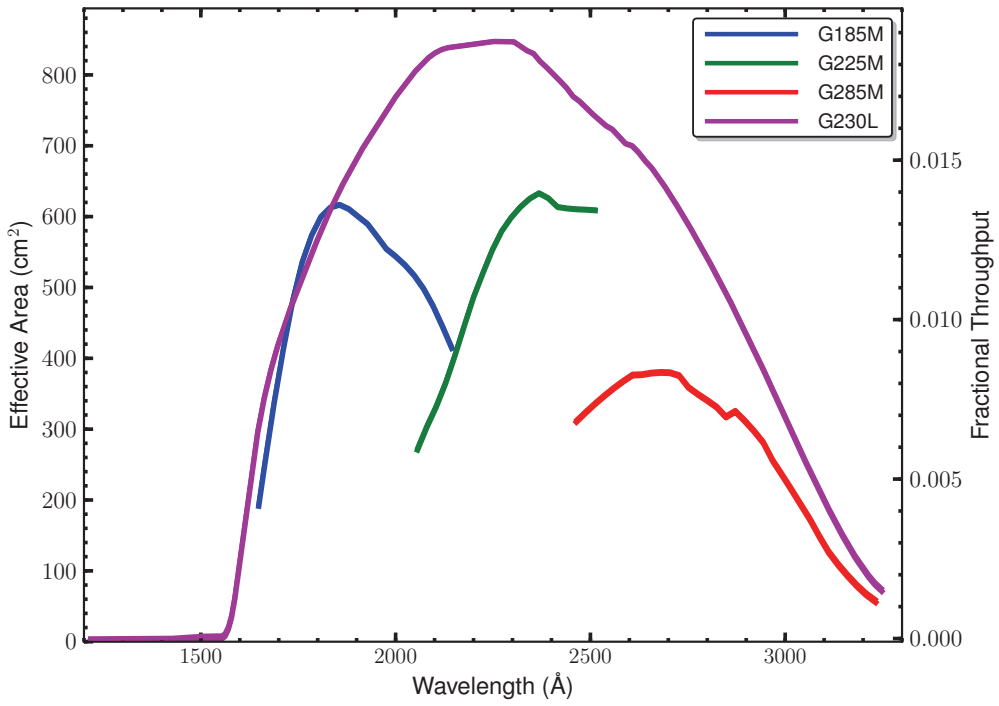

Figure 6.3: Two Estimates of the G140L CENWAVE=1230 FUVB Effective Area

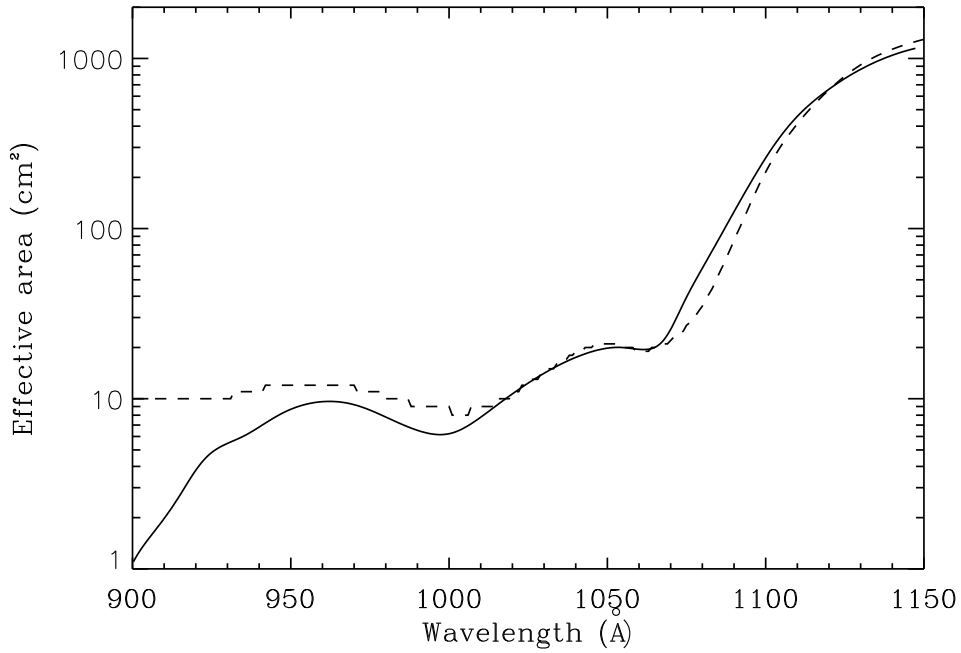

Segment B effective area of the COS G140L grating at wavelengths between 900 and 1150 Å. Dashed line is from McCandliss et al (2009); solid line is from SMOV calibration observations.

6.1.2 Observing below 1150 Å

Figure 6.3 compares the PSA G140L CENWAVE=1230 FUVB effective area measured by McCandliss et al. (2009; arXiv:0909.3878) to the effective area determined from SMOV observations of the spectroscopic standard star LDS 749b. (Given the low S/N of the SMOV observation, the two measurements are consistent.) From this figure, we can draw two fundamental conclusions: First, COS can obtain useful spectra at wavelengths between 900 and 1150 Å. Second, the contrast between the throughput at 1000 and 1150 Å is roughly a factor of 100. This second point is extremely important. Because wavelengths between 900 and 1150 Å fall on the same detector, the count rate at 1150 Å can easily exceed the detector local bright limit, while the count rate at shorter wavelengths is fine. The problem is alleviated somewhat by using FP-POS=3, which moves wavelengths longer than 1137 Å off of the detector. Consequently, turning segment A off and using FP-POS=3 is the recommended approach for observing bright objects below 1100 Å with the G140L grating.

Figure 6.4: Second-order light in G230L Spectrum.

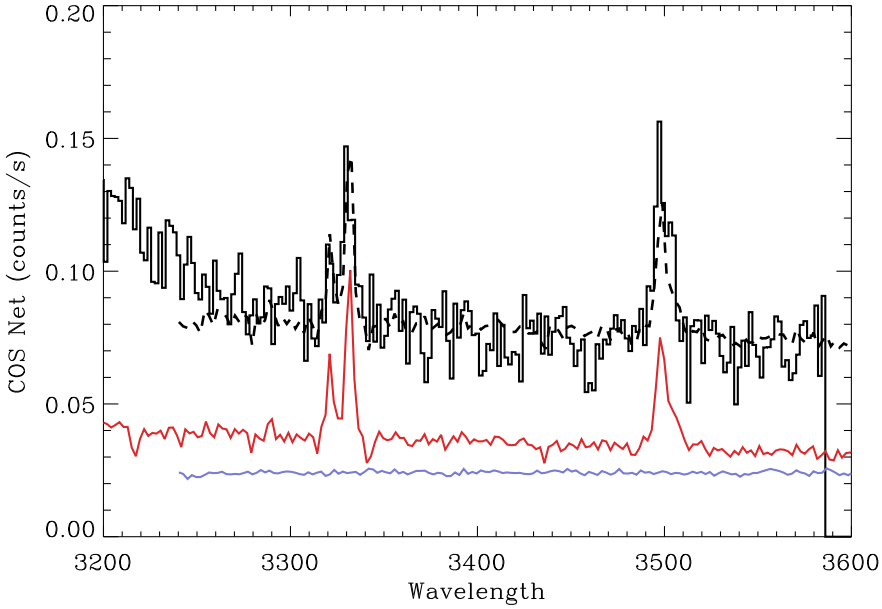

Black curve is stripe B of the G230L CENWAVE = 3360 spectrum of NGC 6833. Blue curve is an FOS spectrum over the same wavelength range (units are Ångstroms). Red curve is an FOS spectrum of the 1600 - 1800 Å region, plotted as $f(2\lambda)$. The FOS spectra have been rescaled by arbitrary amounts for display purposes. The dashed curve, a combination of the two FOS spectra, reasonably reproduces the COS spectrum.

6.1.3 Second-Order Sensitivity

Because the MAMA detector is sensitive to wavelengths as short as 1150 Å, NUV spectra longward of 2300 Å are vulnerable to second-order contamination. To mitigate this problem, the COS NUV optics were designed to provide peak reflectivities between 1600 and 2000 Å. Gratings G225M and G285M are coated in bare aluminum, which when oxidized has poor reflectivity below 1800 Å. After six reflections (two in the *HST* OTA and four within COS), light from below 1250 Å is reduced by 99%. Mounted directly on gratings G230L and G285M are 2 mm-thick fused-silica order-sorting filters that block second-order light from below 1700 Å.

For G230L, stripes B and C are still affected by second-order flux. When `CENWAVE=3360`, stripe B is contaminated by second-order light beyond 3200 Å. In a spectrum of the planetary nebula NGC 6833 obtained with `CENWAVE=3360`, second-order light accounts for roughly 40% of the flux at 3320 Å and more that 50% at 3500 Å (Figure 6.4). Above 1700 Å, stripe C is more sensitive to second-order light than first-order by design (Table 6.5), but on-orbit observations reveal that first-order light is detectable at a level of 5% from wavelengths greater than 3700 Å at all central-wavelength settings.

In the FUV channel, second-order light is suppressed by the three reflections from optics coated with Al and MgF_2 (two in the *HST* OTA plus the COS grating).

6.1.4 Zero-Order Image

The 1105 Å central wavelength setting of grating G140L places the zero-order image from the grating on segment B of the FUV detector, while a useful first-order spectrum falls onto segment A. For this central wavelength, observations can be made only in single-segment mode, with the high voltage for segment B reduced (Section 6.6). After final alignment of COS on-orbit, the zero-order image was also found to fall on segment B for the 1230 Å setting with `FP-POS=4`. Beginning in Cycle 18, `CENWAVE=1230` is being replaced with `CENWAVE=1280` to keep the zero-order image off the detector. Two-segment observations are allowed with `CENWAVE=1280`.

6.1.5 Spectroscopic Resolving Power

The spectroscopic resolving power (R) of each COS grating is listed in Table 6.1. The quoted values correspond to the FWHM of the model LSFs that are described in Chapter 5 and presented in Chapter 15. Because the COS LSF is not a Gaussian, simple rules relating R to the detectability of narrow spectral features may not apply. Careful modeling of the LSF may be required to determine the feasibility of an observation.

Use of the BOA degrades the resolving power, decreasing G130M to R = 5900, G160M to 4400, G140L to 1100, G185M to 3500, G225M to 4600, G285M to 5000, and G230L to 500.

6.1.6 Spatial Resolution and Field of View

The spatial resolution of COS is affected by the mid-frequency wavefront errors via the non-Gaussian wings they introduce (Chapter 5). The NUV channel's optics correct for the telescope's spherical aberration, but not the mid-frequency errors. In spectroscopic mode, ground tests show that COS can separate the spectra of two equally bright objects that are 1 arcsec apart in the cross-dispersion direction using either the FUV or the NUV channel.

The COS field of view is determined by the entrance apertures (which are 2.5 arcsec in diameter), but the aberrated light entering the aperture means that objects up to 2 arcsec from the center of the aperture will contribute to the recorded spectra.

6.1.7 Photometric (Flux) Precision

The limits on the precision and accuracy of fluxes measured with COS are expected to be the same as for STIS. COS has the advantage of a fairly large aperture so that there are only small aperture losses (at most 5%; see Section 8.3). The on-orbit photometric accuracy of COS has yet to be determined, but for now we take it to be the same as STIS, namely 5% accuracy on absolute fluxes and 2% on relative fluxes (within a single exposure). The experience with the NUV MAMA of STIS shows that the repeatability of a flux is good to well under 0.5%. The level of repeatability for the FUV detector is not yet known.

6.1.8 Wavelength Accuracy

The COS specifications for absolute wavelength uncertainties within an exposure are:

- 15 km s^{-1} for medium-resolution spectra (the "M" gratings),
- 150 km s^{-1} for G140L, and
- 175 km s^{-1} for G230L.

The error budget for wavelength accuracy for the various gratings is shown in Table 6.2. Note that all quantities are 1σ. To arrive at the last two columns, the error budget has been divided equally between internal and external sources. The internal sources include the accuracy of the wavelength scale, the dispersion relation, aperture offsets, distortions, and drifts. The external tolerance budget is dominated by target mis-centering in the aperture. For more on this subject, see Section 8.3.2.

Table 6.2: Wavelength Calibration Uncertainties.

Grating	Error goal (1σ)		Internal error (1σ)	External error (1σ)	Plate scale[1]
	km s^{-1}	pixels	pixels	arcsec	pixel $arcsec^{-1}$
G130M	15	5.7 – 7.5	3.0 – 4.0	0.09 – 0.12	45.1
G160M	15	5.8 – 7.2	3.1 – 3.8	0.10 – 0.12	44.6
G140L	150	7.5 – 12.5	4.0 – 6.6	0.12 – 0.21	47.1
G185M	15	7.2 – 10.0	1.2 – 1.7	0.03 – 0.04	41.85
G225M	15	9.7 – 13.3	1.6 – 2.3	0.04 – 0.06	41.89
G285M	15	9.7 – 14.7	1.6 – 2.6	0.05 – 0.07	41.80
G230L	175	8.3 – 15.5	1.4 – 2.6	0.03 – 0.07	42.27

1. The plate scale is shown to indicate the centering precision needed during acquisition. The values are for the along-dispersion direction.

The COS grating mechanisms (OSM1 and OSM2) continue to move after reaching their commanded positions. Though small, the drift is significant enough to degrade spectral resolution, especially during the first few minutes after a grating motion. To measure and remove this effect, the TAGFLASH operating technique was developed. In this mode, the wavelength calibration lamp is turned on periodically during TIME-TAG science observations with the PSA so that spectral drifts can later be removed in data processing. Because the wavelength calibration spectrum is recorded on the detector well away from the science spectrum, one does not contaminate the other. TAGFLASH is the default mode for TIME-TAG observations with the PSA; it is described further in Section 6.7.1.

Figure 6.5: Internal Scattered light in the FUV.

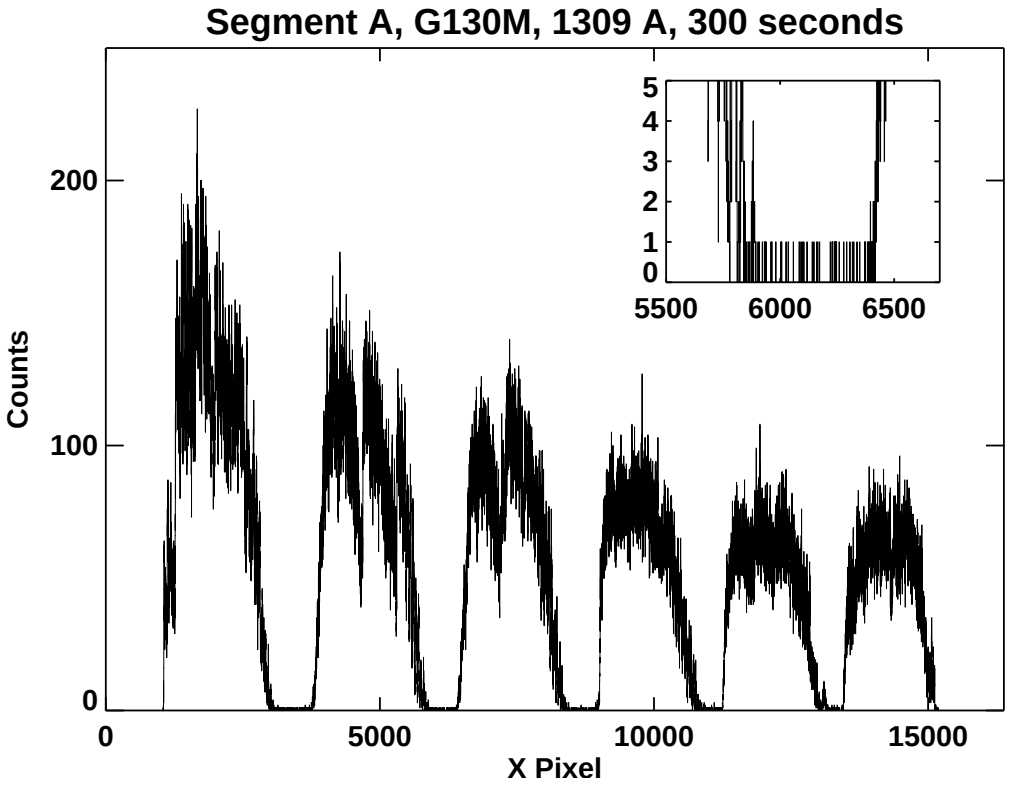

A test exposure obtained during ground calibration using a CO absorption cell. The inset shows an enlargement of the bottom of one of the absorption troughs.

6.1.9 Internal Scattered Light

The internal scattered-light level within the COS is quite low. Figure 6.5 shows an observation obtained during ground testing, in which a CO absorption cell was placed into the beam of an FUV continuum source. The inset shows the bottom of one of the absorption troughs. Light scattered along the dispersion axis represents less than 1% of the nearby continuum.

The extended wings of the COS LSF may fill in the cores of saturated absorption features that would otherwise appear black (Chapter 5). This effect can be modeled using the synthetic line profiles presented in Chapter 15.

Figure 6.6: Vignetting Profile for NUV M Gratings.

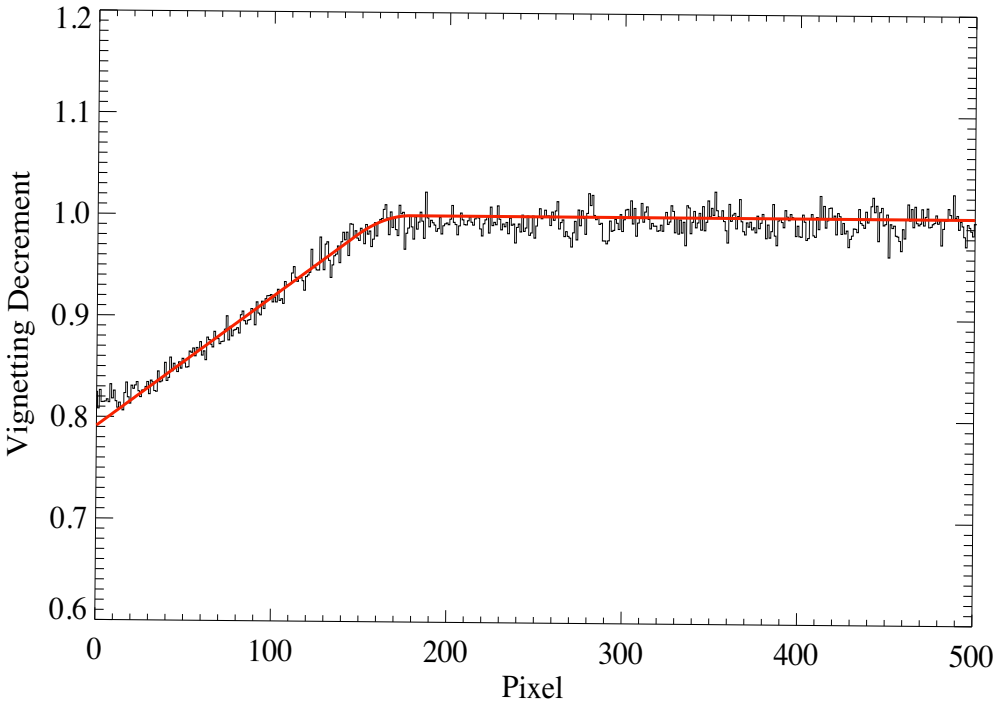

Vignetting profile of the medium-resolution gratings as a function of pixel location showing the linear decrease in throughput near the low-pixel edge of the NUV detector. The red line shows the best fit to the profile obtained from observations of the white dwarf G191-B2B.

6.1.10 Vignetting of the NUV Channel

After on-orbit alignment of COS in *HST*, fluxes of external targets in the PSA were found to be depressed at the short wavelength ends of the NUV stripes. For the medium-resolution gratings, the reduction is about 20% at the first pixel and ramps up linearly to expected levels over approximately the next 160 pixels (Figure 6.6). For G230L, the reduction is about 15% at the first pixel and extends about 110 pixels. (The slope is the same as in Figure 6.6; it is as though the ramp were shifted by 50 pixels.) The depression is thought to be due to vignetting of the beam at the NUV camera mirrors that image the spectrum on the detector. The vignetting correction is the same for all stripes and grating settings. The effect is corrected in pipeline processing, but is not included in the COS ETC.

6.2 TIME-TAG vs. ACCUM Mode

COS exposures may be obtained in either a time-tagged photon-address mode (TIME-TAG), in which the position, arrival time, and pulse height (for FUV observations) of each detected photon are saved in an event stream, or in accumulation (ACCUM) mode, in which only the positions of the photon events are recorded.

6.2.1 TIME-TAG Mode

In TIME-TAG mode, each photon is kept as a separate event in a list in COS memory. Each entry in that list contains the (*x, y*) coordinates of the photon together with the pulse height of the charge cloud generated by it (for FUV observations). Time markers are inserted in the list every 32 msec by the instrument electronics. When data are processed by the ground system, arrival times are assigned to the events according to the time marker preceding the event.

COS observations should be obtained in TIME-TAG whenever possible, because it provides significant opportunities for temporal sampling, exclusion of poor quality data, and, for the FUV, improved thermal correction (by tracking the stim-pulse positions as a function of time) and background removal (by using the pulse-height information). TIME-TAG mode should always be used for exposures that will generate count rates of 21,000 counts sec^{-1} or less from the entire detector (including both detector segments for the FUV). At count rates between 21,000 and 30,000 counts sec^{-1}, TIME-TAG may be used to obtain properly flux-calibrated data, but the loss of some continuous time periods within extended exposures will occur (see the discussion under BUFFER-TIME below). At present, TIME-TAG should not be used for count rates greater than 30,000 counts sec^{-1}. ACCUM mode should be used only when absolutely necessary, such as for high count-rate targets.

We recommend that TIME-TAG mode always be used with FLASH=YES (the so-called TAGFLASH mode) unless circumstances prevent it.

Doppler Correction for TIME-TAG Mode

No on-board corrections are made for shifts in the spectrum from orbital motion of *HST* while in TIME-TAG mode; this is done later in pipeline processing.

Pulse-height Data for TIME-TAG

In FUV TIME-TAG mode, the individual pulse height amplitudes are recorded along with the position and time information of the photon events, so the PHD can be screened by time or position on the detector if desired during the calibration process. Post-observation pulse height screening is useful for reducing unwanted background events, and can often improve the signal-to-noise ratio in the extracted science spectrum. Pulse-height information is not provided by the NUV detector.

6.2.2 ACCUM Mode

In ACCUM mode, an image of the detector is stored in a 16-bit memory buffer. As each photon arrives from the detector, the location in the buffer at coordinates *(x, y)* is incremented by one. Each location can hold at most 65,535 counts; the next event will cause the value to roll over to zero. To conserve memory, only a 16384 × 128 region of each segment is stored. Timing and pulse-height information is not saved, preventing the application of the data-correction techniques available in TIME-TAG mode.

ACCUM mode should be used primarily for bright targets whose high count rates would fill the on-board buffer memory too rapidly if the data were taken in TIME-TAG mode. In some instances it may be possible to observe a relatively bright object in TIME-TAG mode if the BOA is used instead of the PSA, although the BOA degrades the spectroscopic resolution. Observers wishing to use ACCUM mode will be asked to justify doing so when submitting their Phase II program.

Observing Efficiencies with ACCUM

In certain cases, on-board readout overheads can be minimized with ACCUM mode. FUV ACCUM images do not include the entire detector. To conserve memory, photons are collected only from the stim regions and that portion of the detector actually illuminated by the target (1/8 of the full detector area, or 128 pixels in *y*). Each FUV ACCUM image fills one-half of the total COS memory, so it is possible to acquire two FUV images before dumping the on-board buffer.

NUV ACCUM images cover the entire detector. Because they are smaller, up to nine of them can be stored in the memory buffer. Unlike TIME-TAG mode, no data may be acquired during an ACCUM readout. NUV ACCUM mode is thus most efficient when repeated identical observations are stored in memory, then read out all at once. (The number_of_iterations parameter in APT can be a useful tool to this end.)

Doppler Correction for ACCUM Mode

In ACCUM mode, the COS flight software adjusts the pixel coordinates of detected events to correct for the orbital motion of *HST*. The correction (always an integral pixel shift) is updated whenever *HST*'s motion changes enough to cause the spectrum to cross a pixel boundary. This is done via a small table of times relative to the start of each exposure when integral pixel shifts should occur, based on the orbital motion and the dispersion of the grating in use.

Note that ACCUM mode exposures longer than 900 seconds that use the G130M or G160M gratings may blur the FUV spectra by 1 to 2 pixels (about 1/6 to 1/3 of a resolution element) since shifts are performed in pixel, not wavelength, space.

Pulse-Height Distribution Data for ACCUM Mode Observations

Some limited pulse-height information is available for FUV ACCUM observations. A PHD histogram is dumped for every ACCUM mode image with the FUV detector, consisting of 256 bins (128 bins for each segment) of 32 bits each. Pulse-height data are not provided for NUV exposures.

6.3 Exposure Time Considerations

All COS exposure times must be an integer multiple of 0.1 seconds. If the observer specifies an exposure time that is not a multiple of 0.1 sec, its value is rounded *down* to the next lower integral multiple of 0.1 sec, (or set to 0.1 seconds if a smaller value is specified). The minimum COS exposure time duration is 0.1 seconds (but `FLASH=YES TIME-TAG` exposures impose a longer minimum; see FLASH section below). The maximum COS exposure time is 6,500 seconds. Bear in mind that exposure time values much larger than about 3,000 seconds are normally appropriate only for visits with the CVZ special requirement because the visibility period of a typical orbit is ~50 minutes. See the *HST Primer* for information about *HST*'s orbit and visibility periods.

For `TARGET=WAVE` exposures, `DEF` (default) must be entered as the exposure time. The value appropriate for the optical configuration will be chosen from a table established at STScI for best performance. At present, `TARGET=WAVE` flash durations are identical to those given in Table 6.3

6.4 Estimating the BUFFER-TIME in TIME-TAG Mode

COS maintains two on-board data buffers, each with a capacity of 9 MBytes (2.35×10^6 counts). The time set aside to fill one of these buffers is called the `BUFFER-TIME`. COS uses the `BUFFER-TIME` to establish the pattern and timing of memory dumps during a `TIME-TAG` exposure: For the first `BUFFER-TIME` of an exposure, counts are recorded in the first COS data buffer. At the end of this time, data recording switches to the second data buffer, and the first buffer is read out while the second is being filled.

If the `BUFFER-TIME` is overestimated, the buffer may fill before input switches to the other buffer. Subsequently-arriving photons will be lost, leaving a gap in the data. The pipeline will correct actual exposure times for any such gaps, so flux calibrations will be correct, but the overall S/N will be lower than expected. If BUFFER-TIME is underestimated, input will switch to the second buffer before the first buffer is full. No data will be lost, but the resulting drain on spacecraft resources could preclude other activities, including parallel observations.

For all external `TIME-TAG` observations, a value of the `BUFFER-TIME` must be specified in the Phase 2 proposal. The `BUFFER-TIME` is 2.35×10^6 counts divided by the anticipated count rate in photons per second. The `BUFFER-TIME` calculation should include counts from the detector dark current and stim pulses as well as the detected photon events, factoring in the instrument quantum efficiency and dead time. We recommend use of the COS Exposure Time Calculator (ETC) to compute an accurate value of the `BUFFER-TIME`. **Give yourself a margin of error of about 50%; i.e., multiply the ETC `BUFFER-TIME` by 2/3.**

6.4.1 Very Bright Targets

The minimum allowed value of the BUFFER-TIME is 80 seconds. This value corresponds to a count rate of 30,000 counts per second over the entire detector, the maximum rate at which the flight electronics are capable of processing counts. If 2/3 of the ETC BUFFER-TIME is less than 80 seconds, then the source is very bright and should be observed in ACCUM mode. If your exposure is less than 80 seconds in length, set BUFFER-TIME=80. The buffer will be read out immediately after the exposure ends, and there will be no idle time.

6.4.2 Bright Targets

While the minimum value of the BUFFER-TIME is 80 seconds, it actually takes 110 seconds to empty a buffer. A BUFFER-TIME of 110 seconds corresponds to a count rate of 21,000 counts per second. If the count rate exceeds this value, the second data buffer will be filled before the first buffer has been completely read out. In this situation, you have two options: You can shorten your exposure, or you can accept gaps in the recorded data stream. In either case, **calcos** will compute the actual exposure time and will calculate fluxes correctly, but the total number of collected counts, and hence the S/N, will be limited by the 21,000 counts per second rate.

- Option A: You wish to receive all the data and are willing to shorten the exposure time. In this case, use 2/3 of the BUFFER-TIME returned by the ETC. If the BUFFER-TIME is less than 111 seconds, APT will issue a warning and truncate the exposure time at 2 × BUFFER-TIME to ensure that all data are recorded.
- Option B: You can tolerate data drop-outs, but want control of the total exposure time. In this case, choose a BUFFER-TIME of 111 seconds. You will lose some fraction of the data during each BUFFER-TIME interval (see example below), but APT will not truncate your exposure.

As an example, suppose that 2/3 × (BUFFER-TIME returned by the ETC) is 100 seconds, and you want an exposure time of 360 seconds.

- With Option A, you would specify BUFFER-TIME=100. Because it takes longer than that to read out the buffer, APT limits you to an exposure time of 2 × 100 = 200 sec. In this case, COS records all the events that arrived during the exposure.
- With Option B, you would specify BUFFER-TIME=111. Since the COS buffer may be full after the first 100 seconds, the last 11 seconds of data may not be recorded and are lost each time the buffer fills. With this option you will get a series of data blocks as follows: **100**, *11*, **100**, *11*, **100**, *11*, **27**, where the bold numbers represent periods when the data are recorded, and the italic numbers represents periods when the data are lost. The COS shutter remains open for the full 360 seconds, and the data are properly flux calibrated by the pipeline.

6.4.3 Faint Targets

For faint targets, the predicted BUFFER-TIME may be considerably longer than the exposure time. In such cases, set BUFFER-TIME equal to the exposure time. In orbits with multiple science exposures, you can minimize overheads – and squeeze out a few more seconds of observing time – by setting the BUFFER-TIME for each exposure to the exposure time minus 100 seconds. The buffer takes about 110 seconds to empty, so most of the data will be read out before the exposure is completed, leaving only a fraction for the end of the exposure. This allows the next exposure to begin sooner. You can test the effects of such trade-offs by trying them out within APT.

The software and parameters that control dumps of the data buffer have been designed to avoid any loss of data from an observation. The duration and timing of data dumps depend on several factors, and observers are urged to use APT for observation planning to ensure that they are scheduled properly.

6.5 Spectral Gap Coverage

Single exposures for both the FUV and NUV channels have gaps in the spectra due to the physical layout of the detectors and optics.

The FUV detector consists of two segments whose active areas are separated by a gap approximately 9 mm wide. The optical image of the spectrum is continuous across the segments, but the wavelengths that fall in the gap are not recorded. These wavelengths can be brought onto the active area of the detector by choosing one of the alternate central-wavelength settings listed in Table 6.4.

For the FUV M gratings, the gap (14-18 Å) is about twice the size of the difference in central wavelength shifts (9 Å). Thus the missing wavelengths are recovered by a second exposure two central wavelength settings from the original exposure. For the G140L grating, both central wavelengths are needed to obtain a complete spectrum from below 1100 Å to Lyman α.

For the NUV channel, dispersed light from the gratings is imaged onto the detector by three camera mirrors, resulting in three non-contiguous spectral stripes being recorded at once. The gaps between the stripes are 64 Å for the G185M and G225M gratings, 74 Å for G285M, and 700 Å for G230L (Table 6.5). To acquire a complete medium-resolution spectrum requires six settings with G185M, six with G225M, and eight with G285M. A full spectrum with G230L requires all four central wavelength settings. Such a complete spectrum can probably be acquired more efficiently with STIS, but COS may be a better choice when a limited number of specific wavelengths is desired.

6.6 FUV Single-Segment Observations

The FUV detector segments are operated and read out independently. For all FUV gratings, segment A detects the longer-wavelength light and segment B the shorter wavelengths. Normally, both segments are used for a science exposure; however, there are circumstances in which operating with one detector segment at the nominal high voltage and the other effectively turned off may be beneficial. The `SEGMENT` optional parameter allows this choice. STScI strongly recommends use of both segments (the default for all but the G140L 1105 Å setting) unless special circumstances exist. Such circumstances include, but are not limited to

- Sources with unusual spectral energy distributions at FUV wavelengths (bright emission lines or rapidly increasing/decreasing continuum slopes), for which the count rate on one detector segment exceeds the bright-object protection limit, while the other segment is safe for observing.
- Sources for which the count rate on one detector segment is high but safe, while the other segment has a relatively low count rate. If the science to be done were on the low count-rate segment, operating just that segment may result in a substantially reduced dead-time correction.

The optional parameter `SEGMENT` (`=BOTH` (default), `A`, or `B`) specifies which segment of the FUV detector to use for an observation. A value of `BOTH` will activate both segments. If `A` is selected, only segment A of the detector will be activated for photon detection, and the spectrum will contain data from only the long-wavelength half of the detector. If `B` is selected, only the short-wavelength segment B of the detector will be activated and used to generate data. Wavelength and flat-field calibration procedures remain the same for a particular segment whether the other segment is operating or not.

If grating G140L is specified with the 1105 Å wavelength setting, then the value must be `SEGMENT=A`. Switching from two-segment to single-segment operation (or back again) incurs a substantial overhead time; see Table 10.4.

6.7 Internal Wavelength Calibration Exposures

Three types of internal wavelength calibration exposures may be inserted in the observation sequence by the scheduling system or by the observer:

1. `FLASH=YES` (so-called TAGFLASH) lamp flashes (`TIME-TAG` observing with the PSA only),
2. AUTO wavecals, and
3. User-specified wavecals.

Note that all wavelength calibration exposures are taken in TIME-TAG mode. Wavelength calibration exposure overheads are higher when the BOA is used for science observation as the aperture mechanism must be moved to place the WCA in the wavelength calibration beam.

For TIME-TAG observing, we strongly recommend use of the default FLASH=YES mode of wavelength calibration.

6.7.1 Concurrent Wavelength Calibration with TAGFLASH

The Optional Parameter FLASH (=YES (default), NO) indicates whether or not to "flash" the wavelength calibration lamp during TIME-TAG exposures utilizing the PSA. These flashes provide data used by the **calcos** pipeline to compensate for drifts of the Optics Select Mechanisms. In this mode, when the external shutter is open to observe an external target, the wavecal lamp is turned on briefly at the beginning and at intervals throughout the exposure. Light from the science target and the internal wavelength calibration source is recorded simultaneously on different portions of the detector. Other than the flash at the start, the timing of flashes is determined by the elapsed time since the last OSM motion. As a result, flashes may occur at different times in different exposures. The grating-dependent flash durations (Table 6.3) and the flash intervals will be defined and updated as necessary by STScI. Observers may not specify either flash duration or interval. When flashing is enabled, the exposure time must be at least as long as a single flash.

TIME-TAG sequences with FLASH=YES provide the highest on-target exposure time, as no on-target time is lost to wavelength-calibration exposures. We thus strongly recommend use of Optional Parameter FLASH=YES with all TIME-TAG observations. (Since FLASH=YES is the default for TIME-TAG spectroscopic exposures, the observer need not specify it.) FLASH=YES may not be specified for ACCUM mode or when the BOA is selected.

6.7.2 AUTO Wavecals (when TAGFLASH is not used)

For ACCUM, BOA, or TIME-TAG exposures with FLASH=NO, a separate wavelength calibration exposure will be automatically performed for each set of external spectrographic science exposures using the same spectral element, central wavelength, and FP-POS value. These AUTO wavecals are always obtained in TIME-TAG mode with the external shutter closed. This automatic wavelength calibration exposure will be added before the first associated science exposure and after each subsequent science exposure if more than 40 minutes of visibility time has elapsed since the previous wavelength calibration exposure and if the same spectrograph set-up has been in use over that time. The calibration exposure will often use some science target orbital visibility. The calibration lamp configuration and exposure time will be based on the grating and central wavelength of the science exposure. Utilization of a GO wavecal (see below) resets the 40 minute interval timer. Insertion of a FLASH=YES exposure in the time-line does not affect the 40-minute clock.

Table 6.3: TAGFLASH Exposure Durations

Grating	Central Wavelength (Å)	Flash duration (sec)	Grating	Central Wavelength (Å)	Flash duration (sec)
G130M	1300	10	G225M (cont.)	2339	5
	all others	5		2357	10
G160M	1600	10		2373	5
	all others	5		2390	5
G140L	all	5		2410	5
G185M	1786	10	G285M	2617	5
	1817	5		2637	5
	1835	10		2657	5
	1850	20		2676	10
	1864	30		2695	5
	1882	15		2709	5
	1890	10		2719	5
	1900	20		2739	5
	1913	10		2850	5
	1921	10		2952	5
	1941	10		2979	15
	1953	15		2996	5
	1971	15		3018	10
	1986	10		3035	5
	2010	10		3057	5
G225M	2186	5		3074	5
	2217	10		3094	10
	2233	5	G230L	2635	5
	2250	10		2950	5
	2268	10		3000	5
	2283	5		3360	5
	2306	10	MIRRORA	...	5
	2325	10	MIRRORB	...	17

`AUTO` wavecals may not be turned off by the observer. If there is a science requirement to turn off `AUTO` wavecals, specific permission must be sought from the STScI Contact Scientist.

`FLASH=NO` observations will be less efficient than `FLASH=YES` observations in terms of on-target utilization of orbital visibility and in the quality of their wavelength calibration due to possible OSM residual motions.

6.7.3 User-specified Wavelength Calibration Exposures (GO Wavecals)

Observers may insert additional wavelength calibration observations in the visit by specifying target=WAVE (so-called GO wavecal exposures). Note that the default modes of operation (TIME-TAG, ordinarily, or ACCUM) automatically secure needed wavelength calibration information to go with your science data, and so the need for user-specified wavecals should be rare. Exposure time must be set to DEF for these exposures, TIME-TAG must be used, and FLASH=NO should be explicitly selected. Exposures specified with the WAVE internal target will use the same calibration lamp configuration and exposure time as the automatic wave calibrations discussed above.

6.8 Signal-to-Noise Considerations

The signal-to-noise ratio (S/N) of COS observations are improved through two techniques, flat fielding and coadding spectra taken at different grating settings using the FP-POS option. Flat fielding removes the high frequency, pixel-to-pixel detector variations by dividing the data by a high S/N flat-field response image. FP-POS exposures smooth out the detector variations without degrading the science spectrum by aligning in wavelength space data taken at different locations on the detector.

6.8.1 COS Flat Fielding

The internal flat-field calibration system consists of two deuterium lamps and the flat-field calibration aperture (FCA). The system was designed such that light from the lamps follows nearly the same optical path as that from an external target. The FCA is inserted near the location of the PSA, and the lamp beam illuminates the gratings and mirrors from this slightly offset position. The FCA restricts the area exposed on the detectors to regions where external spectra fall (Chapter 4).

Ground flat-field data for the FUV are not useful due to low lamp levels, so the FUV flat field is being constructed from on-orbit observations of bright white dwarfs. A preliminary version is shown in Figure 6.7. The dark, vertical stripe is a shadow cast by a grid wire in front of the detector (Section 4.1.1). A detector dead spot and the hexagonal pattern of the fiber bundles in the micro-channel plate are also visible. Although significant structure is present in the FUV flats, it is reproducible and can be removed during data reduction.

The COS FUV detector can achieve a S/N of about 18 per 6-pixel resel with a single grating setting. By using multiple FP-POS settings, it is possible to reach S/N = 35 per 6-pixel resel. Using high S/N data obtained during SMOV at four FP-POS settings of the G160M grating at a central wavelength 1600 A, and using a data-reduction technique that estimates the flat field from the data itself, we have achieved S/N values greater than 100 per resel over small wavelength ranges. This result demonstrates the capability of the FUV detector to achieve S/N > 100 per resel in special circumstances.

Figure 6.7: Section of a flat-field image for the FUV XDL.

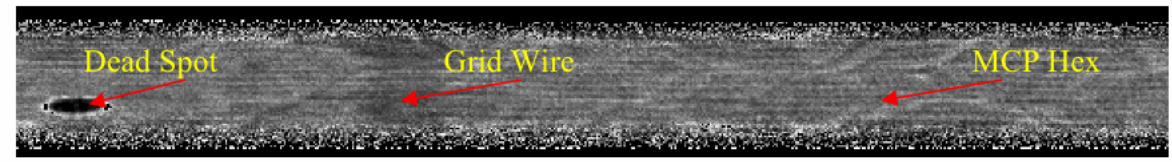

A section of the FUV flat field showing representative detector features and a grid wire.

The NUV flat field used by **calcos** was built from a combination of external PSA deuterium lamp exposures taken on the ground and internal observations taken on the ground and on-orbit. Figure 6.8 presents a comparison between two NUV flat-field frames, one obtained on orbit and one during thermal vac. Each image was divided by a low-order polynomial to isolate the high-order fringe pattern characteristic of the NUV detector. Their ratio is consistent with the noise in the on-orbit image, indicating that the thermal-vac image can be used to flat-field data taken on orbit. Pre-flight ground tests with COS show that the NUV MAMA can deliver S/N up to about 50 without using a flat field. Using a flat field, S/N of 100 or more per resolution element should be routinely achievable.

Figure 6.8: Example of flat-field exposures for the NUV MAMA.

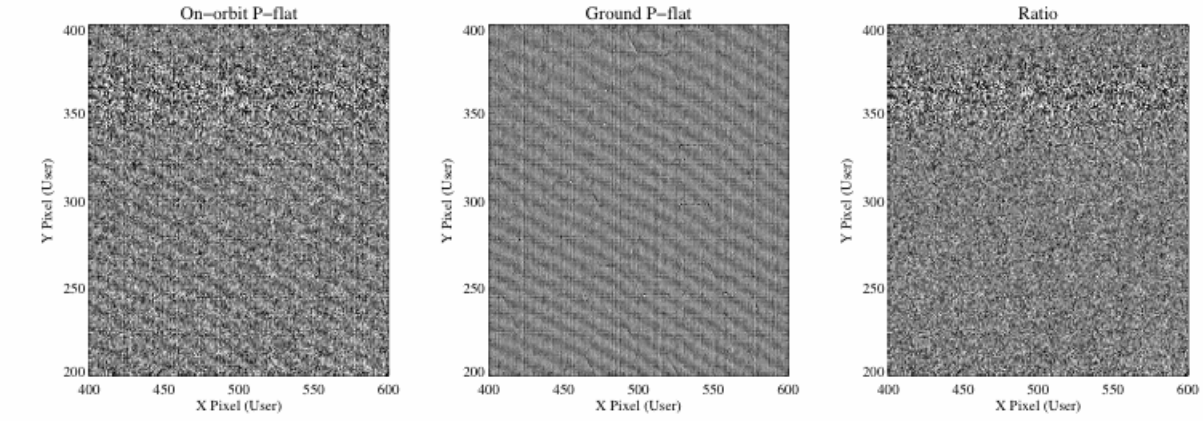

6.8.2 Use of Optional Parameter FP-POS

Fixed-pattern noise in the COS detectors limits the S/N that can be achieved in a single exposure to ~18 per resolution element for the FUV and 50 for the NUV. To achieve higher S/N ratios, one can obtain a series of exposures, each slightly offset in the dispersion direction, causing spectral features to fall on a different part of the detector. For STIS and GHRS, these motions are known as FP-SPLITs. For COS, these motions are specified by the `FP-POS` optional parameter.

Four FP-POS offset positions are available: a nominal position (0), two positions toward longer wavelengths (–2 and –1), and one position toward shorter wavelengths (+1). Positions –2, –1, 0, and +1 are designated respectively as `FP-POS=1`, `FP-POS=2`, `FP-POS=3`, and `FP-POS=4`. The nominal position, `FP-POS=3`, is the

default and is the setting used to define the wavelength range associated with the grating central wavelengths (Table 6.4 and Table 6.5). In pipeline processing, **calcos** creates individual calibrated spectra for each FP-POS exposure, then aligns and combines them into a merged spectral product, using only good-quality data at each wavelength.

The optical mechanism is rotated by one step for each adjacent FP-POS position. The amount that a particular spectral feature moves in the dispersion direction on the detector is 244-259 pixels per step for the FUV channel and 52 pixels for the NUV. The corresponding wavelength shifts for each grating are given in Chapter 15. There is a preferred direction for moving the grating mechanism, so overheads are reduced if FP-POS exposures are obtained in increasing order (see Section 10.3). Note that FP-POS indicates the relative position of a grating, not the number of separate exposures and steps. FP-POS=4, for example, takes a single spectrum at position number 4 for the specified exposure time.

Wavelength calibrations will be obtained each time the FP-POS changes. For FLASH=YES exposures, the time-since-grating-move clock is not reset by an FP-POS movement; however, there will always be at least one lamp flash during each individual FP-POS exposure. For FLASH=NO exposures, a separate wavelength calibration exposure will be taken for each FP-POS position change. FP-POS is not allowed for internal targets except TARGET=WAVE.

FP-POS at low S/N

In cases where a spectrum with low S/N will suffice, multiple FP-POS positions can be disadvantageous. We recommend that two FP-POS positions be used so that you can confirm that an apparent feature is real.

FP-POS and gap coverage in the FUV

The two segments of the COS FUV detector have a gap between them. If you require a spectrum that covers all available wavelengths at medium resolution, the best strategy is to use the grating at one FP-POS but at four consecutive central wavelengths. For example, use of G130M at central wavelengths 1300, 1309, 1318, and 1327 Å, all with FP-POS=3, will efficiently cover the full range available with G130M and will provide the equivalent of four FP-POS positions. To construct a complete FUV medium-resolution spectrum, we recommend using G130M at its four shortest central wavelengths plus G160M at its four longest wavelengths. You will have to combine the observation manually, as the pipeline does not combine spectra with different central wavelengths.

Figure 6.9: Techniques for Improving the S/N

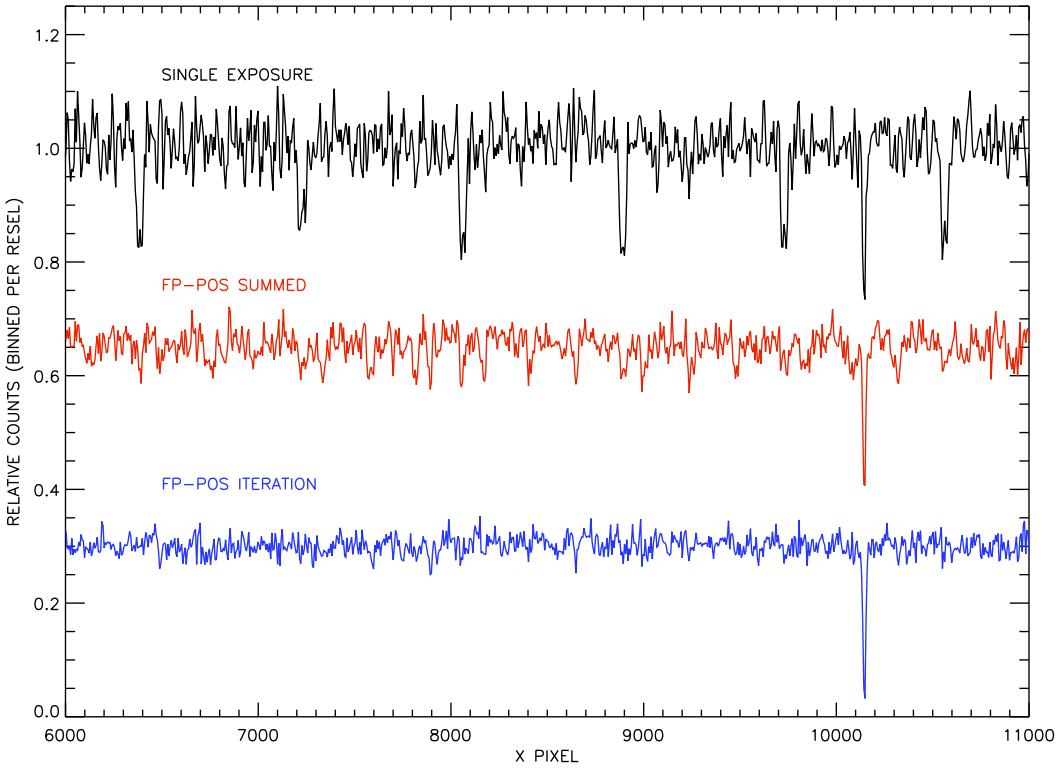

On-orbit FUV observations of a white dwarf. The black curve represents a single exposure. The red curve represents the sum of spectra taken at several FP-POS settings. The blue curve represents the sum of spectra taken at several FP-POS settings, each flat-fielded before being combined.

6.8.3 A Simple Example

To illustrate how these techniques can improve the S/N of COS spectra, Figure 6.9 presents on-orbit spectra of a white dwarf. The black spectrum represents a single exposure, taken with segment A of the FUV detector. The regularly-spaced absorption features are shadows cast by the grid wires; the narrow, deeper feature is astrophysical. Summing the spectra from multiple `FP-POS` settings significantly reduces the depth of the grid-wire features (red spectrum), but does not remove them completely. The blue spectrum is the result of an iterative technique that uses the data to construct and subtract a flat field from each spectrum before combining them. Its S/N is roughly twice that of the red curve. At the time of this writing, **calcos** does not apply a flat-field correction, but should do so in the near future.

6.9 EXTENDED Optional Parameter

Optional Parameter `EXTENDED` (default = `NO`) sets a science header keyword to inform the **calcos** pipeline that the target is an extended source. The keyword may be used in the future to activate special data-reduction procedures, although none are currently in the pipeline. No aspect of on-board data-taking is affected by this parameter.

COS spectra of extended objects could have significantly lower resolution than those of point sources, depending on the spatial distribution of the source. For example, measurements of Lyman α airglow lines, which uniformly fill the COS aperture, show R = 1450 for G130M and R = 165 for G140L. Filled-aperture observations of SNR N132D from the COS ERO program confirm $R \sim 1500$ for both FUV M gratings (France et al. 2009, ApJ, 707, L27). In the NUV, the situation is much worse, because a source that fills the aperture will lead to cross-contamination among the three spectral stripes on the MAMA detector.

A similar but more favorable situation arises in the case of multiple point sources that fall within the aperture. COS was designed to resolve two point sources that are one arcsec apart in the cross-dispersion direction, and ground tests confirm that it is possible. However, a point source that is more than 0.5 arcsec from the center of the PSA will not have all of its light transmitted; see Section 8.3.1.

6.10 Wavelength Settings and Ranges

Table 6.4 and Table 6.5 show the wavelength ranges recorded on the detectors for each valid combination of grating and central-wavelength setting at the default `FP-POS=3` position (Section 6.8.2). The wavelength ranges spanned at other `FP-POS` settings may be estimated using the `FP-POS` step values provided in Chapter 15. Note, however, that uncertainties in the positioning of the Optics Select Mechanisms (Section 3.3.3) correspond to about half of an FP-POS step. These wavelength ranges are subject to change as the instrumental calibration evolves. The most recent measurements are available from the COS Web site.

Table 6.4: Wavelength Ranges for FUV Gratings for `FP-POS =3`.

Grating	Central wavelength setting (Å)[1]	Recorded wavelengths	
		Segment B	Segment A
G130M	1291	1132 – 1274	1291 – 1433
	1300	1141 – 1283	1300 – 1442
	1309	1153 – 1294	1309 – 1449
	1318	1163 – 1303	1319 – 1459
	1327	1173 – 1313	1328 – 1468
G160M	1577	1386 – 1559	1577 – 1749
	1589	1398 – 1571	1589 – 1761
	1600	1410 – 1581	1601 – 1772
	1611	1421 – 1594	1612 – 1784
	1623	1433 – 1606	1625 – 1796
G140L	1105	HV OFF	1120 – 2246[2]
	1230[3]	<900 – 1155	1260 – 2385[2]
	1280	<900 – 1165	1280 – 2405[2]

1. The central wavelength is (approximately) the shortest wavelength recorded on segment A.
2. The G140L grating is flux calibrated up to 2150 Å. At longer wavelengths, second-order light may be present.
3. In Cycle 18, central wavelength 1230 will be replaced with 1280 to move the zero-order image off the detector (Section 6.1.4).

Table 6.5: Wavelength ranges for NUV gratings for `FP-POS=3`

Grating	Central wavelength setting (Å)[1]	Recorded wavelengths		
		Stripe A	Stripe B	Stripe C
G185M	1786	1670 – 1705	1769 – 1804	1868 – 1903
	1817	1701 – 1736	1800 – 1835	1899 – 1934
	1835	1719 – 1754	1818 – 1853	1916 – 1951
	1850	1734 – 1769	1833 – 1868	1931 – 1966
	1864	1748 – 1783	1847 – 1882	1945 – 1980
	1882	1766 – 1801	1865 – 1900	1964 – 1999
	1890	1774 – 1809	1872 – 1907	1971 – 2006
	1900	1783 – 1818	1882 – 1917	1981 – 2016
	1913	1796 – 1831	1895 – 1930	1993 – 2028
	1921	1804 – 1839	1903 – 1938	2002 – 2037
	1941	1825 – 1860	1924 – 1959	2023 – 2058
	1953	1837 – 1872	1936 – 1971	2034 – 2069
	1971	1854 – 1889	1953 – 1988	2052 – 2087
	1986	1870 – 1905	1969 – 2004	2068 – 2103
	2010	1894 – 1929	1993 – 2028	2092 – 2127
G225M	2186	2070 – 2105	2169 – 2204	2268 – 2303
	2217	2101 – 2136	2200 – 2235	2299 – 2334
	2233	2117 – 2152	2215 – 2250	2314 – 2349
	2250	2134 – 2169	2233 – 2268	2332 – 2367
	2268	2152 – 2187	2251 – 2286	2350 – 2385
	2283	2167 – 2202	2266 – 2301	2364 – 2399
	2306	2190 – 2225	2288 – 2323	2387 – 2422
	2325	2208 – 2243	2307 – 2342	2406 – 2441
	2339	2223 – 2258	2322 – 2357	2421 – 2456
	2357	2241 – 2276	2340 – 2375	2439 – 2474
	2373	2256 – 2291	2355 – 2390	2454 – 2489
	2390	2274 – 2309	2373 – 2408	2472 – 2507
	2410	2294 – 2329	2393 – 2428	2492 – 2527

Grating	Central wavelength setting (Å)[1]	Recorded wavelengths		
		Stripe A	Stripe B	Stripe C
G285M	2617	2480 – 2521	2596 – 2637	2711 – 2752
	2637	2500 – 2541	2616 – 2657	2731 – 2772
	2657	2520 – 2561	2636 – 2677	2751 – 2792
	2676	2539 – 2580	2655 – 2696	2770 – 2811
	2695	2558 – 2599	2674 – 2715	2789 – 2830
	2709	2572 – 2613	2688 – 2729	2803 – 2844
	2719	2582 – 2623	2698 – 2739	2813 – 2854
	2739	2602 – 2643	2718 – 2763	2837 – 2878
	2850	2714 – 2755	2829 – 2870	2945 – 2986
	2952	2815 – 2856	2931 – 2972	3046 – 3087
	2979	2842 – 2883	2958 – 2999	3073 – 3114
	2996	2859 – 2900	2975 – 3016	3090 – 3131
	3018	2881 – 2922	2997 – 3038	3112 – 3153
	3035	2898 – 2939	3014 – 3055	3129 – 3170
	3057	2920 – 2961	3036 – 3077	3151 – 3192
	3074	2937 – 2978	3053 – 3094	3168 – 3209
	3094	2957 – 2998	3073 – 3114	3188 – 3229
G230L	2635	1334 – 1733[2]	2435 – 2834	**1768 – 1967[3]**
	2950	1650 – 2050	2750 – 3150	**1900 – 2100[3]**
	3000	1700 – 2100	2800 – 3200	**1950 – 2150[3]**
	3360	2059 – 2458[4]	3161 – 3560[5]	**2164 – 2361[3]**

1. The central wavelength setting is the wavelength at the midpoint of stripe B.
2. For central wavelength 2635 Å, the stripe A wavelengths are listed for completeness only (and in case a bright emission line falls onto the detector). The NUV detector's sensitivity at these wavelengths is extremely low. To obtain a low-resolution spectrum at wavelengths below ~ 1700 Å, we recommend G140L and the FUV channel.
3. The values in shaded cells are wavelength ranges seen in second-order light. In these cases, the achieved dispersion is twice that for first-order mode. Longward of 3700 Å, first-order light may be present.
4. Lyman α may be present in second order.
5. Longward of 3200 Å, second-order light may be present. No flux calibration is performed for these wavelengths.

CHAPTER 7:

NUV Imaging

In this chapter…

7.1 Essential Facts About COS Imaging

- Imaging with COS may be performed only with the NUV channel.
- With a plate scale of 23.8 mas per pixel, COS provides the highest spatial sampling of any instrument aboard *HST*. The image is corrected for the *HST* spherical aberration, but is degraded by zonal (polishing) errors on the *HST* primary and secondary mirrors.
- Because the optics image the sky onto the detector – not the aperture – the image records some light from sources out to a radius of about 2 arcsec. Only point sources within about 0.5 arcsec of the aperture center have essentially all their light imaged (see Figure 7.1), so the photometric interpretation of a COS image can be inherently complex.
- COS is very sensitive, and there is a limit to the allowed count rate per pixel (50 counts per second for the NUV, which corresponds to a point-source AB magnitude of 17.6). The imaging mode of COS concentrates an object's entire NUV flux into a diffraction-limited image, so the limiting count rate can easily be exceeded.
- MIRRORB and/or the BOA can be used to obtain images of bright objects, but MIRRORB produces a secondary image, and the BOA produces an image with coma that degrades resolution; see Section 8.4.2.

7.2 Configurations and Imaging Quality

COS offers an NUV imaging mode; no FUV imaging is possible. It is anticipated that the greatest use of this imaging capability will be for target acquisition (see Chapter 8), but science exposures may be obtained as well. With OSM1 set to mirror NCM1 (which occurs automatically when any NUV mode is selected), and with OSM2 set to MIRRORA, an image of the sky is formed on the NUV MAMA detector. The plate scale is 23.8 mas per pixel. Because the entrance aperture is out of focus at the detector, the image receives light out to a radius of about 2 arcsec; however, as can be seen from Figure 7.1, once a point source is more than about 0.5 arcsec from the aperture center, its flux is significantly diminished.

The NUV imaging mode requires that the observer make two optical-element selections, the aperture and the mirror. The PSA is completely open and provides maximum throughput. For bright targets, the BOA's neutral-density filter attenuates the image by a factor of approximately 200 (Figure 3.4), but degrades the image quality significantly (see Figure 8.5 and Figure 8.6).

MIRRORA refers to the usual position of the TA1 mirror on OSM2. MIRRORB refers to an arrangement in which OSM2 rotates this mirror slightly so that the front surface of its order-sorting filter is used. This provides an attenuation factor of approximately 25 compared to MIRRORA. Because of the finite thickness of the order-sorting filter, MIRRORB produces a doubled peak in the image that may impede its use for imaging. The secondary peak contains about half of the flux of the primary image. The secondary peak is located about 20 pixels in the $+x$ direction on the MAMA detector from the primary image. It is thus easily separable for an isolated point source, but may present difficulties for extended sources or crowded fields; see Section 8.4.2 for details.

To record an image, specify `CONFIG` = `COS/NUV`, together with `MODE` = `ACCUM` or `TIME-TAG`. If `TIME-TAG` mode is selected, the minimum allowable `BUFFER-TIME` is 80 seconds, which may be longer than the expected exposure time. `ACCUM` mode is recommended for such short exposures.

To track motions of the optics selection mechanisms during TIME-TAG exposures longer than ~ 6 minutes, lamp flashes may be requested by setting `FLASH=YES`; a lamp flash in imaging mode will illuminate the WCA, whose position relative to the PSA is known. By default, `FLASH=NO` for all imaging modes.

COS imaging in `TIME-TAG` mode allows for high-speed NUV photometry with a temporal resolution of 32 msec. STIS is capable of much finer time resolution (125 microseconds), but at lower sensitivity.

The minimum COS exposure duration is 0.1 seconds, and all COS exposure times must be integer multiples of 0.1 seconds. If the observer specifies an exposure time that is not a multiple of 0.1 sec, its value is rounded down to the next lower integral multiple of 0.1 sec (or set to 0.1 seconds if a smaller value is specified). The maximum COS exposure time is 6,500 seconds. Bear in mind that exposures longer than 3,000 seconds are normally appropriate only for observations in the CVZ.

Figure 7.1: Relative Throughput of the COS PSA in NUV Imaging Mode

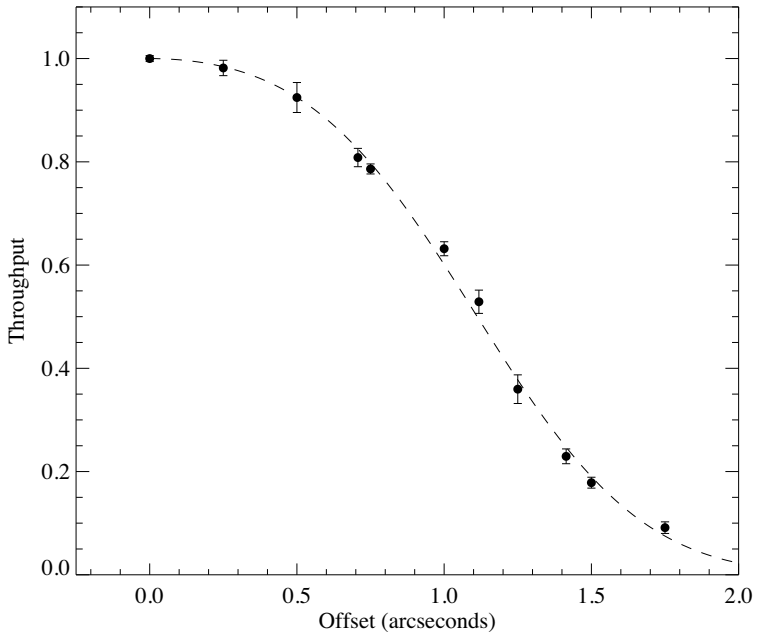

7.3 Sensitivity

COS is a sensitive instrument (Figure 7.2), and its imaging mode concentrates the target's NUV flux into a diffraction-limited image rather than dispersing the light. The local count rate limit for COS/NUV is 50 counts per pixel per second (Table 9.1), and that limit is easily reached, even for fairly faint objects. Observers should use the COS ETC (see Chapter 11) to get an accurate estimate of expected count rates, but the following values will provide a guide. These have been calculated for a flat-spectrum source (flux independent of wavelength), and the limiting count rate is reached at the following approximate flux levels:

Aperture and Mirror	Flux Limit (erg cm^{-2} s^{-1} $Å^{-1}$)
PSA + MIRRORA	2×10^{-15}
BOA + MIRRORA	4×10^{-13}
PSA + MIRRORB	3×10^{-14}
BOA + MIRRORB	6×10^{-12}

Because the COS NUV channel is sensitive to wavelengths longer than 3200 Å, care should be taken when observing cool stars ($T_{eff} < 5{,}000$ K) and other red objects, lest high count rates at long wavelengths damage the detector.

Figure 7.2: Effective Area for COS NUV Imaging with the PSA/MIRRORA.

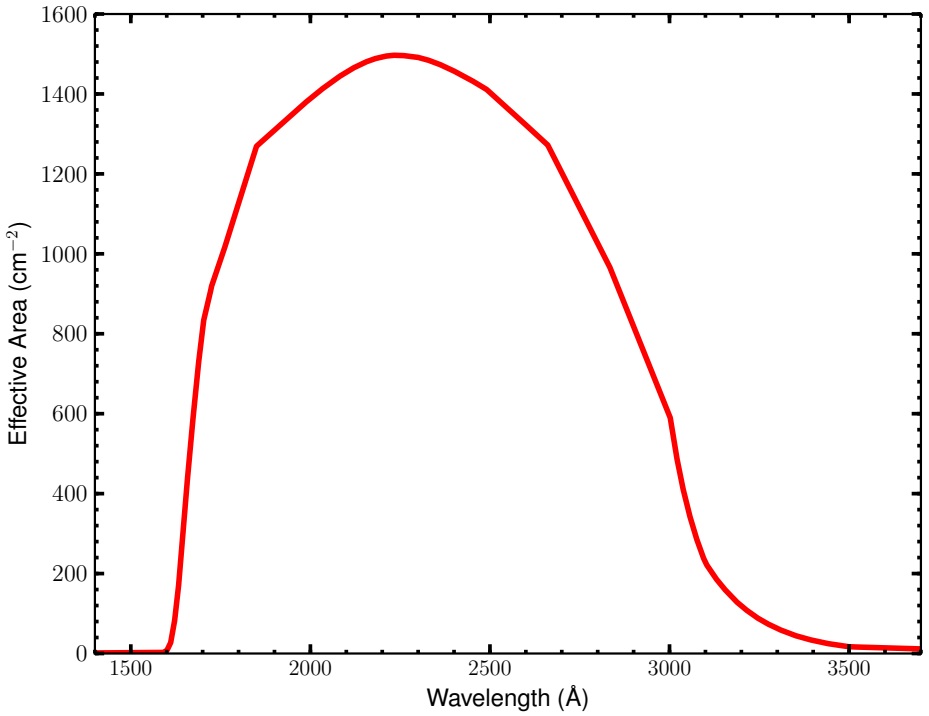

7.4 Image Characteristics

Figure 7.3 shows a typical image of a point source obtained during early in-flight testing of the NUV channel. Figure 7.4 shows a cut through this image along the *x* dimension. A two-dimensional Gaussian fit to the PSF has the following characteristics:

FWHM: 1.97 pixels = 47.1 mas

Fraction of light in brightest pixel: 13.4%

Note that the focus of *HST* changes during its orbit around the Earth. During the first few months of COS in-flight operations, typical image PSF FWHM values ranged from 1.8 to 2.4 pixels.

Figure 7.3: Two-dimensional PSF for COS in imaging mode.

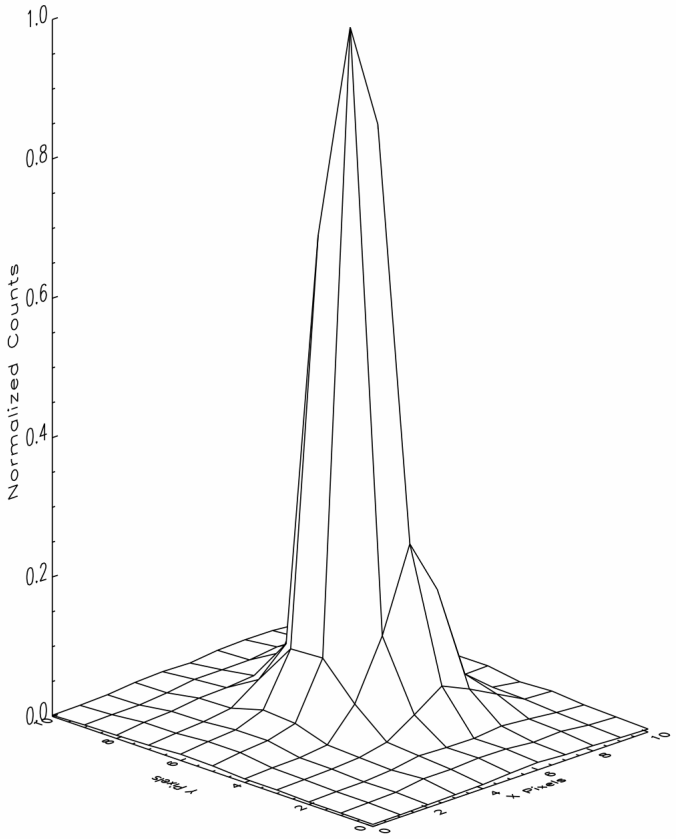

Figure 7.4: Profile through COS imaging PSF in the *x* direction.

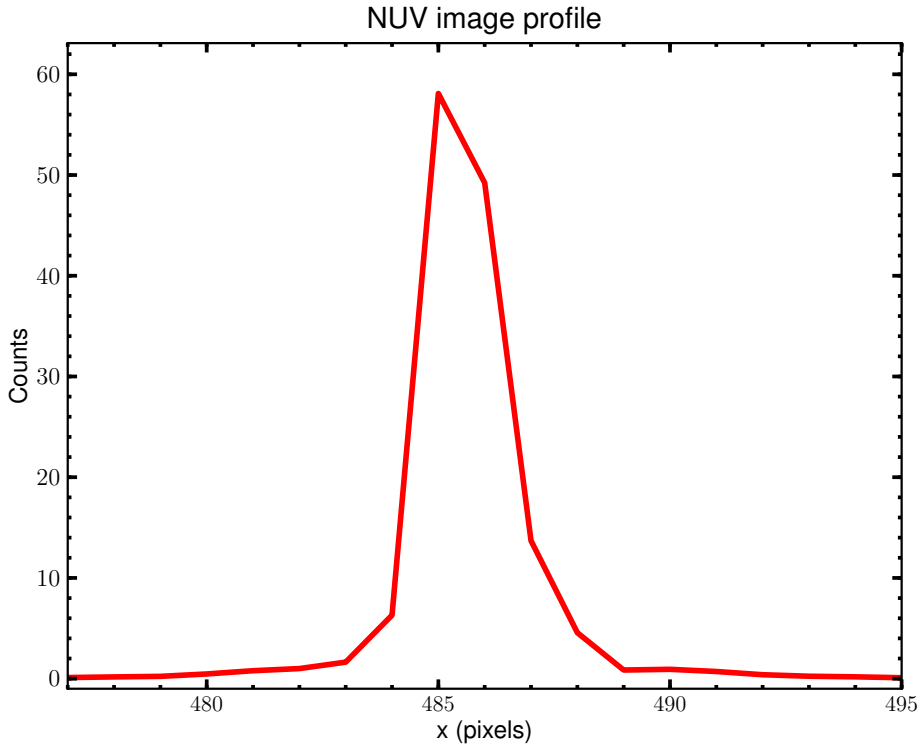

Profile through COS imaging PSF in the *x* direction. The red solid line represents a slice through the central row of the profile.

In imaging mode, COS sums all the light from about 1600 to 3300 Å. As discussed in Chapter 5, mid-frequency WFEs contribute significantly to the PSF wings at wavelengths < 2500 Å, so the spatial resolution of a point source will depend somewhat on its spectral energy distribution. For an M star, which has little flux at the shortest wavelengths, the image would be close to diffraction limited. For a hot star or a white dwarf, the mid-frequency WFEs would have the maximum impact on the spatial resolution.

Deep images taken during the first few months of on-orbit operations have revealed the detailed shape of the COS imaging PSF. Figure 7.5 shows the COS imaging PSF, averaged over 180 degrees of azimuth, and plotted on a log scale to reveal its extended wings. Figure 7.6 shows a 2-dimensional grey-scale image of a deep imaging observation that reveals two low-level "ghosts" located approximately 20 pixels to the right and the upper left of the center of the PSF. The peak intensity of the brightest of the two ghosts is roughly 0.1% of that of the main PSF. These features may complicate the analysis of faint objects located in the wings of a brighter object.

Figure 7.5: Extended wings in the COS imaging PSF.

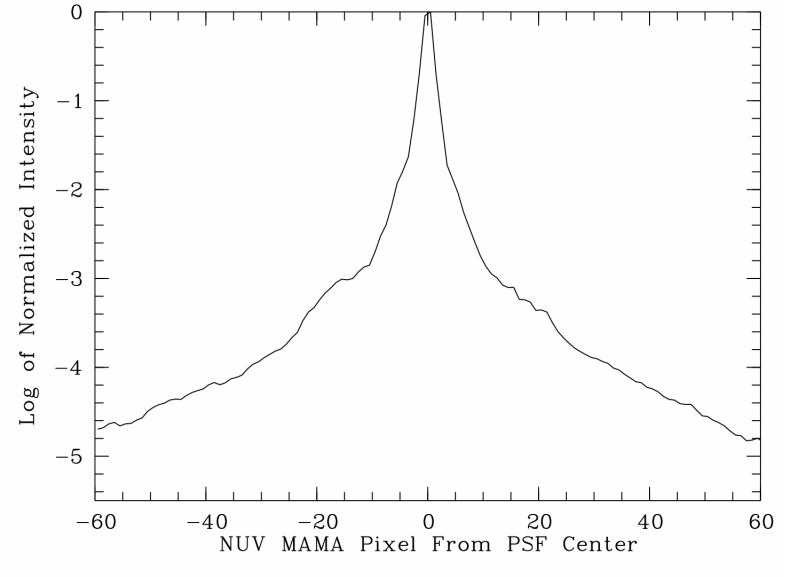

Azimuth-averaged COS imaging PSF plotted with a logarithmic intensity scale.

Figure 7.6: Ghosts in COS NUV Images.

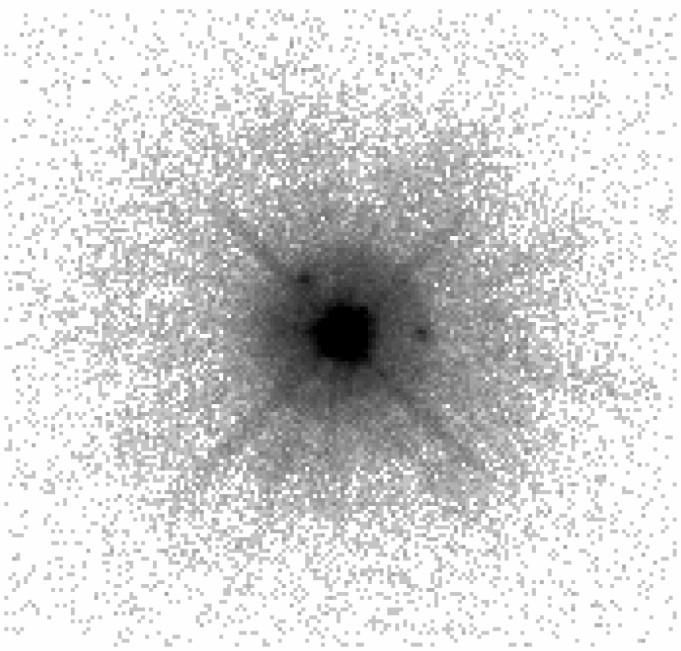

Negative greyscale rendering of a deep COS NUV image of a point source. This figure is plotted with a logarithmic intensity scale and covers about 6.5 arcsec along each axis. Note the two ghost images to the right and upper left of the center of the PSF.

CHAPTER 8:

Target Acquisitions

In this chapter…

8.1 Introduction

The COS apertures are 2.5 arcsec in diameter. An observation will yield good-quality data only if the target is properly centered. This chapter reviews the available acquisition methods, demonstrates the dependence of data quality on centering accuracy, and explains the available acquisition methods in detail.

Due to the combined uncertainties in the COS-to-FGS alignment and target coordinates in the GSC2/ICRS reference frame, we recommend that each visit begin with an `ACQ/SEARCH` target acquisition. APT will issue a warning if an acquisition is omitted. You are not required to perform a target acquisition with COS; however, if a visit does not begin with an `ACQ/SEARCH` exposure, and the observations fail because of an unsuccessful acquisition, then the observations will not be repeated.

Bright Object Protection

The COS detectors are vulnerable to damage or performance degradation if exposed to too much light. Imaging acquisitions are a special risk because they concentrate the light of an object on a small area of the detector. Users of COS must demonstrate that their targets are safe. Information on bright-object protection and screening is in Chapter 9.

8.2 A Quick Guide to COS Acquisitions

COS has four acquisition modes:

- **ACQ/SEARCH** performs a search in a spiral pattern by executing individual exposures at each point in a square grid pattern (details are in Section 8.5.2). This mode can use either dispersed-light or imaging exposures.
- **ACQ/IMAGE** obtains an NUV image of the target field, moves the telescope to center the object, and secures a second NUV image as a confirmation (details are in Section 8.3.3). This is generally the fastest method of target acquisition.
- **ACQ/PEAKXD** determines the centroid of the dispersed-light spectrum in the direction perpendicular to dispersion and moves the telescope to center the object in the cross-dispersion direction (details are in Section 8.5.3).
- **ACQ/PEAKD** centers the target in the dispersion direction by executing individual exposures at each point in a linear pattern along the dispersion axis (details are in Section 8.5.4). ACQ/PEAKXD should always precede ACQ/PEAKD, and the two should always be performed together.

Coordinate accuracy and target brightness will inform your choice of target-acquisition strategy and optional parameters. Table 8.1 lists the basic target acquisition scenarios and types discussed in later in this chapter.

Table 8.1: Basic COS Target Acquisition Scenarios.

Type	Step 1	Step 2	Step 3
Imaging	ACQ/SEARCH	ACQ/IMAGE	none
Dispersed-Light	ACQ/SEARCH	ACQ/PEAKXD	ACQ/PEAKD

Suggestions on acquisition strategy

An observer has many options for acquiring an object with COS, and each has its strengths and limitations. In particular, imaging acquisitions can be fast and precise, but the restrictions on local count rate (Chapter 9) can prohibit use of the PSA, even with MIRRORB. We suggest that you try the options in this order:

1. Imaging target-acquisition sequence (ACQ/SEARCH and ACQ/IMAGE) using the NUV channel and the fastest allowable aperture and mirror combination.
2. Dispersed-light acquisition using the same configuration as for the first science exposure that follows the acquisition, if it will use less time overall.
3. Dispersed-light acquisition with a different configuration, if it will use less time overall.

Recommendation: Begin each visit with an ACQ/SEARCH

Given the current uncertainties in the alignment of COS and the FGS and typical target-coordinate uncertainties in the GSC2/ICRS frame, STScI recommends that the target acquisition of each visit begin with an `ACQ/SEARCH` using a minimum 3 × 3 grid (`SCAN-SIZE=3`). You may use `SCAN-SIZE=2` if your coordinates are extremely good ($\sigma \leq 0.4$ arcsec) and should use `SCAN-SIZE=4` or `5` if your coordinates are uncertain (see Table 8.2). We recommend that grid points be separated by 1.767 arcsec (`STEP-SIZE=1.767`, which is the default).

Table 8.2: Recommended `ACQ/SEARCH SCAN-SIZE` values as a function of coordinate quality.

Recommended `SCAN-SIZE`	Coordinate uncertainty (arcsec)
3	σ <= 1.0
4	1.0 < σ < 1.3
5	1.3 < σ < 1.6

STScI does not recommend using an `ACQ/SEARCH` as your sole target-acquisition exposure, but in certain circumstances (e.g., extremely faint targets requiring long dwell times), you may chose to do so. In this event, the coordinate uncertainties in Table 8.2 must all be decreased by 0.5 arcsec. Please contact a COS Instrument Scientist if you are uncertain about the appropriate value of any target-acquisition parameter.

What happens if an acquisition fails?

The COS flight software takes the information gathered in an `ACQ/SEARCH` or `ACQ/IMAGE` exposure and applies a centroiding algorithm. If any stage of the target acquisition should fail, then the subsequent acquisition procedures in that visit (such as `ACQ/PEAKXD` or `ACQ/PEAKD`) will not be executed, but the science exposures will be. Note that *HST* will be left pointing at the last commanded position, which may differ substantially from the initial pointing.

Do I need to use the same set-up to acquire as to observe?

No. An NUV imaging acquisition is recommended in many cases because it is fast and accurate, even if you are then obtaining a spectrum with the FUV channel. If it is advantageous, you could, for instance, acquire with the FUV channel using dispersed light and then take an NUV spectrum. Any combination in any order is permissible, because both COS channels are always available for observations. The overheads involved in switching between various optical elements cost time; these can be evaluated using APT. We suggest that you compare using an NUV `ACQ/IMAGE` and a dispersed-light acquisition that uses the same configuration as your science exposure to see the relative times needed.

The specifications of a COS acquisition are left to the observer. However, if in Cycle 18 you do not use an appropriate ACQ/SEARCH at the beginning of a visit, and your observations fail because COS failed to find the target, then STScI will not repeat those observations. Should future improvements in the alignment of COS and FGS allow us to relax this requirement, new instructions will be published before the Cycle 18 Phase II deadline.

8.3 Centering Accuracy and Data Quality

8.3.1 Centering Accuracy and Photometric Precision

Figure 8.1 shows the relative transmission of the PSA as a function of the displacement of a point source from the aperture center, as measured through each of the three FUV gratings. The NUV throughput is plotted in Figure 8.2. The curves are nearly identical, though the throughput of the low-resolution gratings falls off more steeply at offsets greater than 0.5 arcsec.

The spatial resolution of COS is sufficient to separate spectra of equally bright objects that are 1 arcsec apart in the cross-dispersion direction; see Section 6.1.6. If placed at ± 0.5 arcsec from the aperture center, both objects will receive essentially full throughput.

8.3.2 Centering and Wavelength Accuracy

To achieve a wavelength accuracy of 15 km/s, the target should be centered to within about 0.05 arcsec for NUV observations and 0.1 arcsec for FUV (approximately 2 pixels for the NUV and 4 pixels for the FUV, or 2/3 of a resolution element). COS imaging acquisitions can achieve a centering precision of about 0.025 arcsec.

Dispersed-light `ACQ/SEARCH` acquisitions, whether with the FUV or NUV detector, typically provide centering accuracies of only about 0.3 arcsec. Therefore, additional peak-up acquisitions in both the cross-dispersion and along-dispersion directions are required. Typical centering accuracies for both `ACQ/PEAKXD` and `ACQ/PEAKD` sequences are less than 0.05 arcsec.

As noted above, the throughput of COS is little affected by centering errors of less than 0.5 arcsec, so a high centering precision is not strictly necessary if your science goals do not require an absolute wavelength scale. For example, the spectra of some objects may include foreground interstellar or inter-galactic absorption lines that can be used to establish relative velocities.

Figure 8.1: Relative Transmission of the COS PSA at FUV Wavelengths

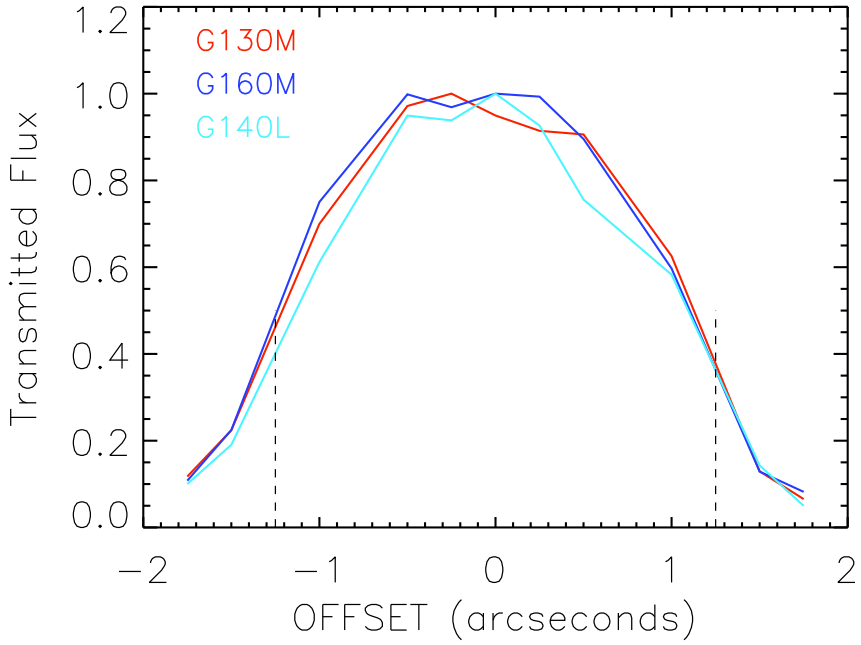

Transmitted flux as a function of displacement from aperture center in the cross-dispersion direction for all three FUV gratings. The dotted lines mark the edge of the aperture (1.25”). For all gratings, the absolute transmission for a centered point source is at least 95%.

Figure 8.2: Relative Transmission of the COS PSA at NUV Wavelengths

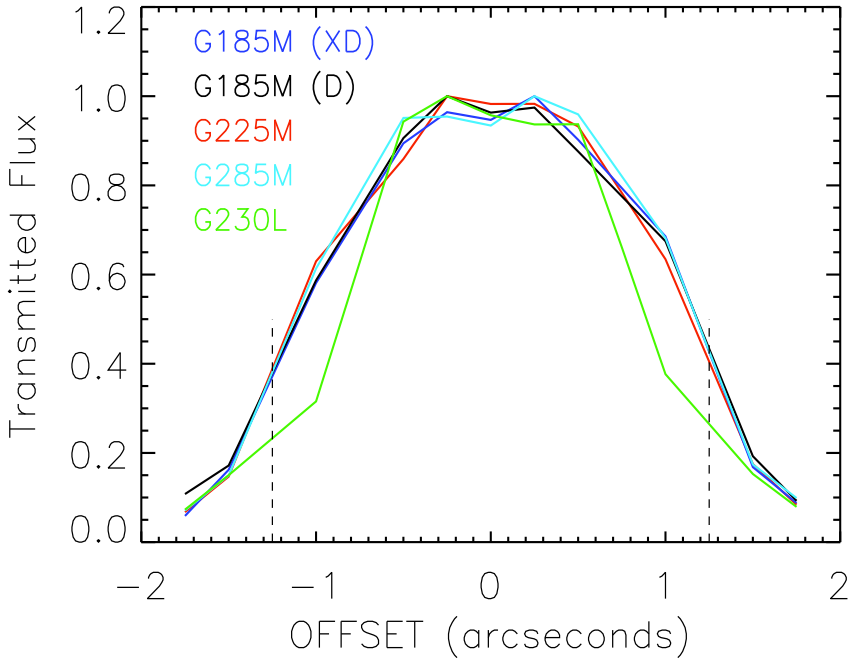

Transmitted flux as a function of displacement from aperture center for all four NUV gratings. The dotted lines mark the edge of the aperture (1.25”). The two curves labeled D and XD refer to offsets along the dispersion and cross-dispersion axes, respectively. The other curves trace offsets in the cross-dispersion direction. For all gratings, the absolute transmission for a centered point source is at least 95%.

8.3.3 Centering Accuracy and Spectroscopic Resolution

Targets centered within the central 0.5 arcsec of the science aperture will achieve maximum spectral resolution. Centering errors larger than 0.5 arcsec will lead to progressively poorer resolution. Targets at the edge of the aperture have approximately half the throughput and spectral resolution of well-centered targets.

8.4 Imaging Acquisitions

Observers will often acquire their targets in imaging mode using `ACQ/SEARCH` and `ACQ/IMAGE` in sequence. Imaging-mode acquisitions employ the COS NUV detector and either `MIRRORA` or `MIRRORB` instead of a grating. (In all other respects, the `ACQ/SEARCH` procedure is the same as for an acquisition in dispersed light; see Section 8.5). As noted above, both COS detectors are available for use, so little time is lost in switching from an NUV acquisition to an FUV spectrum (approximately 2 minutes; see Chapter 10). Occasionally, an FUV dispersed-light acquisition may be more efficient than an imaging acquisition, so you should always check.

An `ACQ/IMAGE` exposure consists of the following steps:

1. The shutter is opened and a target-acquisition image is obtained. The telescope is not moved, meaning that an acquisition using `ACQ/IMAGE` will be successful only if the target lies within the aperture. An area of 170 × 170 pixels, which corresponds to approximately 4 × 4 arcsec, centered on the aperture, is then read out. This image is recorded and downlinked, and becomes part of the archived data package.
2. A 9 × 9 pixel checkbox array is then passed over the 170 × 170 pixel image. First, the checkbox with the most counts is identified. In the unlikely instance that two checkboxes have equal counts, the first one encountered is used. The 9 × 9 array centered on that brightest pixel is then analyzed using a flux-weighted centroiding algorithm to calculate the target position.
3. An exposure of the internal PtNe lamp is obtained through the WCA aperture. The centroid of the WCA image is calculated by the onboard software. Using the known offset between the center of the WCA and the science apertures (PSA or BOA), the location of the center of the science aperture on the detector is computed.
4. Finally, *HST* is moved to place the calculated centroid at the center of the selected aperture, as calculated in step 3 above. Another exposure is taken and recorded for later downlink as a verification of the centering. Note that NUV `ACQ/IMAGE` exposures require two minutes plus twice the exposure time specified for the acquisition image.

Figure 8.3: Exposure Time Needed for ACQ/IMAGE Acquisition.

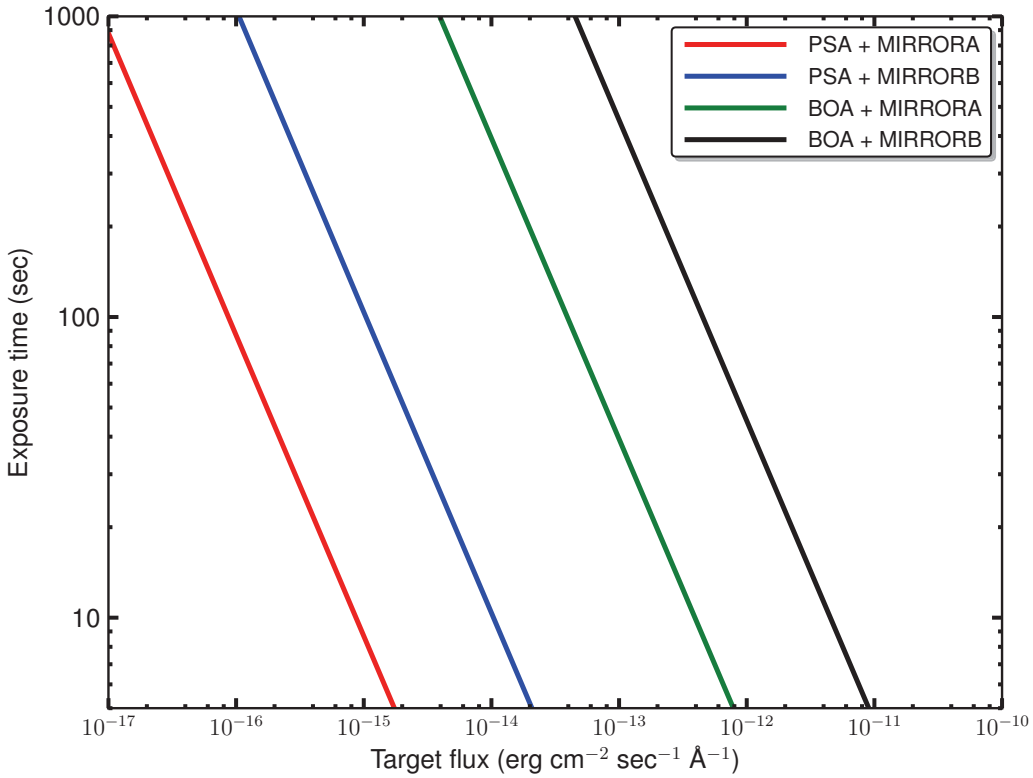

Exposure time needed to achieve S/N = 40 (PSA) or 60 (BOA) as a function of target flux. This calculation assumes a flat source spectrum.

8.4.1 Exposure Times

Acquisition images obtained through the PSA should strive for a minimum S/N = 40; those obtained through the BOA should have S/N = 60. Figure 8.3 shows approximate acquisition exposure times needed to reach these S/N levels for various target fluxes. A flat source spectrum is assumed. For more on acquisition exposure times, see Section 8.7.

8.4.2 Imaging Acquisitions with MIRRORB and/or the BOA

`MIRRORB` is not a separate optical element but is instead `MIRRORA` oriented so that light is reflected by the order-sorting filter in front of the mirror. Light reflecting off the back of this filter forms a secondary peak with approximately half the intensity of the primary peak and displaced by 20 pixels (about 0.5 arcsec) in the *x* (dispersion) direction. There is some overlap between the wings of the primary and secondary peaks, but they are well enough separated to allow for reliable acquisitions (see Figure 8.4). The recommended S/N for `MIRRORB` acquisitions refers only to the primary image; the COS ETC performs this calculation appropriately.

Figure 8.4: Cross section of an image obtained with MIRRORB.

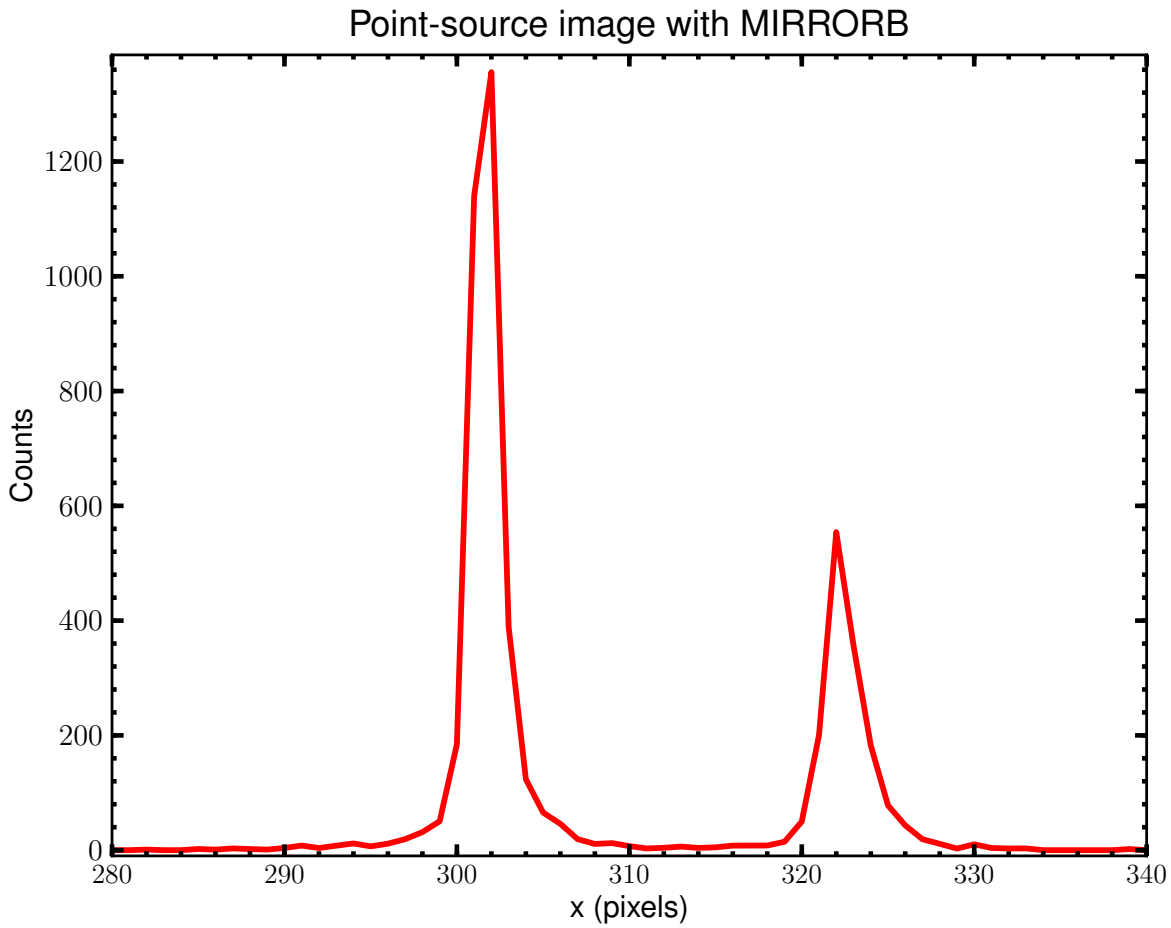

Cross section through the center of an image obtained with the PSA and `MIRRORB`. The secondary peak has an amplitude about half that of the primary peak and is displaced by 20 pixels (center to center) in the *x* (dispersion) direction.

Figure 8.5: NUV image of a point source observed with the BOA.

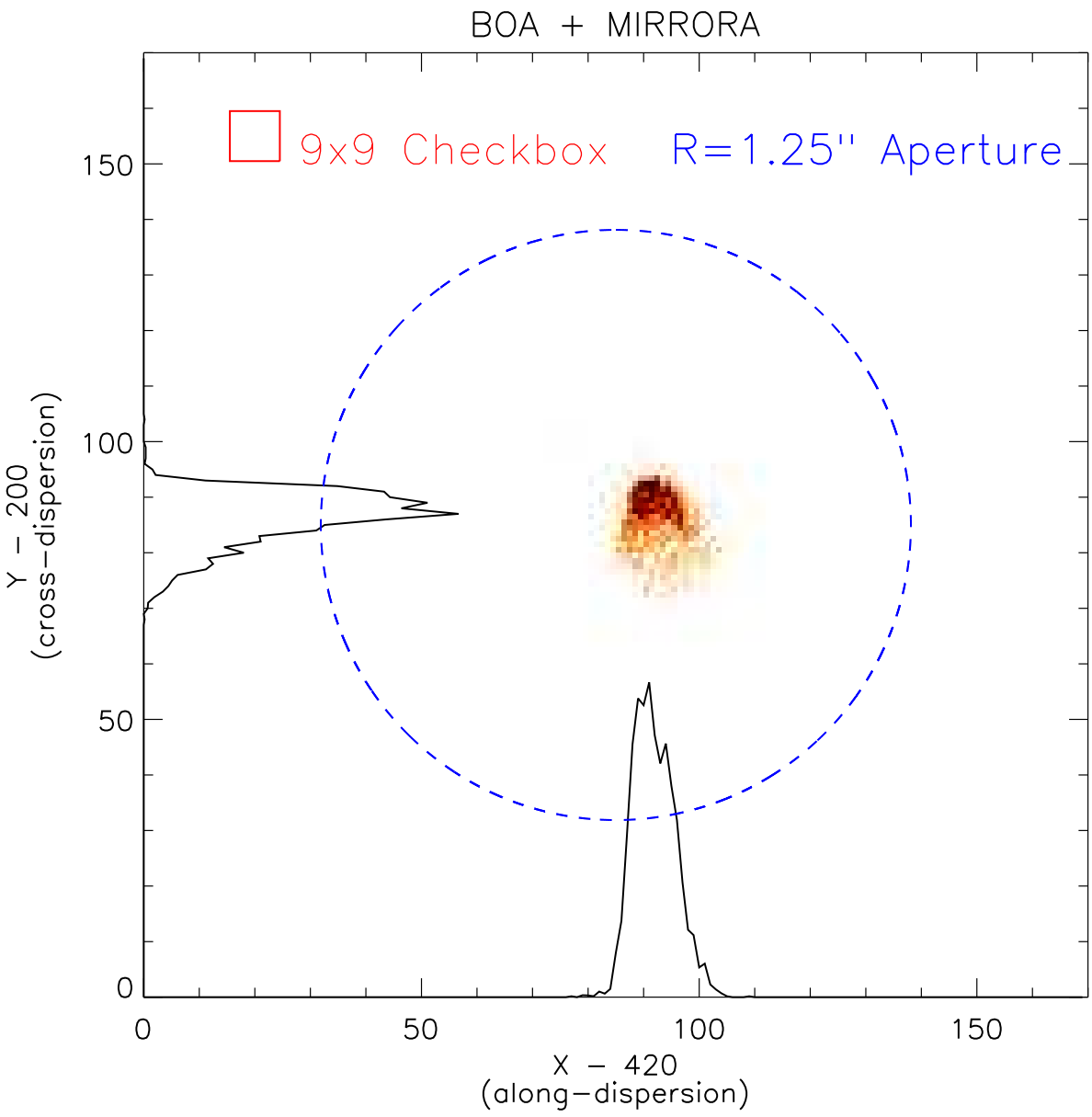

NUV image of a point source observed through the BOA aperture using MIRRORA. The limits of the plot represent the 170 × 170 pixel image discussed in Section 8.3.3. Also shown are the COS aperture (blue circle of radius 1.25") and the 9 × 9 checkbox used by ACQ/SEARCH. The dispersion and cross-dispersion axes show the one-dimensional light distributions on this un-centered target. This pointing is typical of that expected after an ACQ/SEARCH, but before additional peak-ups.

When the BOA is used, the slight wedge shape of its neutral-density filter produces a chevron-like image whose peak is displaced in both the dispersion and cross-dispersion directions (Figure 8.5). When the BOA is used with MIRRORB, two distorted peaks result (Figure 8.6). Because of the complex shape of images obtained through the BOA, a S/N of 60 in the primary image is required to center the target.

Figure 8.6: NUV image of a point source observed using both the BOA and MIRRORB.

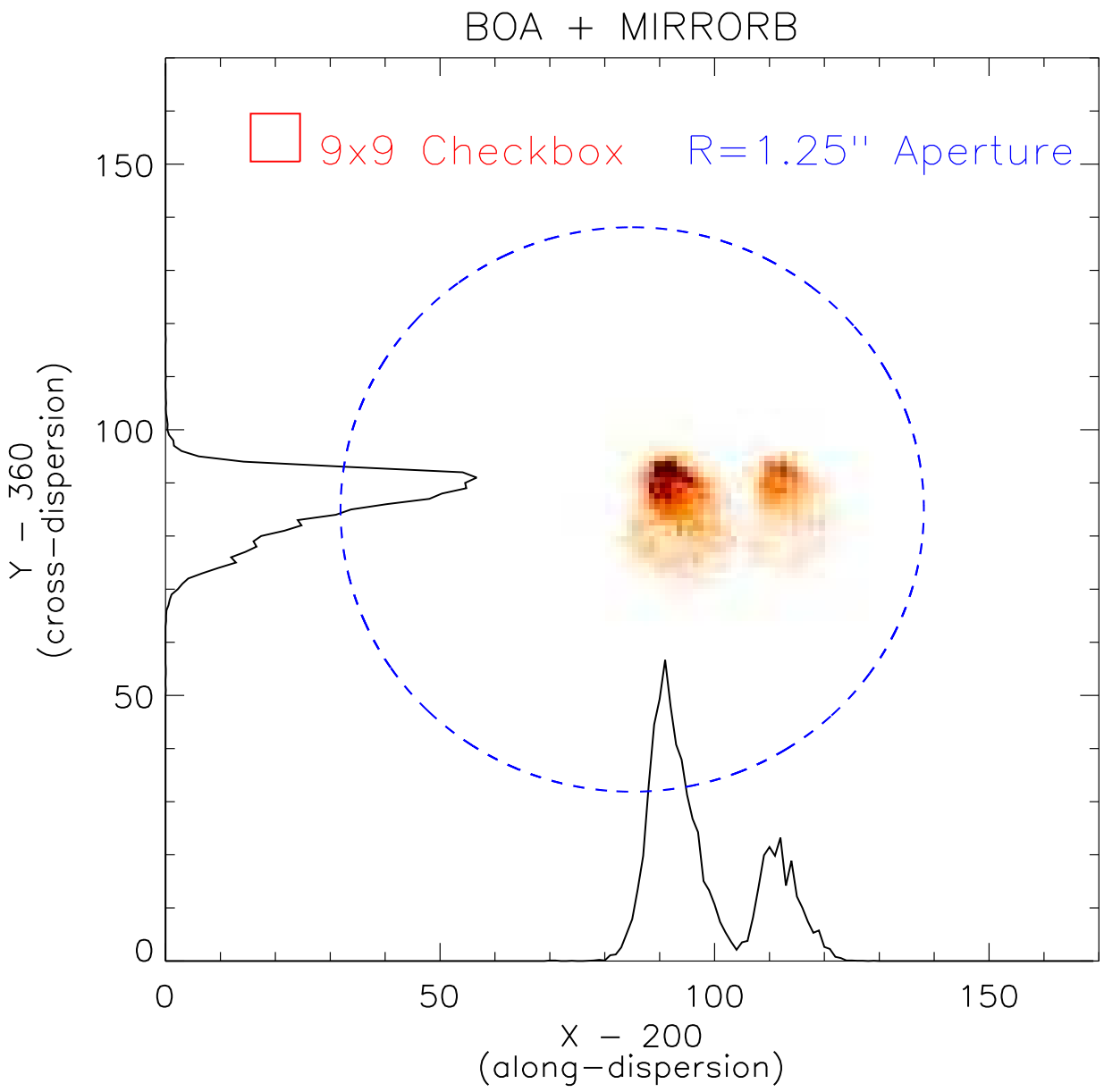

NUV image of a point source observed through the BOA aperture using MIRRORB. The secondary peak is offset along the dispersion dimension. The limits of the plot represent the 170 × 170 pixel image discussed in Section 8.3.3. Also shown are the COS aperture (blue circle of radius 1.25") and the 9 × 9 checkbox used by ACQ/SEARCH. The dispersion and cross-dispersion axes show the one-dimensional light distributions on this un-centered target. This pointing is typical of that expected after an ACQ/SEARCH, but before additional peak-ups.

8.5 Dispersed-Light Acquisitions

COS can find and center a source in the selected aperture using either its FUV or NUV dispersed spectrum. Depending on the relative target fluxes and instrument efficiencies, a dispersed-light acquisition may be more efficient than an imaging one.

8.5.1 Dispersed-light Acquisition Summary

A typical dispersed-light acquisition consists of three steps:

1. A search (using ACQ/SEARCH) is carried out, in a spiral pattern, making a square with 2, 3, 4, or 5 points on a side. At each scan point, the telescope stops and an integration is taken. After completion of the full $n \times n$ pattern, the target's position is calculated, and the telescope is moved to center the target.
2. A peak-up in the cross dispersion direction is performed to improve the centering (PEAKXD).
3. A peak-up in the along-dispersion direction is performed (PEAKD).

The last two steps should be always be performed in the order indicated (PEAKXD then PEAKD). In rare circumstances (discussed below), the peak-up stages may be omitted or replaced by a 2 × 2 ACQ/SEARCH. Any step may be performed more than once to improve the centering. As a result, there is a huge number of ways to acquire a target and improve its centering. Here we will concentrate on some specific scenarios that generally achieve good results in a reasonable amount of time.

Note: Airglow (or geocoronal) emission features fill the aperture and could confuse the centering algorithms. The problem is averted by ignoring portions of the detector illuminated by airglow features. It is done by using sub-arrays on the detector and is performed automatically by the flight software.

8.5.2 ACQ/SEARCH: The Spiral Target Search

Specifications and considerations for dispersed-light ACQ/SEARCH acquisitions are similar to those for imaging ACQ/SEARCH acquisitions. In ACQ/SEARCH mode, the telescope is moved in a spiral pattern to cover a square grid up to 5 × 5 steps in size (Figure 8.7). If the uncertainty in your target coordinates is <= 1 arcsec in the GSC2/ICRS reference frame, then a 3 × 3 search using a STEP-SIZE of 1.767 arcsec should work well (see Table 8.2).

You will need to specify:

- The aperture to use, either PSA or BOA.
- The spectral element (i.e., grating) to be used and the central wavelength setting. In general this will be the same as the grating and central wavelength to be used for the science observation. However, an observer may acquire with a different grating + central wavelength combination if there are advantages to doing so.
- The SCAN-SIZE, which is 2, 3, 4, or 5, corresponding to spiral patterns of 2 × 2, 3 × 3, etc.

- The STEP-SIZE, or spacing between grid points. A value of 1.767 arcsec is recommended.
- The exposure time per dwell point.
- For FUV searches, you can choose to use just one of the segments, A or B, but use of both (the default) is recommended.

Large SCAN-SIZE values should be used only in cases where the target coordinates have large uncertainties (see Table 8.2). A 3 × 3 pattern should be adequate in virtually all cases. Note that the even SCAN-SIZE values (2 or 4) trigger an additional overhead because of the telescope motion required to displace the aperture by half of a STEP-SIZE in both the dispersion and cross-dispersion directions. This is so the overall pattern remains centered on the initial pointing.

The STEP-SIZE parameter determines the spacing, in arcsec, between dwell points in the pattern. It may be any value from 0.2 to 2.0 arcsec, but we strongly recommend using the default value of 1.767 arcsec. This value has been chosen so that no part of the sky is missed, given the 2.5 arcsec diameter aperture ($2.5/\sqrt{2} = 1.767$).

To calculate the total time needed for an FUV ACQ/SEARCH:

1. Add 20 sec to the exposure time to be used at each dwell point.
2. Multiply this value by the number of dwell points *n* (or, for even values of SCAN-SIZE, *n+1*).
3. Add any overheads (from Table 10.2) required to put in place the spectral element you will use. Note that G130M at central wavelength 1309 is in position by default at the start of a new visit.

Finding the Source

Once the integrations are complete, the flight software determines what point in the array contains the source. There are three options:

1. The default option is CENTER=FLUX-WT, which uses a flux-weighted centroiding procedure to determine the center of light.
2. A variation on CENTER=FLUX-WT is FLUX-WT-FLR. In this case, a floor is subtracted from the counts at each dwell point before the centroid is computed. The floor is taken as the minimum number of counts seen in any one dwell point. FLUX-WT-FLR has the advantage of removing background counts, but leaves one or more points in the array with zero. This can cause computational problems; as a result, FLUX-WT-FLR may not be used with SCAN-SIZE=2.
3. The last option for centering is to use CENTER=BRIGHTEST, which simply centers the dwell point with the most counts. This is straightforward but not as accurate as the centroiding methods. Some examples where CENTER=BRIGHTEST is appropriate: you are uncertain of your coordinates and will follow the initial ACQ/SEARCH and CENTER=BRIGHTEST with an a second ACQ/SEARCH using flux-weighted centering or ACQ/IMAGE; or your source is extended and you want only to be sure that the brightest point is in the aperture.

For all values of `SCAN-SIZE` ***greater than 2, we recommend*** `CENTER=FLUX-WT-FLR`.

Figure 8.7: Example of a 3 × 3 Spiral Search Pattern.

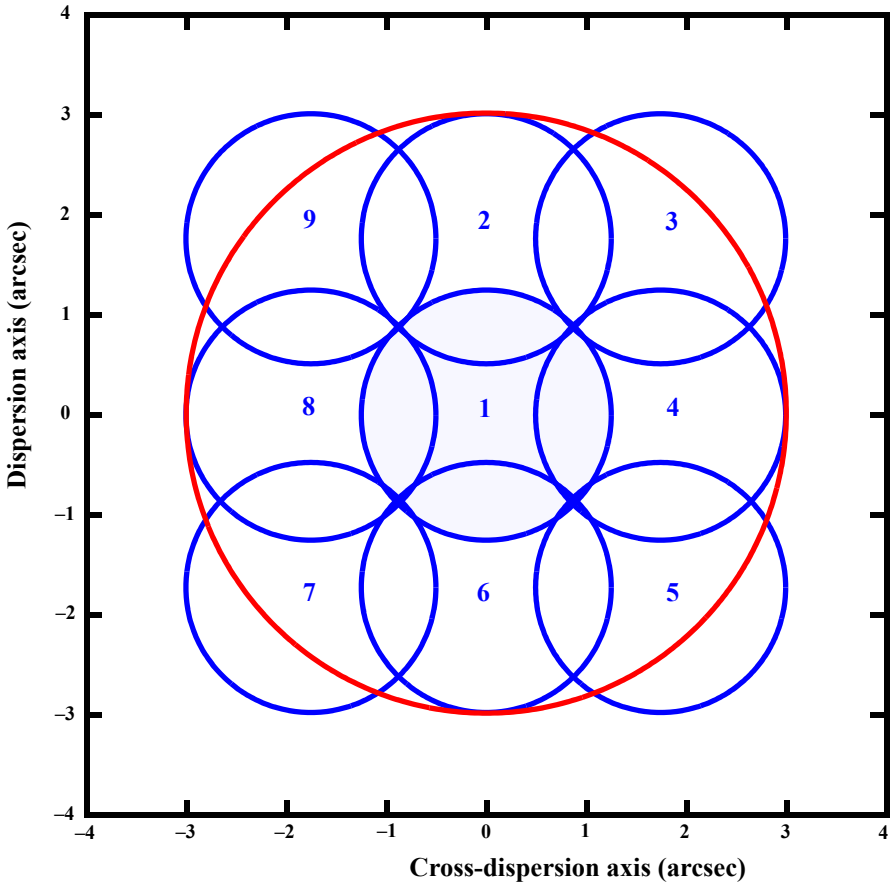

This example was executed with the default STEP-SIZE of 1.767 arcsec. The blue circles represent the nine positions of the aperture, each 2.5 arcsec in diameter, and the numbers show the sequence of steps. The large outer circle in red has a radius of ~ 3 arcsec. An initial pointing that was good to 1 arcsec (1σ) would result in a successful acquisition with a 3 × 3 pattern 99.5% of the time.

Figure 8.8: Exposure Times for Dispersed-Light Acquisitions.

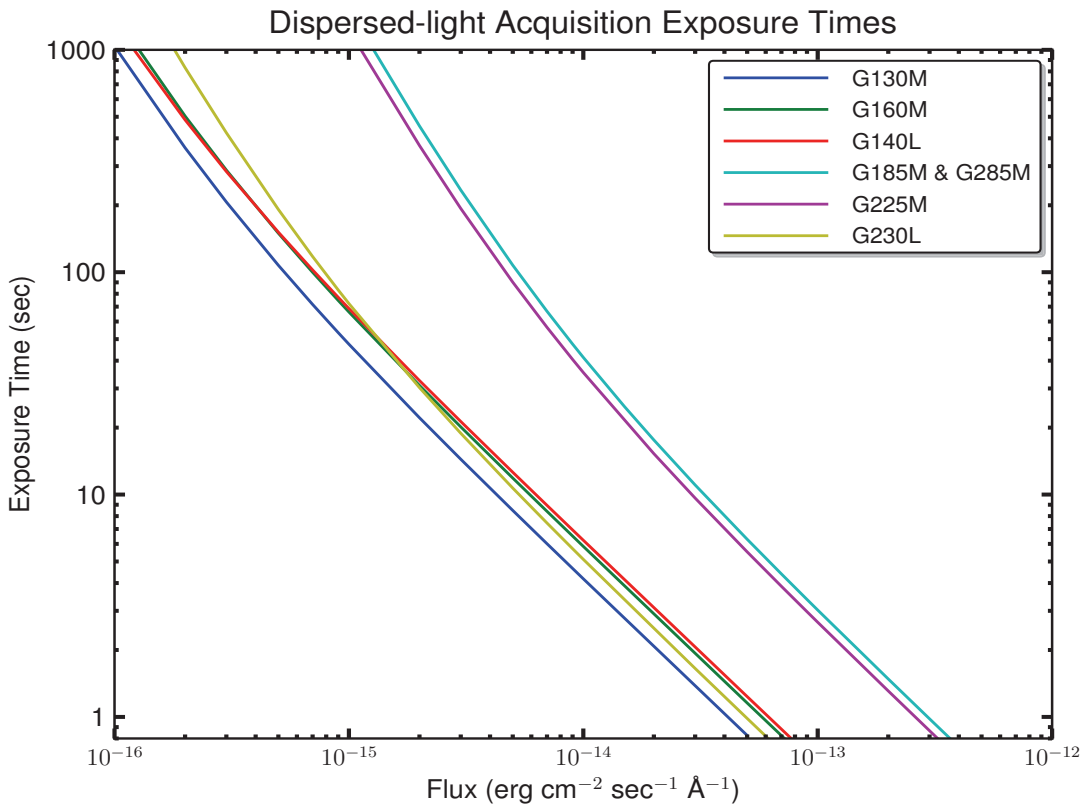

Approximate exposure time needed to achieve a S/N of 40, assuming a flat source spectrum.

Exposure Times

Figure 8.8 is a guide to the exposure time needed for a dispersed-light acquisition. The COS acquisition ETC should always be used to get actual values. Note that these exposure times apply to each separate dwell point of a pattern, which is the quantity entered into APT in Phase II. For more on acquisition exposure times, see Section 8.7.

Quality of Centering After ACQ/SEARCH

A single `ACQ/SEARCH` stage, using `CENTER=FLUX-WT` or `CENTER=FLUX-WT-FLR`, generally places a source within 0.3 arcsec of the aperture center in both in the dispersion and cross-dispersion directions. `ACQ/SEARCH` stages using `FLUX-WT-FLR` are slightly more accurate due to better sky and detector background suppression; however, `FLUX-WT-FLR` should not be used in `ACQ/SEARCH` stages with `SCAN-SIZE=2`.

See Table 8.3 for a summary of ACQ/SEARCH parameter choices.

8.5.3 PEAKXD: Peaking up in the Cross-dispersion Direction

To improve centering in the cross-dispersion direction after an initial ACQ/SEARCH, an ACQ/PEAKXD sequence may be used. The steps executed in an ACQ/PEAKXD sequence are

- A spectrum is recorded for the user-specified time using a sub-array (to remove edge effects and airglow lines) tailored to each grating setting.
- The location of the spectrum in the cross-dispersion direction is computed.
- This location is compared to a similar calculation for an automatically generated short exposure of the PtNe wavelength calibration lamp through the WCA aperture, and the shift necessary to center the target spectrum in the desired aperture is computed.
- The telescope is then slewed by this offset to center the target in the cross-dispersion direction.

The total duration of an ACQ/PEAKXD is 80 seconds for FUV, 70 seconds for NUV, plus the exposure time, plus any overhead required for an OSM movement (Table 10.2). ACQ/PEAKXD centers a source in the cross-dispersion direction to within 0.05 arcsec in almost all cases.

To schedule an ACQ/PEAKXD exposure, specify the aperture (PSA or BOA, the same as for your science exposure, in general), the grating and central wavelength, and the exposure time. (Because ACQ/PEAKXD is used only for dispersed-light acquisitions, the use of MIRRORA or MIRRORB is not allowed.) For NUV ACQ/PEAKXD acquisitions, you can specify which stripe (SHORT, MEDIUM, or LONG, corresponding to stripes A, B, or C) to use for the computations; however, the default stripe B (MEDIUM) is usually appropriate and achieves better centering than the other stripes. For FUV ACQ/PEAKXD acquisitions, you can choose to use just one of the segments, A or B, but use of both (the default, except for G140L) is recommended. By default, only segment A is used with G140L.

We recommend a minimum S/N = 40 for ACQ/PEAKXD exposures. STScI calibration programs routines use up to S/N = 100 when precise pointing is required.

See Table 8.3 for a summary of ACQ/PEAKXD parameter choices.

8.5.4 PEAKD: Peaking up in the Along-dispersion Direction

Centering in the dispersion direction helps to ensure the accuracy of the wavelength scale. ACQ/PEAKD works very much like ACQ/SEARCH except that, instead of a spiral, the spacecraft is moved linearly along the dispersion axis between exposures. The centroid is computed, and the telescope is moved to center the target in the aperture.

The user must specify the aperture, grating and central wavelength, and the exposure time at each dwell point. (The use of MIRRORA or MIRRORB is not allowed.) The number of steps may be 3, 5, 7, or 9. Although NUM-POS=3 is currently the default, we recommend using NUM-POS=5. The STEP-SIZE depends on the number of positions sampled. If NUM-POS=3 or 5, then we recommend

STEP-SIZE=1.2 arcsec. If NUM-POS = 7 or 9, then STEP-SIZE=1.0 arcsec is recommended.

As with ACQ/SEARCH, there are three options for the centering algorithm, CENTER=FLUX-WT, FLUX-WT-FLR, and BRIGHTEST, and they work just as described above. We recommend use of the special parameter CENTER=DEFAULT, which uses FLUX-WT if NUM-POS=3, but FLUX-WT-FLR if NUMPOS=5, 7 or 9.

To determine the duration of an ACQ/PEAKD sequence, add 20 seconds to the exposure at each dwell point and multiply the sum by the number of dwell points. Overheads for OSM movements (Table 10.2 and Table 10.3) must also be added.

For FUV ACQ/PEAKD acquisitions, you can choose to use just one of the segments, A or B, but use of both (the default, except for G140L) is recommended.

We recommend a minimum S/N = 40 for ACQ/PEAKD exposures. STScI calibration programs routines use up to S/N = 100 when precise pointing is required.

See Table 8.3 for a summary of ACQ/PEAKD parameter choices.

8.5.5 Examples of Dispersed-Light Acquisitions

Here are some examples of dispersed-light acquisition strategies that were successfully employed during SMOV:

1. QSOs often have both a blue continuum and strong FUV emission lines (such as Ly α or C IV λ1550), making them brighter in the FUV than the NUV. Observations of Mrk 817 and PKS 0405-123 used a 3 × 3 ACQ/SEARCH in dispersed light, followed by ACQ/PEAKXD and ACQ/PEAKD.
2. Cool stars are characterized by strong FUV emission lines and a weak NUV continuum. The brown-dwarf program employed a 3 × 3 ACQ/SEARCH and an ACQ/PEAKXD for the brightest target, but dropped the peak-ups altogether for the fainter targets, because the acquisitions became prohibitively long.
3. The supernova remnant N13D has bright OIV] λ1400, CIV λ1550, and OIII] λ1664 emission lines. Monte Carlo simulations indicated that a 3 × 3 ACQ/SEARCH followed by a 2 × 2 ACQ/SEARCH (with no peak-ups) was the best approach.

Several SMOV calibration programs used a 3 × 3 ACQ/SEARCH followed by a 2 × 2 ACQ/SEARCH to achieve centering equivalent to that obtained by programs using a combination of ACQ/PEAKXD and ACQ/PEAKD stages.

Table 8.3: COS Acquisition Modes

Acquisition Type	Description	SCAN-SIZE	STEP-SIZE (arcsec)	Optional Parameters	Recommended Values	Required S/N
ACQ/ SEARCH	Spiral pattern; multiple exposures	2	1.767	CENTER= FLUX-WT, FLUX-WT-FLR, BRIGHTEST	FLUX-WT	40
		3[1]			FLUX-WT-FLR	
		4			FLUX-WT-FLR	
		5			FLUX-WT-FLR	
ACQ/ PEAKXD	One exposure			For FUV: SEGMENT= A, B, BOTH For NUV: STRIPE= SHORT, MEDIUM LONG	SEGMENT=BOTH STRIPE=MEDIUM (These are the default values.)	40 to 100
ACQ/ PEAKD[2]	Linear pattern; multiple exposures	3	1.2	CENTER= FLUX-WT, FLUX-WT-FLR, BRIGHTEST	FLUX-WT	40 to 100
		5[1]	1.2		FLUX-WT-FLR	
		7	1.0		FLUX-WT-FLR	
		9	1.0		FLUX-WT-FLR	
ACQ/ IMAGE	Initial and confirm images					40 (PSA) 60 (BOA)

1. Recommended value.
2. For ACQ/PEAKD, use of the special parameter CENTER=DEFAULT, which sets CENTER=FLUX-WT if NUM-POS=3, but FLUX-WT-FLR if NUMPOS=5, 7 or 9, is recommended.

8.6 Acquisition Techniques for Crowded Regions

Acquiring targets that lie in crowded regions can be difficult. For the present, it is necessary to first acquire a nearby point source that is isolated enough not to cause problems (at least 5 arscec from another UV source), and to then offset to the desired object. This method would also work for objects that are not quite point sources themselves. Table 10.1 lists spacecraft movement overheads that typically require less than one minute.

When performing offset acquisitions, you should refine the centering of the initial target before offsetting. Be aware that bright object concerns will apply over a broader region. In some cases, you may be able to use a roll-angle constraint to avoid nearby objects in a crowded region.

8.7 Acquisition Exposure Times

Always use the COS ETC to calculate acquisition exposure times for your target and APT to estimate the time required to perform the acquisition. Separate ETC tools are provided for imaging and dispersed-light acquisitions. In either case, be sure to bracket the parameters of the source you are acquiring. For example, if you are acquiring a star and its unreddened color corresponds to about A5V, you may wish to try the different versions of "A5V" that are available as options in the ETC to see what range of exposure times results; they will not be identical. In general, the Kurucz models are to be preferred in the ultraviolet. The library spectra that are used to carry out these calculations can be downloaded from the ETC so that one can examine the alternatives. In addition, we recommend that you try model atmospheres that are one type hotter and cooler than the nominal type to get a sense of the possible range of UV brightness the source may produce. The COS ETC includes QSO spectra, blackbodies, and power-law continua. Estimating ultraviolet fluxes from optical data introduces many uncertainties. These can be reduced by using actual UV data (*FUSE, Galex, HST*, etc.); see below.

Acquisition exposure times for variable objects

With variable objects (such as AGNs) it is important to calculate the acquisition exposure time carefully. The following strategy has been adopted by the COS GTOs in preparing their Phase II programs:

1. Start by using the brightest flux that has been observed for the object. Use this brightest flux both for BOP checking (Chapter 9) and for the acquisition strategy. If only one observation is available for the source, use a value higher by a factor of 2.5 (one magnitude) for BOP checking.

2. When calculating the Time_per_exposure to reach a particular S/N, use the minimum flux that has been observed. If only one observation is available, use 1/2 that flux.

Using *Galex* fluxes to calculate exposure times

Much of the sky has now been mapped by the *Galaxy Evolution Explorer*, or *Galex*. *Galex* images are taken in two broad UV passbands that are centered at about 1400 Å (*Galex* FUV) and 2300 Å (*Galex* NUV).

The *Galex* NUV images are especially helpful for planning acquisitions since the *Galex* NUV passband is similar to the NUV imaging passband for COS. Within APT, you can retrieve both *Galex* images (on the left side of the Load window), and the *Galex* source catalog from MAST (click the bottom button on the right side of the Load window). The *Galex* images can be helpful for clearing objects when doing Bright Object Protection (BOP) checking (Chapter 9). For acquisitions, the *Galex* NUV AB magnitude can be used in the COS ETC as a value to which the calculation is normalized. The choice of source type can still be important even with this measured UV flux.

Note that in some cases the display of *Galex* catalog sources within Aladin may appear odd. This is because only 10,000 sources can be displayed at one time. This problem should go away once you zoom in on your target or specify a smaller display region.

8.8 Early Acquisitions and Preliminary Images

In some situations, an observer may need to get an independent ultraviolet image of a region in order to be sure that no objects violate safety limits and that the target to be observed can be acquired by COS successfully. Such an early acquisition should be included in the Phase I proposal, and the observation should not use a photon-counting detector. The UVIS channel on WFC3 is recommended, but observers are encouraged to consult with an STScI instrument scientist.

CHAPTER 9:

Bright-Object Protection

In this chapter…

9.1 Introduction

Both the FUV XDL and the NUV MAMA detectors are subject to damage or destruction by excessive illumination. An excessive local count rate can reduce the sensitivity of the affected detector region; the most likely causes are a spectral emission line or direct imaging (in the NUV). A global over-illumination of the detector can result in its loss. To protect the detectors, on-board software monitors the local and global counts rates, shuttering the instrument in case of a local violation, and lowering the high voltage if a global violation is detected. The local rate is checked before an exposure is begun, while the global rate is monitored continuously during the exposure. Under certain circumstances, damage could result despite the onboard mechanisms, and in any event lowering the high voltage will disrupt the *HST* schedule and operations, so all proposed COS observations must meet count-rate screening limits with safety margins to allow for uncertainties. COS is currently the only *HST* instrument to use UV detectors for acquisitions; such acquisitions must be screened, as well. It is the responsibility of the observer to screen all proposed targets and of STScI to check and enforce these limits. The COS Bright Object Protection (BOP) policies and procedures are described in this chapter.

Table 9.1: COS Count Rate Screening Limits.

Detector	Source type[1]	Type of limit	Limiting count rate (counts / sec)
FUV	predictable	global	15,000 per segment
		local	0.67 per pixel
	irregular	global	6,000 per segment
		local	0.67 per pixel
NUV	predictable	global	170,000 (imaging) or 30,000 per stripe
		local	50 per pixel[2] (imaging) or 70 per pixel (spectroscopic)
	irregular	global	68,000 (imaging) or 12,000 per stripe
		local	50 per pixel (imaging) or 70 per pixel (spectroscopic)

1. "Predictable" means the brightness of the source can be reliably predicted for the time of observation to within 0.5 magnitude.
2. For imaging acquisitions, a count rate of 300 in the 9×9-pixel box surrounding the target (as computed by the COS Imaging Acquisition ETC) represents an equivalent safe upper limit.

9.2 Screening Limits

The global and local count-rate screening limits for each COS configuration are given in Table 9.1. The limits are independent of observing mode (TIME-TAG or ACCUM). Compliance with these limits must be checked for all proposed COS targets by means of the Exposure Time Calculator (ETC), which issues warnings if they are exceeded.

In Phase I, all proposed targets must be screened against these limits. In Phase II, the results of more detailed target and field checks must be submitted by the corresponding deadline; further details about the procedures and overlight remedies are discussed below.

It is useful to consider relationships between the BOP limits and the data-rate limits discussed in Chapter 4. In the FUV, TIME-TAG data will be lost above 21,000 cts/sec (buffer time of 110 sec), but one can observe up to 30,000 cts/sec (buffer time 80 sec), provided that neither segment exceeds the 15,000 cts/sec screening limit. In this regime, one can either accept the data loss, which doesn't affect the quality (pipeline fluxes will be correct), or switch to ACCUM mode (and accept possible resolution loss due to the OSM drifts). Analogous considerations apply in the NUV, albeit with a

higher BOP limit of 30,000 cts/sec/stripe. In particular, a target could satisfy the 30,000 cts/sec/stripe BOP limit and still be too bright to observe in TIME-TAG mode, for which the global count-rate limit is 30,000 counts per second (Section 6.2.1).

9.3 Source V or Flux Limits

As an approximate guide, bright limits calculated with the ETC, corresponding to the screening limits in Table 9.1, for various sources observed with each COS configuration are given in the following tables. They list V magnitudes for unreddened stellar spectral types and fluxes for other sources. These values are not meant to be a substitute for the ETC, but rather an indication of whether a given object may be near the limit. The most sensitive spectroscopic setting and/or the global vs. local rate limit determines the listed values. Table 9.2 corresponds to spectroscopy through the PSA, Table 9.3 through the BOA, and Table 9.4 to NUV imaging for both apertures.

Table 9.2: V Magnitude Bright-Object Limits for PSA Spectroscopy

Spectral Class	FUV			NUV			
	G130M	G160M	G140L	G185M	G225M	G285M	G230L
O5 V	14.8	14.2	15.2	10.1	9.6	8.9	12.5
O7 V	14.6	14.0	15.0	10.0	9.5	8.8	12.4
O9 V	14.4	13.8	14.8	9.9	9.4	8.7	12.3
B0 V	14.3	13.7	14.7	9.8	9.3	8.6	12.2
B1 V	13.9	13.4	14.3	9.4	9.1	8.4	11.9
B3 V	12.9	12.7	13.5	8.8	8.5	8.0	11.3
B5 V	12.1	12.1	12.8	8.3	8.0	7.6	10.8
B8 V	11.1	11.2	11.6	7.5	7.3	6.9	10.1
A1 V	8.7	9.1	9.5	6.4	6.2	6.0	9.0
A3 V	6.6	8.1	8.6	6.1	6.0	5.8	8.8
A5 V	3.1	7.2	7.6	5.8	5.8	5.7	8.5
F0 V	0.0	5.1	6.0	4.8	5.3	5.5	7.8
F2 V	-1.1	4.3	5.3	4.5	5.0	5.4	7.6
F5 V	-3.2	2.2	3.5	3.7	4.5	5.2	7.3
F8 V	-4.6	0.8	2.3	3.2	4.1	5.0	7.2
G2 V (Solar)	1.9	-0.2	3.5	1.4	2.7	4.6	6.8
G8 V (Tau Ceti)	3.1	-0.2	4.8	0.5	2.2	4.1	6.4
K2 V (Epsilon Eri)	4.1	0.1	5.9	-0.7	1.1	3.4	6.2
KM III (Eta Ser)	-1.4	-1.2	0.2	-0.7	1.1	3.1	5.7
KM III (Alpha Boo)	-0.7	-2.1	1.0	-3.1	-1.0	1.1	4.7
KM III (Gamma Aql)	-2.1	-4.3	-0.4	-5.4	-3.8	-2.1	3.8
KM III (HD 146051)	-3.0	-4.8	-1.3	-7.0	-5.0	-2.9	3.3
KM III (Alpha Cet)	0.3	-1.3	2.0	-4.2	-1.9	-0.8	3.3
KM III (HD 123023)	0.1	-0.8	1.7	-3.2	-1.2	-0.1	3.7
KM III (Beta Gru)	-0.1	-0.5	1.6	-2.9	-1.0	0.9	3.4
T~50,000 Blackbody	14.7	14.2	15.1	10.1	9.5	8.8	12.5
$F_\lambda \sim \lambda^{-1}$	11.1	10.8	11.6	7.2	7.3	6.9	10.0
Flat limit surface brightness	11.2	11.1	11.9	7.8	8.1	7.9	10.7
Flat limit point source flux	9.5	9.4	10.2	6.0	6.4	6.1	9.0

Table 9.3: V Magnitude Bright-Object Limits for BOA Spectroscopy

Spectral Class	FUV			NUV			
	G130M	G160M	G140L	G185M	G225M	G285M	G230L
O5 V	9.6	8.8	9.8	4.6	3.9	3.0	7.0
O7 V	9.3	8.6	9.6	4.5	3.8	3.0	6.8
O9 V	9.1	8.4	9.4	4.3	3.7	2.9	6.7
B0 V	9.0	8.3	9.3	4.2	3.6	2.8	6.6
B1 V	8.6	7.9	9.0	3.9	3.4	2.6	6.3
B3 V	7.7	7.2	8.2	3.2	2.8	2.1	5.6
B5 V	6.8	6.7	7.5	2.7	2.3	1.7	5.2
B8 V	5.7	5.7	6.2	1.9	1.5	1.0	4.4
A1 V	3.2	3.6	4.0	0.8	0.5	0.1	3.3
A3 V	1.2	2.5	3.0	0.5	0.3	0.0	3.1
A5 V	-2.3	1.7	2.1	0.2	0.1	-0.2	2.8
F0 V	-5.4	-0.4	0.4	-0.8	-0.5	-0.5	2.0
F2 V	-6.5	-1.3	-0.3	-1.2	-0.8	-0.6	1.7
F5 V	-8.7	-3.4	-2.1	-1.9	-1.3	-0.8	1.4
F8 V	-10.0	-4.7	-3.3	-2.5	-1.7	-0.9	1.2
G2 V (Solar)	-3.5	-5.8	-1.8	-4.3	-3.1	-1.3	0.8
G8 V (Tau Ceti)	-2.2	-5.7	-0.5	-5.2	-3.6	-1.8	0.4
K2 V (Epsilon Eri)	-1.1	-5.4	0.5	-6.4	-4.7	-2.5	0.1
KM III (Eta Ser)	-6.8	-6.7	-5.1	-6.3	-4.7	-2.8	-0.4
KM III (Alpha Boo)	-6.0	-7.6	-4.3	-8.7	-6.8	-4.9	-1.3
KM III (Gamma Aql)	-7.5	-9.8	-5.8	-11.1	-9.6	-8.0	-2.2
KM III (HD 146051)	-8.3	-10.2	-6.7	-12.6	-10.8	-8.8	-2.8
KM III (Alpha Cet)	-5.0	-6.8	-3.3	-9.7	-7.6	-6.8	-2.8
KM III (HD 123023)	-5.3	-6.3	-3.6	-8.8	-6.9	-6.2	-2.3
KM III (Beta Gru)	-5.4	-5.9	-3.7	-8.6	-6.7	-5.0	-2.6
T~50,000 Blackbody	9.4	8.7	9.7	4.5	3.8	3.0	6.9
$F_\lambda \sim \lambda^{-1}$	5.8	5.3	6.2	1.6	1.5	1.0	4.2
Flat limit surface brightness	5.9	5.6	6.5	2.2	2.3	2.0	5.0
Flat limit point source flux	4.2	3.9	4.7	0.5	0.6	0.2	3.3

Table 9.4: V Magnitude Bright-Object Limits for Imaging

Spectral Class	PSA+MirrorA	PSA+MirrorB	BOA+MirrorA	BOA+MirrorB
O5 V	19.2	16.3	13.5	10.7
O7 V	19.1	16.2	13.4	10.5
O9 V	19.0	16.0	13.3	10.4
B0 V	18.9	15.9	13.2	10.3
B1 V	18.7	15.6	12.9	10.0
B3 V	18.1	15.0	12.4	9.3
B5 V	17.6	14.5	11.9	8.9
B8 V	16.9	13.7	11.1	8.0
A1 V	15.8	12.6	10.1	6.9
A3 V	15.6	12.3	9.9	6.6
A5 V	15.3	12.0	9.6	6.2
F0 V	14.7	11.3	8.9	5.5
F2 V	14.5	11.0	8.6	5.2
F5 V	14.0	10.6	8.1	4.7
F8 V	13.7	10.3	7.8	4.4
G2 V (Solar)	13.0	9.6	7.1	3.7
G8 V (Tau Ceti)	12.6	9.1	6.6	3.2
K2 V (Epsilon Eri)	11.8	8.3	5.8	2.4
KM III (Eta Ser)	11.4	8.0	5.5	2.0
KM III (Alpha Boo)	9.6	6.1	3.6	0.2
KM III (Gamma Aql)	7.1	3.6	1.1	-2.3
KM III (HD 146051)	6.2	2.7	0.2	-3.3
KM III (Alpha Cet)	8.0	4.6	2.1	-1.3
KM III (HD 123023)	8.7	5.2	2.7	-0.7
KM III (Beta Gru)	8.9	5.5	3.0	-0.4
T~50,000 Blackbody	19.2	16.2	13.5	10.6
$F_\lambda \sim \lambda^{-1}$	16.8	13.6	11.0	7.9
Flat limit point source flux	15.8	12.6	10.1	6.9
Flat limit surface brightness	9.8	7.0	4.1	1.3

9.4 Policies and Procedures

All proposers of COS observations are required to confirm that their targets (Phases I and II) and fields (Phase II) include no excessively bright sources. In Phase II, STScI will verify all targets and fields before any COS observations are scheduled.

STScI has developed a Bright Object Tool (BOT) to facilitate detailed target and field checking prior to COS program implementation. This tool is based on automated analysis of the fields by means of data from the second Guide Star Catalogue (GSC2) and displays of the Digital Sky Survey (DSS). GSC2 provides two magnitudes (photographic J and F), hence one color, for most fields down to about 22nd mag, which, combined with conservative spectral-type vs. color relationships, supports determinations of safety for individual objects. In the best cases, these procedures allow expeditious target and field checks, but in some cases the GSC2 is inadequate because of crowding or absence of one of the filters, for instance. In such cases, supplementary information must be provided by the proposers to support the BOP process. Always check the target in the ETC, using the more detailed information generally available there, rather than relying on the BOT field report.

The BOT is implemented within the Astronomer's Proposal Tool (APT), with an Aladin interface, and uses target and exposure information from the proposal. Thus, the BOP procedures are conveniently accessible for GO use. Help files and training movies are available within APT. While the procedures may appear complex at first, their straightforward application rapidly become apparent. As proposers conduct BOP reviews of their targets and fields in conjunction with their Phase II preparations, they will become aware of any problems, such as the need for supplementary data, and thus avoid lengthy implementation delays following the Phase II deadline. (An exception is moving target fields, which must be cleared after the scheduling windows have been established.) To assist with these procedures, a COS Contact Scientist (CS) will be assigned to each COS program, to interact with the GO as necessary during the Phase II preparations and through program execution.

Briefly, for a single default COS pointing with unconstrained orientation, a field of 43 arcseconds in diameter must be cleared. The APT/BOT automatically reports on all GSC2 stars within that field. If any displacements from the default pointing (e.g., acquisition scans, POS TARGs, patterns, or mosaics) are specified, the field to be cleared increases commensurately. POS TARG vectors and the enlarged, rotated field circles are conveniently displayed in APT/Aladin. Because both the PSA and BOA are exposed to the sky at all times, no unsafe or unknown star may lie within 7 arcseconds of either aperture at any orientation. (The BOT automatically allows for the reduced throughput of the BOA aperture.) Orientation restrictions may be introduced to avoid bright objects in the field, but will constrain scheduling of the observation.

Light from a bright nearby source could scatter into the PSA. The region of concern is an annulus extending from 5 to 15 arcsec from the center of the PSA. Any object falling in this annulus may not produce a global count rate in excess of 1×10^5 per segment for the FUV channel or 2×10^5 for the NUV, or a local count rate over 200

cts/sec/resel in the FUV or 400 cts/sec/resel in the NUV. Count rates must be estimated using the ETC as though the source were in the center of the aperture.

A COS GO must send to his/her CS, by the Phase II deadline, results of ETC calculations for each discrete target, and reports on any unsafe or unknown stars from APT/BOT for each field, either showing that the observations are in fact safe, or documenting any unresolved issues. In the latter case, including inadequacy of BOT/GSC2 to clear the observations, other photometric or spectroscopic data sources must be sought by the GO to clear the fields. Many of these are available directly through the APT/Aladin interface (although automatic BOP calculations are currently available only with GSC2), including the STScI Multimission Archive (MAST), which contains data from *IUE* and *Galex,* in addition to *HST*. An existing UV spectrogram of the target or class may be imported directly into the ETC; *IUE* data must be low-resolution, large-aperture spectra. If model spectra are used, the original Kurucz (not Castelli & Kurucz) set should be used for early-type stars. None of the provided models is adequate for late-type stars, since they lack chromospheric emission lines; actual UV data must be used for them. When importing data into the ETC, remember that it does not convolve spectra to the COS resolution. To be conservative, assume that the entire flux of an emission line falls within a single COS resolution element. In worst cases, new ground-based data or *HST* CCD UV exposures may be required to clear the fields for BOP; in general, the latter must be covered by the existing Phase I time allocation.

If a given star has only a V magnitude, it must be treated as an unreddened O5 star. (The older Kurucz O5 model with higher Teff in the ETC should be used for BOP purposes.) If one color is available, it may be processed as a reddened O5 (which will always have a greater UV flux than an unreddened star of the same color). If two colors are available, then the actual spectral type and reddening can be estimated separately. The APT/BOT now clears automatically stars with only a single GSC2 magnitude, if they are safe based on the unreddened O5 assumption. Any other unknowns must be cleared explicitly.

In some cases, the 2MASS JHK may be the only photometry available for an otherwise "unknown" star. It is possible to estimate V and E(B-V) from those data on the assumption of a reddened O5 star, and thus determine its count rates in the ETC. Martins & Plez (2006, A&A, 457, 637) derive $(J-H)_0 = -0.11$ for all O stars and $(V-J)_0 = -0.67$, $(V-H)_0 = -0.79$ for early O types. (The K band should be avoided for BOP because of various instrumental and astrophysical complications.) Bessell & Brett (1988, PASP, 100, 1134), Appendix B, give relationships between the NIR reddenings and E(B-V). These data determine the necessary parameters. Note that the ETC also supports direct entry of observed J and H magnitudes with E(B-V).

It is not expected that all such issues will be resolved by the Phase II deadline, but they should at least be identified and have planned resolutions by then. Another possible resolution is a change to a less sensitive COS configuration, i.e., the BOA, MIRROR B for imaging, or a higher spectral resolution or less sensitive wavelength setting. Again, note that unlike any other instrument, for COS all acquisition exposures must also be cleared; acquisition fields may be relatively large because of the associated pointing steps. Any COS targets or fields that cannot be demonstrated

to be safe to a reasonable level of certainty in the judgement of the CS will not be observed. In that case, it is possible that equivalent alternative targets may be approved upon request; but any observations that trigger the onboard safety mechanisms will not be rescheduled.

A related issue is COS pointing-specification changes after the targets and fields have been cleared by the STScI BOP review. Any such changes must be approved by the COS Team on the basis of a specific scientific justification and a new BOP review by the GO, which may be submitted via the CS if absolutely necessary. In general, such requests should be avoided by ensuring that submitted COS specifications are final, to prevent a need for multiple BOP reviews.

GOs planning COS observations of unpredictably variable targets, such as cataclysmic variables, should be aware of the special BOP procedures in effect for them, including quiescence verification immediately preceding the COS observations, as detailed in ACS ISR 2006-04, which applies to all *HST* detectors subject to BOP. Observations of flare stars are allowed with COS (and STIS) only if the Contact Scientist is convinced that the target would not violate BOP limits even in its brightest state.

9.5 On-Orbit Protection Procedures

Should an overly-bright object be observed with COS, on-board software will act to protect the instrument from damage. The most serious response is to reduce the high voltage of the affected detector; subsequent observations will not take place until COS undergoes a safe-mode recovery procedure that is run from the ground. Activating any of the instrument protection levels listed below is regarded as a serious breach of our health and safety screening procedures and is cause for an investigation. Observers are responsible for ensuring that their observations do not endanger the instrument.

FUV Bright Object Protection

There are five levels of protection for the COS FUV detector:

1. At the lowest level are the screening limits imposed on observers in order to provide a margin of safety for the instrument. The screening limits (Table 9.1) are set about a factor of two below actual risk levels, and we expect observers to work with us to ensure these limits are adhered to. They are determined by estimating the expected count rate from an object, both globally over the detector and locally in an emission line if appropriate. The COS ETC is the tool used for this check.
2. At the next level, within COS the “Take Data Flag” (TDF) is monitored during an exposure. If an event occurs that causes the TDF to drop (such as loss of lock on a guide star, which could lead to the telescope’s drifting), then the COS external shutter is commanded closed. If this occurs, only that exposure is lost.

3. Next comes local rate monitoring. It is possible to permanently damage a localized region of the micro-channel plates without necessarily exceeding the global rate limits. This could occur if an object with bright emission lines were observed, for example. At the beginning of each exposure, the COS flight software bins the FUV spectrum by 4 pixels in *x* and 1024 in *y*; if the count rate in any bin exceeds 1000 counts per 15 seconds, the external shutter is closed and the calibration lamps turned off. Again, if this occurs, only the one exposure is lost. Special commanding is required to turn the detector high voltage, so subsequent COS observations are likely to be lost.
4. Global rate monitoring is next. The COS flight software continuously monitors the total event rate for both FUV detector segments. If the rate for either segment exceeds 60,000 counts per second, the high voltage to both segments is turned off.
5. At the highest level, the instrument is protected by software that senses an overcurrent condition in the high-voltage power supply; if triggered, the software shuts down the high voltage.

NUV Bright Object Protection

Similar protections also apply to the NUV detector:

1. At the lowest level are the screening limits imposed on observers to provide a margin of safety for the instrument. The screening limits (Table 9.1) are set at about a factor of two below actual risk levels, and we expect observers to work with us to ensure these limits are adhered to. They are determined by estimating the expected count rate from an object, both globally over the detector, and locally in an emission line if appropriate. The COS ETC is the tool used for this check.
2. At the next level, within COS the "Take Data Flag" (TDF) is monitored during an exposure. If an event occurs that causes the TDF to drop (such as loss of lock on a guide star, which could lead to the telescope's drifting), then the COS external shutter is commanded closed. If this occurs, only that one exposure is lost.
3. Next comes local rate monitoring. It is possible to permanently damage a localized region of the micro-channel plates without necessarily exceeding the global rate limits. This could occur if an object with bright emission lines were observed, for example. At the beginning of each exposure, the flight software in COS analyzes the NUV spectrum and takes a short exposure to check for groups of pixels exceeding a threshold value (750 counts per second in an 8 × 8-pixel area for imaging mode, 1300 counts per second in a 4 × 8-pixel area for spectroscopic mode). This short exposure is not recorded. If the local rate limit is exceeded, the COS flight software closes the external shutter and turns off the calibration lamps. Again, if this occurs only the one exposure is lost.

4. Global rate monitoring is next. The COS flight software continuously monitors the total event rate for the NUV MAMA. If the total count rate exceeds 20,000 in 0.1 sec the high voltage to the MAMA is turned off, the external shutter is closed, and the calibration lamps are turned off. COS can resume operations only after a safemode recovery procedure, so all subsequent COS exposures are likely to be lost.
5. At the highest level, the NUV MAMA is protected by the detector electronics. The so-called Bright-Scene Detector (BSD) monitors the output of 2 of every 32 anode wires across the detector. The wires are parallel to the dispersion axis. If the total count rate exceeds 17,000 in 138 msec, then the high voltage is turned off. COS can resume operations only after a safe-mode recovery procedure. BSD differs from global-rate monitoring in two ways: it is done in hardware, not software, and what is measured is not a digitized count rate, but current in the anode grid wires.

Further information about these mechanisms can be found in COS ISR 2002-01, although some details reported there have been superseded.

CHAPTER 10:

Overheads and Orbit Usage Determination

In this chapter…

10.1 Observing Overheads

Overheads are the times required to execute various instrumental functions that are over and above an actual exposure time. For instance, mechanisms take a finite time to move into place, and electronic components must be configured properly for use.

This chapter helps you determine the total number of orbits that you need to request in your Phase I observing proposal. This process involves compiling the overheads for individual exposures or sequences of exposures, packing the exposure plus overhead time into orbits, and adding up the total number of orbits required. This will most likely be an iterative process as you modify exposures or their order to most efficiently use orbital visibilities.

The Phase I *Call for Proposals* includes information on the observatory policies and practices with respect to orbit time requests. The *HST Primer* provides specific advice on orbit determination. Below we provide a summary of the generic observatory overheads, the specific COS overheads, and several examples that illustrate how to calculate your orbit requirements for a Phase I proposal.

All overheads provided here are accurate as of the writing of this handbook and reflect both the specifications of the COS instrument commanding and the results of actual Phase II runs of APT. These numbers may be used in conjunction with the values in the *HST Primer* to estimate the total number of orbits for your Phase I proposal. After your HST proposal is accepted, you will be asked to submit a Phase II proposal to support scheduling of your approved observations. At that time you will use the APT scheduling software, which will contain the most up-to-date COS overheads. Allowing sufficient time for overhead in your Phase I proposal is important; additional time to cover unplanned or overlooked overhead will not be granted later.

Accounting properly for all the overheads involved in an observation can be complicated. The information provided here is accurate but is meant only to be illustrative. Proposers are urged to use APT to derive complete and accurate determinations of these times.

10.2 Generic Observatory Overheads

The first time that you acquire an object you must include a 6-minute overhead for the *HST* guide-star acquisition. In all subsequent orbits of the same visit you must include the 5-minute overhead for the guide-star reacquisition; if you are observing an object in the Continuous Viewing Zone (CVZ), then no guide-star re-aquisitions are required.

You must allocate additional time for each deliberate movement of the telescope; e.g., if you are performing a target acquisition exposure on a nearby object and then offsetting to your target, or if you are taking a series of exposures in which you move the target on the detector (`POS-TARG`), you must allow time for telescope motion. The time varies depending on size of the slew; see Table 10.1.

Table 10.1: Generic Observatory Overhead Times

Action	Overhead type	Time needed
Guide star acquisition	Initial acquisition	6 min
	Re-acquisition	5 min per orbit
Spacecraft movements	10 arcsec < Offset < 1.5 arcmin[1]	60 sec
	1 arcsec ≤ Offset ≤ 10 arcsec	30 sec
	Offset < 1arcsec	10 sec

1. Spacecraft motions larger than ~ 1.5 arcmin are likely to result in the loss of guide stars.

10.3 Spectral Element Movement Overheads

For any COS exposure, including target acquisition exposures, overhead must be included to allow for the time required for any change of spectral elements. Note that a transition from FUV to NUV requires movement of OSM1 to the NCM1 position, followed by a possible OSM2 movement. On the other hand, a transition from NUV to FUV requires only the movement of OSM1 from NCM1 to the desired FUV grating. Table 10.2 gives the times required for movement between all OSM1 spectral elements and Table 10.3 gives the times for movement between OSM2 spectral elements.

Note that all COS visits start with OSM1 at the G130M position and OSM2 at the G185M position. (These gratings are highlighted in Table 10.2 and Table 10.3.) OSM1 and OSM2 move sequentially, so that the net overhead is the sum of the two separate overheads. The time required to move from one optical element to another is independent of the initial and final values of the central wavelength.

Table 10.2: Overhead Times (seconds) for Motions Between OSM1 Spectral Elements.

Movement times (seconds) from	to G140L	to G130M	to G160M	to NCM1
G140L	—	158	200	115
G130M	164	—	112	116
G160M	206	116	—	159
NCM1	121	109	154	—

Table 10.3: Overhead Times (seconds) for Motions Between OSM2 Spectral Elements.

Movement times (seconds)	to G230L	to G185M	to G225M	to G285M	to MIRRORA	to MIRRORB
G230L	—	209	140	176	105	99
G185M	204	—	136	102	169	175
G225M	135	141	—	108	100	106
G285M	170	107	103	—	136	142
MIRRORA	100	174	105	141	—	71
MIRRORB	94	181	112	147	77	—

10.4 Acquisition Overheads

Target acquisition is required only once for a series of observations in contiguous orbits (i.e., once per visit). The drift rate in pointing induced by the observatory is less than 10 milliarcseconds per hour. Thermal drifts internal to COS are expected to be even smaller. The various target-acquisition procedures are described in detail in Chapter 8. The exposure overheads associated with each are given below:

NUV ACQ/IMAGE: The associated overhead is 120 seconds plus twice the specified exposure time; this includes OSM1 and OSM2 movements. The exposure time is doubled because, after *HST* is slewed to center the target, a confirmation image is taken by the on-board flight software.

NUV ACQ/SEARCH: Multiply the number of dwell points by (20 seconds + exposure time at each dwell) to account for slewing and exposure time overheads. Add the grating change overheads from Table 10.2 and Table 10.3.

NUV ACQ/PEAKXD: The overhead is 70 seconds plus exposure time. Add the grating change overhead from Table 10.2 and Table 10.3.

NUV ACQ/PEAKD: Multiply the number of dwell points by (20 seconds + exposure time at each dwell) to account for slewing and exposure time overheads. Add the grating change overhead from Table 10.2 and Table 10.3.

FUV ACQ/SEARCH: Multiply the number of dwell points by (20 seconds + exposure time at each dwell) to account for slewing and exposure time overheads. Add grating change overhead from Table 10.2 and Table 10.3.

FUV ACQ/PEAKXD: Overhead is 80 seconds plus exposure time. Add the grating change overhead from Table 10.2 and Table 10.3.

FUV ACQ/PEAKD: Multiply the number of dwell points by (20 seconds + exposure time at each dwell) to account for slewing and exposure time overheads. Add grating change overhead from Table 10.2 and Table 10.3.

BOA: Moving the BOA into position to replace the PSA requires 8 sec.

10.5 Science Exposure Overheads

Science exposure overheads are dominated by the time required to move OSM1 and OSM2 and to read out the on-board memory buffer at the end of each exposure. While the Phase II overheads computed by APT may be less than the values presented below, it is important to plan Phase I proposals using the conservative overheads given below to ensure adequate time for each exposure.

The full overhead calculation for science exposures depends upon a number of factors including generic exposure setups (which depend on the detector and observing mode), whether an aperture change is required, whether a grating change is required, whether the central wavelength setting for the grating is changed, and the directional sense of any required motion to implement an `FP-POS` change. Table 10.4 lists these additional overheads.

Table 10.4: Science Exposure Overhead Times

Add the values for grating change, wavelength change, aperture change, or segment reconfiguration only if those actions are being undertaken.

Overhead times (sec)	FUV		NUV	
	TIME-TAG	ACCUM	TIME-TAG	ACCUM
Exposure set-up	71	79	36	38
Grating change	see Table 10.2		see Table 10.3	
Central wavelength change	72		75	
FP-POS forward[1]	3		3	
FP-POS backward[1]	70		70	
PSA – BOA Change	8		8	
WCS – BOA Change	10		10	
SEGMENT reconfiguration	330		N/A	
Memory readout[2]	110	108[2]	110	48[2]

1. "Forward" refers to the preferred direction of motion of OSM1 or OSM2 and "backward" to the opposite direction. The preferred direction is toward larger FP-POS value.
2. ACCUM mode readout overheads can be hidden within subsequent exposures under certain circumstances, but the rules are complex. Use these values as safe upper limits for proposals.

To calculate a complete science (or FLASH=NO wavecal) exposure overhead, round the desired exposure time up to the next whole second and add the generic exposure setup overhead from Table 10.4. If a grating change has occurred from the previous exposure, add the appropriate values from Table 10.2 and/or Table 10.3. If a central wavelength change is made, add the appropriate value from Table 10.4. If an FP-POS movement is made, add the appropriate value for motion in the preferred direction (toward larger FP-POS) or non-preferred direction. For FUV observations, if a detector SEGMENT reconfiguration is employed (options are A, B, or BOTH) add 330 sec for the associated overhead. Lastly, add the appropriate detector memory readout overhead from Table 10.4.

10.6 First Exposure Overhead Adjustment

To increase observing efficiency, a special feature of the COS instrument commanding allows a portion of the instrumental overheads for the first (and only the first) exposure of a visit to be performed during the initial guide-star acquisition. These will usually be target-acquisition exposures. As a result, up to 300 seconds of instrumental overheads (Table 10.2, Table 10.3, and Table 10.4) but ***not*** observatory or acquisition overheads (Table 10.1 and Section 10.4) may be hidden in this fashion. See Section 10.7 for examples.

10.7 Examples of Orbit Estimates

10.7.1 FUV Acquisition plus FUV TIME-TAG

In this example we start with an FUV `ACQ/SEARCH`, followed by `ACQ/PEAKXD` and `ACQ/PEAKD` target acquisitions, then add an FUV `TIME-TAG` exposure with G140L and `SEGMENT=A`.

Table 10.5: Overhead Values for FUV Acquisition and FUV TIME-TAG Science.

Action	Time required	Comment
Initial guide star acquisition	6 min	Required at start of a new visit
FUV `ACQ/SEARCH`, G130M at 1309 Å, 3 × 3 pattern, 15 sec exp.	9×(20+15) = 315 sec = 5.3 min	COS starts from G130M 1309 Å on OSM1 so no initial move; 9 `ACQ/SEARCH` sub-exposures, so overhead includes 9 slews (20 sec each) plus 9 exposures (15 sec each)
First exposure overhead adjustment	0 min	No instrument movements prior to first exposure in this example
FUV `ACQ/PEAKXD`, G130M at 1309 Å, 20 sec exp.	80 + 20 sec = 100 sec = 1.7min	No OSM1 movement; generic `PEAKXD` overhead; exp time
FUV `ACQ/PEAKD`, G130M at 1309 Å, 5 steps, 25 sec exp.	5×(20+25) = 225 sec = 3.8 min	No OSM1 move; five slews (20 sec each) plus 5 exp (25 sec each)
FUV G140L at 1280 Å, `TIME-TAG`, `FLASH=YES`, `FP-POS=3` (default value), `SEGMENT=A`, 1500 sec exp.	71 + 164 + 330 + 110 + 1500 = 2175 sec = 36.3 min	Generic FUV `TIME-TAG` setup; OSM1 grating change (164 sec); no `FP-POS` change; `SEGMENT` reconfiguration change; `TIME-TAG` memory readout; exp time
Total science time	1500 sec = 25 min	
Total time used in orbit	53.1 min	

10.7.2 NUV TIME-TAG

In this example we start with an NUV ACQ/IMAGE target acquisition, then add two NUV TIME-TAG exposures that use the same grating but different central wavelengths, both utilizing the default FP-POS setting and FLASH=YES.

Table 10.6: Overhead Values for NUV TIME-TAG.

Action	Time required	Comment
Initial guide star acquisition	6 min	Required at start of a new visit
NUV ACQ/IMAGE with 2 sec exposure time	116 + 169 + 120 + 4 = 409 sec = 6.8 min	COS starts at G130M on OSM1, so move to NCM1 requires 116 sec. OSM2 home position is G185M, so move to MIRRORA takes 169 sec; Add 2 min ACQ/IMAGE setup and twice the exposure time.
First exposure overhead adjustment	-(116 + 169) sec = -285 sec = -4.8 min	OSM1 and OSM2 movements may be hidden in guide star acquisition.
NUV G185M at 1850 Å, TIME-TAG, FLASH=YES, FP-POS=3, 1200 sec exp.	36 + 174 + 110 + 1200 = 1520 sec = 25.3 min	Generic NUV TIME-TAG setup; change from MIRRORA to G185M (174 sec); no FP-POS change (3=default); no aperture change from PSA; TIME-TAG memory readout; exp time
NUV G185M at 1812 Å, TIME-TAG, FLASH=YES, FP-POS=3, 600 sec exp.	36 + 75 + 110 + 600 = 821 sec = 13.7 min	Only change central wavelength, so generic NUV TIME-TAG exposure setup; no grating change; central wavelength change (75 sec); no FP-POS change; TIME-TAG memory readout; exp time
Total science time[1]	30 min	
Total time used in orbit	46.4 min	

1. The indicated science time has been chosen to be the orbit visibility period less the various overheads.

10.7.3 NUV plus FUV TIME-TAG

In this example we start with an NUV ACQ/SEARCH followed by an ACQ/IMAGE target acquisition, then add an NUV TIME-TAG exposure followed by a switch to the FUV channel and an FUV TIME-TAG exposure.

Table 10.7: Overhead Values for NUV ACCUM with FUV TIME-TAG.

Action	Time required	Comment
Initial guide star acquisition	6 min	Required at start of a new visit
NUV ACQ/SEARCH, MIRRORA, 3 × 3 pattern, 10 sec exp.	116 + 169 + 9×(20+10) = 555 sec = 9.3 min	COS starts at G130M on OSM1, so move to NCM1 requires 116 sec; OSM2 home position is G185M, so move to MIRRORA takes 169 sec; 9 ACQ/SEARCH sub-exposures, so overhead includes 9 slews (20 sec each) plus 9 exposures (10 sec each)
First exposure overhead adjustment	-(116 + 169) sec = -285 sec = -4.8 min	OSM1 and OSM2 movements may be hidden in guide star acquisition.
NUV ACQ/IMAGE with 10 sec exposure time	120 + 2×10 sec = 140 sec = 2.3 min	No OSM2 movement; so overhead includes only ACQ/IMAGE setup and twice exp time
NUV G225M at 2250 Å, TIME-TAG, FLASH=YES, FP-POS=3, 1200 sec exp.	36 + 105 + 110 + 1200 = 1451 sec = 24.2 min	Generic NUV TIME-TAG setup; change from MIRRORA to G225M (105 sec); no FP-POS change (3=default); no aperture change from PSA; TIME-TAG memory readout; exp time
FUV G130M at 1309 Å, TIME-TAG, FLASH=YES, FP-POS=3, 600 sec exp.	71 + 109 + 110 + 600 = 890 sec = 14.8 min	Switch from FUV to NUV adds no overhead (OSM2 not moved); generic FUV TIME-TAG setup; OSM1 move from NCM1 to G130M (109 sec); no FP-POS change; no SEGMENT change; TIME-TAG memory readout; exp time
Total science time	30 min	
Total time used in orbit	51.9 min	

10.7.4 FUV TIME-TAG with BOA and FLASH=NO

In this example, we start with an NUV ACQ/IMAGE, followed by a switch to the FUV channel and an FUV TIME-TAG science exposure using G160M, a non-default FP-POS=1, the BOA, and, as required with the BOA, FLASH=NO. The science exposure will be followed automatically by a 10-second wavecal (see Table 6.3). The next orbit begins with a longer science exposure using the same set-up as for the first orbit. Because more than 40 minutes will have elapsed since the first wavecal, a wavecal will be inserted automatically following this science exposure, as well.

Table 10.8: Overhead Values for FUV TIME-TAG Using the BOA and FLASH=NO.

Action	Time required	Comment
Initial guide-star acquisition	6 min	Required at start of a new visit
NUV ACQ/IMAGE with 2 sec exposure time	116 + 169 + 120 + 4 = 409 sec = 6.8 min	COS starts at G130M on OSM1, so move to NCM1 requires 116 sec. OSM2 home position is G185M, so move to MIRRORA takes 169 sec; Add 2 min ACQ/IMAGE setup and twice the exposure time.
First exposure overhead adjustment	-(116 + 169) sec = -285 sec = -4.8 min	OSM1 and OSM2 movements may be hidden in guide star acquisition.
FUV G160M at 1600 Å, TIME-TAG, BOA, FLASH=NO, FP-POS=1, 1800 sec exp.	71 + 154 + 70 + 8 + 110 + 1800 sec = 2213 sec = 36.9 min	Generic FUV TIME-TAG setup; NUV to FUV adds no overhead; change from NCM1 to G160M (154 sec); non-preferred direction (3 to 1) FP-POS change (70 sec); aperture change from PSA to BOA; no SEGMENT change; TIME-TAG memory readout; exp time
FUV G160M at 1600 Å, TIME-TAG, AUTO WAVECAL, WCA, FP-POS=1, 10 sec exp.	71 + 10 + 110 + 10 = 201 sec = 3.3 min	AUTO WAVECAL to be inserted, since FLASH=YES is not allowed with BOA; generic FUV TIME-TAG setup; no OSM1 move, no central wavelength change; no FP-POS change; aperture change from BOA to WCA (10 sec); no SEGMENT change; TIME-TAG memory readout; exp time
Total science time in orbit 1	30 min	
Total time used in orbit 1	48.1 min	
Guide star re-acquisition	5 min	required at start of additional orbit
FUV G160M at 1600 Å, TIME-TAG, BOA, FLASH=NO, FP-POS=1, 2400 sec exp.	71 + 10 + 110 + 2400 = 2591 sec = 43.2 min	Generic FUV TIME-TAG setup; continue at same OSM1 position, same central wavelength and FP-POS; aperture change to from WCA to BOA (10 sec); no SEGMENT change; TIME-TAG memory readout; exp time
FUV G160M at 1600 Å, TIME-TAG, AUTO WAVECAL, WCA, FP-POS=1, 10 sec exp.	71 + 10 + 110 + 10 = 201 sec = 3.3 min	Another AUTO WAVECAL required as more than 40 min have elapsed since last one; again generic FUV TIME-TAG exposure setup; no grating change; no central wavelength change; no FP-POS change; aperture change from BOA to WCA (10 sec); no SEGMENT change; TIME-TAG memory readout; exp time
Total science time in orbit 2	40 min	
Total time used in orbit 2	51.5 min	

10.7.5 Multiple FP-POS with FUV TIME-TAG and FLASH=YES

In this example, we start with an NUV ACQ/IMAGE target acquisition followed by a switch to the FUV channel for a set of 900-second exposures, one at each FP-POS position. We will again use TIME-TAG, FLASH=YES, and G130M, but at central wavelength 1327.

First an NUV ACQ/IMAGE will be performed. Next OSM1 is moved to put G130M in place at central wavelength 1327. Since the grating begins in the FP-POS=3 position, any sequence of FP-POS observations using all four positions must include at least one move in the non-preferred direction. We will execute the individual FP-POS exposures in the order FP-POS=1, 2, 3, and 4.

The desired exposures will not fit into a single orbit, so some must be performed in a second orbit. As the second orbit is not completely filled, the observer would typically add additional exposures (not shown here) to fill it.

Table 10.9: Overhead Values for FP-POS=AUTO with FUV TIME-TAG and FLASH=YES.

Action	Time required	Comment
Initial guide star acquisition	6 min	Required at start of a new visit
NUV ACQ/IMAGE with 10 sec exposure time	116 + 169 + 120 + 20 = 425 sec = 7.1 min	COS starts at G130M on OSM1, so move to NCM1 requires 116 sec. OSM2 home position is G185M, so move to MIRRORA takes 169 sec; Add 2 min ACQ/IMAGE setup and twice the exposure time.
First exposure overhead adjustment	-(116 + 169) sec = -285 sec = -4.8 min	OSM1 and OSM2 movements may be hidden in guide star acquisition.
FUV G130M at 1327 Å, TIME-TAG, FLASH=YES	109 sec = 1.8 min	Move OSM1 from NCM1 to G130M (109 sec); default FP-POS=3. Ready for following sequence of FP-POS=1,2,3,4 exposures
FP-POS=1, 900 sec exposure	71 + 70 + 110 + 900 = 1151 sec = 19.2 min	First exposure of FP-POS sequence: generic TIME-TAG set-up (71 sec); move to position 1 (70 sec); TIME-TAG memory read-out (110 sec); exposure time = 900 sec
FP-POS=2, 900 sec exposure	71 + 3 + 110 + 900 = 1084 sec = 18.1 min	Second exposure of FP-POS sequence: generic TIME-TAG set-up (71 sec); move to FP-POS=2 (3 sec); TIME-TAG memory read-out (110 sec); exposure time = 900 sec
Total science time in orbit 1	30 min	
Total time used in orbit 1	47.4 min	
Guide star re-acquisition	5 min	Required at start of additional orbit
FP-POS=3, 900 sec exposure	71 + 3 + 110 + 900 = 1084 sec = 18.1 min	As for FP-POS=2
FP-POS=4, 900 sec exposure	71 + 3 + 110 + 900 = 1084 sec = 18.1 min	As for FP-POS=2
Total science time in orbit 2	30 min	
Total time used in orbit 2	41.2 min	

CHAPTER 11:

Exposure-Time Calculator (ETC)

In this chapter…

11.1 The COS Exposure Time Calculators

To help with proposal preparation, four COS Exposure-Time Calculators (ETCs) are available on the COS Web pages:

http://www.stsci.edu/hst/cos/software/etc

These calculators model spectroscopic science observations, spectroscopic target acquisition, imaging, and imaging target acquisition. They estimate count rates for given source and background parameters and calculate either the signal-to-noise ratio for a given exposure time or the exposure time needed to achieve a desired signal-to-noise ratio. If you have a calibrated spectrum of your source, you can upload it to the Exposure Time Calculators. The ETCs warn if your observations exceed local or global brightness limits (see Table 9.1). They have extensive online help that explains how to use them and provides the details of the calculations.

The spectroscopic ETC can display the input spectrum, a simulated one-dimensional output spectrum, and the S/N and number of counts per resolution element for the selected COS configuration and source. These outputs can also be downloaded by the user in ASCII format.

The imaging ETC is simple, because COS has only a single imaging mode. However, it does allow the selection of either the primary science aperture or bright object aperture and either MIRRORA or MIRRORB. The ETC reports the count rate in the brightest pixel, total counts in the detector, and S/N per resolution element.

The target acquisition ETCs return the acquisition exposure time to be entered in APT for both imaging and spectroscopic acquisitions. Target acquisition is described in Chapter 8.

A unique exposure ID is assigned to each calculation performed by the ETCs, allowing results from previous calculations to be retrieved easily. Proposers are urged to check the COS ETC Web page for any updates or issues related to the COS ETCs before performing any ETC simulation.

11.2 NUV Sensitivity

As shown in Figure 7.2, the COS NUV channel is sensitive to wavelengths above 3200 Å, an important consideration when acquiring or observing red objects. For stars with effective temperatures above 6000 K, the effect is negligible, but it grows to about 20% at 5000 K, and below 5000 K it quickly becomes large.

If you upload a spectrum into the ETC to calculate an exposure time, particularly for an acquisition, please be sure that the spectrum spans the full range of wavelengths to which the NUV channel is sensitive, from about 1600 Å to 12,000 Å. Failure to span the full wavelength range can lead to a misleading result.

The COS ETC expects input spectra to extend out to 12,000 Å and will return a warning message ("Partial overlap between instrument throughput band and input spectrum") if they do not.

11.3 Sensitivity, Count Rate, and S/N

A complete theoretical discussion of the exposure time as a function of instrument sensitivity and signal-to-noise ratio is given in Chapter 6 of the *STIS Instrument Handbook* and will not be repeated here. However, COS has several characteristics which simplify the signal-to-noise calculations.

Both COS detectors are photon counters, which means that they have zero read noise. COS is optimized for point sources, and in this case the signal-to-noise ratio is given by

$$\frac{S}{N} = \frac{C \cdot t}{\sqrt{C \cdot t + N_{pix}(B_{sky} + B_{det}) \cdot t}} \ ,$$

where

C = the signal from the astronomical source, in counts sec^{-1}

t = the integration time, in sec

N_{pix} = the total number of detector pixels integrated to achieve C
B_{sky} = the sky background, in counts sec^{-1} $pixel^{-1}$
B_{det} = the detector dark count rate, in counts sec^{-1} $pixel^{-1}$

With no detector read noise, the signal-to-noise ratio is proportional to the square root of the exposure time whether the target is bright or faint compared to the backgrounds and dark count.

Note that the detector dead-time effects discussed in Section 4.1.7 and Section 4.2.5 are not included in the ETC, which will over-predict the count rates and resulting S/N ratios for bright targets.

11.4 Detector and Sky Backgrounds

The background sources that affect COS observations include

- Detector dark count,
- Earthshine,
- Zodiacal light, and
- Geocoronal emission.

The ETC allows the user to select among several levels of intensity for each of the sky backgrounds, corresponding to different observing environments.

11.4.1 Detector dark background

The following table lists the dark count rate and read noise characteristics of the COS detectors as measured on orbit.

Table 11.1: Detector background count rates (per second) for COS.

Detector:	**FUV XDL**	**NUV MAMA**
Dark rate (counts sec^{-1})	1.5 per cm^2 2.2×10^{-6} per pixel 6.5×10^{-5} per resel	11 per cm^2 6.9×10^{-5} per pixel 6.2×10^{-4} per resel
Read noise	0	0

Note that, due in part to its windowless design, the dark current in the FUV detector is truly small, about 1.4 count $resel^{-1}$ in six hours. It is the "resel," or resolution element, that matters most, since that is the net unit for a spectrum. Here we assume that a resel spans 6×10 pixels on the FUV XDL and 3×3 pixels on the NUV MAMA.

Figure 11.1: Sky Background Intensity as a Function of Wavelength.

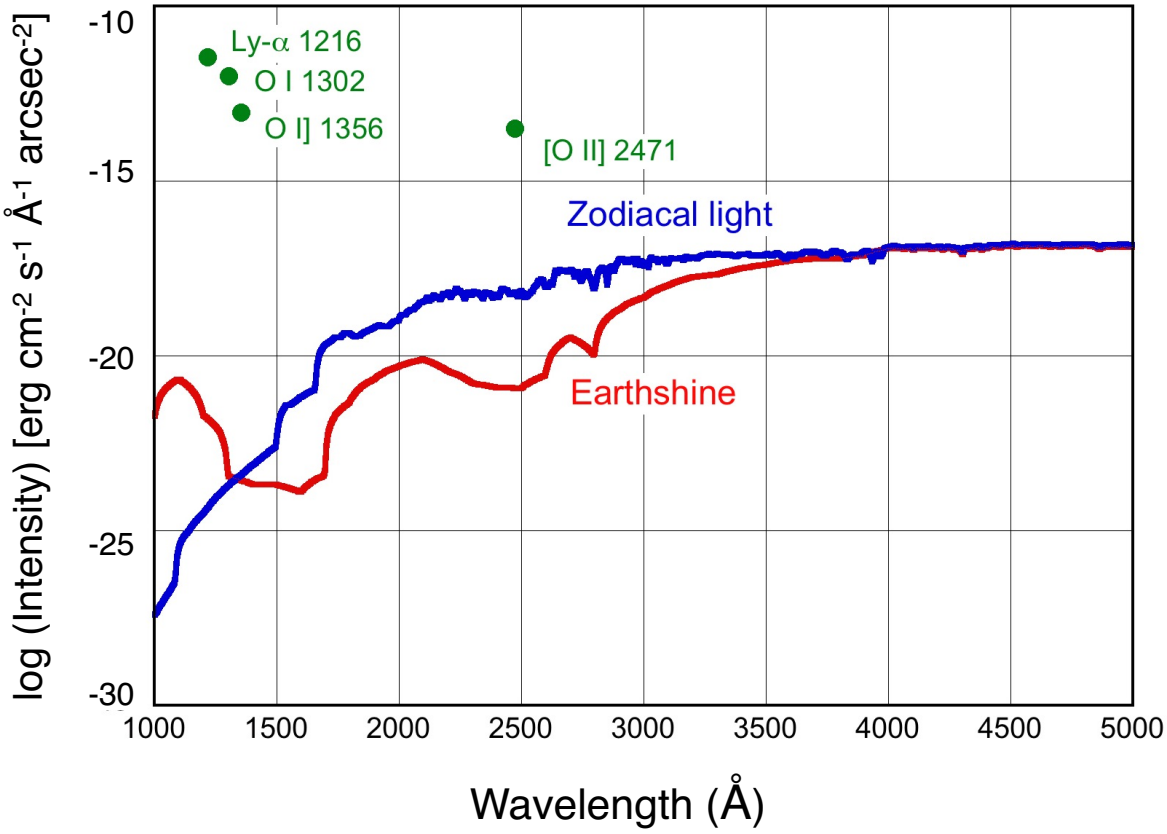

Earthshine for a target 24° above the limb of the sunlit Earth. Use Figure 11.2 to estimate background contributions at other angles. The zodiacal light level (m_V = 22.7 per arcsec^2) corresponds to a helio-ecliptic latitude and longitude of 30° and 180°, respectively. The geocoronal line intensities are integrated fluxes in units of 10^{-15} erg cm^{-2} sec^{-1} arcsec^{-2}. The upper limit to the [OII] 2471 intensity is shown.

11.4.2 Earthshine

Four earthshine intensity levels, with scaling factors of (*none*, *average*, *high*, *extremely high*) = (0.0, 0.5, 1.0, 2.0), are available in the ETC. Earthshine intensity is a strong function of the angle between the target and the bright Earth limb. The earthshine surface brightness for a target 24° degrees above the limb, corresponding to the "high" level, is shown in Figure 11.1. The limb angle is approximately 24° when *HST* is aligned toward its orbit pole (i.e., the center of the CVZ). The variation of earthshine with limb angle is shown in Figure 11.2.

Figure 11.2: Background Contributions from the Moon and Earth.

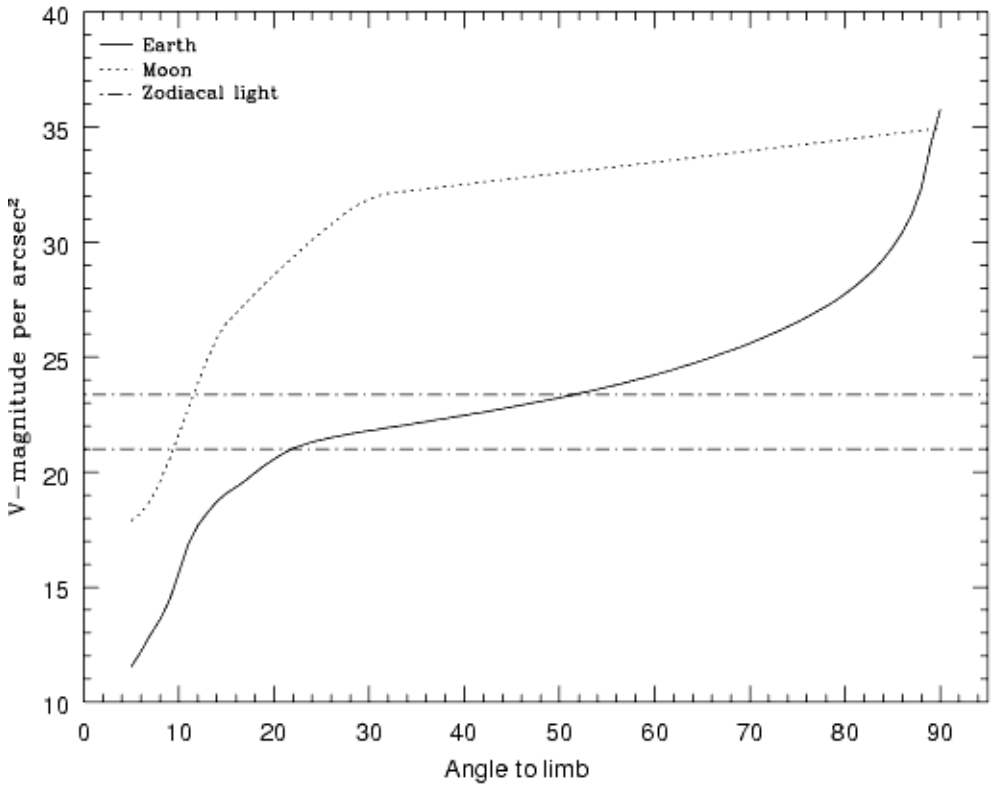

The values are V magnitude per square arcsec due to the moon and the sunlit Earth as a function of angle between the target and the limb of the bright Earth or moon.

11.4.3 Zodiacal Light

Away from the airglow lines, at wavelengths between about 1300 and 3000 Å, the sky background is dominated by zodiacal light and is generally lower than the intrinsic detector background, especially for the NUV detector. Figure 11.1 shows the zodiacal light for the "average" level in the ETC. The selectable levels and the factors by which they are scaled in the ETC are (*none, low*, *average*, *high*) = (0.0, 0.576, 1.0, 1.738).

The zodiacal light intensity does not vary dramatically with time, and varies by only a factor of about three across the sky. For a target near ecliptic coordinates of (50,0) or (–50,0), the zodiacal light is relatively bright at m_V = 20.9, i.e. about 9 times the faintest values of m_V = 23.3. These limits are plotted in Figure 11.2.

Observations of the faintest objects may need the special requirement LOW-SKY in the Phase II observing program. LOW-SKY observations are scheduled during the part of the year when the zodiacal background light is no more than 30% greater than the minimum possible zodiacal light for the given sky position. LOW-SKY in the Phase II scheduling also invokes the restriction that exposures will be obtained only at angles greater than 40 degrees from the bright Earth limb to minimize earthshine and the UV airglow lines. The LOW-SKY special requirement limits the times at which

targets within 60 degrees of the ecliptic plane will be scheduled and limits visibility to about 48 minutes per orbit.

The ETC provides the user with the flexibility to adjust both the zodiacal (*none, low*, *average*, *high*) and earthshine (*none*, *average*, *high*, *extremely high*) sky background components to determine if the use of `LOW-SKY` is advisable for a given program. However, the absolute sky levels that can be specified in the ETC may not be achievable for a given target. As shown in Table 11.2, the zodiacal background minimum for an ecliptic target is $m_V = 22.4$, which is still brighter than both the low and average options with the ETC. By contrast, a target near the ecliptic pole would always have a zodiacal = *low* background in the ETC. The user is cautioned to consider sky levels carefully, as the backgrounds obtained in *HST* observations can span significant ranges.

11.4.4 Geocoronal Airglow Emission

In the ultraviolet, the sky background contains important contributions from airglow lines, which vary from day to night and as a function of *HST* orbital position. Airglow lines may be an important consideration for spectroscopic observations at wavelengths near the lines.

Background due to geocoronal emission originates mainly from hydrogen and oxygen atoms in the exosphere of the Earth. The emission is concentrated in a very few lines. The brightest line by far is Lyman α at 1216 Å. The strength of the Lyman α line varies between about 2 and 20 kilo-Rayleighs (i.e., between 6.3×10^{-14} and 6.3×10^{-13} erg sec^{-1} cm^{-2} arcsec^{-2}, where 1 Rayleigh = 10^6 photons sec^{-1} cm^{-2} per 4π steradians, which equates to 3.15×10^{-17} erg sec^{-1} cm^{-2} arcsec^{-2} at Lyman α) depending on the time of the observation and the position of the target relative to the Sun. The next strongest line is the O I line at 1302 Å, which rarely exceeds 10% of Lyman α. The typical strength of the O I 1302 Å line is about 2 kilo-Rayleighs (about 7×10^{-14} erg sec^{-1} cm^{-2} arcsec^{-2}) on the daylight side and about 150 times fainter on the night side of the HST orbit. The O I] 1356 Å and [O I] 2471 Å lines may appear in observations on the daylight side of the orbit, but these lines are at least 10 times weaker than the O I 1302 Å line. The widths of the lines also vary, but a representative value for a temperature of 2000 K is about 3 km s^{-1}. The geocoronal emission lines are essentially unresolved at the resolution of COS, but the emission fills the aperture in the spectral and spatial directions. For the FUV modes, the aperture width is approximately 114 pixels, or 1.12, 1.36, and 9.46 Å for G130M, G160M, and G140L, respectively. For the NUV modes, the aperture width is approximately 105 pixels, or 3.87, 3.46, 4.18, and 41.21 Å for G185M, G225M, G285M, and G230L, respectively.

The COS ETC provides four airglow intensity levels (*none, low*, *average*, *high*) whose scaling factors depend on the airglow line considered: (0.0, 0.1, 0.5, 1.0) for Lyman α, (0.0, 0.0667, 0.5, 1.0) for O I λ1302, (0.0, 0.006, 0.5, 1.0) for O I] λ1356, and (0.0, 0.005, 0.5, 1.0) for [O I] λ2471.

It is possible to request that exposures be taken when HST is in the umbral shadow of the earth to minimize geocoronal emission (e.g., if you are observing weak lines at 1216 Å or 1302 Å) using the special requirement SHADOW. Exposures using this

special requirement are limited to roughly 25 minutes per orbit, exclusive of the guide-star acquisition (or reacquisition) and can be scheduled only during a small percentage of the year. SHADOW reduces the contribution from the geocoronal emission lines by roughly a factor of ten, while the continuum earthshine is essentially nil. If you require SHADOW, you should request it in your Phase I proposal (see the Call for Proposals).

An alternate strategy for reducing the effects of geocoronal emissions is to use time-resolved observations, so that any data badly affected by geocoronal emission can simply be excluded from the final co-addition. This can be done either by doing the observations in TIME-TAG mode, the default for all COS observations if the target is not too bright, or by taking a series of short (~ 5 min) ACCUM mode exposures over the course of each orbit.

As noted, geocoronal Lyman-α is by far the strongest airglow feature to contend with. Despite this, we estimate that on the day side of HST's orbit, when Lyman α is at its strongest, it will produce a net count rate of 20 counts sec^{-1} $resel^{-1}$, well below rates at which bright lines are a concern.

11.5 Extinction Correction

Extinction can dramatically alter the counts expected from your source, particularly in the ultraviolet. Figure 11.3 shows A_λ/A_V values applicable to our Galaxy, taken from Cardelli, Clayton, & Mathis (1989, ApJ, 345, 245). A value of $R = 3.1$ was used. This corresponds to the "Average Galactic" selection of the ETC.

Extinction curves, have a strong metallicity dependence, particularly at ultraviolet wavelengths. Sample extinction curves can be seen in Koornneef and Code [ApJ, 247, 860 1981 (LMC)], Bouchet et al. [A&A, 149, 330 1985 (SMC)], and Calzetti et al. [ApJ, 429, 582, 1994], and references therein. At lower metallicities, the 2200 Å bump that is so prominent in the Galactic extinction curve disappears, and $A_V/E(B–V)$ increases at shorter UV wavelengths.

The ETC allows the user to select among a variety of extinction curves and to apply the extinction correction either before or after the input spectrum is normalized.

Figure 11.3: Extinction in Magnitude as a Function of Wavelength.

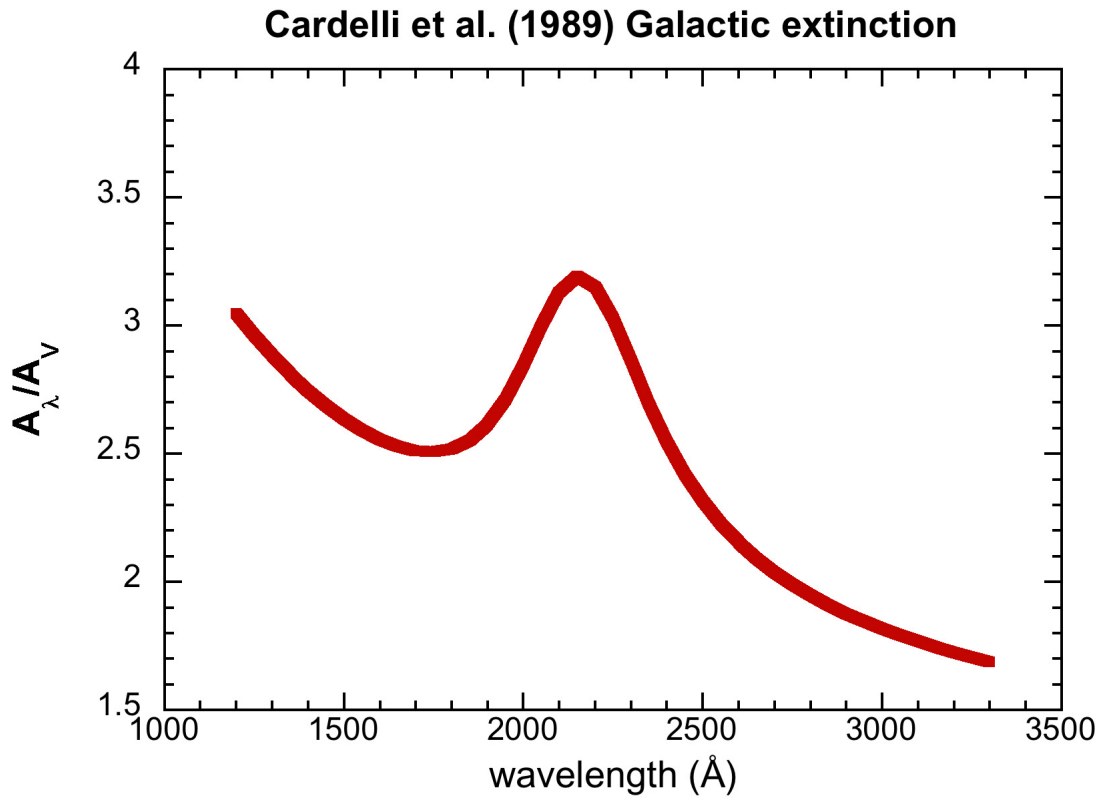

The Galactic model of Cardelli et al. (1989) is shown, computed for $R = 3.1$.

11.6 Tabular Sky Backgrounds

Below is a table of the *high* sky background numbers as plotted in Figure 11.1, for reference. The *high* sky values are defined as the earthshine at 24° from the limb and by the typical zodiacal light of $m_V = 22.7$. Table 11.2 lists the mean value of the zodiacal and earthshine backgrounds (excluding the contributions from geocoronal emission lines) in each wavelength interval.

The line widths and intensities of some important geocoronal emission lines in the COS bandpass are listed in Table 11.3.

Table 11.2: Earthshine and Zodiacal Light in the COS PSA.

Wavelength (Å)	Earthshine	Zodiacal Light	Total
1000	6.48 E–7	1.26 E –12	6.48 E –7
1100	1.66 E –6	6.72 E –11	1.66 E–6
1200	4.05 E–7	6.23 E–10	4.06 E –7
1300	2.66 E–8	3.38 E –9	2.99 E–8
1400	2.28 E –9	1.32 E–8	1.54 E–8
1500	1.95 E–9	2.26 E–7	2.28 E–7
1600	1.68 E–9	1.14 E–6	1.14 E–6
1700	6.09 E–8	3.19 E–5	3.19 E–5
1800	6.19 E–7	6.63 E–5	6.69 E–5
1900	2.30 E–6	1.05 E–4	1.07 E–4
2000	5.01 E–6	2.07 E–4	2.12 E–4
2100	6.97 E–6	5.95 E–4	6.02 E–4
2200	3.94 E–6	9.82 E–4	9.86 E–4
2300	1.83 E–6	9.67 E–4	9.69 E–4
2400	1.27 E–6	1.05 E–3	1.05 E–3
2500	1.37 E–6	1.01 E–3	1.01 E–3
2600	6.33 E–6	2.32 E–3	2.32 E–3
2700	2.66 E–5	4.05 E–3	4.08 E–3
2800	3.79 E–5	3.67 E–3	3.71 E–3
2900	2.17 E–4	7.46 E–3	7.68 E–3
3000	4.96 E–4	8.44 E–3	8.94 E–3
3100	1.04 E–3	9.42 E–3	1.05 E–2
3200	1.72 E–3	1.10 E–2	1.27 E–2
3300	2.18 E–3	1.34 E–2	1.56 E–2
3400	3.12 E–3	1.30 E–2	1.62 E–2
3500	4.06 E–3	1.31 E–2	1.72 E–2
3600	5.15 E–3	1.24 E–2	1.77 E–2
3700	5.89 E–3	1.49 E–2	2.18 E–2
3800	6.19 E–3	1.41 E–2	2.03 E–2
3900	7.80 E–3	1.39 E–2	2.17 E–2
4000	1.14 E–2	2.07 E–2	3.21 E–2
4250	1.13 E–2	2.17 E–2	3.40 E–2
4500	1.33 E–2	2.53 E–1	3.86 E–2
4750	1.35 E–2	2.57 E–2	3.92 E–2
5000	1.30 E–2	2.50 E–2	3.80 E–2

These rates correspond to the *high* level in the ETC and are listed in units of 10^{-15} erg cm^{-2} sec^{-1} Å^{-1} for the total COS PSA, which is 4.91 arcsec^2 in area.

Table 11.3: Typical Strengths of Important Ultraviolet Airglow Lines

Airglow feature	Intensity					
	Day			Night		
	Rayleighs	10^{-15} erg cm^{-2} sec^{-1} arcsec^{-2}	10^{-15} erg cm^{-2} sec^{-1} per PSA	Rayleighs	10^{-15} erg cm^{-2} sec^{-1} arcsec^{-2}	10^{-15} erg cm^{-2} sec^{-1} per PSA
O I 911	17	0.7	3.5	8.3	0.35	1.7
O I 989	161	6.2	30	0.6	–	–
H I 1025	571	21	105	2.7	–	–
O I 1027	64	2.4	12	0	–	–
O I 1152	28	0.93	4.6	0	–	–
H I 1216	20,000	630	3100	2,000	63	310
O I 1302	2,000	59	290	13	0.38	1.9
O I] 1356	204	5.8	28	12.5	0.35	1.7
O I 2471	45	0.70	3.4	1	–	–

11.7 Examples

In this section we present a few examples of the way in which the COS ETCs may be used. They illustrate the information that is returned by the ETCs, and how they can be used to plan your observations.

11.7.1 A Flat-spectrum Source

One often does not know the exact spectrum shape of the object to be observed, so the answer to a simple question is desired: How long will it take to achieve a given signal-to-noise ratio at a given wavelength if the flux at that wavelength is specified? The easiest way to determine this is to use a flat spectrum as input. How long will it take to achieve S/N=10 per resolution element at 1320 Å with a source flux of 10^{-15} erg cm^{-2} sec^{-1} Å^{-1}, using a medium resolution mode?

Only the G130M grating covers the desired wavelength at medium resolution, but several choices of central wavelength are available. We select a setting of 1309 Å. We enter these values into the spectroscopic ETC, select the Primary Science Aperture (PSA), select "Exposure time needed to obtain a S/N ratio of 10.0," and enter the specified wavelength of 1320 Å. For the spectrum distribution, choose a flat continuum in F_λ. Make sure the reddening, *E(B–V)*, is set to 0. Normalize the target to 10^{-15} erg cm^{-2} sec^{-1} Å^{-1}. The zodiacal light, earthshine, and airglow were not specified, so we choose average values.

When this case is computed with the ETC, we find the required time is 11,458 sec; the total count rates are 60 and 298 counts sec^{-1} in detector segments A and B, respectively, well below the safety limit; the count rate in the brightest pixel is 0.113 counts sec^{-1}, also well within the safe range; and the buffer time indicated by the ETC is 6602 sec.

What if somewhat higher *S/N* were desired and one were willing to devote 5 *HST* orbits to the observation? Assuming each orbit allows 50 minutes of observing time (ignoring the acquisition time here), we find that in 15,000 sec we will get *S/N* = 11.4 per resel. Note that $(15{,}000/11{,}458)^{1/2} = (11.4/10.0)$. That is, the *S/N* ratio scales as $t^{1/2}$, as stated in Section 11.3.

If a low-resolution observation is acceptable, then one could switch to the G140L grating. With a grating setting of 1105 Å and *S/N* = 10 per resel, we find the required exposure time is 1956 sec, considerably shorter than the medium resolution case required.

However, also note that the sensitivity of G130M is higher than that of G140L once resolving power is taken into account. In other words, a G130M spectrum that is rebinned to the same resolution as a G140L spectrum can be obtained in less time for a given S/N, although, of course, with diminished wavelength coverage. If only a limited portion of the source's spectrum is of interest, using G130M is more efficient than using G140L.

These cases also illustrate that the earthshine and zodiacal light are completely negligible in the FUV unless the target flux is much lower than that considered here. This is also true of the airglow if the wavelength of interest is away from the airglow lines. Of course, the airglow cannot be ignored in terms of the total count rate of the detector, or the local count rate if the source contributes at the same wavelengths as the airglow lines.

11.7.2 An Early-type Star

We wish to observe an O5 star at medium spectral resolution at a wavelength of 1650 Å. We know that the star has a magnitude of *V* = 16. How long will it take to obtain *S/N* = 15?

We select the G160M grating set to 1623 Å. We select a Kurucz O5 stellar model, and set the normalization to be Johnson *V* = 16. All other settings remain the same as in the previous example. We find that the required exposure time is 629 sec.

Suppose this star is reddened, with *E(B–V)* = 0.2. We select the *Average Galactic* extinction law, which is shown in Figure 11.3. We must now decide if this extinction is to be applied before or after the normalization. Since the star has a measured magnitude, we want to apply the reddening before normalization. Otherwise, the extinction would change the *V* magnitude of the stellar model. Making this selection, we find that *S/N* = 15 can be obtained in 1477 sec.

11.7.3 A Solar-type Star with an Emission Line

We want to observe a solar-type star with a narrow emission line. Consider the Si II 1810 Å line, with the following parameters: FWHM = 30 km sec^{-1} or 0.18 Å at 1810 Å, and integrated emission line flux = 1×10^{-14} erg cm^{-2} sec^{-1}. The measured magnitude of the star is $V = 12$. The desired exposure time is 1000 sec.

In the ETC we select a G2V star and an NUV grating, G185M, set to a central wavelength of 1817 Å. Select a 1000 sec exposure, with the *S/N* specified to be evaluated at 1810 Å. We add an emission line with the line center at 1810, FWHM=0.18, and integrated flux of 10^{-14} erg cm^{-2} sec^{-1}. We specify the normalization as Johnson $V = 12$. We set the zodiacal and earthshine to be *average*.

The ETC returns $S/N = 16.7$ per resel. The local and global count rates are within safe limits. The buffer time recommended is 32,322 seconds. As in the flat-spectrum case above, this `BUFFER-TIME` exceeds the exposure time of 1000 sec, and so the `BUFFER-TIME` should be set at 1000.

11.7.4 A Faint QSO

An important science goal for the design of COS was to obtain moderate S/N spectra of faint QSOs in the FUV. In the ETC, use the FOS-based QSO spectrum provided, and choose G130M at 1309 Å, S/N = 20, and a continuum flux of 10^{-15} erg cm^{-2} sec^{-1} $Å^{-1}$ at 1320 Å. The indicated exposure time is 41,528 sec, or about 14 orbits. The source count rate is 0.002 (counts per second), with a background rate of 1.06×10^{-4} counts per second, 20 times lower than the source. The background is completely dominated by the dark current of the detector. The count rate over the entire detector is 375, well below any safety limits, and the maximum `BUFFER-TIME` is 6289 sec. In this case, to be conservative, use 2/3 that value, or about 4193 sec, for `BUFFER-TIME`.

CHAPTER 12:

Observing Strategies and Proposal Preparation

In this chapter…

The Phase II Proposal Instructions define the capabilities of HST. Those Instructions take precedence over this handbook if there is any conflict of information.

12.1 Designing a COS Observing Proposal

Here are the steps to follow when designing a COS observing proposal. The process is likely to be iterative.

- Identify your science requirements and select the basic instrument configuration to satisfy those requirements.
- Gather target information. Estimate exposure time to achieve required signal-to-noise ratio and check count-rate and bright-object limits. Check for near-by objects.
- Develop a target-acquisition plan. Identify any additional non-science (target acquisition, peakup, and calibration) exposures required.
- Determine the total number of orbits required, taking into account all overheads.

This handbook provides the information needed to estimate exposures and timing, but proposers are urged to use APT to achieve the most accurate results.

12.1.1 Identify Science Requirements

- List your targets. You will probably want to start with more candidate targets than end up in the final proposal so that you can balance factors once you know how long the exposures will be.
- Note your spectroscopic data requirements. What features at what wavelengths are needed for your program? What resolving power is needed? What COS gratings and settings are necessary to get those wavelengths? What level of signal-to-noise is needed for the science?
- Are there other observing requirements? Does a particular target need an unusual acquisition, perhaps because of nearby objects? Is the object variable and needs to be observed at a particular time or phase?

12.1.2 Determine Instrument Configuration

Spectroscopy: For spectroscopic observations, select a detector (FUV or NUV), operating mode (TIME-TAG or ACCUM), aperture (PSA or BOA), grating, central wavelength, and wavelength dither offset (FP-POS). See Chapter 6 for detailed information about these parameters.

Imaging: All imaging observations use the NUV detector, but the user must select the operating mode (`TIME-TAG` or `ACCUM`), aperture (PSA or BOA), and mirror (spectral element = `MIRRORA` or `MIRRORB`).

12.1.3 Gather Target Information

Depending on the type of source, you should be able to obtain target coordinates, magnitudes, and fluxes from on-line databases. For COS, target coordinates need to be accurate to 1.6 arcsec or better for an `ACQ/SEARCH` to successfully center the target in the aperture. Ideally, you want to base your exposure estimates on measured UV fluxes at or near the wavelengths of interest. For much of the sky, observations from the *Galex* mission provide accurate UV fluxes for almost any object bright enough to observe with COS. In other areas, rougher estimates must be made by comparing the source to an analogous object for which better data exist. You will also need at least rough estimates of line fluxes and line widths if there are emission lines in your object's spectrum. This is so you can check to ensure local rate counts will not be excessive.

The HST *Phase II Proposal Instructions* provide information on how the names, coordinates, and fluxes of targets should be specified.

12.1.4 Check for Neighboring Objects

Are there other objects near your targets? First, you want to avoid having more than one source within the COS 2.5 arcsec aperture, otherwise the recorded spectrum will be a blend. Second, other objects that lie within the COS acquisition radius must be checked to ensure they are not too bright. *Galex* data work for much of the sky, but in other areas the available information is much sparser.

Within APT, the Aladin tool allows you to display the Digital Sky Survey in the vicinity of a target and to overplot *Galex* sources if they are available. It is possible for a bright object to fall within the BOA when the PSA is in use (or vice versa), causing a violation of count-rate limits. The Bright Object Tool in APT allows the observer to deal with these situations.

12.1.5 Calculate Exposure Time and Assess Feasibility

You can determine the expected count rate and the recommended `BUFFER-TIME` value (for `TIME-TAG` mode) for your targets with the COS ETC. Determine acquisition exposure times with the COS Target Acquisition ETC. Count rates and exposure times from the ETC will help you to determine the feasibility of using `TIME-TAG` and NUV `ACQ/IMAGE`. Determine the number of exposures needed to cover your desired spectral range.

Once you've selected your basic COS configuration, the next steps are:

- Estimate the exposure time needed to achieve your required signal-to-noise ratio, given your source brightness. (You can use the COS ETC for this.)
- Ensure that your observations do not exceed the count-rate limits discussed in Chapter 9.
- For observations using `ACCUM` mode, ensure that, for pixels of interest, your observations do not exceed the limit of 65,535 accumulated counts per pixel per exposure imposed by the COS 16 bit buffer.

12.1.6 Develop Target Acquisition Strategy

Acquisition strategy is not ordinarily a concern in Phase I, but you may wish to check that an ordinary acquisition will work for your targets, because sophisticated acquisition strategies will use some time in the first orbit that would otherwise be available for science exposures. Some considerations include:

- Check for nearby objects. Other UV-bright objects near your source could cause confusion during the acquisition, so extra care must be taken in crowded fields.

- Check target brightness. Some targets may be observable with COS in spectral mode, but may be too bright for a safe imaging acquisition. The ETC provides a means of checking this. It is unlikely that a source would be too faint to acquire if a spectrum can be obtained of it. Again, the ETC will provide guidance.
- Estimate acquisition times. Use the COS acquisitions ETC to determine the exposure time needed, and then APT to get the full time required, including overheads. Special acquisitions will take longer, and you may wish to consult with a COS Instrument Scientist.

12.1.7 Identify the Need for Additional Exposures

Having identified a sequence of science exposures, you next need to determine what additional exposures you may require to achieve your scientific goals. Specifically:

- If preliminary observations with another *HST* instrument are required to confirm the target's flux or coordinates (Section 8.8), they must be included in the Phase 1 orbit request.
- If the success of your science program requires calibration to a higher level of precision than is provided by routine STScI calibration data, and if you are able to justify your ability to reach this level of calibration accuracy yourself, you will need to include the necessary calibration exposures in your program, including the orbits required for calibration in your total orbit request.

12.1.8 Compute Total Orbit Request

In this step, you place all of your exposures (science and non-science, alike) into orbits, including tabulated overheads, and determine the total number of orbits required. Refer to Chapter 10 when performing this step.

At this point, if you are satisfied with the total number of orbits required, you're done! If not, you can adjust your instrument configuration, lessen your acquisition requirements, or change your target signal-to-noise or wavelength requirements, until you find a combination which allows you to achieve your science goals.

12.2 Parallel Observations with COS

Because the COS aperture is small, it makes sense to use COS as the prime instrument even if a camera, say, is used in parallel. Also, COS is intended to be used on point sources that are centered in its aperture, and that may prevent dithering any camera exposures obtained in parallel. Small displacements (up to 0.3 arcsec on either side of the center) in the cross-dispersion direction should allow some movement of

the image at a camera without degrading the COS spectrum and with only slight loss in throughput.

Proposers with an interest in developing parallel observations with COS are urged to contact an Instrument Scientist and to check the STScI Web pages for new information before the proposal deadline. Also, the HST *Call for Proposals* should be consulted for policies on using COS in parallel with other instruments.

12.3 Phase I - Constructing a Proposal

At this point, you should have assembled all of the information needed to complete your Phase I observing proposal. Before proceeding, you should review the items listed below.

- Check the catalog of previously executed and accepted programs to search for any duplications and, if present, provide a justification for duplicate observations.
- Justify any special requirements (e.g., CVZ targets, targets of opportunity, or time-critical scheduling).
- Allocate time for target acquisitions with appropriate centering accuracy.
- Check your exposure times and configurations to ensure that they are sufficient to provide the desired signal-to-noise ratios and accuracies.
- Check that your source does not exceed the local or global count-rate limits for your detector. Consider both target acquisition and the science observation itself.
- If you require special calibration observations (e.g., additional non-automatic wave-cal exposures) or early acquisition images to determine an object's flux, include them in your Phase I request.
- Consider the need for and benefit of coordinated parallel exposures with other instruments. Take into account any applicable data-volume restrictions.
- Include all applicable overheads so that in Phase II you will have enough orbits to successfully implement your observations.
- Check that no visit is longer than five orbits.
- Make sure that all configurations used in your proposal are included in the summary table.
- Be aware of limits on the number of targets allowed for STIS/MAMA and COS snapshot and survey programs (Section 2.2.2).

12.4 Phase II - Scheduling Approved Observations

Below, we provide a checklist for observers filling out Phase II proposal forms. You should do the following prior to submitting your program.

- Update the text in the Phase II template "Observing Description" and "Special Requirements," which were copied from your Phase I proposal. Make any necessary modifications based on TAC comments and the evolution of your observing plan.
- Specify your coordinates (accurate to one arcsec or better) in the GSC2 reference frame. If accurate coordinates are not available, then consider acquiring a nearby object with well-determined coordinates and offsetting to your target (Section 8.6).
- Specify accurate V magnitude, fluxes, spectral type, and colors for your target.
- Properly specify your instrument configurations.
- Include target acquisitions and peakups as needed.
- Specify any orientation and/or timing requirements. To facilitate scheduling, please allow the broadest ranges for these requirements that are consistent with your scientific goals. If multiple `ORIENT`s are possible, please include the alternatives.
- Include any additional wavecal exposures if needed.
- Verify the correct use (i.e., direction) of `POS-TARG`s (if used).
- Check the Phase II Web page for any updates. You can also find there observing policies and instructions for requesting changes to your program.
- Verify that your targets do not violate bright-limit restrictions.
- For TIME-TAG observations, verify the value of `BUFFER-TIME`.

CHAPTER 13:

Data Products and Data Reduction

In this chapter…

In this chapter, we provide basic information about COS data files that may be helpful to observers preparing Phase I proposals. COS data products are fully described in the *COS Data Handbook*.

13.1 Overview

Raw COS data are processed through the STScI **OPUS** pipeline. Data first undergo Generic Conversion, by which bits from individual exposures are unpacked and combined into files containing raw, uncalibrated data. Next, the raw files are processed through the COS calibration pipeline, **calcos**, which performs image and spectroscopic reduction to produce output files useful for scientific analysis. Finally, the data are ingested into the Hubble Data Archive through the Data Archive and Distribution System (DADS). This system populates a database containing header keywords that is accessible to users via the Multimission Archive at STScI (MAST). Both calibrated and uncalibrated data are then available for distribution by MAST to the user.

13.2 COS File Names

The naming convention for COS files is `rootname_suffix.fits`, in which the rootname follows the standard HST naming convention. All data files associated with a single observation share a unique rootname. COS rootnames begin with the letter l (lowercase L). The suffix identifies the type of data within the file (described below). All FUV data files, with the exception of the _x1d and _x1dsum files, have an additional suffix of _a or _b (e.g., `rootname_rawtag_a.fits`) to denote the detector segment. For the _x1d and _x1dsum files, data from both segments are combined into a single file.

13.3 FUV TIME-TAG

13.3.1 Raw FUV TIME-TAG Data

- File Suffix: _rawtag_a, _rawtag_b

COS FUV raw TIME-TAG data are written to two files, one for each detector segment. These files have two extensions.

The first extension consists of detected events for each segment in sequential order, based on the time that the event was detected. For each event, the FITS table lists

- TIME: The time of the event (to the nearest 32 msec, floating point) after the start of the exposure.
- RAWX: The raw coordinate value in the dispersion direction. These are 16-bit integers between 0 and 16383.
- RAWY: The raw coordinate value in the cross-dispersion location. These are 16-bit integers between 0 and 1023.
- PHA: The pulse-height amplitudes. These are 8-bit integers between 0 and 31.

The raw data include source counts, sky background, detector background, and stim pulses.

The second extension contains two arrays:

- START: These are the starting points of good time intervals in seconds from the start of the exposure.
- STOP: These are the stopping points of the good time intervals in seconds from the start of the exposure.

13.3.2 Corrected FUV TIME-TAG Data

- File Suffix: _corrtag_a, _corrtag_b

The COS pipeline produces corrected TIME-TAG events lists and stores them in binary tables with the suffix _corrtag. These files contain two extensions. The first consists of the 11 quantities listed in Table 13.1.

Table 13.1: Data in corrected FUV TIME-TAG files.

Column name	Description
TIME	time of event in seconds after start of exposure
RAWX	raw *x* pixel location
RAWY	raw *y* pixel location
XCORR	*x* (column) pixel location, corrected for geometric and thermal distortion
XDOPP	XCORR, corrected for doppler shifts.
YCORR	*y* (row) pixel location, corrected for distortion
XFULL	XDOPP corrected for offset in the dispersion direction, based on the wavecal spectrum
YFULL	YCORR corrected for offset in the cross-dispersion direction, based on the wavecal spectrum
EPSILON	weight for the event, based on the flat field and dead time
DQ	data quality flag
PHA	pulse height amplitude

- TIME is the time for each event, recorded to the nearest 32 msec, copied from the raw file.
- RAWX is the *x* location copied directly from the raw data file.
- RAWY is the *y* location copied directly from the raw data file.
- XCORR and YCORR represent the location of the event in detector coordinates, corrected for thermal distortion (characterized by the stim pulses) and geometric distortion (determined during ground testing). These new *x* and *y* values are floating-point numbers, rather than integers.
- XDOPP is the *x* position of the event corrected for orbital and heliocentric doppler effects.

- XFULL is copied from XDOPP and YFULL from YCORR. XFULL and YFULL are then corrected for any spectral drifts as determined from the wavecal spectrum. For TIME-TAG data, offsets in both the dispersion and cross-dispersion directions are interpolated in time from each exposure of the wavecal lamp.
- `EPSILON` is the sensitivity or weighting term for a photon event. It combines pixel-to-pixel response variations and the dead-time correction.
- `DQ` represents the quality factor for a given event, based on its location. It flags events that land on regions of known detector blemishes and anomalies or that occur during time intervals that are deemed to be bad for some reason. See Table 3.10 of the *COS Data Handbook* for a full explanation.
- `PHA` is the pulse height for an event. The pulse height represents the amount of charge extracted from the micro-channel plate for that photon, or, alternatively, the electron gain for that event. The pulse height can be used later as a filter to select the most significant events as a way of reducing noise. The `PHA` values range from 0 to 31 and are copied directly from the raw data file.

The second extension contains copies of the START and STOP times contained in the raw files.

13.3.3 Corrected FUV TIME-TAG Image

- File Suffix: _flt_a, _flt_b

The _flt files contain three extensions, each a 16384 × 1024 image. The first is the corrected image. It is the sum of all the `EPSILON` factors associated with the photon events in a given pixel, divided by the exposure duration. Units are effective counts per second. The image is corrected for flat-field and dead-time effects, but is not background subtracted.

The second extension contains the error array. Errors are calculated from the gross counts using Poisson statistics, then combined with the uncertainties in the flat-field and dead-time corrections. The units are the same as for the corrected image.

The third extension is the DQ (data quality) array. For each pixel, data-quality conditions are flagged by setting individual bits in a 16-bit integer word.

13.3.4 FUV TIME-TAG Science Spectrum

- File Suffix: _x1d, _x1dsum, _x1dsum[n]

The pipeline produces a fully-calibrated, extracted spectrum for each spectroscopic exposure (suffix _x1d) and a combined spectrum representing the mean of all exposures obtained during a single visit (suffix _x1dsum). In cases where several FP-POS offsets were used, there can be additional files with suffixes of the form _x1dsum1, _x1dsum2, etc., for which the number corresponds to the FP-POS position. Each represents the mean of the exposures obtained at that FP-POS position. In

addition, there will be an _x1dsum file without a number, corresponding to the mean of all the FP-POS sums.

In most cases, the FUV _x1d files contain a single file extension consisting of 12 quantities (Table 13.2). Each extension contains a 16384 × 2 array, with one dimension for each detector segment. For observations in which one detector segment was turned off, SEGMENT will have only one entry, and the WAVELENGTH, FLUX, and other arrays will be one-dimensional. In such cases, the keyword SEGMENT in the main header will be FUVA or FUVB, instead of BOTH, as is normally the case.

Table 13.2: Data in extracted FUV TIME-TAG science spectrum files.

Column name	Description
SEGMENT	FUVA or FUVB
EXPTIME	exposure time, in seconds, corrected for any gaps [double precision]
NELEM	the length of the arrays that follow [integer]
WAVELENGTH	array of wavelengths (Å) [double precision]
FLUX	array of fluxes [floating point]
ERROR	array of error estimates for fluxes [floating point]
GROSS	array of count rate [floating point]
GCOUNTS[1]	array of counts [floating point]
NET	array of count rates corrected for background, flat field, and dead time
BACKGROUND	array of background count rates
DQ	Logical OR of all data quality flags in the extraction region
DQ_WGT	1 or 0 in _x1d files; number of good spectra averaged into sum for that wavelength point in _x1dsum files

1. A recent addition to the file, the GCOUNTS array represents the GROSS count-rate array multiplied by the exposure time appropriate for each element.

These quantities are explained in detail in the *COS Data Handbook*. The count rates are computed for bins of equal physical width. The detector background rate is determined from regions of the detector above and below the science spectrum and is averaged over a several spectral elements to improve the statistics, since the background rate is quite low. Since no airglow features fall on this region of the detector, they are not included in the background spectrum.

The net count rate is converted to units of flux using calibration reference files. The final error σ is in flux units and includes all the known sources of error. The DQ array is a logical OR of all the DQ flags in the extraction window. DQ_WGT is either 0 or 1 in the x1d files, depending on whether all of the points contributing to that wavelength point are reliable. In the x1dsum files, DQ_WGT represents the number of good spectra that contribute to that wavelength point.

13.4 NUV TIME-TAG Data

13.4.1 Raw NUV TIME-TAG Data

- File Suffix: _rawtag

For the NUV, no pulse heights are recorded, so the raw data consist of *t*, *x*, and *y*. The coordinate ranges are 0 to 1023 in the raw files.

13.4.2 Corrected NUV TIME-TAG Data

- File Suffix: _corrtag

For the NUV, the corrected array of `TIME-TAG` events consists of the same quantities as for the FUV, except that the entries for PHA are set to 0. Because the corrections applied by the pipeline may shift photon events beyond the physical boundaries of the 1024 × 1024-pixel MAMA, allowed values of XDOPP and XFULL range from 0 to 1273.

13.4.3 Corrected NUV TIME-TAG Image

- File Suffix: _flt

These files have the same structure as the FUV files. In this case, the image, error, and DQ arrays are 1274 × 1024 images, formed from the corrected array of `TIME-TAG` events.

13.4.4 NUV TIME-TAG Science Spectrum

- _x1d, _x1dsum, _x1dsum[n]

These files are similar to the FUV files, except that they consist of 1274 × 3-point arrays, with one dimension for each of the three NUV spectral stripes.

13.5 FUV ACCUM Data

13.5.1 Raw FUV ACCUM Data

- File Suffix: _rawaccum_a, _rawaccum_b

These files have three extensions.

The first extension is an array of 16384 × 1024 pixels. Each pixel is 16 bits deep, so can handle up to 65,535 counts. Note that the actual image sent from the instrument is only 128 pixels high to minimize data volume, but the full image size is maintained in ground processing to allow for future movements of the spectrum on the detector (Section 4.1.9). The unused pixels are filled with zeroes. There are separate sub-arrays for the stim pulses. No pulse-height information is available for data obtained in ACCUM mode.

The second extension consists of only a header.

The third extension is a set of DQ flags that indicate which pixels lay outside of the region that contains actual data.

13.5.2 Corrected FUV TIME-TAG List

- File Suffix: _corrtag_a, _corrtag_b

For ACCUM data, these files serve primarily as place holders to make the time-tag and ACCUM reduction processes as similar as possible. All of the PHA entries are set to 0, and the TIME values to the mean of the observation. XCORR and XDOPP are identical, since the Doppler correction is performed on board.

13.5.3 Corrected FUV ACCUM Data

- File Suffix: _flt_a, _flt_b

These files contain three extensions, each a 16384 × 1024-pixel image.

The first extension is the corrected image, constructed by summing the counts in each pixel, multiplying by that pixel's ε factor, and divided by the exposure duration. The resulting units are effective counts sec^{-1}. The image is corrected for the doppler motion of the spacecraft (done on-board in the flight software), flat-field response, detector dead time, and geometric distortion, but not for background or thermal drift.

The second extension is the error array. Poisson errors, computed from the gross counts in each pixel, are combined with the uncertainties in the flat-field and dead-time corrections. Units are effective counts sec^{-1}.

The third extension is the revised data-quality array.

13.5.4 FUV ACCUM Science Spectrum

- File Suffix: _x1d, _x1dsum, _x1dsum[n]

These files include the same quantities described for FUV TIME-TAG data in Section 13.3.4.

13.6 NUV ACCUM Data

The data products for the NUV ACCUM mode are all as for the FUV except that both the raw and _flt images are 1024 × 1024, with all of the pixels containing actual data. The extracted spectra (the _x1d files) contain 1274 wavelength points, which are needed to accommodate drifts that may shift different exposures obtained during the same visit.

13.7 NUV IMAGE Data

13.7.1 Raw NUV IMAGE Data

- File Suffix: _rawtag, _rawaccum

NUV images can be obtained in either TIME-TAG or ACCUM modes. In each case, the raw file extensions and contents are the same as for NUV spectroscopic data.

13.7.2 Corrected NUV Image Data

- File Suffix: _flt, _fltsum

The _flt files for image data are similar to the spectroscopic data, except that the images in the files are 1024 × 1024 in size instead of 1274 × 1024. A further difference is that when several image exposures are grouped together, an _fltsum file is produced, which contains the mean image.

13.8 Additional COS Output Files

Several additional files are used in the processing of COS data. These include association files (_asn), which are used to control calibration processing; engineering support files (_spt), which contain information used in the pipeline processing; and lampflash files (_lampflash), which contain extracted wavelength calibration spectra used in the processing of `TIME-TAG` data with `FLASH=YES`. For a full description of these and other files, see the *COS Data Handbook*.

CHAPTER 14:

The COS Calibration Program

In this chapter. . .

14.1 Introduction

In this chapter, we provide a brief guide to the calibration observations obtained during ground testing and on-orbit during SMOV4 and Cycle 17. Potential Cycle 18 observers should assume that all of these calibrations will be completed by the time that Cycle 18 begins.

Observers wishing to use instrument configurations that are not addressed by these calibration plans should assess their specific calibration needs and include time in their Phase I proposal for any additional calibrations that are required. Proposers who believe that more extensive calibration observations or analysis may be of general benefit to the COS user community should consider submitting a Cycle 18 Calibration Outsourcing Proposal (see the Cycle 18 "Call for Proposals" for details).

14.2 Ground Testing and Calibration

The COS Instrument Definition Team (Principal Investigator, James Green, University of Colorado) was responsible for the ground testing and ground calibration of COS. Most of the ground test data was obtained in 2003 and 2006 during thermal vacuum testing at Ball Aerospace and Goddard Space Flight Center, respectively. These tests characterized the basic properties of the optics, the detectors, and the mechanisms. While some measurements (e.g., FUV full-detector flat-field images) cannot be repeated in orbit, most of the ground-test data will be superseded by on-orbit measurements obtained during SMOV4.

14.3 SMOV4 Testing and Calibration

The primary goal of Servicing Mission 4's Orbital Verification program (SMOV4) was the timely commissioning of *HST* for normal science operations. For the newly-installed COS, this included testing the focus (internal and external), verifying the target-acquisition procedures, monitoring instrument stability (both in terms of image motions and sensitivity), and measuring plate scales, line-spread functions, and other instrument parameters. SMOV4 observations were completed in October, 2009, and a series of Instrument Science Reports detailing the results of their analysis is forthcoming.

Brief descriptions of the COS SMOV activities are provided below. Details are provided in COS TIR 2009-01 (Keyes et al. 2009). The observing programs used to implement these activities are listed Table 14.1. Data from calibration programs are non-proprietary and can be obtained from the archive using the proposal IDs listed in the table.

COS-01: COS Safemode Recovery

- Includes turn-on and telemetry checks that verify the capability to enter required instrument and detector states during normal operations.

COS-02: COS Dump Test and Verification of COS Memory Loads

- Load, dump and compare sections of memory with stored images to verify operations.

COS-03: COS Science Data Buffer Check with Self-Test

- Check the COS science buffer for bit flips during SAA passages.
- Load a test pattern into the science data buffer. The buffer contents are subsequently examined using memory and exposure dumps.

COS-04: COS NUV Detector Initial HV Turn-On and Ramp-Up

- The NUV MAMA high voltage is slowly ramped up to its full operating voltage.
- TIME-TAG dark images are taken to test basic detector function at full operating voltage.

COS-05: COS NUV Detector Dark

- Measure the NUV detector dark rate by taking twenty long (3250 second) exposures with the shutter closed.

COS-06: COS NUV Detector Internal Functionality and Operation

- Verify lamp operation under various grating and central wavelength combinations with a single deuterium lamp exposure and twelve wavecal lamp exposures.
- Estimate OSM drift through a long exposure with regular lamp flashes.

COS-07: COS NUV Fold Test

- A deuterium lamp exposure measures the performance of the MAMA micro-channel plates.

COS-08: COS to FGS Alignment (NUV)

- Target positioning accuracy using FGS guiding is measured using NUV `MIRRORA` images of an astrometric target and field.

COS-09: COS NUV Optical Alignment and Focus

- NUV `MIRRORA` images are taken of the same field observed by COS-08 to obtain the fine focus.
- The alignment and focus is repeated a total of three times to assure convergence to the optimal alignment and image quality.
- The COS `ACQ/IMAGE` functionality is also verified during this program.

COS-10: COS Internal NUV Wavelength Measurement

- A series of NUV internal wavelength calibration exposures are obtained, testing all grating and central wavelength combinations at the default FP-POS, and one grating/central wavelength combination at all FP-POS values. These exposures are wavelength calibrated in order to measure the COS on-orbit wavelength calibration.

COS-11: COS NUV Imaging Acquisition Algorithm Verification

- Testing that the COS target acquisition flight software can properly identify the centroid of a point source in its field and then move that centroid to the center of the aperture.

COS-12: COS NUV Dispersed-light Acquisition Algorithm Verification

- Verify the ability of the COS flight software to place an isolated point source at the center of the aperture (both BOA and PSA) using dispersed light from the object via an NUV grating.
- Test `ACQ/SEARCH`, `ACQ/PEAKD`, and `ACQ/PEAKXD` acquisitions.

COS-13: COS NUV Imaging Performance Verification

- Assess the PSF quality and measure the plate scale for both `MIRRORA` and `MIRRORB`, using both the PSA and BOA.
- Assess OSM drift and image stability over several orbits.

COS-14: NUV Internal/External Wavelength Scales

- Test wavelength calibration by observing radial velocity standard targets in `TIME-TAG` mode with `FLASH=YES` at all NUV grating and central wavelength combinations.

COS-15: COS Internal NUV Wavelength Verification

- Verify the COS wavelength zero-point and spectral ranges by taking internal PtNe lamp exposures at all grating, central-wavelength, and FP-POS combinations.

COS-16: COS NUV External Spectroscopic Performance, Part 1

- Measure the spectral resolution of absorption lines for all NUV gratings.
- Evaluate the effect of small pointing errors by acquiring additional spectra at spatially offset positions.

COS-17: COS NUV External Spectroscopic Performance, Part 2

- Verify the spatial resolution of COS in the NUV, and characterize the interdependence of the spatial and spectral resolution by stepping a source along the cross-dispersion direction out to the edge of the PSA.

COS-18: COS NUV Flat Fields

- Take long exposures with the internal Deuterium lamp and the G185M grating.
- Take 12 1800-second flat-field exposures at central wavelengths of 1835, 1850, and 1864 Å.

COS-19: COS NUV Spectroscopic Sensitivity

- Establish COS sensitivity vs. wavelength over the entire observable spectrum for all NUV grating and central wavelength combinations.
- Establish a baseline for contamination/sensitivity monitoring.
- Evaluate any changes from ground-based (thermal vacuum) calibrations.

COS-20: COS NUV Structural and Thermal Stability

- Measure COS pointing jitter or drifts over time scales of seconds to hours. In particular, test OSM drift, day-night transitions, and orbital "breathing".
- Test both NUV spectroscopy and NUV imaging.

COS-21: COS NUV High S/N Verification

- Verify that high S/N (S/N = 30) spectra can be obtained in all modes.
- Verify that very high S/N (S/N = 100) spectra can be obtained in medium-resolution modes.

COS-22: COS FUV Detector Door Open

- Open the FUV detector door so that the detector can begin to outgas and light can reach the micro-channel plates.

COS-23: COS FUV Detector Initial High Voltage Turn-On and Ramp-Up

- Turn on the FUV high voltage in stages.
- Obtain short DARK and WAVE exposures as soon as the ramp-up is complete.

COS-24: COS FUV Detector Dark

- Measure the FUV detector dark rate by taking 30 long (3250 second) exposures with the shutter closed.

COS-25: COS FUV Detector Internal Functionality and Operation

- Test lamp and detector functionality with a single deuterium lamp exposure and six wavecal lamp exposures.
- Take a single long exposure with regular lamp flashes to obtain an initial characterization of OSM drift.

COS-26: COS FUV Optical Alignment and Focus

- Produce a fine-focus sweep for each grating by taking 15 FUV exposures of a sharp-lined external target.
- Test FUV dispersed-light target acquisition.
- Verify FUV optical alignment and determine post-alignment spectral resolution and spectrum location.

COS-27: COS Internal FUV Wavelength Measurement

- Derive on-orbit wavelength solutions by taking internal wavecal exposures at all grating and central wavelength combinations at the default `FP-POS`, and all `FP-POS` positions with the default central wavelength of each grating.
- Test the operation of PtNe LAMP 2 with additional exposures.

COS-28: COS FUV Dispersed-light Target Acquisition Algorithm Verification

- Verify the ability of the COS flight software to place an isolated point source at the center of the aperture, for both BOA and PSA, using dispersed light from the object and FUV gratings.

COS-29: COS FUV Internal/External Wavelength Scales

- Obtain zero-point offsets and dispersion relations for all grating and central wavelength combinations by observing radial velocity standard targets in `TIME-TAG` mode with `FLASH = YES`.

COS-30: COS Internal FUV Wavelength Verification

- Verify the COS FUV zero-points and spectral ranges by taking a series of PtNe lamp exposures at all grating, central-wavelength, and FP-POS combinations.

COS-31: FUV External Spectroscopic Performance, Part 1

- Measure the spectral resolution of absorption lines for each FUV grating.
- Characterize the degradation in spectral resolution due to small positioning errors in the peakup process.

COS-32: FUV External Spectroscopic Performance, Part 2

- Verify the spatial resolution of COS in the FUV.
- Characterize the interdependence of the spatial and spectral resolution of COS.

COS-33: COS FUV External Flat Fields

- Obtain exposures of a continuum source with a range of positions in the cross-dispersion direction sufficient to fully cover the region of the FUV detector where spectra will fall.

COS-34: COS FUV Spectroscopic Sensitivity

- Establish COS FUV sensitivity versus wavelength over the entire observable spectrum for all FUV gratings and central wavelength settings.
- Establish a baseline for contamination and sensitivity monitoring.
- Evaluate any changes in sensitivity from ground-based thermal vacuum calibrations.

COS-35: COS FUV Structural and Thermal Stability

- Measure COS pointing jitter or drifts over time scales of seconds to hours. In particular, test OSM drift, day-night transitions, and orbital "breathing".

COS-36: COS FUV High S/N Verification

- Determine whether the effects of detector fixed pattern noise can be compensated for with routine `FP-POS` exposures and flat fielding.

Table 14.1: COS SMOV4 Proposals

ID	Title
11353	COS Dump Test and Verification of COS Memory Loads
11354	COS Science Data Buffer Check/Self-Tests for CS Buffer RAM and DIB RAM
11355	NUV Detector Initial HV Turn On & RampUp, NUV Fold Test
11356	COS FUV Initial On-Orbit Turn-On
11466	NUV Detector Dark
11467	NUV Detector Internal Functionality and Operation
11468	COS to FGS Alignment (NUV)
11469	NUV Optics Alignment and Focus
11470	Internal NUV Wavelength Measurement
11471	NUV Imaging Acquisition Algorithm Verification
11472	NUV Dispersed-light Acquisition Algorithm Verification
11473	NUV Imaging Performance
11474	NUV Internal/External Wavelength Scales
11475	Internal NUV Wavelength Verification
11476, 11477	NUV External Spectroscopic Performance
11478	NUV Flat Fields
11479	NUV Sensitivity Visits
11480	NUV Structural and Thermal Stability

Table 14.1: COS SMOV4 Proposals (Continued)

ID	Title
11481	NUV High S/N Verification
11482	FUV Detector Dark
11483	FUV Detector Functionality and Operation
11484	FUV Optics Alignment and Focus
11485	Internal FUV Wavelength Measurement
11486	FUV Target Acquisition Algorithm Verification
11487	FUV Internal/External Wavelength Scales
11488	Internal FUV Wavelength Verification
11489, 11490	FUV External Spectroscopic Performance
11491	FUV External Flat Fields
11492	FUV Sensitivity Visits
11493	FUV Structural and Thermal Stability
11494	FUV High S/N Verification
11496	SMOV Verification of COS PtNe Lamp 2

14.4 Cycle 17 Testing and Calibration

The Cycle 17 calibration program will continue the testing begun during SMOV. It includes long-term programs to monitor the sensitivity and wavelength scale of both the NUV and FUV detectors. Brief descriptions of each program follow.

11891: NUV Detector Fold Test

- Provides an indication of the gain of the MAMA micro-channel plate by measuring the distribution of charge cloud sizes on the anode.

11892: NUV Detector Recovery after Anomalous Shutdown

- Tests NUV MAMA health after an anomalous shutdown.
- Performs slow HV ramp-up, including dark exposures at full and intermediate voltages.

11893: FUV Detector Recovery after Anomalous Shutdown

- Turn on FUV HV slowly over several cycles after an unexpected shutdown, each time ramping up to a higher voltage than the last.

11894: NUV Detector Dark Monitor

- Take a 25-minute NUV dark exposure twice every week.

11895: FUV Detector Dark Monitor

- Take a 25-minute FUV dark exposure five times every week.

11896: NUV Spectroscopic Sensitivity Monitor

- Obtain a G230L exposure of a standard star every month.
- Obtain a G185M exposure of a standard star every three months and G225M and G285M exposures every month.
- Track any time dependence in detector sensitivity.
- Tie primary to secondary spectrophotometric standards.

11897: FUV Detector Sensitivity Monitor

- Take monthly G140L and quarterly medium-resolution exposures of standard stars to monitor any time-dependence in detector sensitivity.
- Tie primary to secondary spectrophotometric standards.

11899: NUV Imaging Sensitivity

- Observe targets with an appropriate range of colors to establish color terms in the sensitivity formula.

11900: NUV Internal/External Wavelength Scale Monitor

- Monitor zero-point offsets for the wavelength scale (internal wavecal lamp to external standard wavelength scale). Repeat every 1-2 months initially.

11997: FUV Internal/External Wavelength Scale Monitor

- Observe radial-velocity standard targets in TIME-TAG FLASH=YES mode to monitor zero-point offsets between the internal calibration spectrum and the external target.
- Repeat every 2-3 months initially starting at the end of SMOV.

12010: FUV Line Spread Function Characterization

- Observe the star Sk-155 (an O9b star in the SMC) with the high resolution E140H grating on STIS. Compare with COS G130M and G160M spectra obtained during SMOV to characterize the broad non-Gaussian wings in the COS LSF.

Additional Cycle 17 Programs

- As this handbook is being written, a program to determine the sensitivity and wavelength scale of COS at wavelengths between 900 and 1100 A, and perhaps into the EUV, is under development. Another program will characterize the second-order flux seen on the long-wavelength end of FUV detector segment A. Information about these and other additional Cycle 17 calibration programs will be distributed via STScI Analysis Newsletters (STANs).

14.5 Cycle 18 Calibration Plan

The Cycle 18 calibration plan for COS will include the routine calibration and monitoring observations performed in Cycle 17. The priorities assigned to the calibration of various COS modes will be determined by the approved Cycle 18 GO programs.

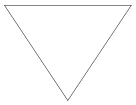

If your program requires calibrations beyond those that are planned for Cycle 17 and that are of direct benefit to other COS users, then you should apply directly for this calibration in your Phase I proposal.

CHAPTER 15:

Spectroscopic Reference Material

In this chapter. . .

15.1 Introduction

The information in this chapter will help you to select a detector, grating configuration, and observing aperture and to develop your observing plan. For each grating, the following information is provided:

- A brief description of the grating, with special considerations for its use.
- Grating parameters, including the dispersion and plate scale.
- Plots showing the available central-wavelength settings and the range of wavelengths covered by each setting and `FP-POS` position.
- Plots and tables of sensitivities and effective areas as a function of wavelength.
- Plots of signal-to-noise ratio as a function of V+STMAG$_\lambda$ (the color-dependent correction from V magnitude to STMAG at wavelength λ), F_λ, and exposure time.
- Line-spread functions as a function of wavelength.

Note that the quoted parameters are based on the measurements available at the completion of SMOV4. Values will be refined throughout Cycle 17. See the COS Web site for the latest information.

15.2 Using the Information in this Chapter

15.2.1 Grating Parameters

For each grating, the resolving power, dispersion, and the size of an `FP-POS` step are taken from Table 6.1. Plate scales in both the dispersion and cross-dispersion directions are derived from data obtained during SMOV.

15.2.2 Wavelength Ranges

For each grating, we plot the wavelengths sampled by each central-wavelength setting. For the NUV gratings, the central wavelength is the midpoint of stripe B. For the FUV gratings, the central wavelength represents the shortest wavelength recorded on segment A (though that value may have changed slightly since the central wavelengths were first defined). Wavelength ranges for each central wavelength at `FP-POS=3` are provided in tabular format in Table 6.4 and Table 6.5; tables of the wavelength ranges for all four `FP-POS` positions are available on the COS Web site.

For the FUV gratings, the wavelength ranges sampled at each `FP-POS` position are plotted separately. For the NUV gratings, the total wavelength range sampled by all `FP-POS` positions is plotted for each central-wavelength setting.

15.2.3 Grating Sensitivities and Effective Areas

This section presents sensitivities and effective areas as a function of wavelength for each grating. The target is assumed to be a point source centered in the PSA.

The total system[1] *spectroscopic point-source sensitivity,* S_λ^p, has units of counts pix_λ^{-1} sec^{-1} per incident erg cm^{-2} sec^{-1} $Å^{-1}$ for both the FUV and NUV detectors, where

- pix_λ = a pixel in the dispersion direction, and
- counts refer to the total counts from a point source integrated over the PSF in the direction perpendicular to the dispersion.

The count rate per pixel is simply the product of the target flux and the point-source sensitivity at a given wavelength. To estimate the S/N ratio achieved at a given count rate and exposure time, follow the directions in Section 11.3 or use the S/N plots in this chapter.

The effective area has units of cm^2.

1. COS plus *HST* Optical Telescope Assembly (OTA).

15.2.4 Signal-to-Noise Plots

For each grating, a plot is provided to help you estimate the signal-to-noise ratio (S/N) that can be achieved from a point source observed at a fiducial wavelength near the peak of the effective-area curve. The fiducial wavelength is indicated in the ordinate label of each plot. To estimate S/N at other wavelengths, scale your source flux or magnitude by the relative sensitivities at the wavelength of interest and at the fiducial. The plots show S/N as a function of F_λ and of V+STMAG$_\lambda$ for a range of exposure times. STMAG$_\lambda$ is the color-dependent correction from V magnitude to STMAG at wavelength λ. Values of STMAG$_\lambda$ for various stellar and extragalactic sources are presented in Table 15.1 and Table 15.2, respectively. In producing these plots, we assumed an average sky background (as described in Chapter 11) and the dark current appropriate for each detector. These plots should be used only for rough estimates of exposure times. When constructing your proposal, use the COS Exposure Time Calculator (ETC) to estimate S/N values.

Note the following:

- The point source S/N has been calculated per resolution element, and has been integrated over the PSF to contain all of the flux in the cross-dispersion direction.
- The symbols in the S/N figures delineate regions of parameter space where the dark current contributes more than half the source counts.
- The vertical shaded area indicates the bright-object *observing* limit, which is slightly higher than the *screening* limit given in Table 9.1.

Follow these steps to use the S/N plots:

1. Look up in Table 15.1 the effective temperature and wavelength region of interest (e.g., 5000 K @ 2000 Å). Interpolate in the table to get STMAG$_\lambda$.
2. Add the V magnitude of the target to STMAG$_\lambda$.
3. Find the appropriate plot for the desired grating and locate V+STMAG$_\lambda$ on the horizontal axis. Read off the S/N for the desired exposure time, or vice-versa. Alternatively, use F_λ directly on the horizontal axis.
4. To get accurate values for repeated or `FP-POS` exposures, use the sub-exposure time when consulting the plot, and then multiply the resulting S/N by $\sqrt{N}$, where N is the number of sub-exposures to be averaged.

For example, consider a V=15 star of spectral type B0 V, for which we want to derive the S/N achieved in a 100 sec exposure using the NUV grating `G230L`. The S/N calculations for G230L are presented in Figure 15.21, where we learn that the fiducial wavelength for this grating is 3000 Å. Assuming an effective temperature of 30,000K, we obtain STMAG$_\lambda$ ~ –2.1 at 3000 Å from Table 15.1, making V+STMAG$_\lambda$ = 12.9. Returning to Figure 15.21, we find this value on the horizontal axis. For an exposure time of 100 seconds, the S/N ~ 9.5.

Table 15.1: $STMAG_\lambda$ as a Function of Wavelength for Stellar Objects. $STMAG_\lambda$ is the color-dependent correction from V magnitude to STMAG at wavelength λ.

Temp (K)	Wavelength (Å)									
	1000	**1200**	**1500**	**2000**	**2500**	**3000**	**3500**	**4000**	**4500**	**5000**
45000	-5.87	-5.46	-4.79	-3.87	-3.02	-2.36	-1.76	-1.27	-0.79	-0.37
30000	-5.38	-4.92	-4.37	-3.50	-2.70	-2.13	-1.56	-1.23	-0.76	-0.35
20000	-3.90	-3.38	-3.45	-2.73	-2.14	-1.66	-1.18	-1.13	-0.72	-0.33
15000	-1.68	-1.24	-2.68	-2.08	-1.53	-1.21	-0.83	-1.05	-0.68	-0.31
10000	9.18	6.27	-0.72	-0.68	-0.26	-0.21	-0.03	-0.88	-0.62	-0.29
9000	12.84	8.67	1.81	-0.19	0.15	0.05	0.16	-0.75	-0.58	-0.26
8000	17.10	11.79	6.33	0.51	0.58	0.21	0.24	-0.56	-0.46	-0.20
7000	20.97	15.07	9.29	1.86	1.26	0.36	0.24	-0.34	-0.32	-0.12
6000	N/A	19.44	14.17	5.50	2.92	0.94	0.47	0.02	-0.15	-0.04
5000	N/A	N/A	20.15	9.80	6.24	2.74	1.24	0.50	0.04	0.10
4000	N/A	N/A	N/A	14.74	9.70	5.53	2.37	0.97	0.24	0.58
3000	N/A	N/A	N/A	17.85	11.46	5.69	2.22	0.71	0.25	0.82

Table 15.2: $STMAG_\lambda$ as a Function of Wavelength for Non-Stellar Objects. $STMAG_\lambda$ is the color-dependent correction from V magnitude to STMAG at wavelength λ.

Spectrum	Wavelength (Å)							
	1500	**2000**	**2500**	**3000**	**3500**	**4000**	**4500**	**5000**
Elliptical	3.35	3.19	4.17	2.92	1.60	0.70	0.17	0.15
S0	4.63	3.95	3.27	2.23	1.61	0.71	0.18	0.13
Sa	2.64	2.27	2.39	1.78	1.31	0.36	0.12	0.07
Sb	1.70	2.59	2.04	1.32	1.12	0.43	0.17	0.10
Sc	-0.18	0.44	-0.17	-0.68	-0.67	-0.51	-0.44	-1.25
Starburst, E(B-V)<0.1	-1.71	-1.15	-0.68	-0.43	-0.13	-0.42	-0.23	-1.24
Starburst, 0.25 < E(B-V) < 0.35	-0.95	-0.87	-0.33	-0.10	0.08	-0.19	-0.19	-0.28
Starburst, 0.51 < E(B-V) < 0.60	-0.40	-0.18	0.01	0.23	0.03	-0.14	-0.12	-0.36
Starburst, 0.61 < E(B-V) < 0.70	0.05	0.31	0.31	0.15	0.27	-0.17	-0.13	-0.11

The $STMAG_\lambda$ values of Table 15.1 are derived from the stellar models of Castelli and Kurucz (2003, 2004), assuming solar metallicity ([Fe/H] = 0.0) and a surface gravity log (g) = 4.5. The $STMAG_\lambda$ values of Table 15.2 are based on observed spectra of each object type.

15.3 Spectrograph Design Parameters

15.3.1 FUV Channel

Table 15.3 presents design parameters of the FUV spectrograph and gratings. The FUV gratings are concave and have holographically-generated grooves to provide dispersion and correct for astigmatism. The gratings have aspherical surfaces to correct for *HST*'s spherical aberration. The FUV "M" gratings have been ion etched to produce triangular groove profiles for better efficiency. The G140L grating has grooves with a laminar profile. All FUV gratings are coated with MgF_2 over aluminum.

The surface of the optic is a sphere of the quoted radius, but with a deviation of $\Delta z = a_4 r^4 + a_6 r^6$, where z is measured along the vertex normal. The quantities γ, δ, r_c, and r_d are the standard positions of the recording sources as defined in Noda, Namioka, and Seya (1974, J. Opt. Soc. Amer., 64, 1031).

Table 15.3: Design Parameters for the FUV Spectrograph and Gratings.

Dimension	G130M	G160M	G140L
secondary mirror vertex to aperture (z, mm)	6414.4		
V_1 axis to aperture (mm)	90.49		
aperture to grating (mm)	1626.57		
α (degrees)	20.1	20.1	7.40745
β (degrees)	8.6466	8.6466	–4.04595
$\alpha - \beta$ (degrees)	11.4534		
grating to detector (mm)	1541.25		
detector normal vs. central ray (degrees)	9.04664		
nominal groove density (lines mm $^{-1}$)	3800	3093.3	480
radius of curvature (mm)	1652	1652	1613.87
a_4	1.45789×10^{-9}	1.45789×10^{-9}	1.33939×10^{-9}
a_6	-4.85338×10^{-15}	-4.85338×10^{-15}	1.4885×10^{-13}
γ (degrees)	–71.0	–62.5	10.0
d (degrees)	65.3512	38.5004	24.0722
r_c (mm)	–4813.92	–4363.6	3674.09
r_d (mm)	5238.29	4180.27	3305.19
recording wavelength (Å)	4880		

15.3.2 NUV Gratings

Table 15.4 presents design parameters of the NUV gratings. The NUV gratings are flat and were not constructed holographically. The NUV MAMA has low but measurable sensitivity at FUV wavelengths, and with some gratings second-order light could contaminate the spectrum. To minimize this effect, the coated optics are optimized for wavelengths above 1600 Å. Given the four reflections used in the NUV channel, wavelengths below 1600 Å, including geocoronal Lyman α, are effectively eliminated. In addition, gratings G230L and G285M have order-blocking filters mounted directly on them to block the second-order spectra below 1700 Å. Even with these filters, it is possible for second-order light with G230L to appear on the NUV MAMA, especially in the long-wavelength stripe.

Table 15.4: Design Parameters for the NUV Gratings.

Dimension	G185M	G225M	G285M	G230L
groove density (mm^{-1})	4800	4800	4000	500
α (degrees)	27.24	33.621	35.707	5.565
β (degrees)	25.85	32.23	34.32	1.088
coating	Al + MgF_2	Al only	Al only	Al + MgF_2

15.4 Gratings

For each COS grating, we present the resolving power, dispersion, plate scales, the wavelength ranges covered at each central wavelength setting and (for the FUV gratings) `FP-POS` position, sensitivities, effective areas, and a tool for estimating S/N. Advice on use is provided where appropriate.

Wavelengths in this handbook and in COS data products are always measured in vacuum.

Gratings:

FUV Grating G130M

Description

The G130M grating samples wavelengths between about 1150 and 1450 Å. It offers higher resolution and effective area than the G140L grating, but less spectral coverage.

Special Considerations

The gap between segments A and B spans 14.3 Å. To fill this gap requires exposures separated by two central-wavelength settings.

Grating	Resolving Power $R = \lambda/\Delta\lambda$	Dispersion (mÅ pixel^{-1})	Plate Scale (milliarcsec pixel^{-1})		FP-POS Step (Å step^{-1})
			Disp. Axis	Cross-Disp. Axis	
G130M	16,000 - 21,000	9.97	22.9	100	2.5

Figure 15.1: Wavelength Ranges for the G130M Grating.

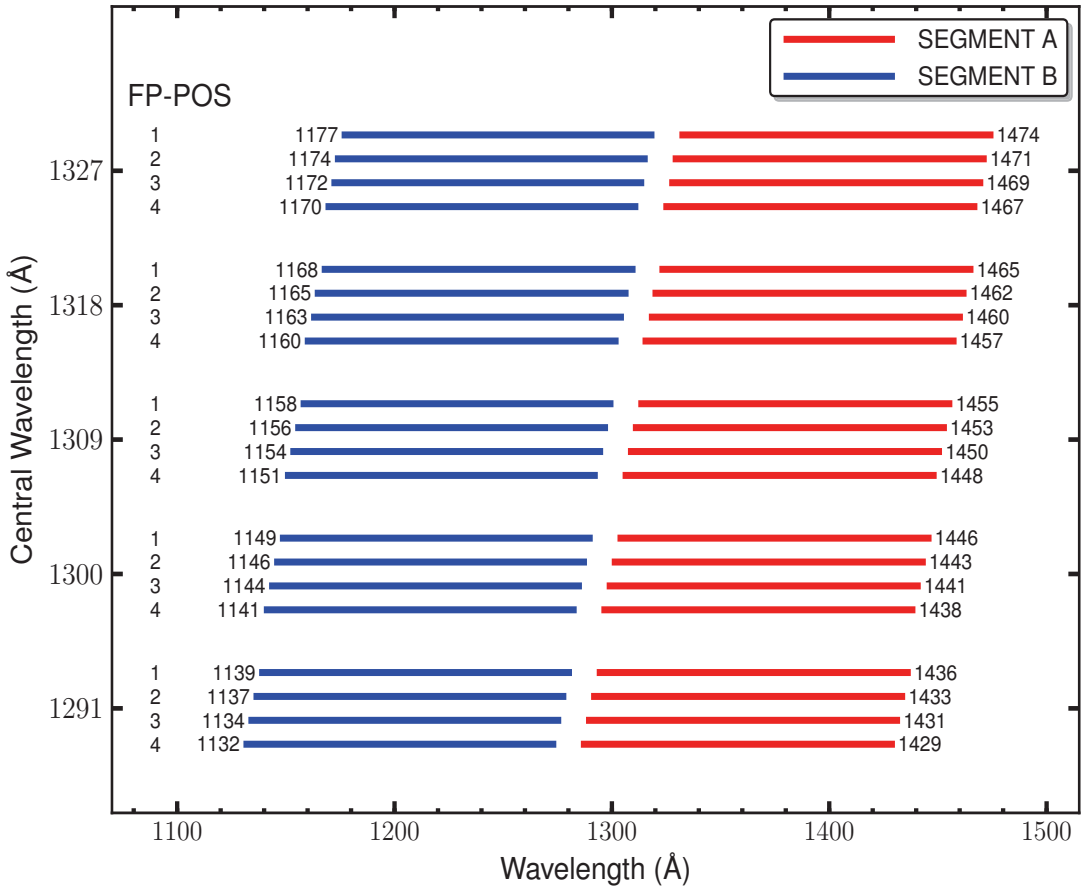

G130M Sensitivities

Table 15.5: G130M Sensitivities & Effective Areas for a Point Source Centered in the PSA.

Wavelength (Å)	Sensitivity (counts pixel^{-1} sec^{-1} per erg cm^{-2} sec^{-1} Å^{-1})	Effective Area (cm^2)
1150	9.7E11	1.69E03
1200	1.4E12	2.35E03
1250	1.8E12	2.94E03
1300	1.7E12	2.59E03
1350	1.5E12	2.25E03
1400	1.4E12	1.97E03
1450	1.1E12	1.52E03

Figure 15.2: G130M Point Source Sensitivity for PSA and BOA.

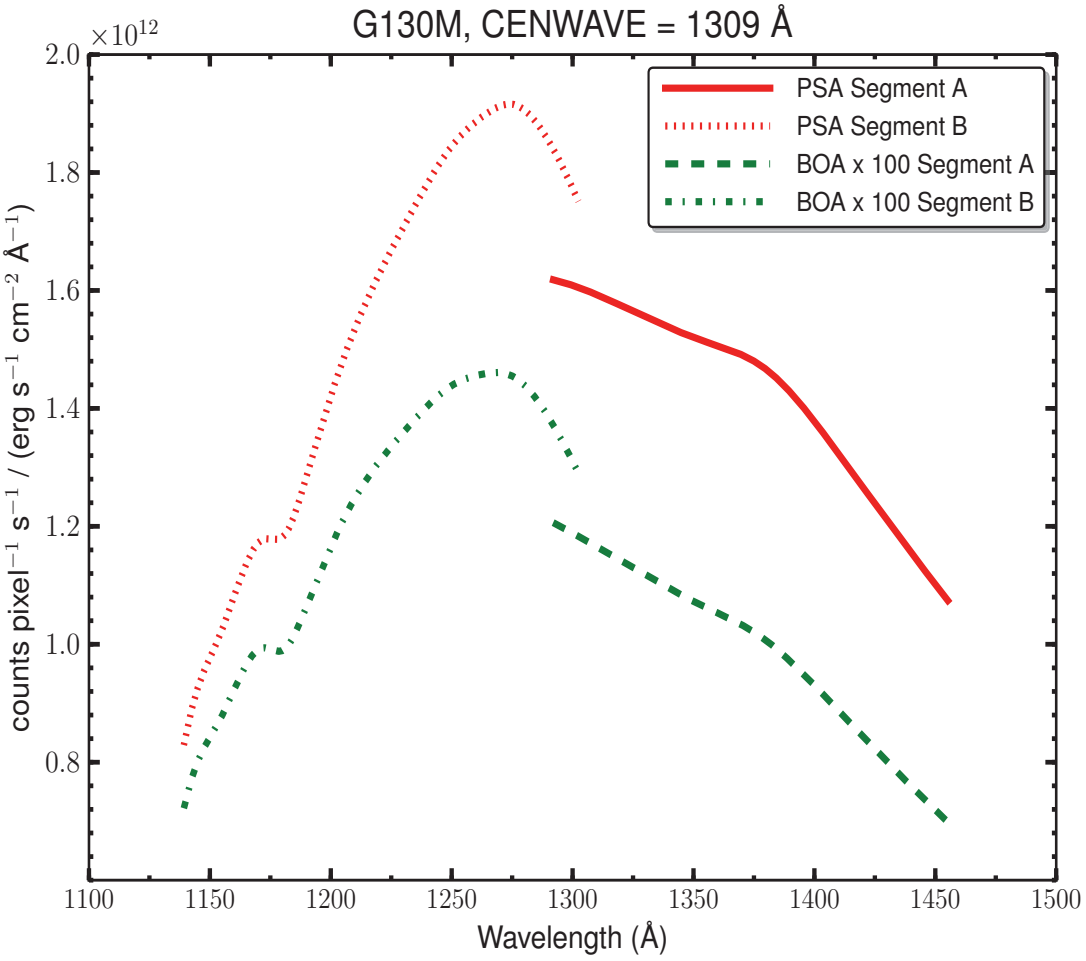

G130M Signal-to-Noise Ratio

Figure 15.3: Point Source Signal-to-Noise as a Function of STMAG for G130M at 1310 Å.

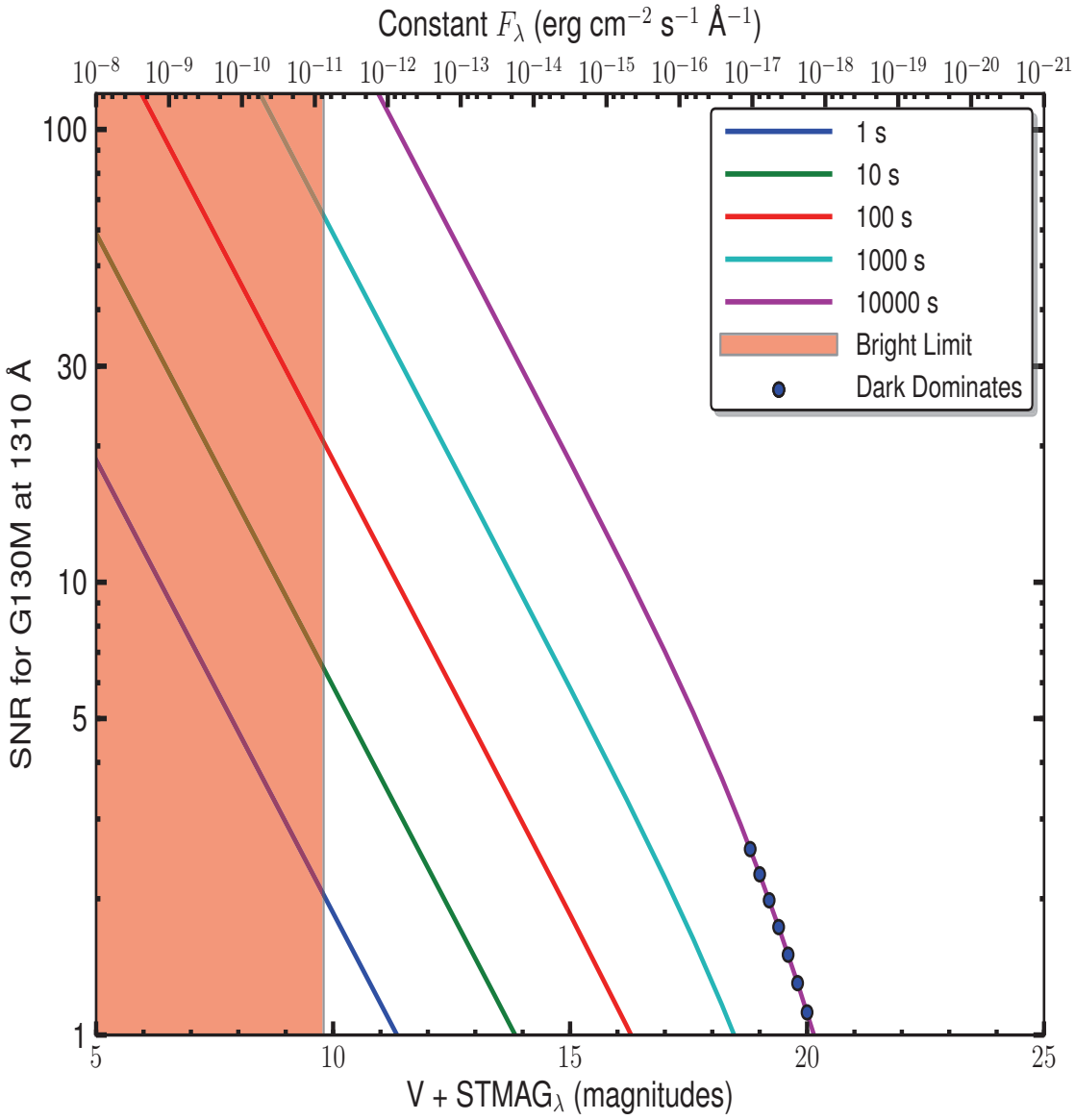

The top axis displays constant F_λ values corresponding to the STMAG units (V+STMAG$_\lambda$) on the bottom axis. Recall that STMAG=0 is equivalent to F_λ = 3.63E-9 erg cm^{-2} s^{-1} Å^{-1}. Colors refer to exposure times in seconds. The edge of the shaded area corresponds to the bright-object limit. Use of the PSA is assumed.

FUV Grating G160M

Description

The G160M grating samples wavelengths between about 1405 and 1775 Å. It offers higher resolution and effective area than the G140L grating, but less spectral coverage.

Special Considerations

The gap between segments A and B spans 18.1 Å. To fill this gap requires exposures separated by two central-wavelength settings.

Grating	Resolving Power $R = \lambda/\Delta\lambda$	Dispersion (mÅ pixel^{-1})	Plate Scale (milliarcsec pixel^{-1})		FP-POS Step (Å step^{-1})
			Disp. Axis	Cross-Disp. Axis	
G160M	16,000 - 21,000	12.23	24.3	90	3.2

Figure 15.4: Wavelength Ranges for the G160M Grating.

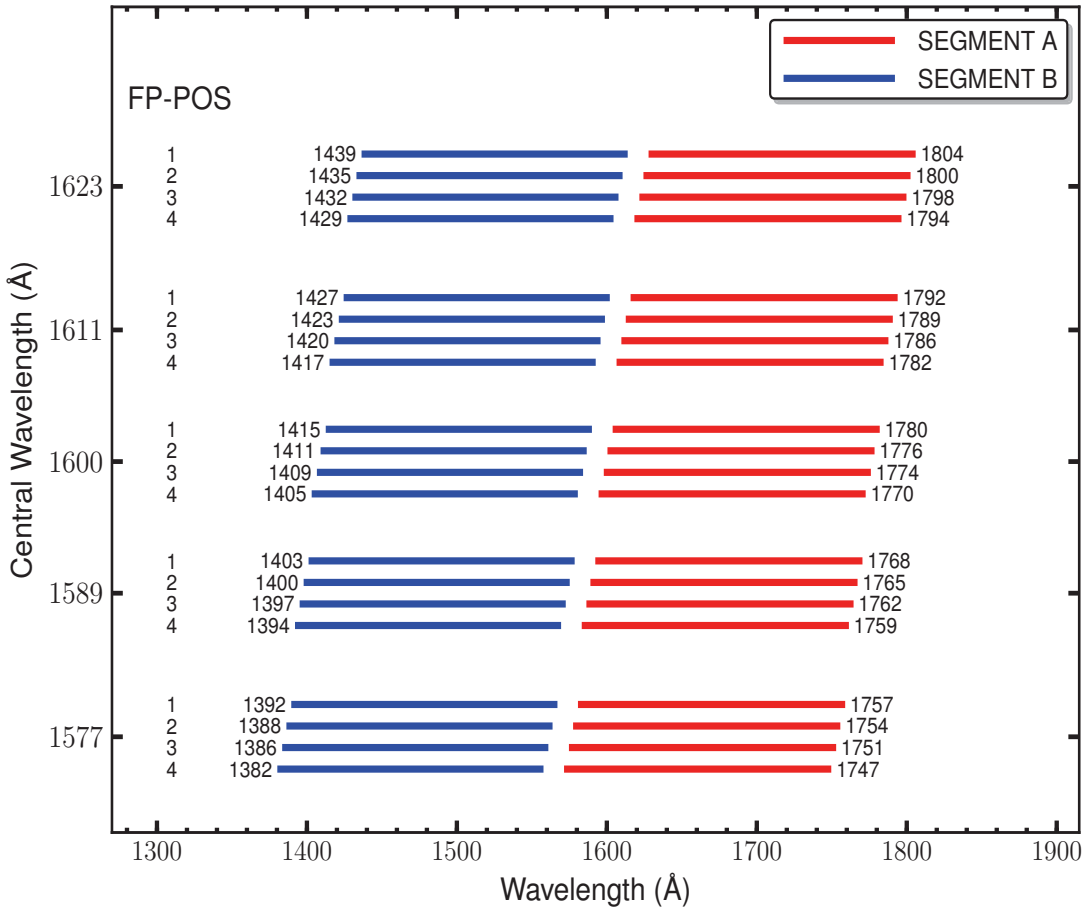

G160M Sensitivities

Table 15.6: G160M Sensitivities & Effective Areas for a Point Source Centered in the PSA.

Wavelength (Å)	Sensitivity (counts pixel^{-1} sec^{-1} per erg cm^{-2} sec^{-1} Å^{-1})	Effective Area (cm^2)
1400	1.9E12	2.25E03
1450	1.7E12	1.92E03
1500	1.4E12	1.48E03
1550	1.1E12	1.18E03
1600	8.1E11	8.18E02
1650	6.8E11	6.70E02
1700	5.8E11	5.56E02
1750	5.1E11	4.69E02

Figure 15.5: G160M Point Source Sensitivity for PSA and BOA.

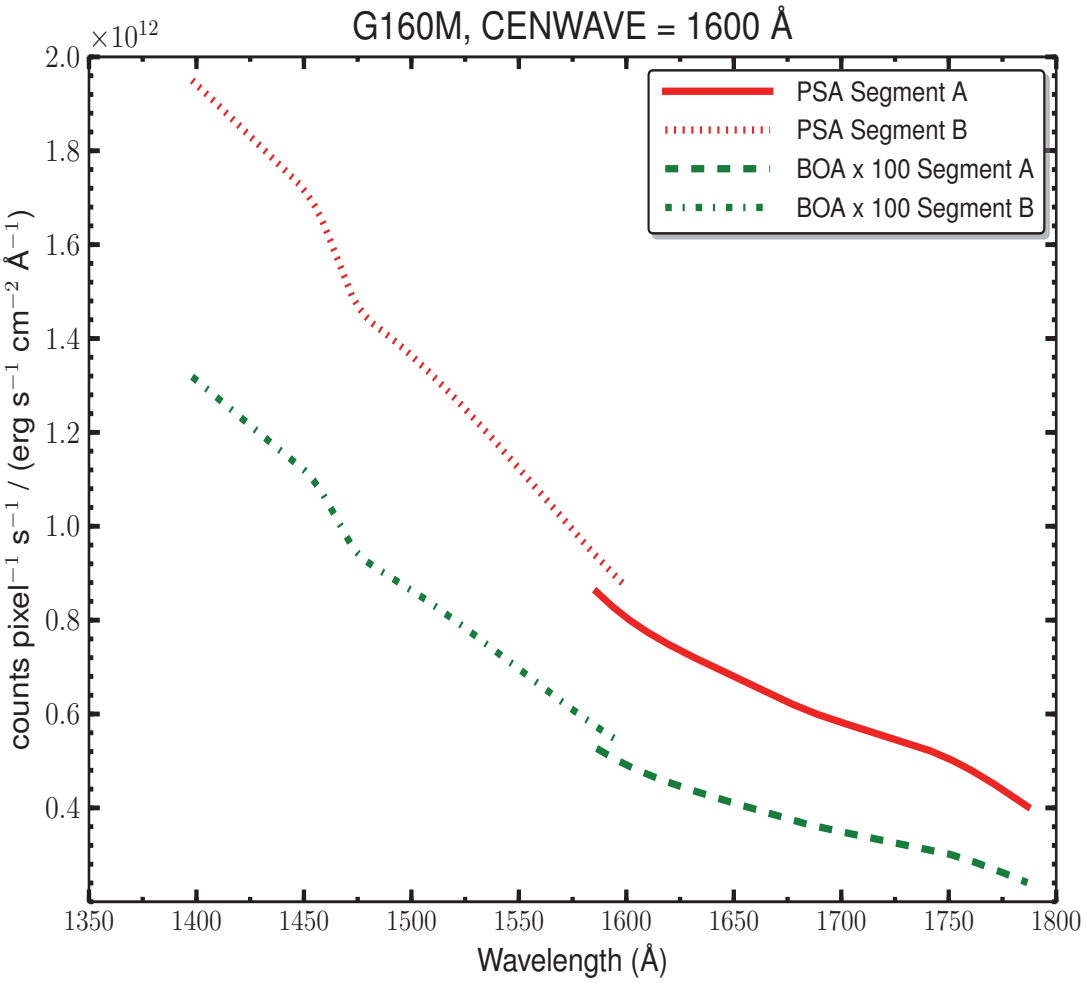

G160M Signal-to-Noise Ratio

Figure 15.6: Point Source Signal-to-Noise as a Function of STMAG for G160M at 1610 Å.

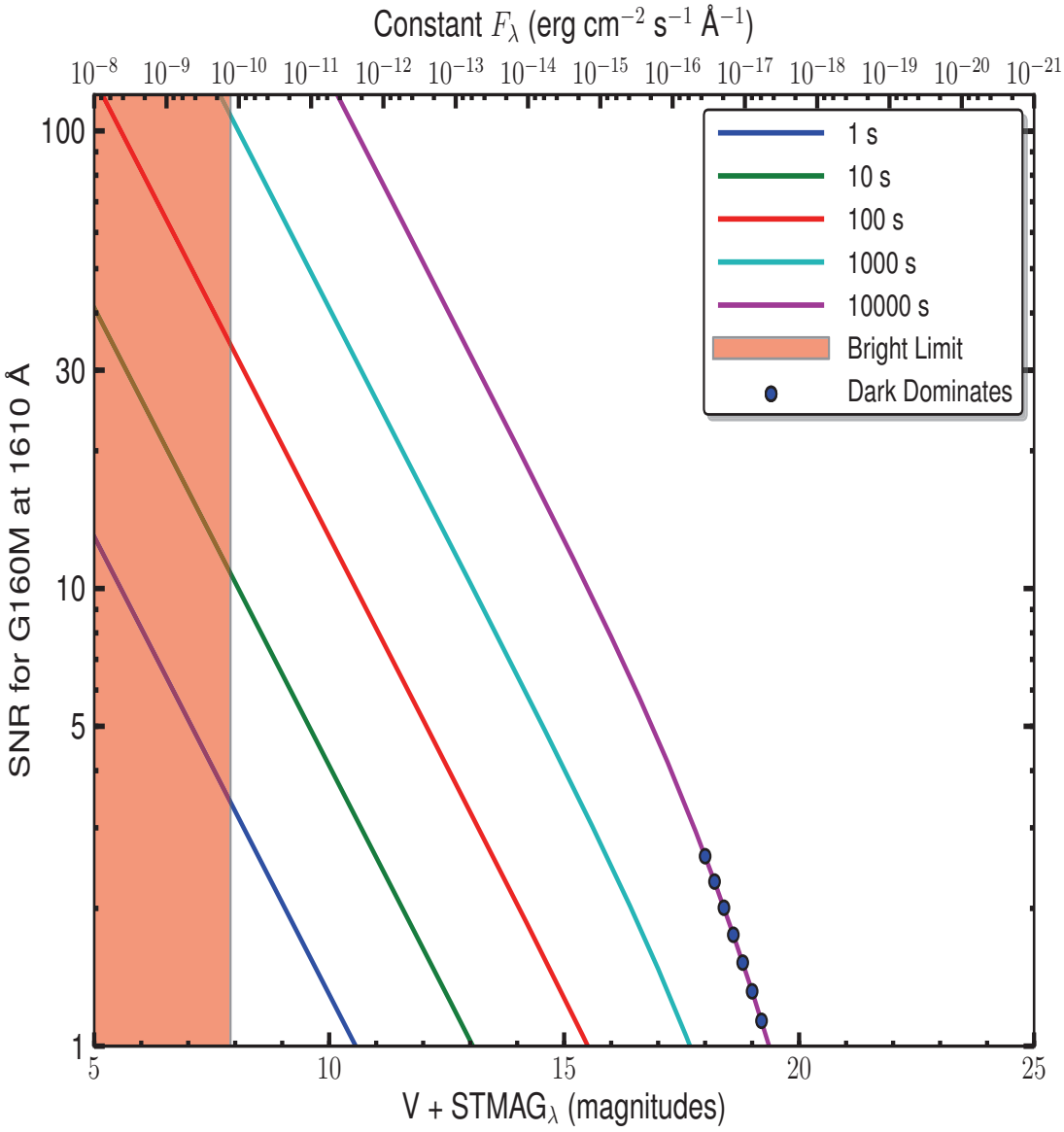

The top axis displays constant F_λ values corresponding to the STMAG units (V+STMAG$_\lambda$) on the bottom axis. Recall that STMAG=0 is equivalent to F_λ = 3.63E-9 erg cm^{-2} s^{-1} Å^{-1}. Colors refer to exposure times in seconds. The edge of the shaded area corresponds to the bright-object limit. Use of the PSA is assumed.

FUV Grating G140L

Description

G140L is a low-resolution grating (R~2,000) with wavelength coverage extending to 900 Å -- and perhaps below. Its sensitivity at EUV wavelengths -- marked in light blue in Figure 15.7 -- has not yet been calibrated. The grating has two central-wavelength settings, 1105 and 1280 Å.

Special Considerations

The gap between segments A and B spans 105 Å. To fill this gap requires exposures at both central wavelength settings. When setting 1105 is used, segment B must be turned off to prevent 0th-order light from falling on the detector.

Grating	Resolving Power $R = \lambda/\Delta\lambda$	Dispersion (mÅ pixel^{-1})	Plate Scale (milliarcsec pixel^{-1})		FP-POS Step (Å step^{-1})
			Disp. Axis	Cross-Disp. Axis	
G140L	1,500 - 4,000	80.3	23.0	90	19.6

Figure 15.7: Wavelength Ranges for the G140L Grating.

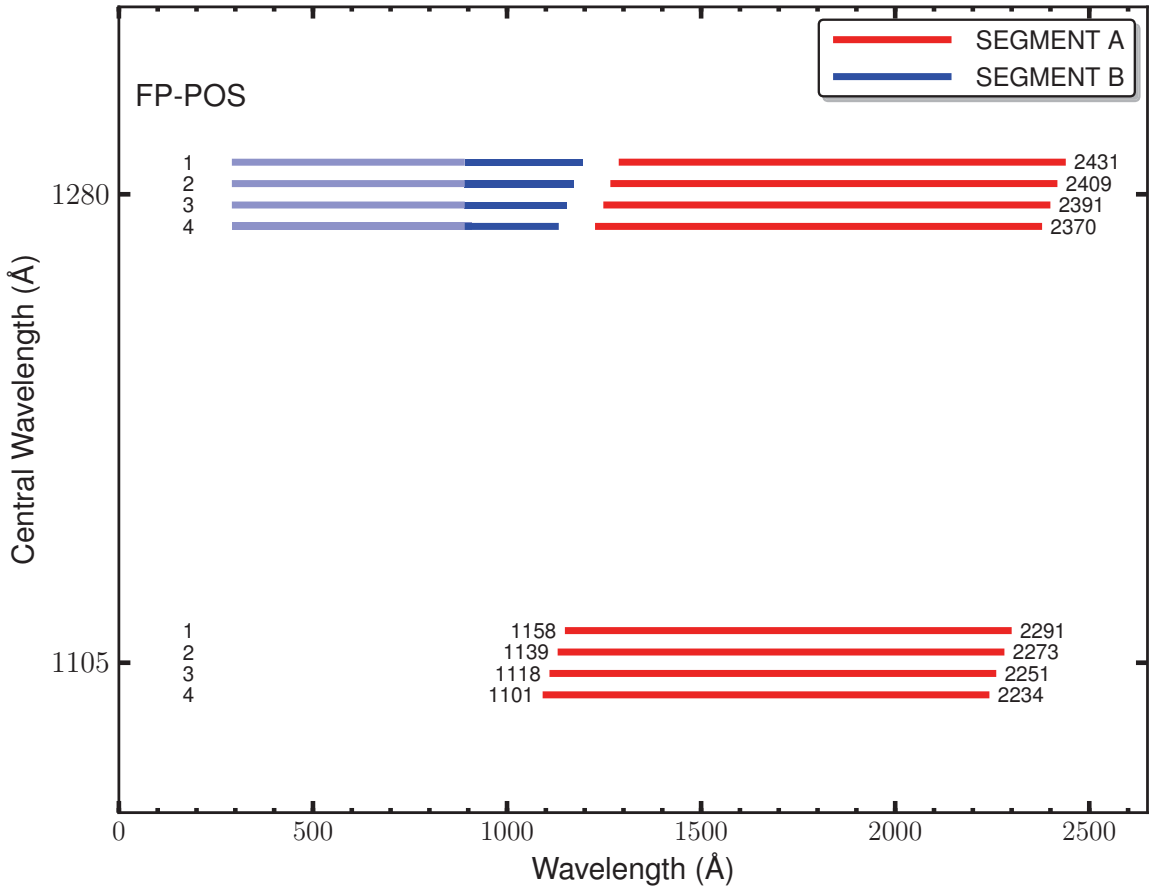

G140L Sensitivities

Table 15.7: G140L Sensitivities & Effective Areas for a Point Source Centered in the PSA.

Wavelength (Å)	Sensitivity (counts pixel^{-1} sec^{-1} per erg cm^{-2} sec^{-1} Å^{-1})	Effective Area (cm^2)
950	3.3E10	8.79E00
1000	3.0E10	7.5eE00
1100	2.3E12	5.17E02
1200	7.4E12	1.53E03
1300	8.9E12	1.72E03
1400	6.8E12	1.21E03
1500	4.9E12	8.17E02
1600	3.2E12	4.99E02
1700	2.3E12	3.41E02
1800	1.7E12	2.29E02
1900	9.6E11	1.27E02
2000	2.2E11	2.75E01
2100	1.5E11	1.82E00

Figure 15.8: G140L Point Source Sensitivity for PSA and BOA.

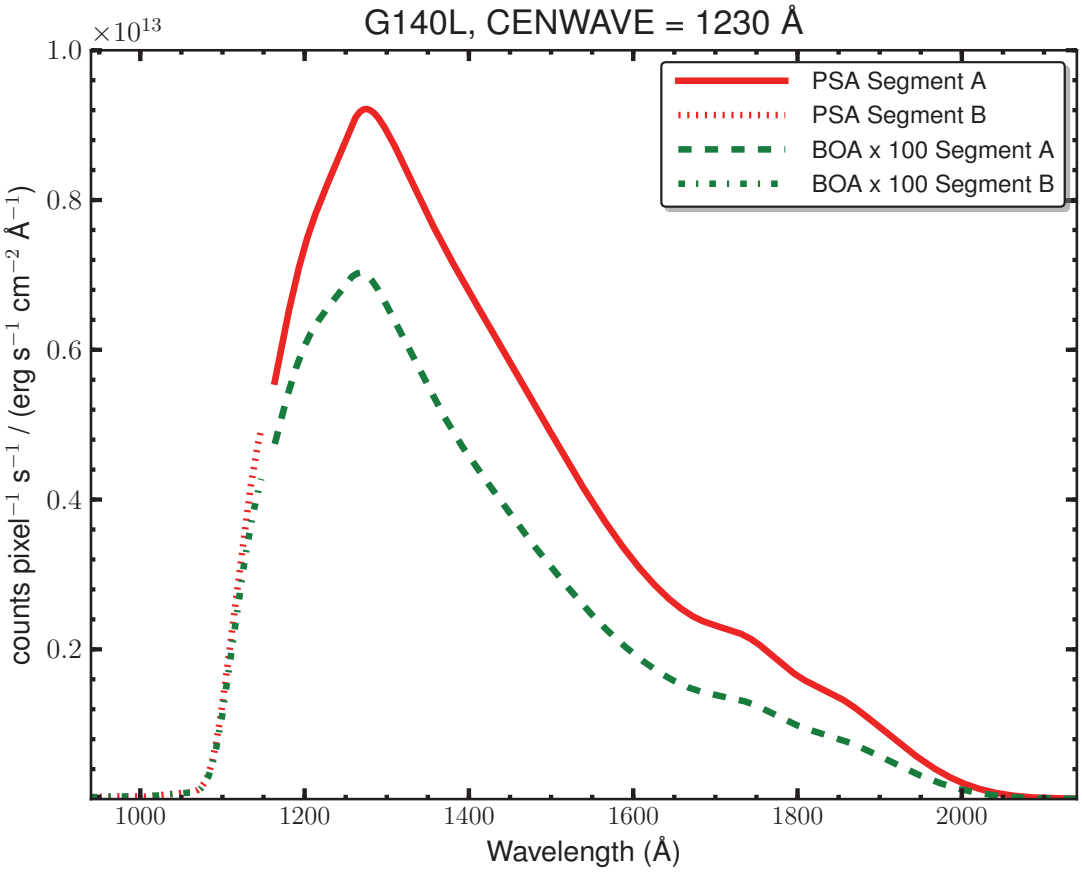

G140L Signal-to-Noise Ratio

Figure 15.9: Point Source Signal-to-Noise as a Function of STMAG for G140L.

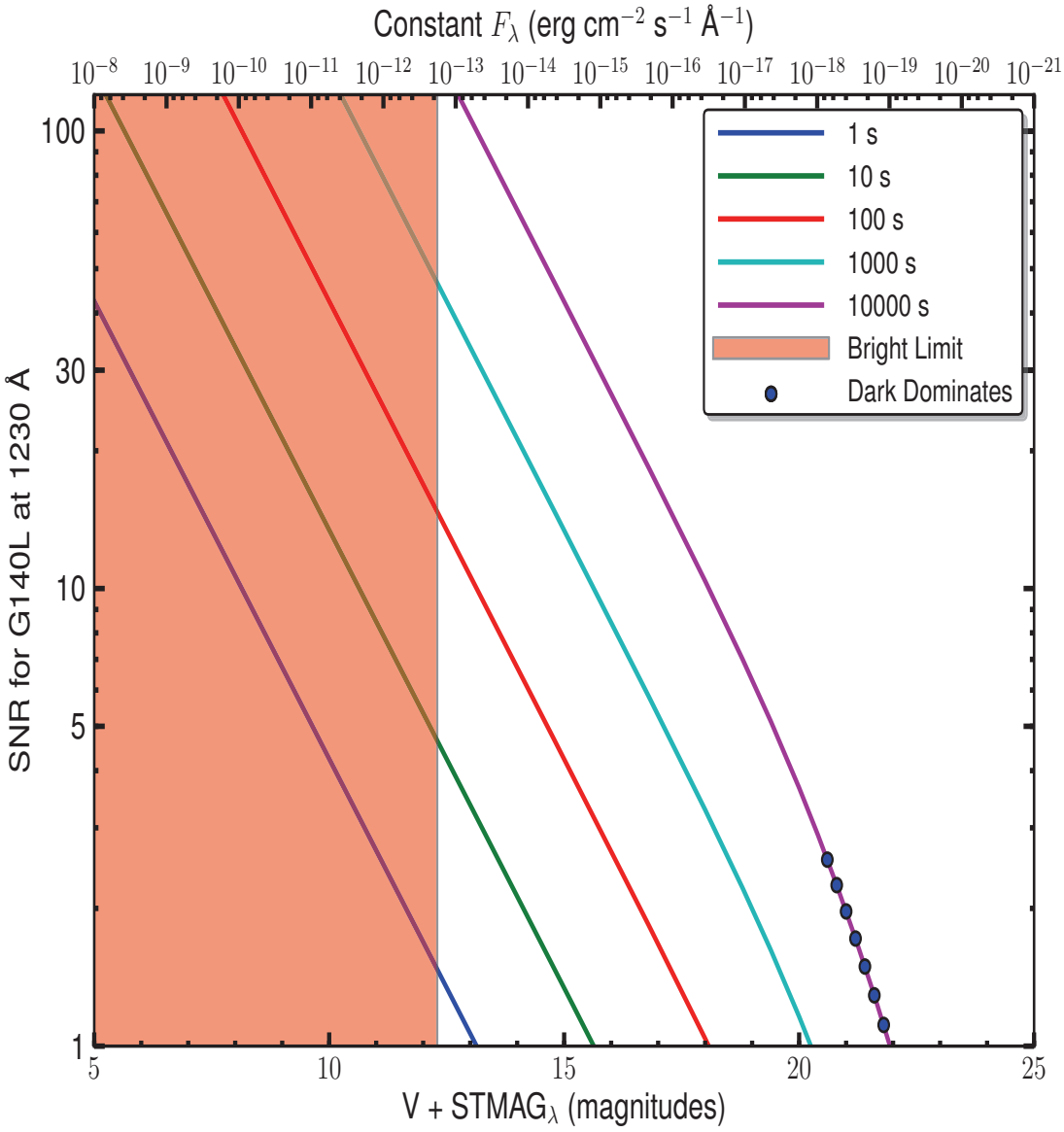

The top axis displays constant F_λ values corresponding to the STMAG units (V+STMAG$_\lambda$) on the bottom axis. Recall that STMAG=0 is equivalent to F_λ = 3.63E-9 erg cm^{-2} s^{-1} Å^{-1}. Colors refer to exposure times in seconds. The edge of the shaded area corresponds to the bright-object limit. Use of the PSA is assumed.

NUV Grating G185M

Description

The `G185M` grating samples wavelengths between about 1700 and 2100 Å. The grating has 15 central wavelength settings.

Special Considerations

G185M spectra consist of three 35-Å stripes separated by two 64-Å gaps. To acquire a complete spectrum requires the use of six central-wavelength settings.

Grating	Resolving Power $R = \lambda/\Delta\lambda$	Dispersion (mÅ pixel^{-1})	Spatial Resolution (milliarcsec pixel^{-1})	Plate Scale (milliarcsec pixel^{-1})		FP-POS Step (Å step^{-1})
				Disp. Axis	Cross-Disp. Axis	
G185M	22,000 - 28,000	37	75 ± 4	24.3	23.8	1.9

Figure 15.10: Wavelength Ranges for the G185M Grating.

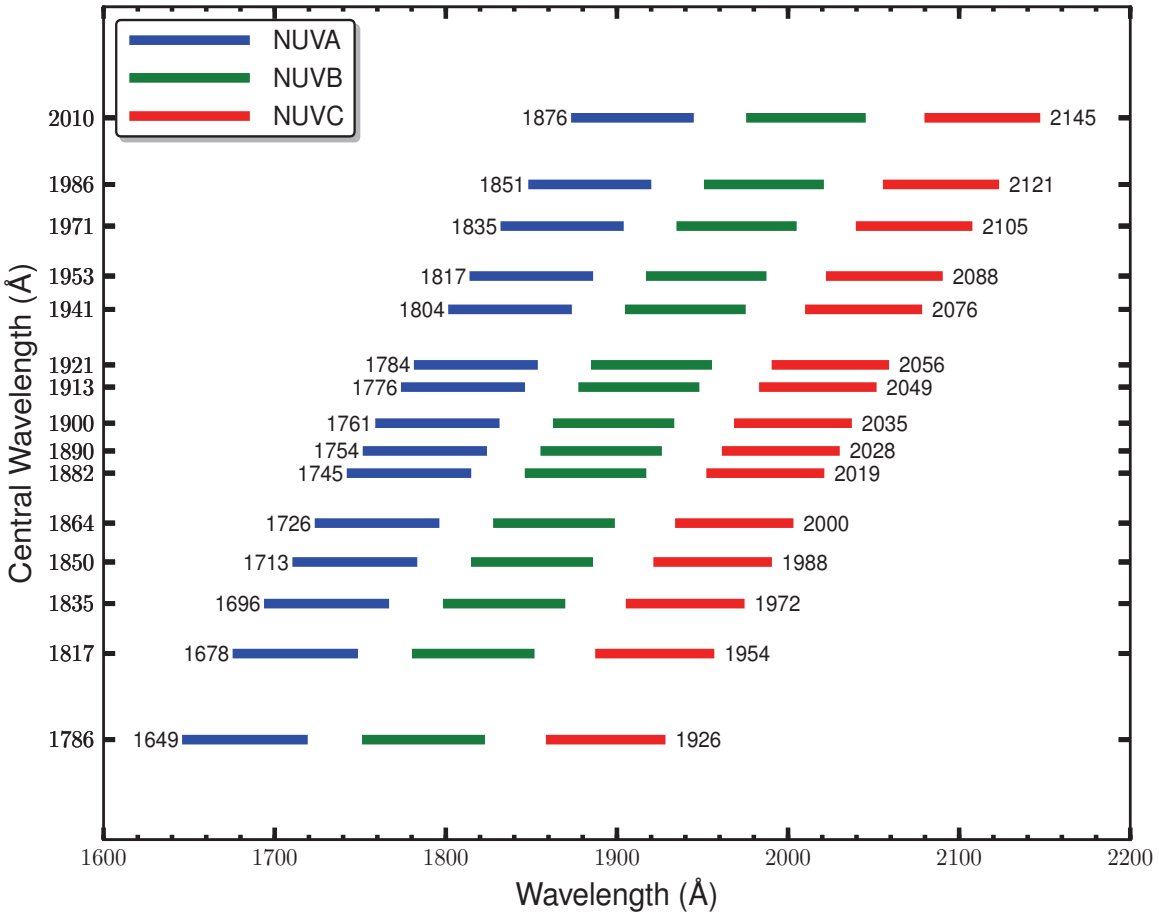

G185M Sensitivities

Table 15.8: G185M Sensitivities & Effective Areas for a Point Source Centered in the PSA.

Wavelength (Å)	Sensitivity (counts pixel^{-1} sec^{-1} per erg cm^{-2} sec^{-1} Å^{-1})	Effective Area (cm^2)
1650	5.9E11	1.95E02
1700	1.2E12	3.76E02
1750	1.7E12	5.15E02
1800	2.0E12	5.92E02
1850	2.1E12	6.17E02
1900	2.1E12	6.01E02
1950	2.1E12	5.80E02
2000	2.0E12	5.43E02
2050	1.9E12	5.14E02
2100	1.8E12	4.69E02

Figure 15.11: G185M Point Source Sensitivity for PSA and BOA.

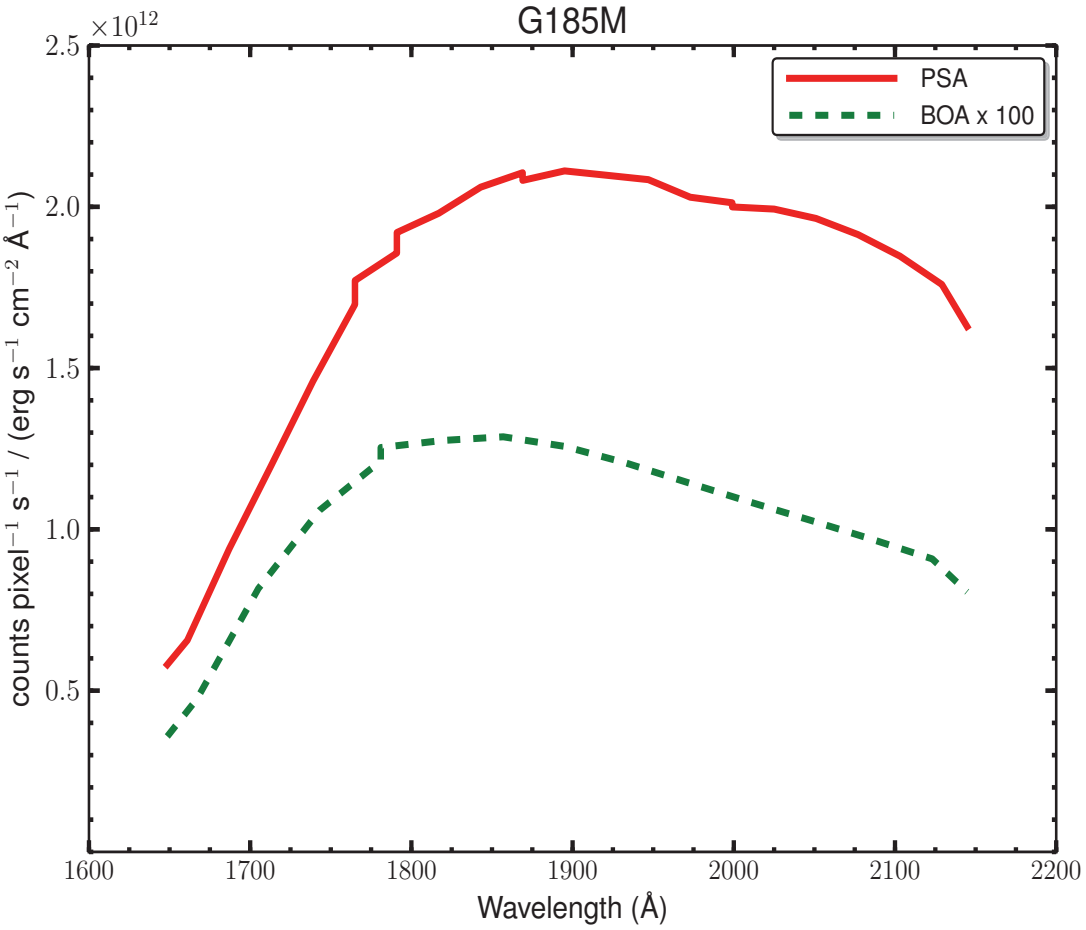

G185M Signal-to-Noise Ratio

Figure 15.12: Point Source Signal-to-Noise as a Function of STMAG for G185M.

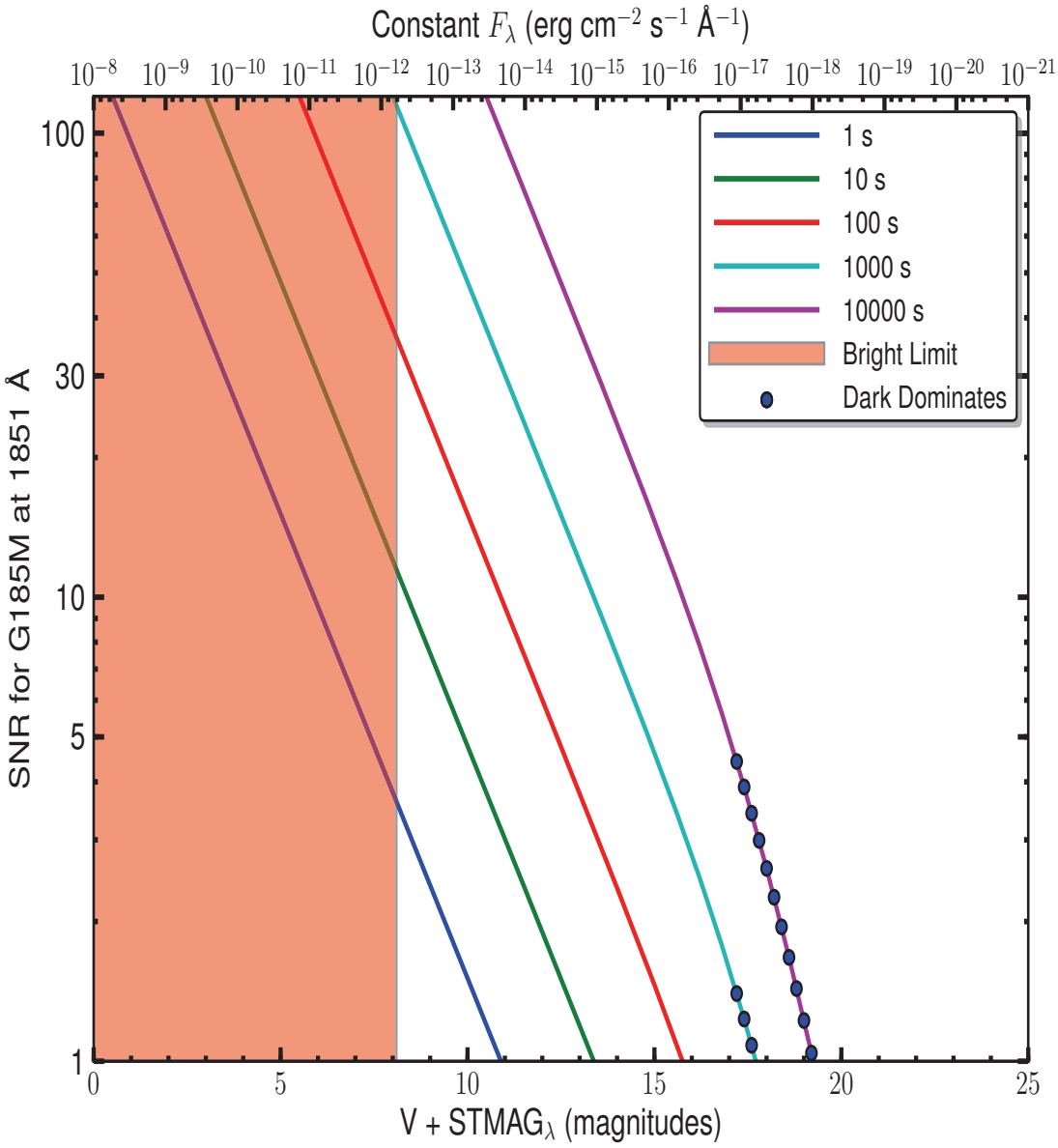

The top axis displays constant F_λ values corresponding to the STMAG units (V+STMAG$_\lambda$) on the bottom axis. Recall that STMAG=0 is equivalent to F_λ = 3.63E-9 erg cm^{-2} s^{-1} Å^{-1}. Colors refer to exposure times in seconds. The edge of the shaded area corresponds to the bright-object limit. Use of the PSA is assumed.

NUV Grating G225M

Description

The `G225M` grating samples wavelengths between about 2100 and 2500 Å. The grating has 13 central wavelength settings.

Special Considerations

G185M spectra consist of three 35-Å stripes separated by two 64-Å gaps. To acquire a complete spectrum requires the use of six central-wavelength settings.

Grating	Resolving Power $R = \lambda/\Delta\lambda$	Dispersion (mÅ pixel^{-1})	Spatial Resolution (milliarcsec pixel^{-1})	Plate Scale (milliarcsec pixel^{-1})		FP-POS Step (Å step^{-1})
				Disp. Axis	Cross-Disp. Axis	
G225M	28,000 - 38,000	33	58 ± 2	24.3	23.1	1.7

Figure 15.13: Wavelength Ranges for the G225M Grating.

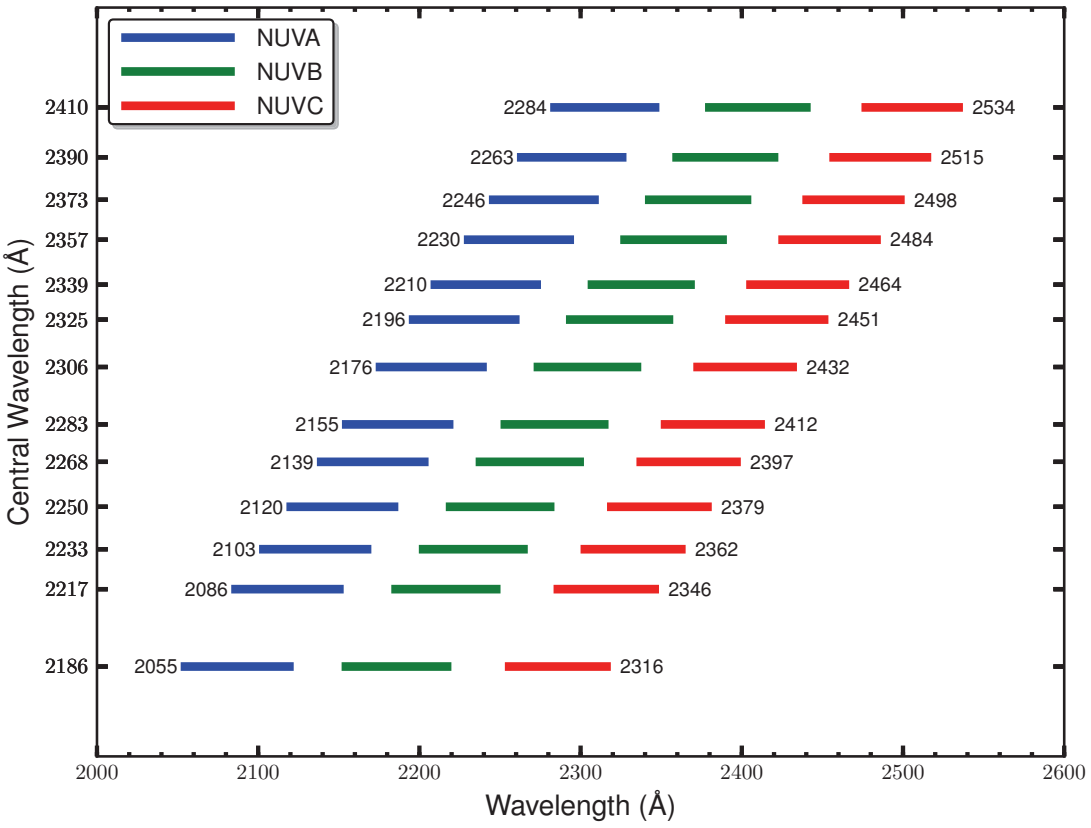

G225M Sensitivities

Table 15.9: G225M Sensitivities & Effective Areas for a Point Source Centered in the PSA.

Wavelength (Å)	Sensitivity (counts pixel^{-1} sec^{-1} per erg cm^{-2} sec^{-1} Å^{-1})	Effective Area (cm^2)
2100	1.2E12	3.26E02
2150	1.5E12	4.00E02
2200	1.8E12	4.86E02
2250	2.2E12	5.55E02
2300	2.4E12	6.01E02
2350	2.5E12	6.27E02
2400	2.6E12	6.26E02
2450	2.6E12	6.11E02
2500	2.6E12	6.09E02

Figure 15.14: G225M Point Source Sensitivity for PSA and BOA.

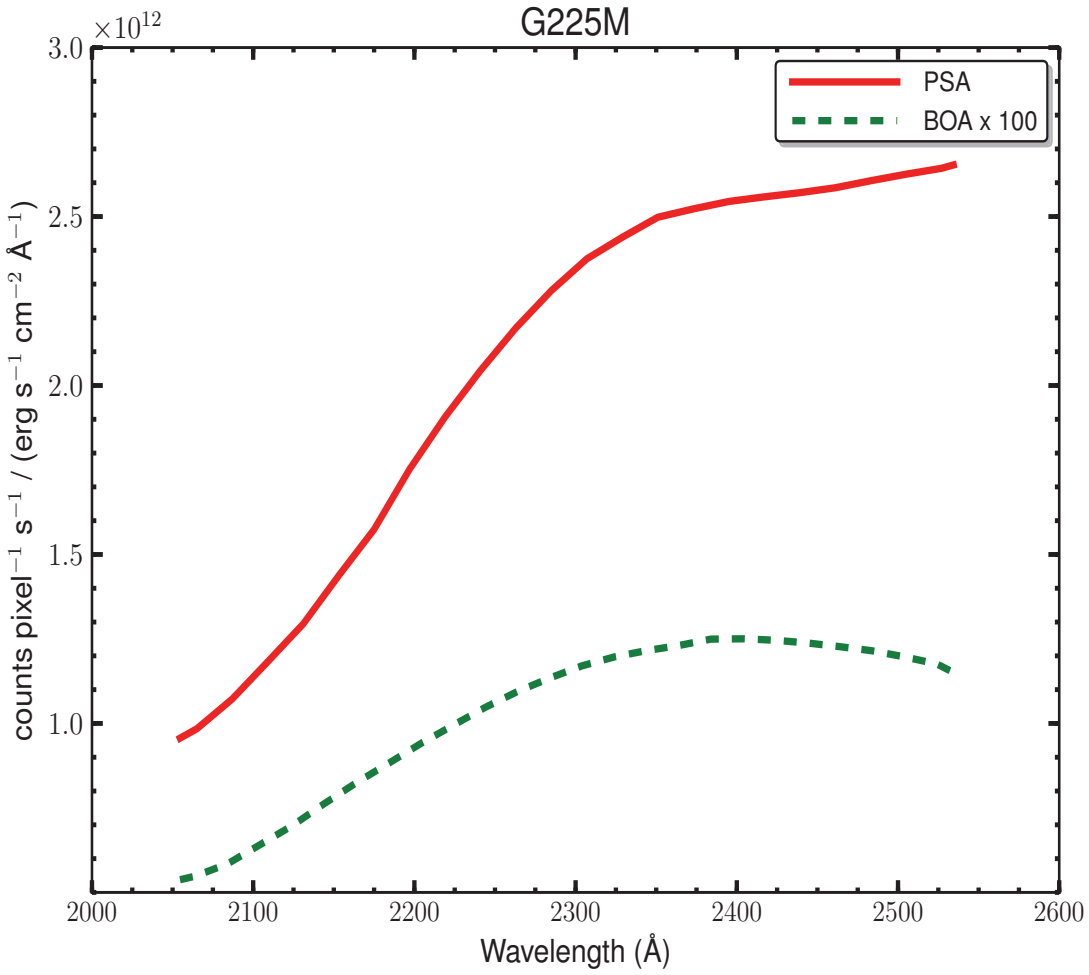

G225M Signal-to-Noise Ratio

Figure 15.15: Point Source Signal-to-Noise as a Function of STMAG for G225M.

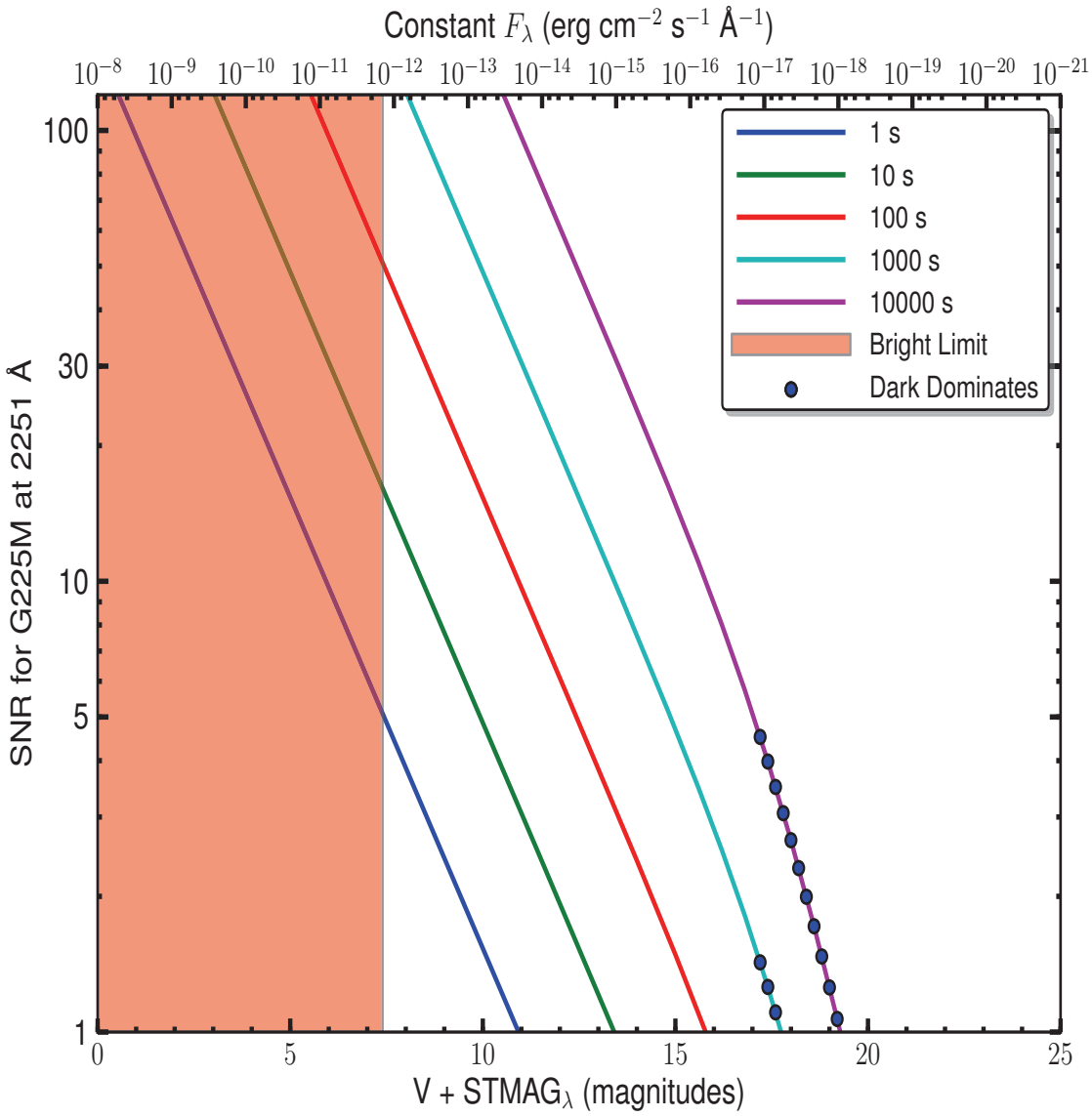

The top axis displays constant F_λ values corresponding to the STMAG units (V+STMAG$_\lambda$) on the bottom axis. Recall that STMAG=0 is equivalent to F_λ = 3.63E-9 erg cm^{-2} s^{-1} Å^{-1}. Colors refer to exposure times in seconds. The edge of the shaded area corresponds to the bright-object limit. Use of the PSA is assumed.

NUV Grating G285M

Description

The G285M grating samples wavelengths between about 2500 and 3200 Å. The grating has 17 central wavelength settings.

Special Considerations

G185M spectra consist of three 41-Å stripes separated by two 74-Å gaps. To acquire a complete spectrum requires the use of eight central-wavelength settings.

Grating	Resolving Power $R = \lambda/\Delta\lambda$	Dispersion (mÅ pixel^{-1})	Spatial Resolution (milliarcsec pixel^{-1})	Plate Scale (milliarcsec pixel^{-1})		FP-POS Step (Å step^{-1})
				Disp. Axis	Cross-Disp. Axis	
G285M	30,000 - 41,000	40	56 ± 1	24.3	24.4	2.1

Figure 15.16: Wavelength Ranges for the G285M Grating.

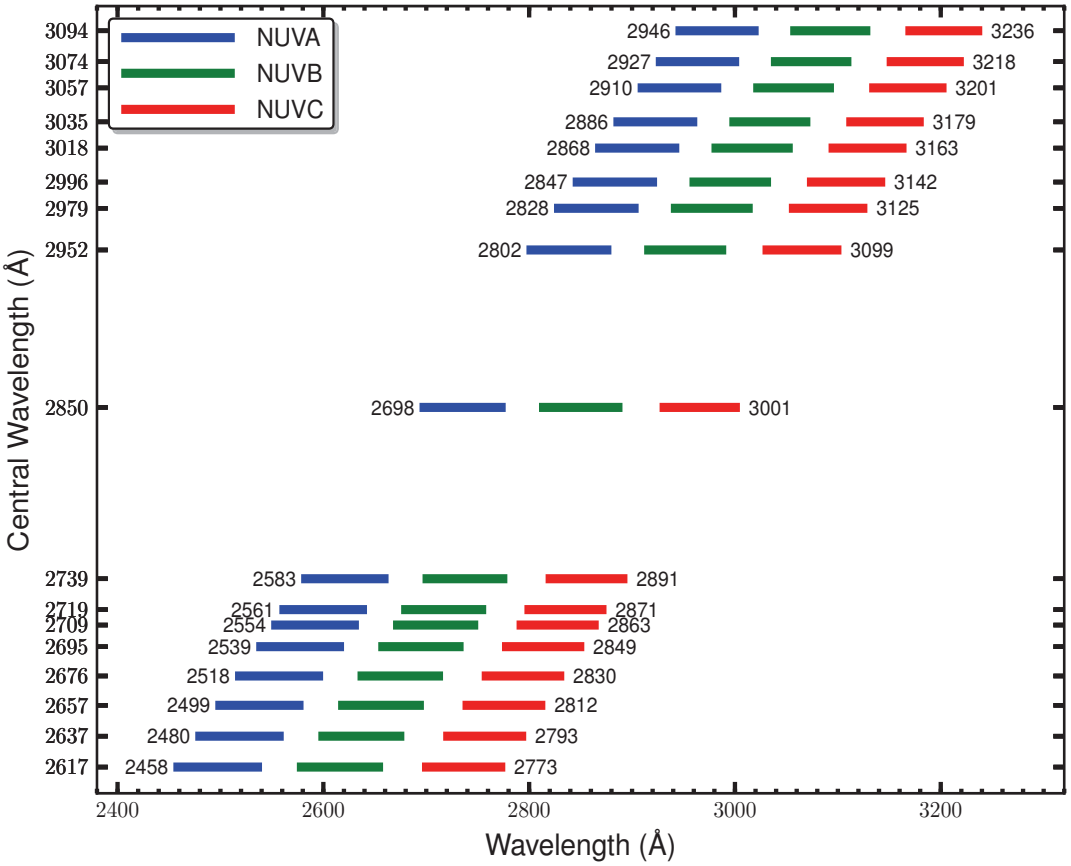

G285M Sensitivities

Table 15.10: G285M Sensitivities & Effective Areas for a Point Source Centered in the PSA.

Wavelength (Å)	Sensitivity (counts pixel^{-1} sec^{-1} per erg cm^{-2} sec^{-1} Å^{-1})	Effective Area (cm^2)
2500	1.7E12	3.29E02
2600	2.0E12	3.73E02
2700	2.1E12	3.79E02
2800	1.9E12	3.39E02
2900	1.8E12	3.08E02
3000	1.4E12	2.27E02
3100	8.5E11	1.34E02
3200	4.5E11	6.90E01

Figure 15.17: G285M Point Source Sensitivity for PSA and BOA.

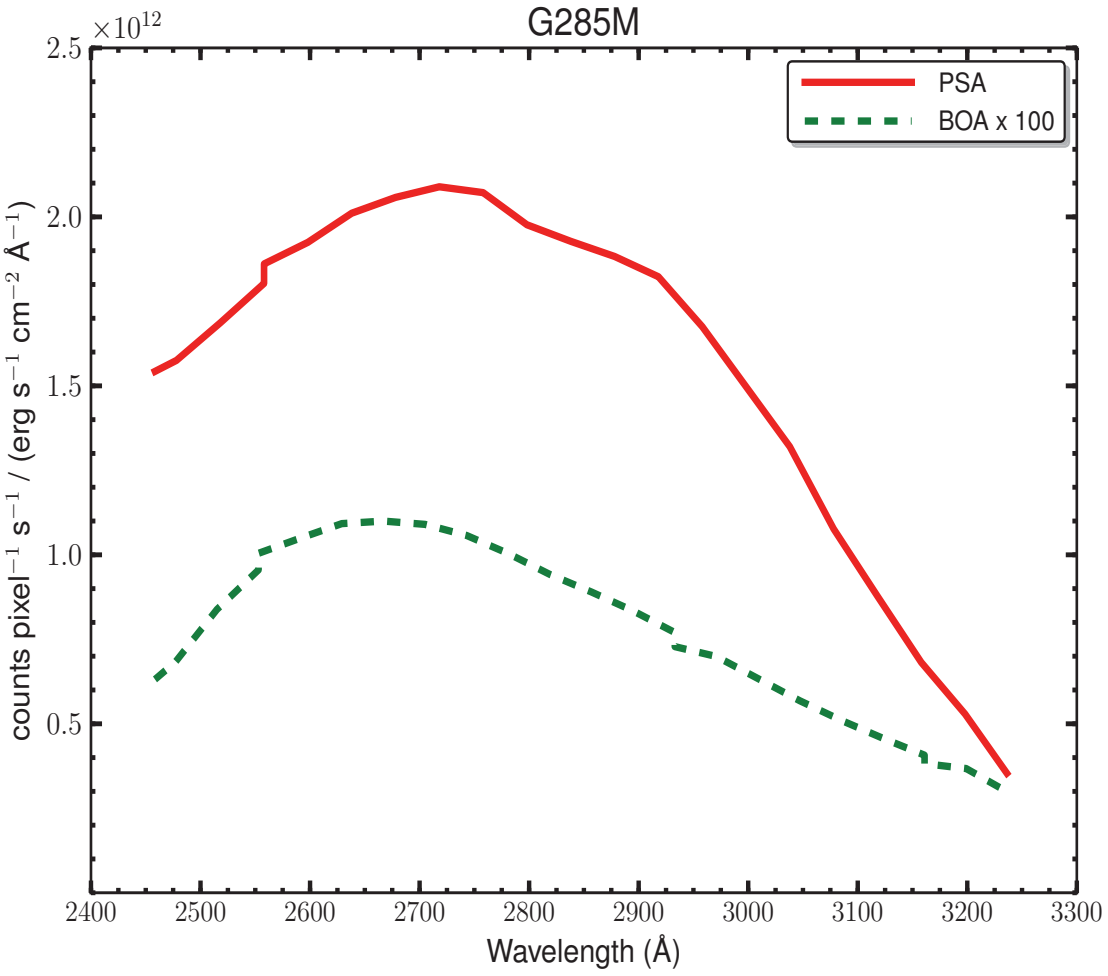

G285M Signal-to-Noise Ratio

Figure 15.18: Point Source Signal-to-Noise as a Function of STMAG for G285M.

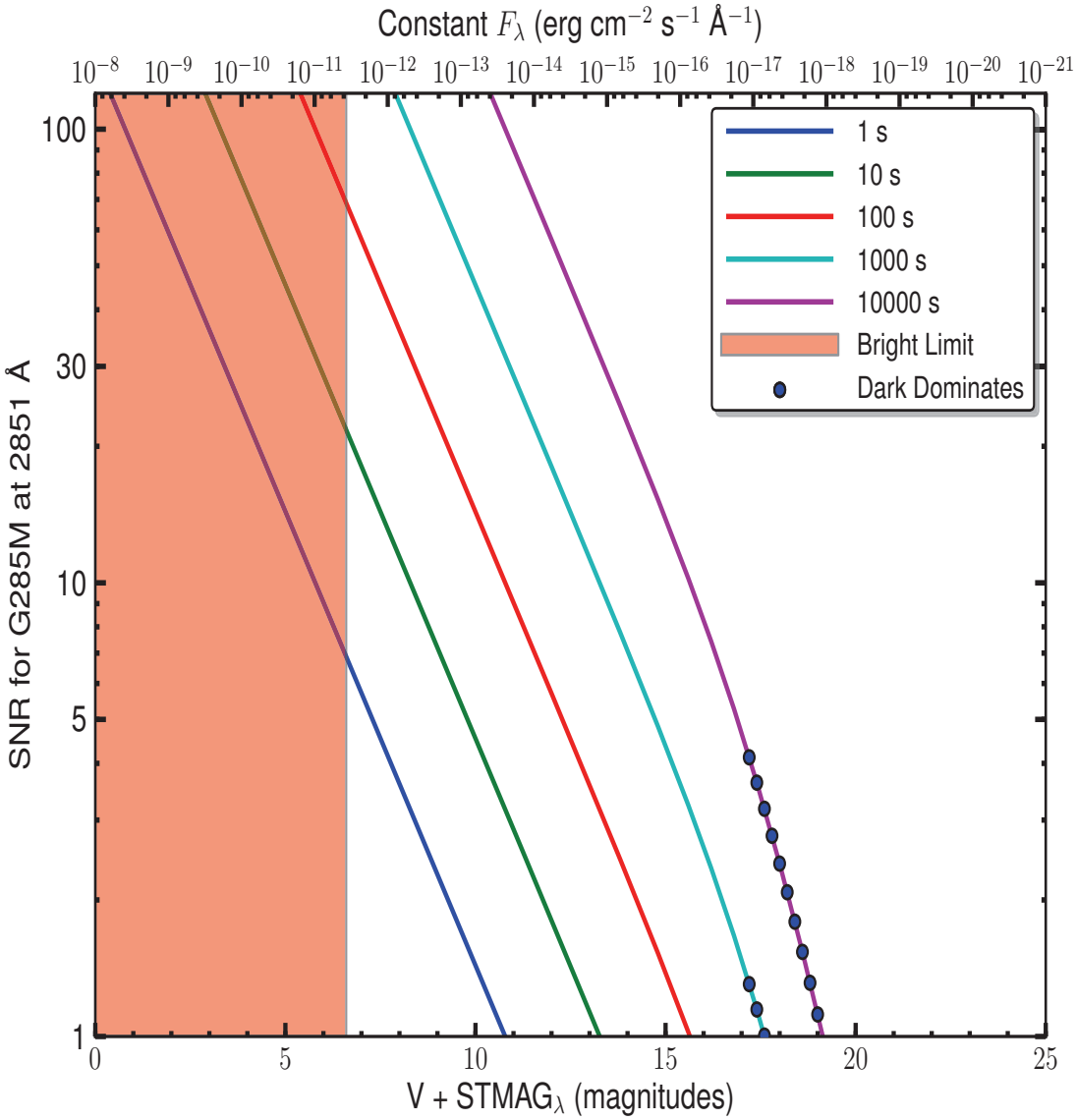

The top axis displays constant F_λ values corresponding to the STMAG units (V+STMAG$_\lambda$) on the bottom axis. Recall that STMAG=0 is equivalent to F_λ = 3.63E-9 erg cm^{-2} s^{-1} Å^{-1}. Colors refer to exposure times in seconds. The edge of the shaded area corresponds to the bright-object limit. Use of the PSA is assumed.

NUV Grating G230L

Description

G230L is a low-resolution grating (R~3000) with wavelength coverage extending from about 1650 to 3200 Å. The grating has four central-wavelength settings.

Special Considerations

G230L spectra consist of three 400-Å stripes separated by two 700-Å gaps. To acquire a complete spectrum requires the use of all four central-wavelength settings.

Only stripes A and B record first-order light, and even they may be contaminated by second-order light when central wavelength 3360 is used. See Table 6.5.

Grating	Resolving Power $R = \lambda/\Delta\lambda$	Dispersion (mÅ pixel^{-1})	Spatial Resolution (milliarcsec pixel^{-1})	Plate Scale (milliarcsec pixel^{-1})		FP-POS Step (Å step^{-1})
				Disp. Axis	Cross-Disp. Axis	
G230L	2,100 - 3,900	390.0	81 ± 1	24.3	24.0	20.3

Figure 15.19: Wavelength Ranges for the G230L Grating.

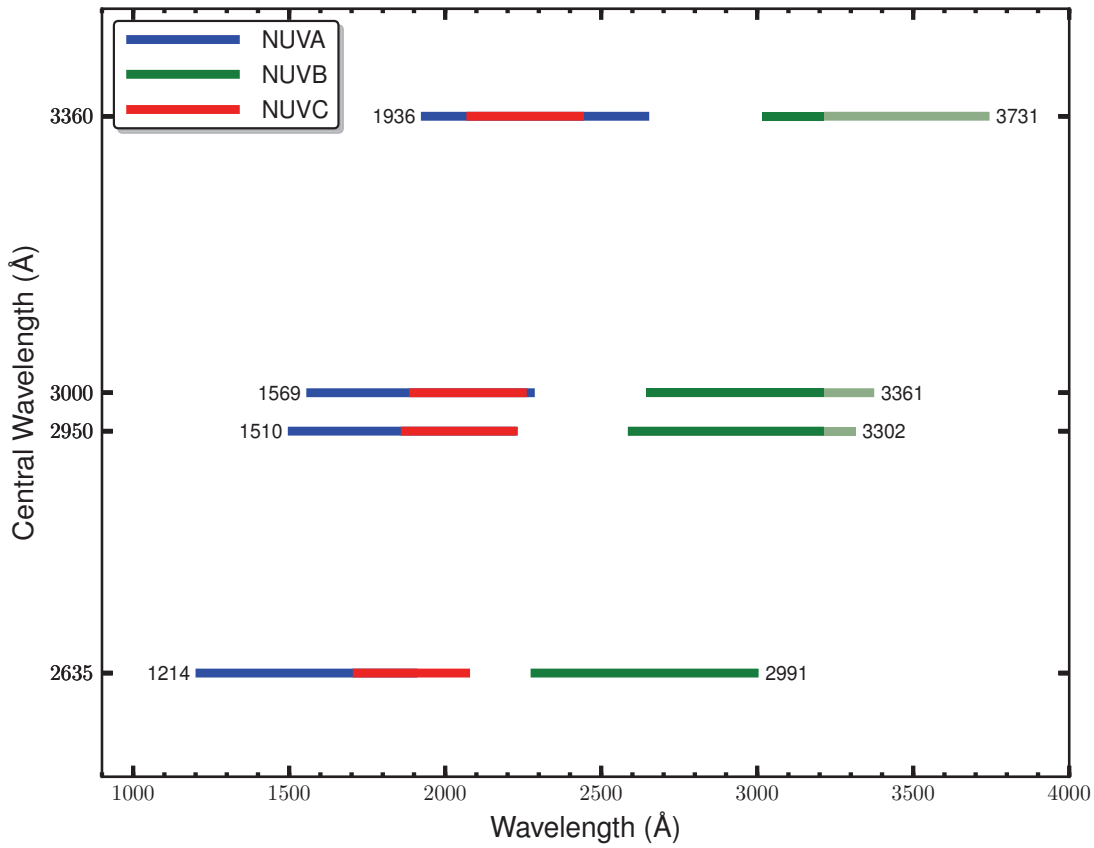

G230L Sensitivities

Table 15.11: G230L Sensitivities & Effective Areas for a Point Source Centered in the PSA.

Wavelength (Å)	Sensitivity (counts pixel^{-1} sec^{-1} per erg cm^{-2} sec^{-1} Å^{-1})	Effective Area (cm^2)
1600	1.9E11	7.13E00
1700	9.9E12	3.55E02
1800	1.6E13	5.30E02
1900	2.1E13	6.59E02
2000	2.5E13	7.55E02
2100	2.9E13	8.26E02
2200	3.0E13	8.42E02
2300	3.2E13	8.48E02
2400	3.2E13	8.09E02
2500	3.1E13	7.47E02
2600	3.0E13	7.00E02
2700	2.8E13	6.24E02
2800	2.4E13	5.23E02
2900	1.9E13	4.08E02
3000	1.4E13	2.81E02
3100	8.3E12	1.62E02
3200	4.0E12	7.51E01
3300	6.0E12	1.10E02
3400	9.8E12	1.75E02

Figure 15.20: G230L Point Source Sensitivity for PSA and BOA.

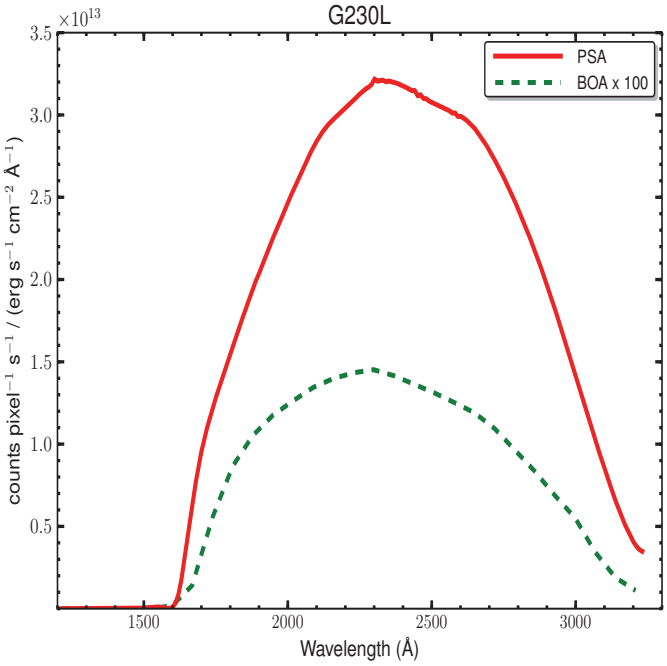

G230L Signal-to-Noise Ratio

Figure 15.21: Point Source Signal-to-Noise as a function of STMAG for G230L.

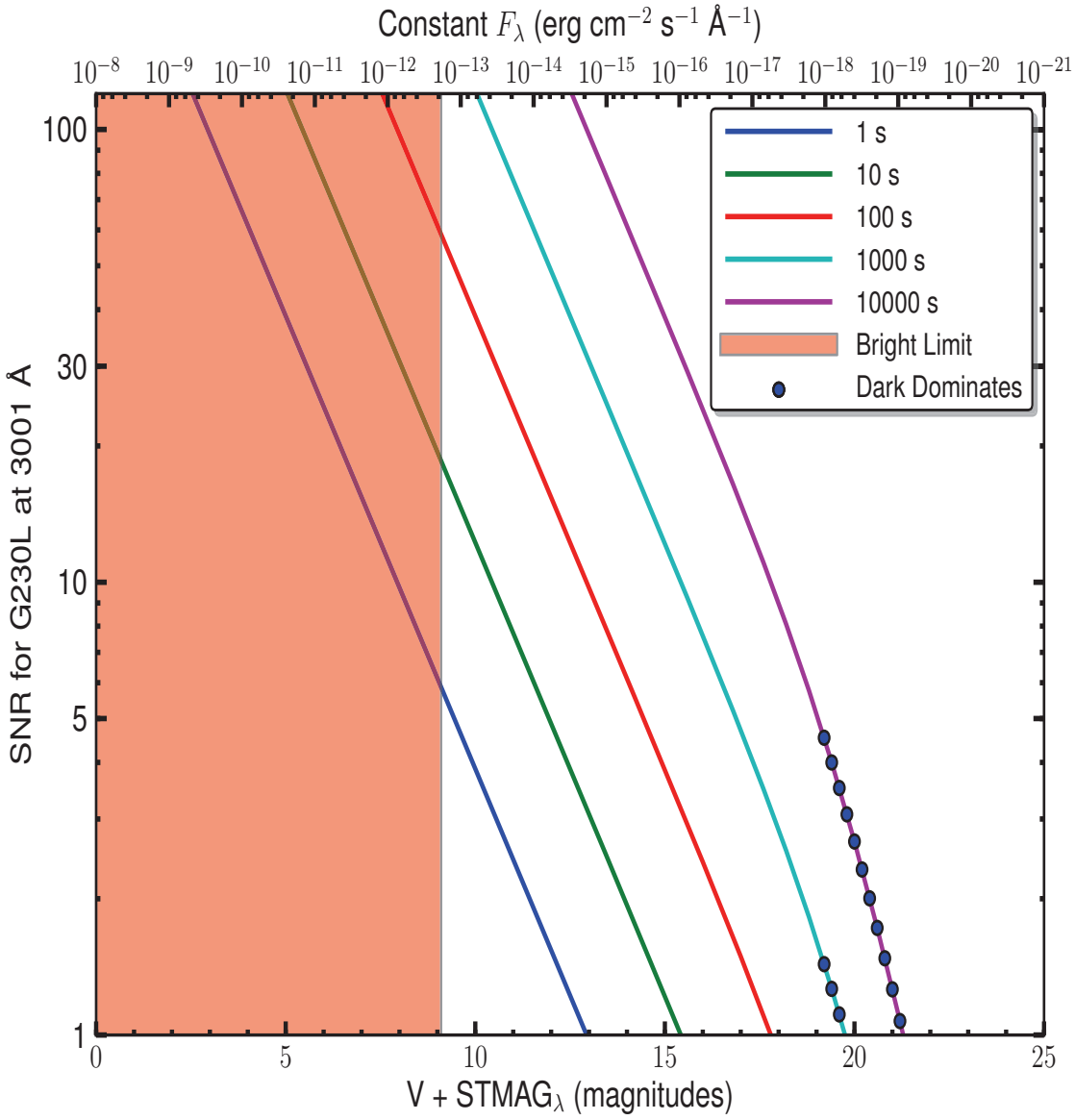

The top axis displays constant F_λ values corresponding to the STMAG units (V+STMAG$_\lambda$) on the bottom axis. Recall that STMAG=0 is equivalent to F_λ = 3.63E-9 erg cm^{-2} s^{-1} Å^{-1}. Colors refer to exposure times in seconds. The edge of the shaded area corresponds to the bright-object limit. Use of the PSA is assumed.

15.5 Line Spread Functions

Model Line Spread Functions (LSFs) for the COS gratings have been computed from the expected aberration of the COS + *HST* optical telescope assembly (OTA) system, the OTA pupil geometry, the OTA mid-frequency wavefront errors (as determined by Krist & Burrows 1995), and estimates of the point response function of the detectors.

The FUV LSF models were calculated at the nominal central wavelength setting of each FUV medium-resolution grating (1309 Å and 1600 Å respectively, for G130M and G160M) and at intervals of 50 Å over the full range of wavelengths covered by each grating. While the aberrations change slightly as the grating is moved to other settings, changes to the LSF at different grating positions are expected to be small.

The NUV optical models assume no variation between gratings or central wavelength settings, since we are dealing with planar gratings used in a collimated beam. The LSFs were computed at intervals of 100 Å over the full spectral range covered by the COS NUV gratings.

More detailed descriptions of the COS LSF are available in COS Instrument Science Report 2009-01.

Line Spread Functions:

G130M

Figure 15.22: Line Spread Functions of G130M as a function of wavelength.

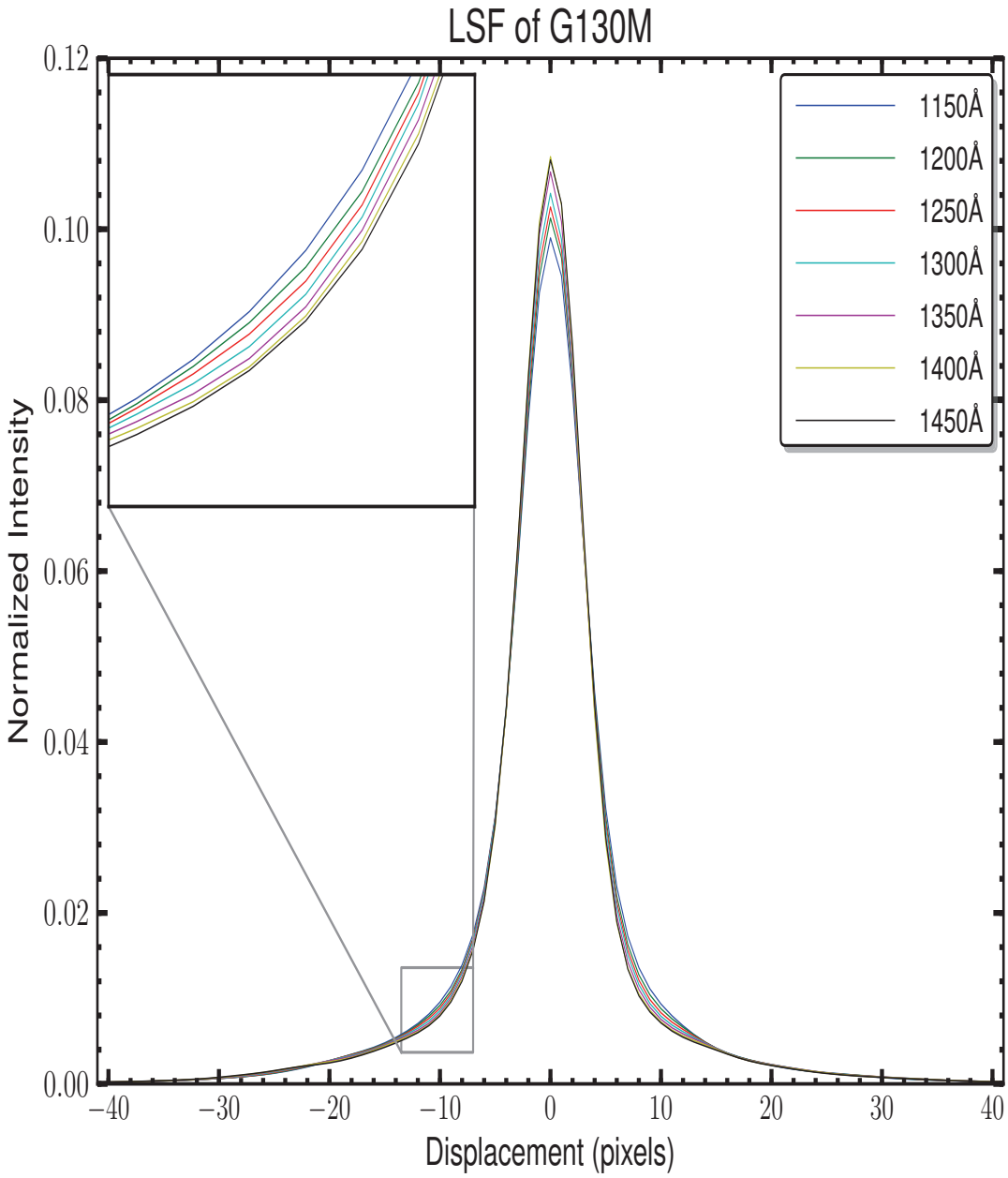

G160M

Figure 15.23: Line Spread Functions of G160M as a function of wavelength.

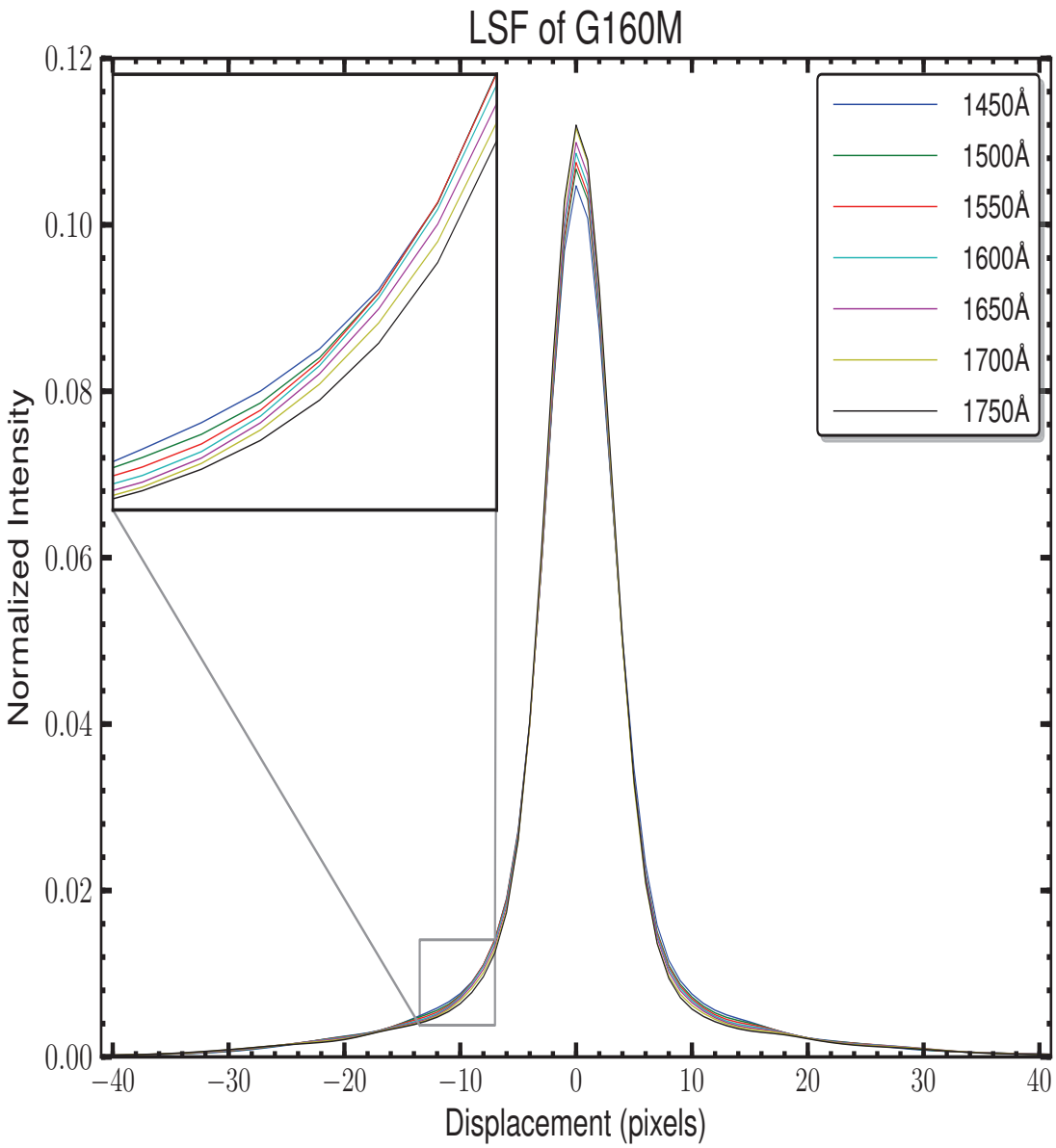

G140L

Figure 15.24: Line Spread Functions of G140L as a function of wavelength.

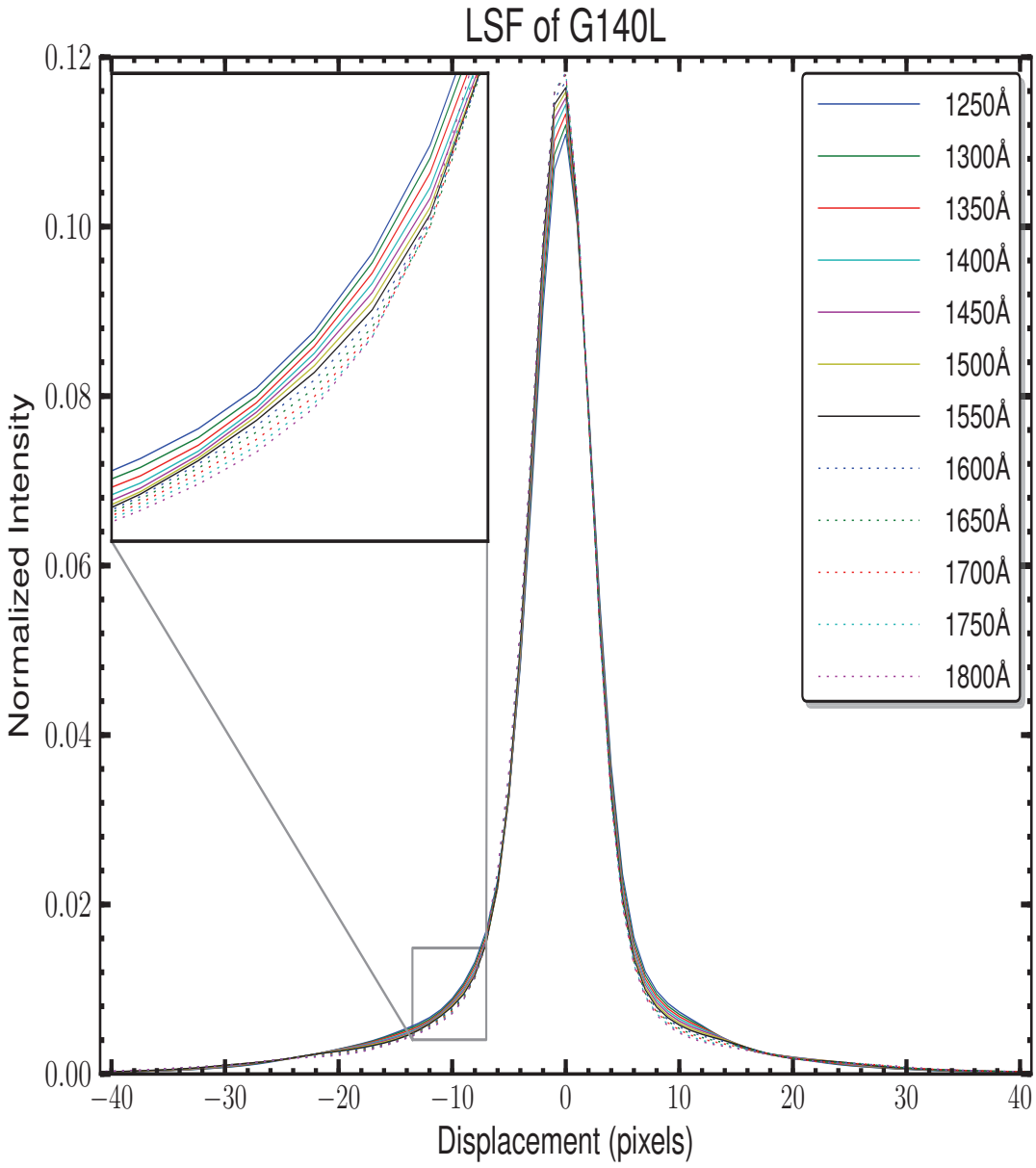

NUV Gratings

Figure 15.25: Line Spread Functions of NUV Gratings as a function of wavelength.

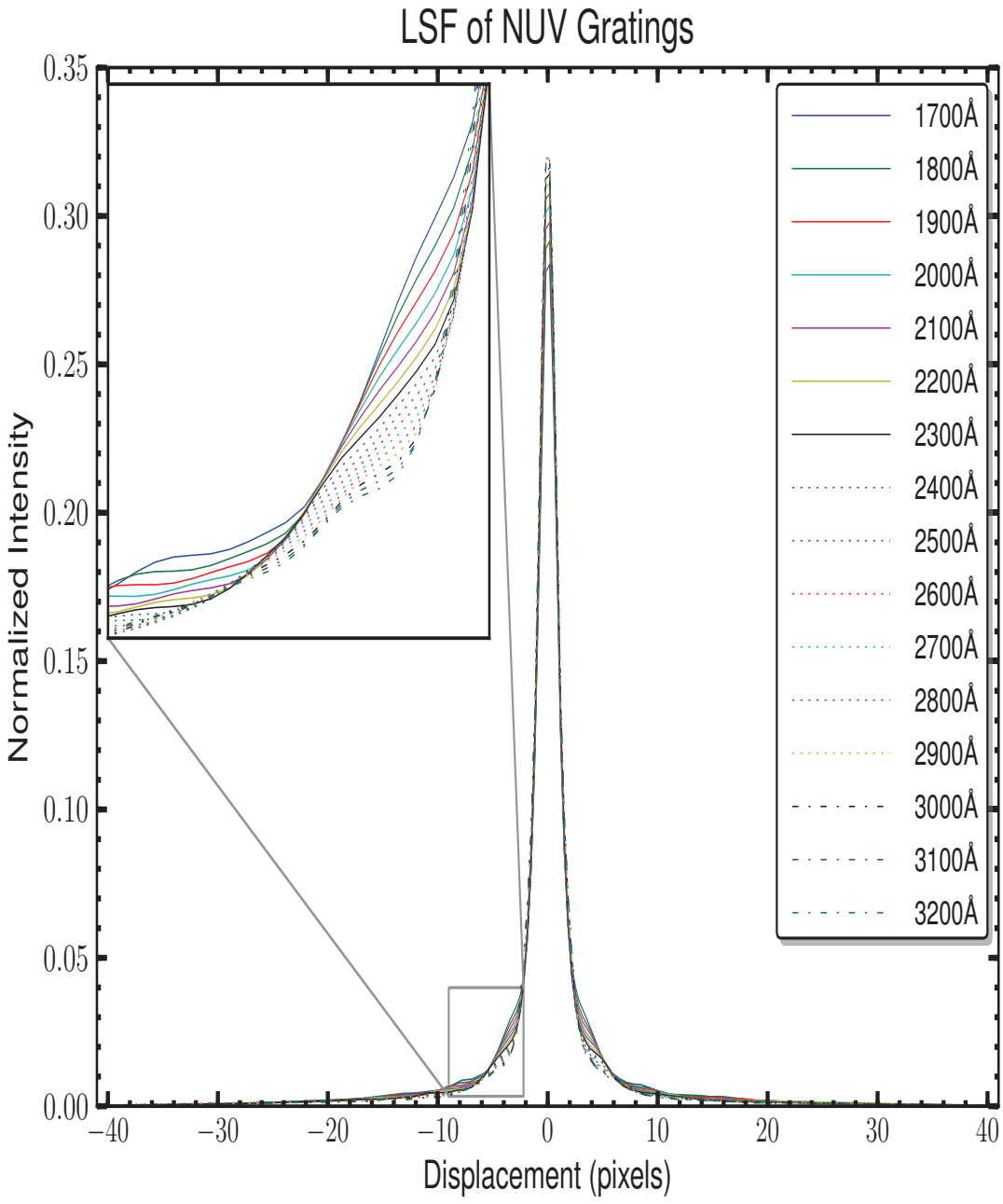

Glossary

A Glossary of Terms and Abbreviations

ACCUM

Operating mode for COS in which only the locations of detected photons are recorded; no time information is recorded. ACCUM mode is designed for brighter object with higher count rates. See also TIME-TAG.

Aperture Mechanism (ApM)

The Aperture Mechanism is used to place either the BOA or PSA into position as the science aperture. The ApM is also moved to place the FCA into position if a flat-field exposure is to be taken.

APT

The Astronomer's Proposal Tool, software provided by STScI for writing Phase I proposals and Phase II programs. The use of APT is encouraged in all cases, even for Phase I proposals, because it provides an accurate estimate of the actual time needed to obtain an observation. For more information, go to

http://apt.stsci.edu

BOA

Bright Object Aperture, which is 2.5 arcsec in diameter with a neutral-density filter that attenuates flux by a factor of about 200.

calcos

The COS calibration pipeline, a software package that performs image and spectroscopic data reduction to produce output files useful for scientific analysis.

central wavelength

For the NUV gratings, the central wavelength is the midpoint of the stripe B spectrum. For the FUV gratings, the central wavelength refers to the shortest wavelength recorded on segment A (though that value is subject to change as the instrument calibration improves).

channel (FUV or NUV)

One of the two COS optical systems, FUV and NUV, including mirrors, gratings, and detectors.

ETC

Exposure Time Calculator, software provided by STScI to estimate exposure times needed to achieve, say, a given signal-to-noise level on a source. Although information is provided in this handbook on exposure estimation, the ETC provides the most accurate way to determine the exposure times required to acquire or observe an object. The ETC is used together with the APT to plan *HST* observations. For more information, go to

http://etc.stsci.edu/webetc/index.jsp

FCA

Flat-field Calibration Aperture, the aperture through which the on-board deuterium lamps illuminate the COS optical system.

FP-POS

A command used to move the spectrum on the detector (in the dispersion direction) to reduce the effects of fixed-pattern noise.

FUSE

Far Ultraviolet Spectroscopic Explorer, a moderate-resolution ($R \sim 15{,}000$), far-UV spectrograph that used micro-channel plate detectors similar to those employed by the FUV channel of COS.

FUV

Far ultraviolet, the channel of COS that spans wavelengths from less than 900 to 1800 Å.

Galex

Galaxy Evolution Explorer, a NASA mission observing the sky in two ultraviolet bandpasses. *Galex* data are useful for determining the UV fluxes of COS targets. For more information, go to

http://www.galex.caltech.edu/

GSC2/ICRS

Guide Star Catalog II / International Celestial Reference System. The GSC2 is an all-sky optical catalog based on 1” resolution scans of the photographic Sky Survey plates from the Polomar and UK Schmidt telescopes. The ICRS is the fundamental celestial reference system adopted by the International Astronomical Union for high-precision astrometry. Uncertainties in this system are dominated by the 0.3” uncertainty of the GSC2.

GTO

Guaranteed Time Observer, a member of the COS science team who has been granted a share of telescope time as part of their involvement in designing and building COS.

home position

The default position for a mechanism. COS is reconfigured at the start of each visit, and mechanisms are returned to their home positions. For the ApM, the home is the PSA; for OSM1, home is G130M, `CENWAVE=1309`; and for OSM2, home is G185M, `CENWAVE=1850`.

IDT

Instrument Development Team, NASA's term for the group that proposed and built COS.

LSF

Line Spread Function, the shape of a spectral feature emitted by a monochromatic point source.

MAMA

Multi-Anode Micro-channel Array, a photon-counting UV detector, used in the NUV channel.

MAST

The Multi-mission Archive at Space Telescope, which makes available data from a number of NASA missions, including *HST*. Go to

`http://archive.stsci.edu`

MCP

Micro-Channel Plate, a resistive glass plate with 10-15 micron-sized holes used within both the XDL and MAMA detectors to amplify photo-electrons into charge pulses large enough for downstream electronic processing.

MIRRORA, MIRRORB

MIRRORA and MIRRORB are used for NUV imaging in COS. MIRRORA provides the highest throughput. MIRRORB uses a reflection off of the order-sorting filter of MIRRORA to get lower throughput, which can be helpful when observing brighter targets.

NUV

The near ultraviolet channel of COS. It spans wavelengths from ~1650 to 3200 Å.

OSM1, OSM2

The Optics Select Mechanisms on COS that place gratings or mirrors in the optical path.

OTA

Optical Telescope Assembly, *HST*'s optical system of primary and secondary mirrors, plus the structure that holds them and maintains alignment.

pixel

The basic stored unit of data. In the NUV channel, MAMA pixels correspond to physical portions of the detector. In the FUV channel, the position of a detected event is assigned to a pixel based on calculations, but there are no physical pixels as such.

PHD

Pulse-Height Distribution, a histogram of the charge cloud sizes collected in a particular exposure or portion thereof. The PHD is a useful measure of data quality and is recorded as a data product for FUV exposures. PHD data are not available for NUV exposures.

POS TARG

The "`POS TARG X, Y`," special requirement is used to request a target offset in APT. POS TARG offsets are specified in the COS user coordinate system, which is used in all COS data products (Section 3.2). Note that the POS TARG coordinates represent motion of the target in the aperture; the telescope moves in the opposite direction.

PSA

Primary Science Aperture, a circular aperture 2.5 arcsec in diameter and completely open.

PSF

Point Spread Function, the two-dimensional distribution of light produced by the *HST*+COS optics.

resel

Resolution element of a spectrum or image. For spectra, a resel corresponds to the FWHM of a narrow wavelength-calibration line. Using pre-flight data, resels were determined to be roughly 6 pixels wide (dispersion direction) by 10 tall for the FUV channel and 3 × 3 pixels for the NUV. On-orbit data suggests that the FUV resel is somewhat larger than this, while the NUV resel is somewhat smaller. Note that spectra are recorded in pixel units and that any rebinning into resels is performed on the ground during data reduction.

segment

The COS FUV detector consists of two independent segments. In all spectroscopic modes, the long-wavelength end of the spectrum falls on segment A, and the short-wavelength end on segment B.

SMOV

Servicing Mission Observatory Verification, the period immediately following a servicing mission in which *HST*'s instruments are activated, tested, and made ready for science observing. Only a minimal set of calibrations are done in SMOV to confirm instrument performance; more detailed calibrations are performed in the ensuing cycle.

stim pulse

Artificially-induced events on each segment of the FUV detector. The stim pulses allow for the correction of thermal distortion and aid in determining the dead-time correction.

STMAG

In this system, the flux density is expressed per unit wavelength, and the reference spectrum is flat in F_λ. $STMAG = -2.5 \log F_\lambda - 21.10$.

stripe

To accommodate the NUV detector format, COS NUV spectra are split into three non-contiguous stripes, each of which covers a relatively small range in wavelength.

TAGFLASH

Use of TIME-TAG mode with FLASH=YES selected. This adds wavelength calibration spectra at periodic intervals during a PSA TIME-TAG observation so that any drifts of the spectrum due to residual motion of the optics can be removed.

TIME-TAG

A COS observing mode in which the locations (pixels) and times (to the nearest 32 msec) are recorded for each detected photon. Doing this consumes memory but allows great flexibility in reducing and analyzing the data.

wavecal

A wavelength calibration exposure; i.e., an exposure of the Pt-Ne wavelength calibration lamp through the WCA.

WCA

Wavelength Calibration Aperture, which is illuminated by a Pt-Ne wavelength calibration lamp.

XDL

Cross Delay Line, the type of detector used in the FUV channel of COS.

Index